Isolation of new genes involved in temperature synchronization of the circadian clock of Drosophila melanogaster

Simoni, Alekos

Isolation of new genes involved in temperature synchronization of the circadian clock of *Drosophila melanogaster*

Alekos Simoni

School of Biological & Chemical Sciences

Queen Mary, University of London

Thesis submitted in fulfilment

of the requirements of the University of London

for the Degree of *Philosophiæ Doctor* (Ph.D.)

September 2010

I certify that this thesis, and the research to which it refers, are the product of my own work, and that any ideas or quotations from the work of other people, published or otherwise, are fully acknowledged in accordance with the standard referencing practices of the discipline. I acknowledge the helpful guidance and support of my supervisor, Professor Ralf Stanewsky.

September 2010

Alekos Simoni

Abstract

Circadian clocks regulate behaviour and physiology of many organisms and keep them in synchrony with the environment. *Drosophila*'s circadian clock is mainly synchronized by natural light-dark cycles and temperature fluctuations, both at molecular and behavioural levels. The mechanisms underlying temperature entrainment are poorly understood, but previous studies have shown that this process can be genetically dissected.

In this work, I isolated several mutants which interfere with the temperature synchronization of *Drosophila*'s circadian clock. Three variants were isolated in a chemical EMS-mutagenesis screen monitoring putative second- and third-chromosomal mutations. The mutants behave normal in light-dark cycles suggesting that they specifically interfere with temperature entrainment. In a different, RNAi-based screen, a Forkhead-domain transcription factor encoding gene was isolated, which shows defective circadian activity of *per* expression and PER accumulation in temperature-entrainment condition, when down-regulated. Finally, a candidate approach led me to identify three genes encoding proteins belonging to the TRP family of ion channels. Mutations in the *pyrexia*, *trpM* and *trpA1* genes show abnormal temperature synchronization of locomotor behaviour, similar to our EMS-candidates.

The isolation and analysis of those mutations are described, as well as a behavioural analysis of the already-known "temperature-mutant" *nocte*. In particular, I discuss the involvement of chordotonal organs as structures required for temperature entrainment of the clock and the role of *nocte* for signalling the temperature information from the periphery to the brain.

The rest-activity pattern is a well-studied circadian output behaviour; the pupal emergence, named eclosion, is another behaviour strictly regulated by the circa-

dian clock. Here we show that genes important for entrainment of adult locomotor behaviour to temperature do not play the same role in regulating the synchronization of eclosion. To gain insight into the synchronization mechanisms of eclosion, I studied how different entrainment conditions affect the phase and free-running period of eclosion.

Ai miei amati genitori,

che anche da lontano

mi siete sempre stati vicini.

Acknowledgements

I think a Ph.D. goes far beyond the 4 years spent in the lab. It is a long and — at time — exhausting process. I could reach the end only thanks to numerous people and it is impossible to mention everyone here. I will try to mention the most important ones, aware that it is inevitable to forget someone. I apologise in advance.

First, I especially thank my supervisor Prof Ralf Stanewsky, who has been my scientific mentor and also a trustful and helpful person. I could consider myself extremely lucky and honoured to have encountered in my early career someone who can teach the "right way" of doing science.

Poche parole non sono sufficienti per ringraziare la mia famiglia, che, come sempre, mi è stata accanto e mi ha accompagnato per tutta la vita. So quanto la lontananza da casa sia dolorosa, per voi quanto per me. Vi ringrazio di non avermelo mai fatto pesare e di avermi sempre sostenuto e incoraggiato a fare quello che volevo. Questa tesi è dedicata a voi, a tutto quello che avete fatto per me e continuate a fare.

A huge thanks goes to all my colleagues, who supported me in many situations, and made the lab a joyful place to work. In particular, I thank (in order of appearance) Niki, Franz, Johannes, Antonio (in Regensburg), Gisela (for the

"Sisyphus task"), Hanka, Ko fan, Carla, Joanna, Chenghao, Werner, Chi and Min (at QMUL).

For the fruitful collaboration and helpful support, I thank Jörg T. Albert.

I thank Fanis Missirilis and Robin Maytum for their advices, help and support. And for showing an example that, sometimes, being a great person is not enough.

I thank Sushi John for the numerous tools that made this Ph.D. possible. In particular, the Agay application, Catenazzo, Delirfrasi (largely utilized in this Thesis), Captchazionario, the countless posts in the "smanettare" blog and the valuable 42 discussions about the Life, the Universe and Everything. The *Richelieu* songs have been the soundtrack in many dolorous situations.

Numerous people and friends made my life in London unforgettable. It is impossible to remember everyone.

I thank: Claudio G. with whom I shared not only the flat, but countless important moments and the best discussions of "filosofia spicciola".
Paolo and the London Buses, for the many hours at the phone and conversations about business, Life, Death and beyond.
Marta who wanted to play.
Sara who did not want to play.
Vahid for showing me the other side of the world.
Claudio V. and "Il circolo del bell'Antonino" for the aglioliopeperoncinate.
Chiara for a shine of light in dark times.
The Barbican Centre for the music.
Google for Gsearch, Gmail, Gimages, Gmaps, Gnews, Gscholar, Gyoutube, Gwasting Gtime, Gprocrastination, ...
Wikipedia for having an answer to everything.
The 11 Marina Court for a place to stay and for the climbers.

Repubblica.it for periodic reminders of the reasons that drove me out of Italy.

The Gate Production for the sleepless nights in North London and the *Odyssey*.

Dilbert, PhD comics, Xkcd for the daily amount of geeky humour.

Vitus for the support. Literal.

Carlo and Valeria for the support and sympathy "off-site", especially on the yearly trip to the Island.

The Island, for reminding us that another year was gone, for the beer and the Jungle Speed.

The Football World Cup, for setting the edges of my Ph.D.

Contents

List of Figures

List of Tables

Abbreviations

♂ male

☿ virgin female

20E 20-hydroxyecdysone peptide

aME Accessory medulla

bHLH basic helix-loop-helix

BO Bolwig's Organ

CCAP Crustacean cardioactive petide

ch chordotonal

ck1ϵ casein kinase 1ϵ

ck2 casein kinase 2

clk Clock

CNS Central nervous system

cps count per second

cry cryptochrome

CT Circadian Time

cwo clockwork orange

cyc cycle

dbt doubletime

DD Constant Darkness

DMAS *Drosophila* Activity Monitor System

DN_1 Dorsal neuron group 1

DN_2 Dorsal neuron group 2

DN_3 Dorsal neuron group 3

DNA DeoxyRibonucleic Acid

EH Eclosion hormone

EMS Ethyl Methane-sulfonate

ERG Electroretinogram

es external sensory

ETH Ecdysis-trigger hormone

FFT-NLLS Fast Fourier transform non-linear least squares

gsk3β glicogensyntase kinase 3β

HB Hofbauer-Buchner

HEK Human Embryonic Kidney cells

iav incative

JO Johnston's Organ

l-LN_v large-ventrolateral neuron

LD Light-Dark cycle

LL Constant Light

LN_d dorsolateral neuron

LPN Lateral posterior neuron

luc luciferase

mya million years ago

nan nanchung

nocte no circadian temperature entrainment

norpA no receptor potential A

pain painless

PAS Per-Arnt-Sim, or period - aryl hydrocarbon receptor nuclear translocator - single-minded

PDF Pigment dispersing factor

Pdk2 Polycystic kidney disease gene-2

Pdp1 Par domain protein 1

per period

PG Prothoracic Gland

PI Pars intercerebralis

PL Pars lateralis

PLC Phospholipase C

PNS Peripheral nervous system

POT Posterior optic tract

pp1 protein phosphatase 1

pp2a protein phosphatase 2a

PTTH Prothoracicotropic hormone

pyx pyrexia

RG Ring Gland

RMS Root mean square

RNA Ribonucleic acid

RNAi RNA interference

s-LN_v small-ventrolateral neuron

SCF Skp1/Cul1/F-box protein complex

SEM Standard Error of the Mean

sgg	shaggy
slimb	supernumerary limbs
TC	Temperature Cycles
tim	timeless
trp	transient receptor potential
trpl	trp-like
UTR	untranslated region
V/P	vrille/Pdp1 site
VDRC	Vienna *Drosophila* RNAi Center
vri	vrille
VS	Vibration-Silence cycles
wt	wild-type
wtrw	water witch
ZT	Zeitgeber Time

There once was a scientist doing an experiment on the reaction of fleas. He had trained a flea to jump on command. The scientist would command the flea "Jump Flea!" and the flea would jump. Then the scientist would proceed to pull off one of the fleas legs with a pair of tweezers and write a comment in his notebook.

The scientist did this many times until the flea had only one leg left. The scientist said "Jump Flea!" and the flea made it's best effort to jump, which the scientist recorded in his notebook.

After he pulled off its last leg, the scientist commanded the flea to jump, and after repeating the command many times without the flea responding he jotted down in his notebook, "After the flea looses all of his legs it becomes completely deaf."

"For every behavioural observation, there is an equal and opposite observation."

Seymour Benzer [1].

[1] Quoted in Mealey-Ferrara et al. (2003)

Chapter 1

Introduction

Time is an illusion. Lunchtime doubly so.

Douglas Adams

1.1 Chronobiology and circadian clocks

The first report of the existence of circadian clock dates back to the eighteen century, and an observation of a French astronomer, Jean-Jacques d'Ortus de Mairan (1729). The leaves of the heliotrope *Mimosa pudica* turn to the sun and open during the day and close during the night (hence the name, *helios*=sun, *tropos*=movement). De Mairan observed that the leaf movement was not a passive response to the environment, but persisted when the plant was enclosed in a dark cabinet and not exposed to the daily oscillation of light and dark. De Mairan cleverly concluded that there must have been some endogenous mechanism which was telling the plant the time of the day and he proposed the existence of a "circadian clock" (although the term *circadian* has been coined only in the 1950s by Franz Halberg, as recalled in the publication Halberg et al., 2003).

Two centuries later the origin of this mysterious mechanism has been revealed

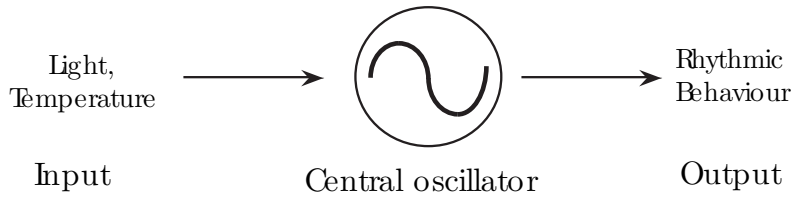

FIGURE 1.1: The three-component structure of circadian clocks. The components of the "input pathway" receive the cycling information from the environment and transmit them to the "central oscillator". Rhythmic behaviours are then generated via the "output pathway".

and the properties described (Dunlap et al., 2004).

Circadian clocks are endogenous oscillators shaped by evolution to make the organisms able to perceive time and to be synchronized with the cycling environment in order to anticipate reproducible environmental changes.

Three properties characterize circadian clocks. First, they are endogenous and self-sustainable. The clocks generate rhythms with a period of about 24 hours (*circa dies*) that persist even in absence of any environmental stimulus. Secondly, the clock can be synchronized (entrained) by cycling environmental conditions in order to be in-phase with the environment. Last, the clocks are temperature compensated, which means that the period is almost the same over a wide range of constant physiological temperatures. This last properties is summarized by the formula $Q_{10} \approx 1$. Q_{10} indicates the rate of change of chemical reactions as a consequence of temperature increase of 10°C [1]. For most biochemical reactions, the rate is generally between 2 and 3. For biological clocks, the rate is about 1, which means that circadian systems are temperature compensated (Pittendrigh, 1954).

The simplified structure of a circadian system is based on three components

[1] Q_{10} is calculated as $Q_{10} = \left(\frac{R_2}{R_1}\right)^{10/(T_2-T_1)}$, where R is the rate and T is the temperature (in Celsius).

(Figure 1.1). The *central oscillator* is capable of generating sustained circa 24-hour cycles of gene expression and protein accumulation. The central oscillator (or pacemaker) can be entrained by rhythmically changing environmental conditions. The second component that constitutes the circadian clock is the *input pathway*, which includes the structures arranged to perceive the cycling stimuli in the environment and to transmit these information to the central oscillator. The stimuli able to entrain the circadian clock are called Zeitgeber (German *Zeit*=time and *Geber*=giver). For *Drosophila*, the main Zeitgebers are daily light-dark cycles and temperature fluctuations (Pittendrigh et al., 1958; Zimmerman et al., 1968), although other factors can synchronize the circadian clocks, for instance social interactions (Levine et al., 2002b). The generation of rhythmic behaviours and physiological processes is regulated through the third component of the circadian clock — the *output pathway*. In *Drosophila*, many complex behaviours are under the control of the circadian clock and the most studied ones are adult emergence (eclosion) and locomotor behaviour (see below).

1.2 The circadian clock of *Drosophila melanogaster*

1.2.1 The central oscillator

The current understanding of circadian systems has achieved great contributions thanks to studies conducted on *Drosophila*. After the pioneering works from Konopka and Benzer (1971) and the isolation of the first clock mutants, the molecular basis of circadian clocks has been established. Now, many "clock genes" are known to be required for the generation of 24 hour rhythms and the picture is

quite complex, though not completely clear.

The generation of a rhythm of 24 hours is determined by the presence of two interlocked feedback loop of gene expression and repression. The basic helix-loop-helix (bHLH) PAS-domain transcription factors CLOCK (CLK) and CYCLE (CYC) (Allada et al., 1998; Bae et al., 1998; Rutila et al., 1998) form heterodimers and bind the E-box sequences (*CACGTG*) (Kyriacou and Rosato, 2000) in the promoters of the target genes *period* (*per*) and *timeless* (*tim*) (Konopka and Benzer, 1971; Sehgal et al., 1994). PER and TIM proteins accumulate in the cytoplasm, dimerize and then migrate to the nucleus (Saez and Young, 1996; Shafer et al., 2002) where they block the CLK/CYC complex (Lee et al., 1999), inhibiting their own transcription. Some studies have proposed that PER and TIM dissociate before entering the nucleus (Shafer et al., 2002), and that PER homodimerization is important for nuclear entry (Landskron et al., 2009).

The time in which PER and TIM accumulate in the cytoplasm is strictly regulated by post-transcriptional events and ubiquitin-mediated degradation. Phosphorylation of PER is mediated by the kinase DOUBLE TIME (DBT), which is the homologue of the mammalian *casein kinase 1*ϵ (Kloss et al., 1998; Price et al., 1998). The F-box protein SLIMB in the ubiquitin-proteasome pathway interacts with DBT-phosphorylated PER and mediates its degradation (Ko et al., 2002). The PER/DBT complex can also enter the nucleus regulating the activity of CLK (Kim and Edery, 2006). TIM is phosphorylated by GLYCOGEN SYNTHASE KINASE 3β/SHAGGY (GSK3β/SGG) (Martinek et al., 2001) and CK2 (Meissner et al., 2008). The action of PROTEIN PHOSPHATASE 2A (PP2A) and PROTEIN PHOSPHATASE 1 (PP1) (Sathyanarayanan et al., 2004; Fang et al., 2007) on PER and TIM, respectively, promotes the accumulation and the stability of the protein in the cytoplasm and the subsequent entry in the nucleus. While PER

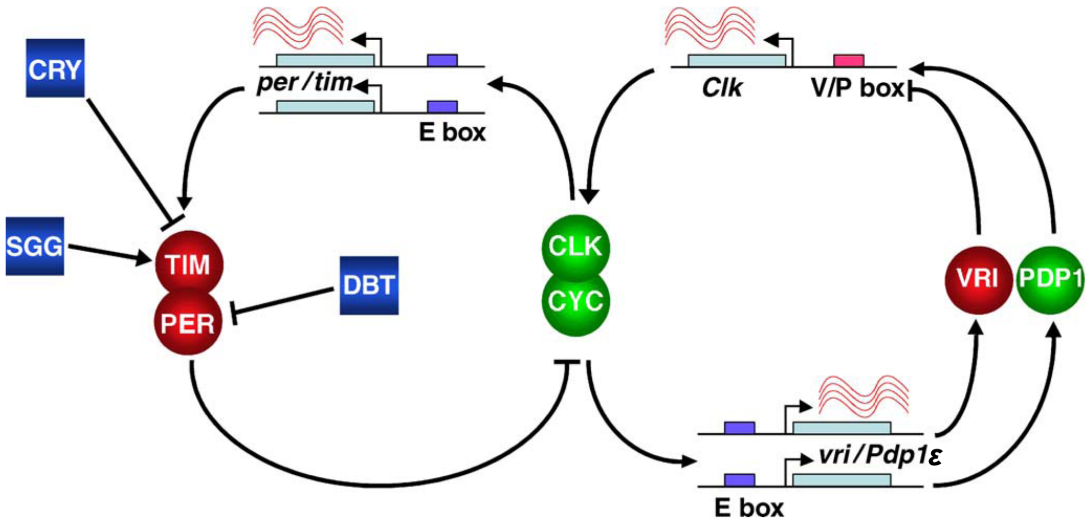

FIGURE 1.2: The schematic of the circadian clock of *Drosophila melanogaster*. Two negative feedbacks loops are interlocked with each other. In the first loop, CLK and CYC regulate the expression of *per* and *tim* by binding the E-box regulatory sequences on their promoter region. The phosphorylation activity of SGG and DBT determines the stability of TIM and PER and the time before the proteins enter the nucleus where they eventually inhibit their own transcription. In the second loop, CLK/CYC activate the expression of *vri* and *Pdp1*ϵ. Once the respective proteins have been translated, VRI and PDP1 repress and activate, respectively, the expression of *Clock*, competing for the same V/P box binding site. CRY mediates the light-dependent degradation of TIM, resetting the clock with the light signal. Figure taken from Collins and Blau (2007).

and TIM repress their own transcription, their concentration gradually decreases. As a result, CLK and CYC are then free to start activating *per* and *tim* again, and the cycle continues. In wild-type (wt) flies, this feedback loop takes circa 24 hour to repeat itself.

In *Drosophila*, a second feedback loop is interlocked with the first. In addition to activating the expression of *per* and *tim*, the CLK/CYC complex activates the transcription of *Par domain protein 1*ϵ (*Pdp1*ϵ), *vrille* (*vri*) and *clockwork orange* (*cwo*) (Cyran et al., 2003; Kadener et al., 2007; Lim et al., 2007). The basic zipper transcription factor PDP1 activates the expression of CLK, whereas VRI represses it, competing for the binding site on its promoter (V/P site). This results in *Clk* mRNA cycling in anti-phase compared to *per* and *tim*: the latter phase peak in

the early night and the former in the morning. CWO belongs to the same feedback loop and acts as a repressor for CLK/CYC-mediated activation of *vri* and *Pdp1*ϵ and for its own transcription (Kadener et al., 2007; Lim et al., 2007). However, CWO has also been proposed to act also as an activator for CLK targets (Richier et al., 2008).

1.2.2 The input of the clock: light and temperature

The two-loop model described above explains the first characteristic of the circadian clocks, such as the ability to generate and self-maintain a circa 24-hour rhythm. The rhythm is *circa* 24 hour, but not *exactly* 24. This means that the clock has to be continuously reset to be constantly in phase with the 24-h environmental cycles. In *Drosophila*, daily temperature oscillations and the light-dark cycle are the strongest known signals perceived by the clock as Zeitgeber. Although light is a more potent signal compared to temperature (Wheeler et al., 1993), the two act together to fine tune and reinforce the fly entrainment in a synergistic way (Boothroyd et al., 2007; Yoshii et al., 2009a).

Light entrainment

The fly possess several photoreceptors which act in orchestra to sense the light signal and transmit it to the central pacemaker. The fly's photoreceptors are the compound eye, the ocelli and the Hofbauer-Buchner eyelet (HB-eyelet) (Helfrich-Förster et al., 2001; Helfrich-Förster, 2002; Veleri et al., 2007). However, the main circadian photoreceptor is the blue-light sensitive protein CRYPTOCHROME (CRY) expressed within the clock neurons where it mediates the light-dependent degradation of TIM (Emery et al., 1998, 2000; Stanewsky et al., 1998). In darkness, CRY is kept in an inactive form by an unknown repressor (Rosato et al.,

2001). When light is on, CRY is activated, and it binds directly to TIM, triggering its degradation via the proteasome (Ceriani et al., 1999; Busza et al., 2004). The light-dependent degradation of TIM is mediated by the F-box protein JETLAG (Koh et al., 2006; Peschel et al., 2006, 2009), which is part of the SCF E3 ubiquitin ligase complex.

Light-dependent degradation of TIM is a crucial event for resetting the circadian clock. In fact, when TIM is degraded, the PER/TIM complex cannot be formed and PER is a target of phosphorylation events by DBT, which leads to PER degradation (see above). This results in a delay of PER and TIM entry in the nucleus and a resetting point for their own transcription (Dunlap, 1999).

Exposure to constant light (and constant temperature) induces arrhythmic behaviour (Konopka et al., 1989) due to continuous degradation of TIM by CRY. The cry^b mutation, which severely affects CRY function, largely prevents light-dependent TIM degradation resulting in a severe reduction of circadian light responses and in rhythmic behaviour under constant light conditions (Stanewsky et al., 1998; Emery et al., 1998, 2000). These data were recently confirmed by the generation of the null mutant cry^0 (Dolezelova et al., 2007). Over-expression of CRY, instead, induces hypersensitivity to light (Emery et al., 1998), confirming the prominent role of CRY in the light entrainment.

CRY mutants are not completely circadian blind, but the circadian light sensitivity is much reduced and light entrainment is slower (Stanewsky et al., 1998; Emery et al., 1998, 2000). Only the removal of all photoreceptors makes the fly circadianly blind and unresponsive to the light stimulus (Helfrich-Förster et al., 2001). However, the input pathways which mediate CRY-independent light entrainment are still unclear.

Temperature entrainment

In addition to LD cycles, temperature cycles (TC) also can entrain the circadian clock. Temperature robustly synchronizes the eclosion rhythm of *Drosophila pseudoobscura* (Zimmerman et al., 1968), the fly's locomotor behaviour (Wheeler et al., 1993) and the molecular oscillations of clock proteins (Stanewsky et al., 1998).

Temperature cycles (TC) can also entrain the circadian clock in LL, both at behavioural (Tomioka et al., 1998; Yoshii et al., 2002, 2005) and molecular levels (Glaser and Stanewsky, 2005), a situation that usually induces the fly to be arrhythmic (Konopka et al., 1989). It is generally believed that LL stops the clock, since TIM and PER are not cycling under LL and constant temperature. However, TC in LL restore the circadian oscillation of PER and TIM (Glaser and Stanewsky, 2005). Work from Tomioka et al. (1998) and Yoshii et al. (2002) suggest an even "better entrainment" to temperature cycles in LL compared to DD, based on the observation that per^s and per^L mutants fail to synchronize their locomotor activity to temperature in DD whereas they do so in LL. Also wild-type flies entrain to TC faster in LL compared to DD. In addition, Yoshii et al. (2002) showed that that wild-type flies can entrain to a wide range of thermoperiods in LL but only to 12:12 hr warm-cold cycles in DD, indicating that temperature is a stronger Zeitgeber in LL than in DD. The effect of temperature as Zeitgeber on the clock is further confirmed by experiments involving temperature pulses and temperature step-up and step-downs, which can change the phase of free-running behaviour (Sidote et al., 1998; Kaushik et al., 2007; Yoshii et al., 2007). Interestingly, the phase response induced by heat pulses (37°C) is mediated by the photoreceptor CRY (Kaushik et al., 2007), since cry^b exhibits reduced (or almost zero) heat phase responses. The model proposes that heat facilitates the interaction between PER and TIM and facilitate also the interaction of the PER-TIM complex with the

active CRY. CRY:TIM-PER interaction leads to TIM degradation, which advance or delay the the clock (Kaushik et al., 2007).

Although CRY seems not to be required for temperature entrainment in a more physiological range (Stanewsky et al., 1998; Busza et al., 2007), it mediates the interaction with PER/TIM in a temperature-dependent manner, similarly to the light-dependent interaction between CRY and TIM/PER (Rosato et al., 2001; Kaushik et al., 2007).

The ability of the circadian clock to synchronize to temperature cycles, with an amplitude as little as 3℃ (Wheeler et al., 1993) is of interest if we consider that the clock is temperature compensated (Pittendrigh, 1954; Konopka et al., 1989). The chemical reactions underlying the circadian system are buffered to keep a constant rate at different physiological temperatures. However, the same system is able to interpret temperature oscillations as a Zeitgeber, in a process which is still mainly unknown. The protein PER is probably involved in the temperature compensation of the clock, since per^s and per^L mutant flies, in addition to having, respectively, a short and long period (Konopka and Benzer, 1971), are not temperature compensated (Konopka et al., 1989). It has also been proposed that the polymorphic repeats of Threonine-Glycine (Thr-Gly) residues in the PER protein mediate the adaptation of various populations of *Drosophila melanogaster* living in different latitudes to keep the same period length at different temperature (Sawyer et al., 1997).

The peak phase of molecular oscillations and behavioural rhythms under temperature entrainment are a few hours advanced compared to LD entrainment (Glaser and Stanewsky, 2005; Busza et al., 2007; Boothroyd et al., 2007). However, the natural profile of temperature cycles is delayed by several hours compared to the one of light (Boothroyd et al., 2007; Yoshii et al., 2009a) and thus the result-

ing phase of rhythms entrained by the respective Zeitgeber in nature is essentially the same. In natural condition, light and temperature act probably synergically to enhance and fine-tune the entrainment (Boothroyd et al., 2007; Yoshii et al., 2009a).

Although the mechanisms by which TC act on the central clock are still unknown, several contributions address the effect of temperature itself on the regulation of *per* and *tim* expression. Also, the pattern of the fly's locomotor activity is modulated by different constant temperatures by a mechanism which involves temperature-dependent alternative splicing of intron 8 in the 3'-untranslated region (UTR) of *per* (Majercak et al., 1999, 2004). At lower temperature (18℃) and short photoperiods, the spliced version of *per* mRNA is preferred, which results in an advanced accumulation of the PER protein, correlated with an early activity phase. In warm temperatures (29℃) the unspliced version is favoured correlated with a later activity phase (Majercak et al., 1999). Interestingly, under these two temperature conditions, difference in *tim* expression are also observed: at 29℃ the expression of *tim* is higher than at 18℃ (Majercak et al., 1999). In addition, *tim* is also expressed in two different transcript according the temperature (Boothroyd et al., 2007). One transcript, named tim^{cold}, is more abundant at 18℃ (in LD) while the other (the normal one) is favoured at 25℃. Interestingly, the tim^{cold} transcript generates a truncated TIM protein (Boothroyd et al., 2007) but its physiological role has not yet been identified. The modulation of the PER and TIM phase in different temperature and photoperiods thus contributes to the "seasonal adaptation" of the fly's behaviour (Collins et al., 2004; Majercak et al., 1999, 2004). In warmer and longer days, the fly's behaviour is shifted towards dawn and dusk, whereas in cold and short days the fly is more active during the relatively mild hours in the afternoon.

Temperature variations are interpreted by the clock not only for the purpose of seasonal adaptation, but also as a Zeitgeber that entrains the clock. However, the molecular mechanisms by which the temperature entrains the clock are still mainly unknown. To date, only two genes have been proposed as components required for the molecular entrainment of the circadian clock to temperature: *nocte* and *norpA* (Glaser and Stanewsky, 2005, 2007; Sehadova et al., 2009).

nocte has been isolated in an EMS chemical mutagenesis screen as a variant with severe defects on synchronization of the circadian clock to temperature cycles (Glaser and Stanewsky, 2005). The *nocte* gene has been cloned and encodes a large Glutamine-rich protein with no evident homology with any known domains or proteins (Sehadova et al., 2009). RNAi-mediated down-regulation of the gene in peripheral tissues, and specifically in the chordotonal (ch) organs, with the *F-gal4* driver (Kim et al., 2003), compromises temperature entrainment, similar to the *nocte* mutants. Analysis of several ch organ mutants revealed these structures to be required for temperature entrainment (Sehadova et al., 2009), although the molecular mechanisms underlying the entrainment remain unclear. Nevertheless, it appears that temperature and light entrainment display clear differences in the way the signal is transmitted to the central clock. Light acts directly on the clock neurons through the photoreceptor action of CRY (see above). The fly's brain, instead, cannot alone interpret the temperature signal, but it requires peripheral sensory tissues for the entrainment to take place (Sehadova et al., 2009).

Part of this thesis contributed to the publication of the work by Sehadova et al. (2009), and it will be addressed in the chapter 7.2.

The product of the gene *norpA* (*no receptor potential A*) is the enzyme Phospholipase C (PLC). PLC has a prominent role in the visual phototransduction cascade in the fly's compound eyes, and *norpA* mutants are completely blind

(Bloomquist et al., 1988). Glaser and Stanewsky (2005) showed that *norpA* mutant flies exhibit defects in entrainment of the circadian clock to temperature, and the phenotype resembles very much the one of the *nocte* mutants. Previous studies have also shown the involvement of PLC in the light input pathway of the clock, by combining to *norpA* and *cry* mutants (Stanewsky et al., 1998; Emery et al., 1998; Helfrich-Förster et al., 2001). An additional involvement for the *norpA* gene has been suggested in the regulation of the temperature-dependent alternative splicing of the 3'-UTR region of *per* (see above). *norpA* mutants favour the spliced version of the *per* mRNA in warm temperature and long photoperiods, in a light-independent manner (Collins et al., 2004; Majercak et al., 2004). This temperature-dependent splicing event of *per* is not required for temperature entrainment (Glaser and Stanewsky, 2005; Currie et al., 2009), since the two transcripts are expressed at equal levels during TC in wild-type and *nocte* mutant flies (Glaser and Stanewsky, 2007). In contrast, *norpA* mutants favour the "cold" variant (the spliced transcript) during the temperature cycles (Glaser and Stanewsky, 2007), confirming the involvement of *norpA* in the temperature regulation of *per* splicing.

PLC has also been proposed to play a role in the themopreference behaviour mediated by TRP channels (Kwon et al., 2008). Larval *norpA* mutants lose the ability to distinguish between 18℃ and 24℃ and the model suggests that the TRPA1 channel — required for thermopreference behaviour (see below) — acts downstream of a temperature dependent signalling cascade mediated by PLC (Kwon et al., 2008). The role played by the TRP channels in temperature sensation will be addressed in more details in Chapter 5 and Section 1.3.

Temperature entrainment in different model organisms

Periodic temperature oscillations with period of around 24 hours, even in the range of 1–2℃ can entrain the circadian clock of all poikilothermic organisms, beside *Drosophila*. In homeothermic organism, temperature cycles can also cause entrainment, although with considerable individual difference, and only of they are of rather high amplitude (reviewed by Rensing and Ruoff, 2002).

In *Neurospora*, temperature entrains the circadian clock by changing the level of the FREQUENCY (FRQ) protein. At higher temperature, FRQ oscillates at higher level than in low temperature, whereas the level of *frq* oscillation varies little between high and low temperature (Liu et al., 1998). Temperature steps-up and steps-down increase or decrease, respectively, the level of FRQ, causing phase-shift, similar to those obtained after light pulse. Interestingly, in *Neurospora* temperature cycles are even a stronger Zeitgeber than light. Conidiation occurs mainly during the dark phase of a LD regime, and during the cold-phase in temperature entrainment regime. With conflicting light and temperature cycles (light and cold temperature to dark and high temperature), the conidiation rhythms follow the temperature rather than the light (Liu et al., 1998).

The molecular clock of Zebrafish (*Danio rerio*) can also be synchronized by temperature cycles. 24-hour oscillations of 4℃ in DD can entrain the expression of clock genes, and setting the phase of free-running after released to constant conditions (Lahiri et al., 2005). Temperature steps shift the phase of clock genes expression and change their expression level: expression of *per4* and *cry3* are down- and up-regulated following a temperature increase and decrease, respectively, while the opposite effect is observed for *cry2a*. Expression of other genes, like *clock1*, *per2* or *β-actin* is not affected by temperature steps, indicating a gene-specific response (Lahiri et al., 2005). In addition, the protein expression level,

amplitude and phosphorylation of CLOCK, one of the central clock-protein, are temperature dependent, suggesting that posttranscriptional effects are also under temperature control.

The effect of periodic temperature changes is a less powerful Zeitgeber on the circadian clock of endothermic animals respect to ectothermic (poikilothermic) animals. The reason is probably that a homeostatic regulation of the body temperature should render the organism less sensitive to temperature fluctuations (Rensing and Ruoff, 2002). However, even for endothermic animals, temperature cycles can entrain the circadian clock: the locomotor activity of rodents can be synchronized to temperature changes but entrainment to temperature is much slower and less strong than light (Refinetti, 2010). Cultured pineal cells of chicks exhibit rhythmic melatonin production in constant conditions and this rhythm can be synchronized to temperature cycles (Rensing and Ruoff, 2002). Cultured rat fibroblast can entrain clock and clock-controlled genes expression to temperature cycles, suggesting the ability of temperature oscillations to autonomously synchronize cells *in vitro* (Brown et al., 2002). In an organismic level, it has been shown that temperature cycles can entrain peripheral clock in mice liver without affecting the phase of the central clock in the SCN (Brown et al., 2002). In addition, natural body temperature fluctuations can delay the dampening of cycling gene expression in peripheral oscillators (Brown et al., 2002).

1.2.3 The neuronal architecture of the circadian clock

The central oscillator of *D. melanogaster* is located in the central nervous system (CNS). Several groups of neurons rhythmically express clock genes, and were named according to their anatomical position and size (Kaneko and Hall, 2000; Shafer et al., 2006; Helfrich-Förster et al., 2007). In the adult *Drosophila*

brain there are circa 150 clock neurons, which can be divided to six main groups (Helfrich-Förster et al., 2007). Three groups of lateral neurons are located in the centro-lateral region of the brain and are named dorsolateral neurons (LN_d) and small and large ventrolateral neurons (s-LN_v and l-LN_v). The three other groups are located dorsally and are called dorsal neurons group 1, 2 and 3 (DN_1, DN_2 and DN_3; Figure 1.3A). All six groups of neurons are required for generating rhythmicity but the LN_vs and LN_ds seem to be more important since they are necessary and sufficient for maintenance of rhythmic behaviour in the absence of environmental cues (Grima et al., 2004; Shafer et al., 2006). As shown in Figure 1.3A, four s-LN_vs neurons and five l-LN_vs neurons are located in the brain. The s-LN_vs project into the accessory medulla (aME) and to few DN_1 and DN_3 cells. The l-LN_vs project through the posterior optic tract (POT) onto the surface of both medullae. The fifth s-LN_v cell, which does not express the PIGMENT DISPERSING FACTOR (PDF), arborizes in the aMe and runs toward the dorsal brain (Helfrich-Förster et al., 2007). Near the posterior surface of the brain, three to four cells of lateral posterior neurons (LPNs) are located close to the dorsal projections of the sLN_vs (Shafer et al., 2006). The more dorsally located 5–8 LN_d also project into the dorsal brain. The dorsal region consists of more than 80 neurons and none of them express *Pdf*. The ∼17 DN_1 cells are subdivided in two subclasses, the two DN_{1A} and the DN_{1P} (for "anterior" and "posterior", Shafer et al., 2006). The two DN_2 cells are located in the proximity of the projection from the LN_vs and are believed to play an important role in temperature entrainment (Yoshii et al., 2005; Shafer et al., 2006). The biggest group of dorsal neurons is the DN_3, which is constituted of ∼40 cells.

The light input pathways from the R1–R6 and R7/R8 photoreceptor cells of the compound eye terminate in the lamina and in the medulla, respectively, whereas

A)

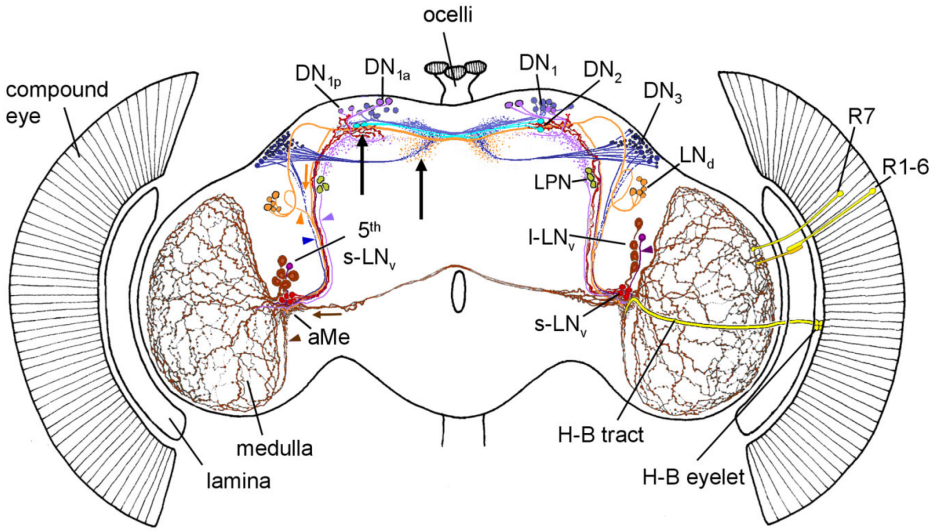

B)

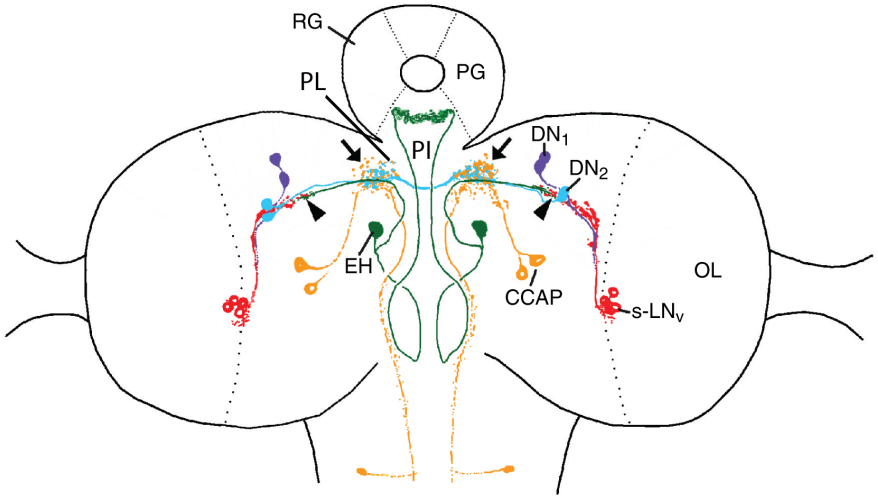

FIGURE 1.3: Anatomy of the clock neurons and their projections in the *Drosophila* brain. A) Clock-gene expressing neurons and light input pathways in the adult brain. B) Neurons expressing clock-genes and eclosion regulating hormones are shown in the larval brain. aMe: accessory medulla. CCAP: crustacean cardioactive peptide cell. DN: dorsal neuron. EH: eclosion hormone cells. LN_d: dorsolateral neuron. LN_v: ventrolateral neuron. LPN: lateral posterior neuron. OL: optic lobe. PG: prothoracic gland. PI: pars intercerebralis. PL: pars lateralis. RG: ring gland. See text for details. Drawings are taken from Helfrich-Förster et al. (2007) and from Helfrich-Förster (2005), respectively.

the projections from the 4 cells of the Hofbauer-Buchner (HB) eyelet overlap with dendritic terminals of the s-LN_vs in the aME (Helfrich-Förster et al., 2007). The circadian photoreceptor CRY is expressed in all the LN_vs (including the 5th PDF-negative), in three of the six LN_ds, in the DN_{1A}s and six of the DN_{1P}s (Yoshii et al., 2009b).

The pathway by which the temperature signals synchronize the central clock is still unclear. Indications suggest that the DN_2 and the LPN neurons are required for temperature entrainment (Yoshii et al., 2005; Glaser and Stanewsky, 2007; Miyasako et al., 2007). Pdf^{01} mutant flies are still able to entrain to temperature cycles (Yoshii et al., 2005) suggesting an important role for the *Pdf*-negative neurons and the non-requirement of this neuropeptide in the process.

The larval brain of *Drosophila melanogaster* is much simpler than the adult one and consists of only three groups of clock neurons: five LNs (four of which express PDF), and two pairs of dorsal neurons (DN_1 and DN_2) (Kaneko et al., 1997; Helfrich-Förster, 2005 and Figure 1.3B). The photoreceptor CRY is expressed only in the PDF-positive LNs and in the DN_1 (Klarsfeld et al., 2004). Interestingly, the DN_2 cells express PER in anti-phase compared to the other groups of neurons (Kaneko et al., 1997; Klarsfeld et al., 2004; Picot et al., 2009) and the phase of PER expression is reversed during metamorphosis (Kaneko et al., 1997). The DN_2 cells seem to be required for temperature entrainment of the larval clock (Picot et al., 2009), whereas the LNs are required for light entrainment through the larval visual system, the Bolwig's Organ (BO) (Kaneko et al., 1997; Malpel et al., 2002).

The contribution of each clock neuronal group to circadian rhythmicity is still object of debate. In 1976 Pittendrigh and Daan proposed the existence of two independent oscillators which govern the morning and evening activity. Their idea was based on studies of free-running activity in rodents and the observation

of the "splitting" phenomenon. Activity sometimes "splits" in two independent components with different free-running periods under certain light or darkness conditions, suggesting the existence of (at least) two oscillators.

In *Drosophila* several studies support the idea of two oscillators. Mosaic analysis revealed that the morning anticipatory activity under light-dark cycles is driven by PDF-positive LN_vs (M, morning cells). The cells which contribute to the evening (E) activity are the 5th-LN_v, the LN_d and some DN_1 and are called E cells (Grima et al., 2004; Stoleru et al., 2005). However, the situation is not completely clear and the original Pittendrigh and Daan's model may not fit to *Drosophila*.

The s-LN_vs (M-cells) seem also to contribute to the evening bout of activity, at least in LL. This observation is based on experiments of cry^b mutants analysed in LL conditions: the free-running evening peak "split" in a long and a short component (Rieger et al., 2006). This split behaviour is observed also in wild-type flies released in low light intensity. Analysis of PER cycling in specific groups of neurons revealed that the short component is driven by the s-LN_v, which are therefore proposed to be "main cells", rather then "morning cells" (Rieger et al., 2006). A recent work by Zhang et al. (2010) showed that the DN_1 neurons, in addition to contribute to the evening bout of activity, control also the morning activity under high intensity light. However, their contribution is under environmental control: at high light intensity and high temperature, the DN1s are unable to generate the evening activity, whereas at low temperature, the morning bout of activity is inhibited (Zhang et al., 2010).

Therefore, the regulation of the activity does not depend only on specific groups of neurons, but by the interaction with the environment. Such complexity of organization is probably required to deal with an environment in which multiple

variables can changes, predictably in many cases, but also erratically (Dubruille and Emery, 2008) and the separation between E and M cells is probably a simplification.

1.2.4 The output: locomotor behaviour and eclosion

Many behavioural and physiological processes are under control of the circadian clocks, ranging from sleep (Shaw et al., 2000), to memory (Lyons and Roman, 2009), feeding (Xu et al., 2008), egg-laying (S. Hari Dass and Sharma, 2008), chemosensation (Chatterjee et al., 2010), courtship and mating (Sakai and Ishida, 2001) and immunity (Lee and Edery, 2008). However, the most studied output behaviours are the locomotor behaviour (activity) and the eclosion rhythm, probably because of the automated nature of the *Drosophila* Activity Monitor System (DAMS).

The first output of the circadian clock that was studied in detail has been the emergence from the pupal case (eclosion). Although the adult emergence occurs only once in the fly's lifetime, it is considered to be a circadian rhythm. This is because a population of pupae manifests an eclosion rhythm if they are not necessarily synchronous developmentally, but are fully synchronous in their circadian oscillations (Skopik and Pittendrigh, 1967).

Eclosion occurs at the early (and wettest) hours of the day because emerging flies lose water at high rate compared to mature flies and they fail to expand their wings at low humidity (Pittendrigh, 1954) — hence *Drosophila* got its name, from the Greek *drosos*, "dew" and *philos*, "lover". The event of eclosion is controlled by a cascade of peptide hormones produced in the prothoracic gland (PG) and in the CNS. Ecdysis, the shedding of cuticle at defined stages of development and growth (Nässel, 2000), initiates with a decreasing titer of 20-hydroexdysone (20E,

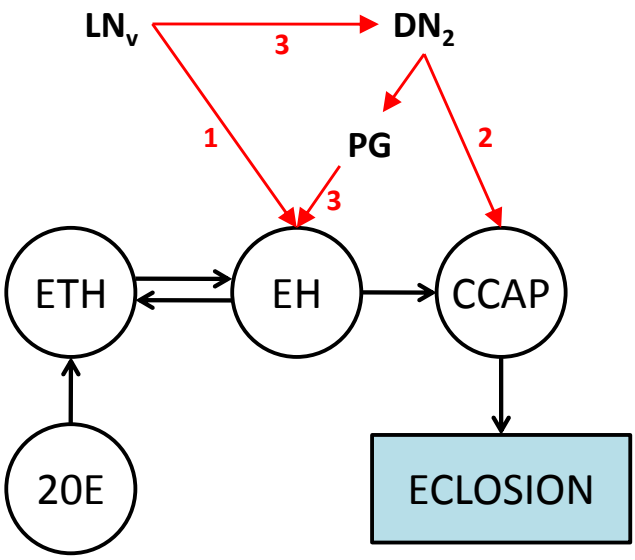

FIGURE 1.4: A model for eclosion control by the circadian clock based on neural connection (Helfrich-Förster, 2005). Black arrows indicate endocrine signalling cascade that leads to eclosion (see text for details). Red arrows and numbers 1, 2 and 3 indicate the three putative pathways of eclosion timing control by the circadian clock.

produced in the PG), which leads to the titer increase of the eclosion hormone (EH) and the ecdysis-trigger hormone (ETH) — produced, respectively, by the neurosecretory EH-cells and crustacean cardioactive petide (CCAP)-cells (Figure 1.3B and reviewed by Helfrich-Förster, 2005). The increase of EH and ETH triggers a rhythmic release of CCAP, which eventually leads to eclosion (Figure 1.4). The regulation of the EH by the PG is under control of the prothoracicotropic hormone (PTTH), which is produced by secretory cells in the pars intercerebralis/lateralis (PI, PL). The circadian clock controls the timing of the eclosion event through three pathways: (i) Projections of the larval LN_vs overlap with the ones of the EH cells (see arrow heads in Figure 1.3B); (ii) DN_2 projections overlap dendritic fibres of the CCAP cells (see arrows); (iii) the third pathway connects the LN_vs to the PTTH cells (via the DN_2) and then to the PG (Siegmund and Korge, 2001; Helfrich-Förster, 2005 and Figure 1.4).

Although the anatomy of the circadian clock neurons is well characterized, little is known about the neurotransmitters implied in the generation of rhythmic behaviour. Only few neurotransmitters are known to be expressed in the clock

neurons. The pigment dispersing factor (PDF) is expressed in the small (except the 5th) and large LN_vs and it is required for maintenance of circadian rhythm under constant conditions and normal locomotor activity under LD (Renn et al., 1999). IPNamide (IPNa) is expressed only in the DN_{1A} (Shafer et al., 2006), and its requirement is still unclear. Recently, other three neuropeptides have been found in a subsets of lateral neurons (Johard et al., 2009). The ion transport peptide (IPT) is expressed in one CRY-positive LN_d and in the 5th PDF-negative s-LN_v. The long neuropeptide F (NPF) is expressed only in 3 LN_ds of male but not female flies, whereas the small neuropeptide F (sNPF) is found in the four PDF-positive LN_vs and in two NPF-negative LN_ds (Johard et al., 2009), but the functional role of those neuropeptides remains uncertain.

1.3 TRP channels and thermosensation

The ability to perceive environmental stimuli is of fundamental importance for the survival of organisms. For poikilothermic organisms such us *Drosophila*, abrupt changes of temperature can have lethal consequences. Temperature is not only a noxious stimulus, though: perceiving environmental changes (e.g. daily temperature fluctuations) can have selective advantages, for instance it allows synchronization of the circadian clock.

Members of the transient receptor potential (TRP) family of ion channels play important roles in sensory physiology and are primary sensors for both physical (heat, light, mechanical stress) and chemical (pH, pheromones, capsaicin) external stimuli (reviewed by Voets and Nilius, 2003; Montell, 2005).

Sensory organs in *Drosophila* fall in two categories. Type I are multicellular organs, consisting of one to four neurons and specialized support cells. Type I

organs are further classified into two subgroups: external sensory (es) organs and chordotonal (ch) organs (see below). Type II are single, non-ciliated, multidendritic neurons (Kernan, 2007). TRP channels are found in both type I and type II sensory organs (see Table 1.1).

The TRP channels get their name from a *Drosophila* mutant (*trp*) that showed a "transient" instead of a "sustained" response to bright light in an electroretinogram (ERG) recording (Figure 1.5 and Montell, 2005). After that, many related channels have been isolated, and have been found in diverse organisms, from *C. elegans*, to humans (Hardie, 2007). In *Drosophila* there are 13 members belonging to the TRP family, which are divided into 7 classes based on sequence comparison (Figure 1.6 and Table 1.1). The common structure of TRP channels is based on six transmembrane domains with the pore loop permeable to cations situated between the fifth and the sixth transmembrane segments. Channels belonging to the TRPC, TRPV, TRPA and TRPN class have ankyrin repeats at the N-terminus, and their basic structure is conserved between organisms (Venkatachalam and Montell, 2007).

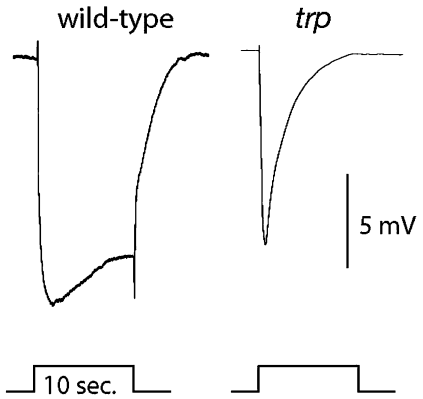

FIGURE 1.5: Electroretinogram (ERG) recordings from wild-type and *trp* mutant flies. *trp* mutants exhibit a "transient" response instead of a "sustained" response to a 10 sec stimulus (from Montell, 2005).

The TRPC class is primarily involved in the visual system via the phototransduction cascade mediated by the PLC, although it is not completely clear by which mechanisms the channels are opened after activation of PLC (Montell, 2005). Many members of the TRP family are activated through mechanical stim-

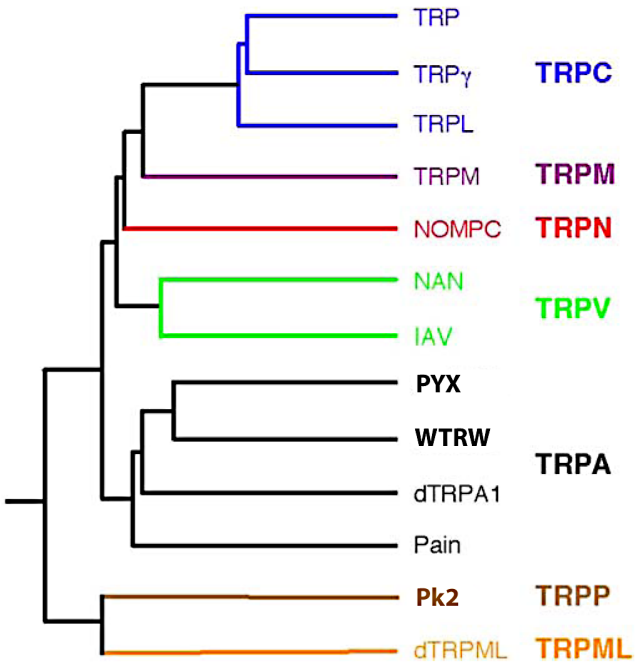

FIGURE 1.6: Dendrogram of the 13 TRP channel proteins in *Drosophila* and their classification into 7 classes based on sequence comparison. Figure modified from Montell (2005).

ulation (reviewed by Damann et al., 2008). Those include the products of the genes *no mechanoreceptor potential C* (*nompC*, TRPN), *painless* (*pain*, TRPA), *nanchung* (*nan*) and *inactive* (*iav*, TRPV). NOMPC is required for the mechanotransduction current in the sensory bristle and mechanosensory organs, whereas NAN and IAV are required in the fly's hearing system, mediated by the Johnston's Organ (JO) (see below). PAIN has been identified as a component required for nociception (Tracey et al., 2003). When wild-type larvae are touched with a heated probe (∼40°C) they vigorously roll sideways to escape the stimulus. *pain* mutants fail to exhibit this behaviour (Tracey et al., 2003). PYREXIA (PYX) and TRPA1 are needed to properly distribute in a thermal gradient, and are specifically required to avoid high temperatures (Lee et al., 2005; Rosenzweig et al., 2005). Recently, a role for TRPA1 in chemical nociception has been indicated: Kang et al. (2010) proposed that the avoiding response to reactive electrophiles (noxious tissue-damaging agents, such as allyl isothiocyanate, *N*-methylmaleimide

or cinnamaldehyde) is entirely TRPA1-dependent and *TrpA1* mutants lack this response. NAN and WATER WITCH (WTRW) have been implicated in hygrosensation and the channels can sense dry and most air, respectively (Liu et al., 2007). IAV, PAIN and PYX seem to be required also for the geotaxis behaviour mediated by the fly's antennae (Sun et al., 2009). TRP and TRPL, in addition to playing a role in the visual signal trunsduction cascade, seem to be implied in cold avoidance (Rosenzweig et al., 2008). TRPML has been implicated in lysosome-mediated autophagy by clearance of toxic macromolecules and of apoptotic cells. *trpml* mutants exhibit impaired autophagy which lead to neurodegenerative processes (Venkatachalam et al., 2008). Recently, the TRPM channels has been proposed to regulate the intake of extracellular magnesium (Mg^{2+}) from the hemolymph. High concentration of Mg^{2+} in fly diet increases lethality of *trpm* mutants and reduces the size of fat bodies and of the whole larva (Hofmann et al., 2010). TRPM is expressed in Malpighian tubules, the fly counterpart of the mammalian kidneys.

In flies, the organ required to sense the temperature is believed to be located in the antennae. Wild-type flies strongly prefer 24℃ if are let to distribute in a thermal gradient within the physiological range (Sayeed and Benzer, 1996). Genetic or surgical removal of the third antennal segment inhibits this thermopreference behaviour, and flies distribute randomly all over the temperature gradient (Sayeed and Benzer, 1996). Mutants for *pyrexia* and *TrpA1* show similar phenotypes, and mutant larvae as well as adult flies have defects in thermotaxis behaviour (Lee et al., 2005; Rosenzweig et al., 2005, 2008). Expression analysis of the PYX channels revealed that they are expressed in the third antennal segment (Lee et al., 2005), confirming the requirement of that organ in thermotaxis. However, thermotaxis behaviour (the ability to chose a preferred temperature in a gradient) and temperature sensation (the perception of temperature as hot or cold noxious stim-

Class	Gene	Described function	Expression	References
TRPM	*trpM*	Mg^{2+} homeostasis	Malpighian tubules	Hofmann et al. (2010)
TRPV	*nanchung* (*nan*)	hearing, hygrosensation, geotaxis	ch organs	Kim et al. (2003); Gong et al. (2004); Liu et al. (2007); Sun et al. (2009)
	inactive (*iav*)	hearing, geotaxis	ch organs	Gong et al. (2004); Sun et al. (2009)
TRPA	*TrpA1*	warm avoidance, chemical nociception	central brain neurons	Hamada et al. (2008); Rosenzweig et al. (2005, 2008); Kang et al. (2010)
	painless (*pain*)	nociception, geotaxis	multidendritic neurons	Tracey et al. (2003); Sun et al. (2009)
	pyrexia (*pyx*)	high temperature tolerance, geotaxis	ch organs, multidendritic neurons	Lee et al. (2005); Sun et al. (2009)
	water witch (*wtrw*)	hygrosensation	mechanosensory neurons?	Liu et al. (2007)
TRPC	*trp*	vision, cold avoidance	photoreceptor cells	Montell and Caterina (2007); Rosenzweig et al. (2008)
	trpl	vison, cold avoidance	photoreceptor cells	Montell and Caterina (2007); Rosenzweig et al. (2008)
	trp-γ	vision	photoreceptor cells	Xu et al. (2000)
TRPN	*nompC*	mechanoreception	ch and es organs	Walker et al. (2000)
TRPP	*Pkd2*	sperm motility, smooth muscle function	testis	Gao et al. (2003, 2004)
TRPML	*trpml*	autophagy		Venkatachalam et al. (2008)

TABLE 1.1: List of the 13 *trp* channel encoding *Drosophila* genes. TRP channels are classified in 7 classes. The functions and expression pattern of TRP channels (if known) are indicated.

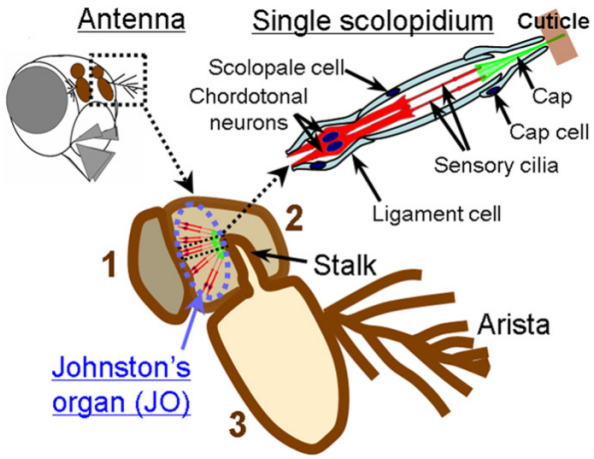

FIGURE 1.7: Schematic of the fly's head, antenna, and a single scolopidium of the Johnston's Organ. Numbers 1, 2 and 3 represent the three antennal segments. Modified from Sun et al. (2009)

ulus), although mediated by overlapping players, are not the same mechanisms. The *pain* mutant larvae do not respond to heat stimulation (Tracey et al., 2003) but mutant adult flies have normal thermotaxis behaviour (Rosenzweig et al., 2008). *pyrexia* and *TrpA1* mutants instead compromise both warm avoidance and thermotaxis (Lee et al., 2005; Rosenzweig et al., 2008).

The diverse spatial distribution of TRP channels throughout the fly body and organs emphasizes the requirement of the TRP channels in the many physiological roles and functions they play. At the same time, the different expression pattern of channels implicated in related processes (e.g. thermosensation) exemplifies the complex nature of the sensory physiology and the requirement of many players to fine tune and regulate temperature sensation.

1.4 Chordotonal organs

As mentioned above, type I sensory organs are classified into external sensory (es) organs and chordotonal (ch) organs (Kernan, 2007). Es organs are formed by external mechanosensory bristles, innervated by a single neuron. In contrast, ch organs lack any external part and are attached to the inside of the cuticle. The

basic unit of a ch organ is called scolopidium, and each ch organ may be formed by hundreds of scolopidia. Each scolopidium contains a liquid-filled capsule called scolopale, which encloses the sensory cilia of one to three ch neurons (Figure 1.7). Chordotonal organs are found at nearly all exoskeletal joints and between joints within limbs and body segments in insects (Field and Matheson, 1998). The known function of ch organs in limbs is proprioception, but a role in vibration detection and graviception is also possible, though unclear (Kernan, 2007). The most prominent ch organ in flies is the Johnston's Organ (JO), the fly's ear (Figure 1.7). It is located in the second antennal segment and it is constituted of almost 480 neurons located in more than 200 scolopidial units specialized in sensing near-field acoustic signals of courtship songs (Eberl and Boekhoff-Falk, 2007). Although the main function of the JO is hearing, it is also required to sense gravity and the JO neurons can be classified into subgroups according to their different role (Kamikouchi et al., 2009).

1.5 Aim of this work

Since the 1970s, with the pioneering research of Seymour Benzer and colleagues — a fascinating account of his work is well depicted by Jonathan Weiner in *Time, Love, Memory* (1999) — the investigation of the fly's behaviour moved down to the scale of single genes and their interactions.

After the truly groundbreaking work of Konopka and Benzer (1971), in which they isolated the first clock mutant *period*, many other components of the circadian clock of *D. melanogaster* have been isolated using genetic screens (reviewed by Stanewsky, 2003; Hall, 2005). Today, the central mechanisms generating circadian rhythmicity are quite well understood. Nevertheless, much remains to be

clarified. In particular, the mechanisms by which temperature cycles synchronize the circadian clock are poorly known. At present, only 2 genes have been reported to be required for temperature entrainment, *nocte* and *norpA*. *nocte* has been isolated in a EMS mutagenesis screen performed by a former Ph.D. student in our group, aimed at the isolation of novel components required for temperature synchronization of the circadian clock (Glaser and Stanewsky, 2005; Glaser, 2006). Similarly to *nocte*, *norpA* also has been reported to be required for temperature synchronization of the clock. However, the exact role of these two genes is not known yet and many questions are still to be answered. Which are the other components that mediate temperature synchronization? Where are the circadian temperature sensors and what is the molecular nature? How does the *nocte* gene play its role in this process? Which structures are necessary to mediate temperature entrainment?

This work tries to answer some of these open questions. In order to address these issues, the main aim of my Ph.D. was to identify new players and novel components that play a role in the circadian temperature entrainment. By isolating new factors and trying to understand their role in the process of circadian rhythmicity we aimed on providing new insight in the mechanisms of temperature entrainment. Following the long path of research conducted in *Drosophila*, we made use of forward and reverse genetic screens to isolate new components. The power of the RNAi technique has been combined with a bioluminescence assay able to monitor real-time expression of one of the central components of the circadian clock as read out for our screens.

Chapter 2

Materials and Methods

2.1 Materials

2.1.1 Fly stock

Drosophila melanogaster were kept and raised in 25℃ or 18℃ in plastic vials containing fly food and dry yeast. The ambient was set to 12:12 hr light-dark cycles and 65% relative humidity.

The fly food was prepared as follow:

Water	1 litre
Agar	10 g
Sucrose	15 g
Glucose	33g
Yeast	35g
Maize meal	15g
Wheat germ	10g
Treacle	30g
Soya flour	1 table spoon
Nipagin	10 ml
Propionic Acid	5 ml

Fly strain	Reference/source
Control	
Canton S	Konopka et al. (1989)
Df(1) y w	Lindsley and Zimm (1992)

period-luciferase	
y w ; ; BG-*luc*	Stanewsky et al. (1997b)
y w ; *plo* ; (LT21)	Stanewsky et al. (1997b)
y w ; ; XLG-*luc* (line 1.1)	Veleri et al. (2003)
Balancers	
y w ; *Bl/CyO* ;	Lindsley and Zimm (1992)
y w ; ; *Dr/TM3*	Lindsley and Zimm (1992)
GAL4 driver	
y w ; *tim-gal4/CyO* ; (line 27)	Kaneko and Hall (2000)
y w ; ; *tim-gal4* ; (line 16)	Kaneko and Hall (2000)
y w ; *tim-gal4* ; (line 62)	Kaneko and Hall (2000)
y w ; ; *tim-gal4* ; (line 67)	Kaneko and Hall (2000)
y w ; ; *cry-gal4BN*	Emery et al. (2000)
y w ; ; *pdf-gal4*	Park et al. (2000)
elav-gal4 ; ;	Luo et al. (1994)
y w ; *F-gal4*;	Kim et al. (2003)
y w ; ; *F-gal4* (line 33-5)	Kim et al. (2003)
y w ; *nocte-gal4* (line B3) ;	Sehadova et al. (2009)
y w ; *repo-gal4*	Sepp et al. (2001)
UAS lines	
y w ; *UAS-cry* ; (line 24.5)	Emery et al. (2000)
Mutant	
y per^{01} *w* ; ;	Konopka and Benzer (1971)
y w ; ; Pdf^{01}	Renn et al. (1999)
$norpA^{P41}$; ;	Pearn et al. (1996)
y w $nocte^{1}$; ;	Sehadova et al. (2009)

RNAi lines were obtained from the Vienna *Drosophila* RNAi Center (VDRC, Dietzl et al., 2007) and the National Institute of Genetics - Fly Stock Center (Japan, `http://www.shigen.nig.ac.jp/fly/nigfly/`), as indicated in the text (see Table 5.1).

Mutants for the *trp* channels encoding genes used in this study and relative references are listed in Table 5.1.

2.2 Methods

2.2.1 EMS mutagenesis

Ethyl Methane-sulfonate (EMS) induces point mutations by ethylation of the *O*-6 position of guanine (G) and the *O*-4 position of thymine, which allows mispairing during DNA duplication (Roberts, 1998). EMS mutagenesis has been performed as described by T.A. Grigliatti (Roberts, 1998). Three-day old male flies were collected in group of 30, placed in a plastic vials containing a piece of filter paper soaked with water and let them to starve for 5–6 hours. The flies were then transferred in a second plastic vial containing a filter paper soaked with 200 μl of EMS-sucrose solution (5% sucrose, 25 mM EMS [1] in water coloured by blue food dye). Flies were let to feed EMS-sucrose solution for 12 to 16 hours, then were transferred to a new vial with fresh food where they were allowed to recover for about 24 h prior to mating.

EMS fed males were then crossed to virgin females according the crossing scheme depicted in Figure 3.2.

2.2.2 Bioluminescence assay

per-luc constructs

In vivo real-time monitoring of gene expression has been performed by the use of fusion constructs in which the central clock component *period* was fused to the sequence of the *luciferase* gene from the firefly *Photinus pyralis*. Analysis of *per-luc* expression in living organisms is possible thanks to the short half-life of the luciferase (Brandes et al., 1996).

[1] The EMS concentration has been increased to 30 mM in the second half of the mutagenesis screen in order to increase the mutagenesis rate.

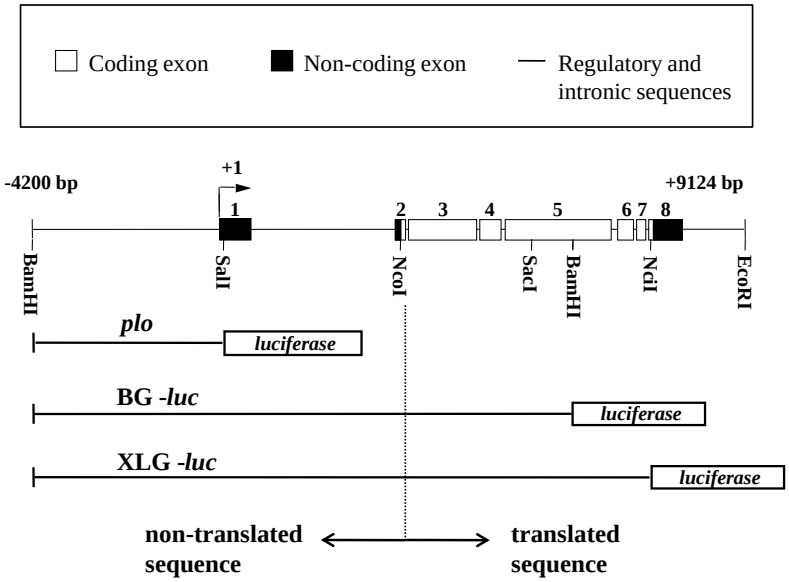

FIGURE 2.1: Structure of the *period* locus and of the *period-luciferase* constructs used in this study. Modified from Stanewsky et al. (1997b).

In this work we used three different constructs (Figure 2.1). *plo* (for promoter luciferase only) carries only the promoter region of *per* fused to the luciferase gene (Stanewsky et al., 1997b). BG-*luc* in addition to *plo* expresses two-third of the PER protein (Stanewsky et al., 1997b) and XLG-*luc* expresses the whole PER except the last 10 aa (Veleri et al., 2003). The presence of the 5'-UTR region of *per* allows the expression of the three constructs in the same spatial and temporal distribution of the endogenous *per* gene. Given that *per* is expressed in almost every tissue, *per-luc* expression was monitored in the whole adult fly and in isolated body parts (namely legs) kept in insect culture medium (Plautz et al., 1997).

Cultures preparation

For monitoring adult flies, alternated-skipped wells of a 96-well Microplate (Packard OptiPlate, Perkin-Elmer) were filled with 100 μl of luciferin-medium (1% Bacto-

agar, 5% sucrose and 15mM Biosynth luciferin). 2–6 day old *per-luc* flies were anaesthetized with diethyl ether, placed in the luciferin-filled well and covered with plastic caps (PCR tube lid with air holes) to keep the flies during the measurement in the correct position relative to the Z-axis. The plate was sealed with an adhesive sealing film (TopSeal, Perkin-Elmer), which was pierced to allow flies to breath.

For tissue cultures preparation, the 96-well Microplate was filled with 100 μl of sterile tissue culture medium (85.9% M3-insect culture medium, 12% heat-inactivated fetal bovine serum, 1% penicillin-streptomycin mixture, 1% Biosynth-luciferin, 0.5% Insulin; all reagents except luciferin from Sigma-Aldrich). Dissection of legs form diethyl ether-anaesthetized flies was carried out on 2% Bacto-agar dissection plates using sharp forceps. The 6 legs of individual flies were placed in a single well. The plate was then covered by an adhesive sealing film (TopSeal, Perkin-Elmer).

Data analysis

period-luciferase expression was monitored in the TopCount automated bioluminescence counter (Perkin-Elmer, TopCount NXT), in 65% relative humidity and in the light and temperature conditions as indicated in each experiments. Temperature cycles conditions were achieved by oscillating the temperature of the room where the TopCount counter was located. This resulted in a gradual ramping of temperature, which lasted for about 2 hours from cold to warm and about 4–6 hours from warm to cold.

Raw data were collected and analysed with the Brass analysis software (Andrew Millar lab) operating in Excel. Data were plotted as bioluminescence readings (counts per second, cps) as a function of time (Zeitgeber Time, h). Only

cultures that showed robust and uniform expression within the approximately 1 week of monitoring were included in data analyses.

Rhythmicity analysis has been performed as described (Plautz et al., 1997; Stanewsky et al., 1997b; Glaser and Stanewsky, 2005) via a Fast-Fourier transform-non-linear least square (FFT-NLLS) multicomponent cosine analysis to determine period, phase, and a metric called relative-amplitude error (rel-amp error).

The statistical significance of each derived rhythmic component is assessed by way of the relative amplitude error, defined as the ratio of, in the numerator, the amplitude error (one-half the difference between the upper minus the lower 95% amplitude confidence limits) to, in the denominator, the most probable derived amplitude magnitude. Theoretically, this metric will range from 0.0 to 1.0; 0.0 indicating a rhythmic component known to infinite precision (i.e. zero error), 1.0 (or greater) indicating a rhythm that is not statistically significant (i.e. error equal to (or exceeding) the most probable amplitude magnitude), and intermediate values indicative of varying degrees of rhythmic determination. In this study, all flies and cultures that had a period value within the range of 24 $\pm$ 1.5 hr and rel-amp error < 0.7 were considered rhythmic (as in Plautz et al., 1997; Stanewsky et al., 1997b).

2.2.3 Locomotor behaviour

Analysis of locomotor activity was performed using the *Drosophila* Activity Monitor System (Trikinetics Inc., Massachusetts). 2–6 day old flies were placed inside a small glass tube (5 mm diameter $\times$ 65 mm length), in which at one side fly food (2% Bacto-agar, 4% sucrose) was placed to sustain the fly over the course of the experiment. The food end of each tube was then sealed with paraffin wax to prevent desiccation and the tube was plugged with cotton. The DAM locomotor

monitor measures the simultaneous individual activity of 32 flies. As a fly walks back and forth from one end of its tube to the other, its passage is detected by an infra-red beam which bisects the tube, and counted. The data are sampled every 30 min.

The DAM monitors were located inside a light- and temperature-controlled incubator where the fly's activity was monitored for up to three weeks.

The raw data were then collected and analysed using a signal-processing toolbox (Levine et al., 2002a,c) implemented in Matlab (MathWorks), which generated the graphical representation of the activity and analysis of rhythmicity.

Actogram: Graphical double-plotted representation of activity versus time. A given row shows two consecutive days of activity; the second such day is re-plotted in the left half of the next row down (thus, consecutive days of locomotion can be viewed both horizontally and vertically); heights of bars within a given actogram row reflect varying amounts of locomotion per half-hour data-collection bin. Shaded areas represent dark phase (or cold phase during temperature cycles conditions) (Figure 2.2A).

Histogram: Daily average activity of several individual flies during entrainment conditions. Every bar indicates average activity during 30 min bin. Dots indicate SEM. Grey bars indicate average activity during lights-off (or cold) and white bars during lights-on (or warm) (Figure 2.2B).

Filtered histogram: Filtered version of the daily average activity to which a 4-h low-pass Butterworth filter has been applied. In addition, the peaks of activity are automated calculated, and the relative intensity values (normalized to the highest peak) are shown in percentage. Pink and blue areas represent lights-on and lights-off (or warm and cold), respectively (Figure 2.2C).

Autocorrelation: Correlogram has been used to determine periodicity and whether the rhythms were statistically significant. The asterisk above the third peak indicates the point used to assess the Rhythms Index (RI), a measure of rhythm strength. If RI is equal to or greater than the numerical height of the confidence line, then the rhythm is significant (by definition, the height of the peak is $\geq$ the height of the confidence interval used to determine statistical significance). The Rhythmicity Statistic (RS) is obtained from the ratio of the RI value to the 95% confidence line. Thus, RS provides a numerical accounting of significance for an individual specimen or an average signal. When RS is ≥ 1, the rhythm is statistically significant. In this study we considered the rhythmicity significant when the RS value was $\geq$ 1.5 (Figure 2.2D).

Maximum entropy spectral analysis (MESA): Spectral density analysis calculates the period of the rhythm. Asterisks are placed over the highest peak shown. Autocorrelation and MESA provide numerical estimates of periodicity using different statistical approaches, but in this study autocorrelation was used to determine rhythmicity (Figure 2.2E).

X-Y activity plot: Activity data are plotted as counts (in 30 min) vs. time. This representation was mainly used for plotting eclosion activity (Figure 2.2G).

X-Y filtered activity plot: Filtered version of the X-Y activity plot to which a 4-h low-pass Butterworth filter has been applied to "smooth" the activity profile (Figure 2.2H)

Circular phase: An average estimate of peak phase, obtained for each specimen, is plotted as a point on a unit circle. A mean vector, extending from the centre of the unit circle towards the diameter is calculated for each group

of points; the direction of the vector indicates mean peak phase for the group and the length of the vector represents the variability or dispersion between the points (phase estimates for each specimen). The internal black circumference represents 100% coherence between individuals of the same group. The closer the vector is to the black line, the more coherent the group is. The Watson-Williams-Stevens test returns an F-statistic that is used to evaluate whether the mean (M) phase vectors are significantly different from one another and whether the dispersion (D) within the groups is statistically significant (Figure 2.2F).

Statistical analysis: Daily-average activity of individual flies was imported in the GraphPad PRISM 4 software (GraphPad Software, San Diego California, United States). A Two-way analysis of variance (ANOVA) was performed in order to determine statistical interaction of a given genotype with the wild-type control. A Bonferroni Post-test was then performed to determine the time points that showed significant difference of activity compared to control ($P<0.05$).

Statistical analysis was performed with the aid of GraphPad PRISM 4 software (GraphPad Software, San Diego California, United States).

2.2.4 Uncoordination behaviour

Uncoordination behaviour has been performed as described in Sehadova et al. (2009), see Chapter 7.

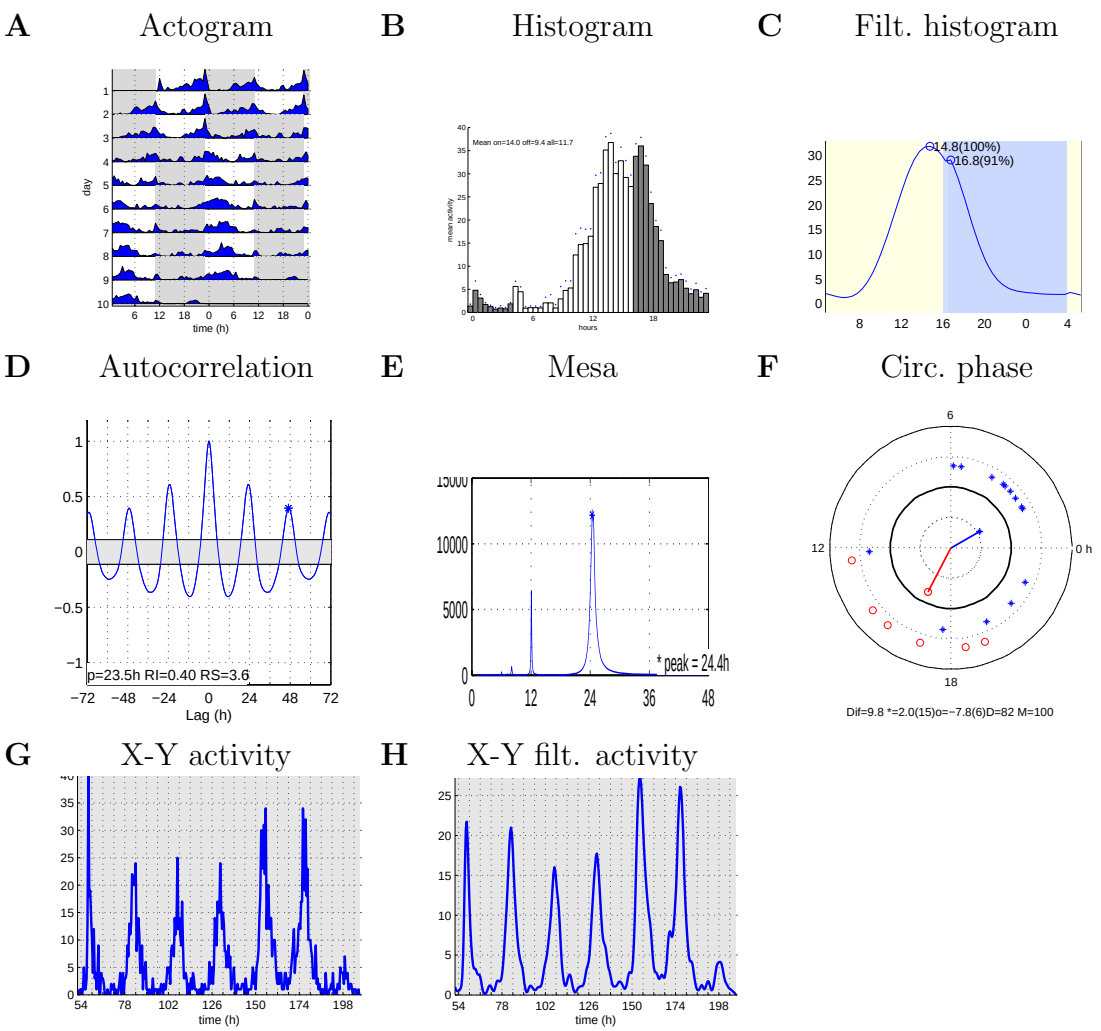

FIGURE 2.2: Graphical output of the signal-processing toolbox software used to analyse rhythmic behaviour and periodicity. See text and (Levine et al., 2002a,c) for details.

2.2.5 Eclosion monitoring

Four to eight bottles of the desired genotype were raised in 12:12 hr LD conditions at 25°C or 18°C or as stated in each specific experiment. Pupae of various ages were then harvested by fluctuation method in a plastic tub filled with 20–22°C water: A given bottle was submerged in the tub and vigorously shaken in order to release the pupae from the bottle walls. With the use of a brush, all the pupae were removed from the bottles. Pupae were collected by fluctuation with a metal

sieve and positioned on a dry paper towel to dry. Larvae were separated from the pupae, and the former discarded. Once the pupae were dry, they were glued (with standard glue stick) over the surface of the eclosion disc (Trikinetics Inc.) and let dry for 5–10 min. The disc was inverted and placed on top of a glass funnel, whose inside surface had been siliconized by a non-toxic sigmacote (Jersey-Cote, Lab Scientific) to prevent newly hatched flies to stick to the funnel. The funnel plus disc were inserted into an eclosion monitor (Trikinetics Inc.) and placed into a light- and temperature-controlled incubator. The eclosion monitor included a solenoid device that "taps down" on top of the disc 3 times every 15 minutes to help the eclosed flies to pass through the funnel stem, where an infrared detector was automated recording every eclosion event. Eclosion was usually monitored for 6–7 days.

The data were then acquired as eclosion events per 30 min intervals by the *Drosophila* Activity Monitor System (Trikinetics Inc.) similarly to that used to register locomotor activity. Data were analysed by the signal-processing toolbox (Levine et al., 2002a,c) implemented in Matlab (MathWorks). Data were plotted as number of eclosed flies as a function of time (per 0.5 hr bin, "raw activity") and also after smoothing them by application of a 4-h low-pass Butterworth filter ("filtered activity"). Rhythmicity analysis has been performed as for locomotor activity (see above and Levine et al., 2002a,c).

2.2.6 Western Blot

For analysis of PER protein oscillation, 20–25 flies per time points were collected in liquid nitrogen and stored at -80°C. Heads were removed by vortex and counted on dry ice. The proteins were extracted in 40 μl of extraction buffer (20 mM HEPES pH 7.5, 100 mM KCl, 5% glycerol, 10 mM EDTA, 0.1% Triton X-100, 20mM β-

glycerophosphate, 100 μM Na_3VO_4 pH 10–12, 0.5 mM PMSF, 20 μg/ml aprotinin, 1 mM DTT, 5 μg/ml Leupeptin, 5 μg/ml pepstatin) to which protease inhibitor was added. After discarding the cell residues, the SDS loading buffer (0.3M TRIS, 10% SDS, 50% glycerol, 25% β-mercapto-ethanol, 0.01% Bromophenol blue) was added, the sample was boiled for 5 min and load on the 4.5% SDS stacking gel and 6% resolving gel. The protein separation was carried out at 70 V, 400 mA and 5W for 16 hours. The separated proteins were transferred into a nitrocellulose membrane (Protran, Whatman) by a "semi-dry blotter" for 1 h at 25 V, 400 mA and 150 W. Ponceau staining was used to control the proteins transfer. The membrane was then blocked for 2 h in 2% BSA in TBST (8.18 g NaCl, 5 ml 2M Tris-HCl pH 7.5, 0.05% Tween-20 for 1 L water) at room temperature. The membrane was incubated with the primary antibody (Rabbit anti-PER, 1:10000, Stanewsky et al., 1997a) at 4°C overnight and with the HRP secondary antibodies (Goat anti-Rabbit, 1:166000) for 2 h at room temperature. The blot was incubated for 5 min with the Pierce SuperSignal HRP kit and developed on X-ray film.

Quantification of the bands was performed with the ImageJ software, by subtracting the background signal and normalizing to the maximum value.

2.2.7 Mechanical stimulation

The effect of mechanical stimulation of the fly's daily pattern of locomotor behaviour was investigate by mounting a DAMS monitor (Trikinetics Inc.) on top of a loudspeaker (ProSound, Power Amp 1600). A ∼5 cm thick polystyrene separator was placed between loudspeaker and DAMS monitor to insulate the monitor from possible temperature oscillations generated by the loudspeaker. The stimulus sequence, which was played continuously for 12 hours, consisted of a 40 Hz tone (duration: 0.5 sec; root mean square (RMS) amplitude: 1 V; acceleration:

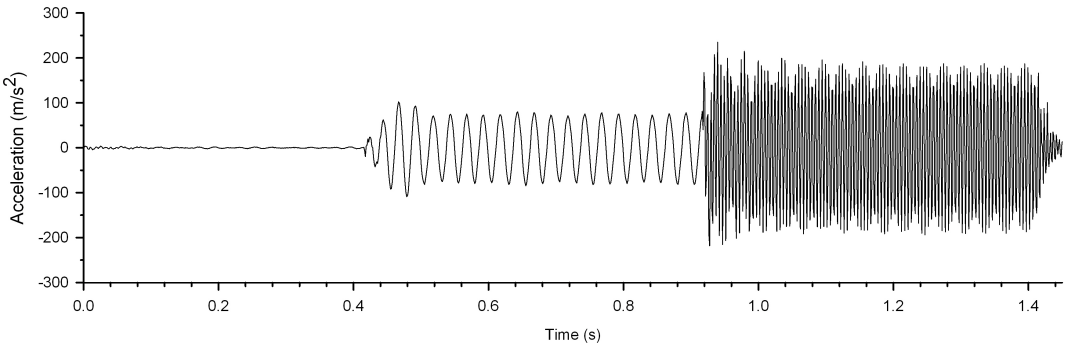

FIGURE 2.3: Recording of the vibration stimulus sequence applied to flies. 0.5 sec of 40 Hz tone (RMS amplitude of 1 V and acceleration of 63 m/s^2) was followed by 0.5 sec of 200 Hz (RMS amplitude 2.5 V and acceleration of 158 m/s^2) and 0.5 sec of silence. The sequence was repeated for 12 hour followed by 12 hours of silence (background noise).

63 m/s^2) followed by a 200 Hz tone (0.5 sec, 2.5 V and 158 m/s^2) and 0.5 sec of silence (Figure 2.3). The 12-hour stimulus was followed by 12 hours without any stimulation ("silence"). The resulting vibration of the fly vials were measured with an accelerometer (Brüel & Kjær, Charge Amplifier type 2635) that was coupled to the behaviour monitor. "Silence" is defined as background noise in the room, with an intensity of the order of a ten thousandth lower compared to the stimulus applied.

The vibration stimulus was sampled for 3 sec every 30 min together with the temperature. The temperature was measured with a thermosensor located inside one of the behaviour tubes where flies were placed. Data acquired using the Spike2 software coupled with the Power 1401 mkII (CED, Science Products).

Experiments were conducted in darkness at 21℃.

For the antennae ablated experiments, flies were anaesthetized under CO_2 and the antennae were manually ablated using sharp forceps. All the three antennal segments were removed. Wild-type flies with and without antennae were monitored at the same time.

Chapter 3

Results

Mutagenesis Screen

3.1 EMS mutagenesis screen

To isolate novel genes which play a role in temperature synchronization of the circadian clock of *Drosophila melanogaster*, we performed a screen of chemically-induced mutants. Ethyl Methane-sulfonate (EMS) induces point mutations by ethylation of the *O*-6 position of guanine (G) and the *O*-4 position of thymine, which allows mispairing during DNA duplication (Roberts, 1998). The concentration of 25 to 30 mM EMS used for the mutagenesis (see Materials and Methods) is expected to generate 50–80% lethal recessive mutations on each autosome (Roberts, 1998). An average of 47.3% of lines generated following our EMS treatment were recessive lethal (see Table 3.1), suggesting an effective ratio of inducing mutations in essential genes along the two autosomes. Although, we noticed a large variability between different treatments (from 15 to 85% lethality). If 47.3% of lines generated were recessive lethal, we can estimate that a similar number of

	Total (n)	Homozygous viable (n)	Homozygous lethal (%)
Lines generated	3044	1637	47.3
Chromosome *2*	1738	962	45.7
Chromosome *3*	1306	675	51.1

TABLE 3.1: Summary of the EMS mutagenesis screen. The total number of mutant lines generated is indicated. All the homozygous viable lines have been tested in temperature entraining conditions.

non-essential genes (and hypomorphic — non lethal — alleles of essential genes) have been induced.

We generated 3044 EMS mutant lines, 1738 for chromosome *2* and 1306 for chromosome *3*. A total of 1637 lines were homozygous viable and have been tested in an automated bioluminescence assay monitoring real-time expression of *period-luciferase* (*per-luc*) in living flies, as previously described (Plautz et al., 1997; Stanewsky et al., 1997b; Glaser and Stanewsky, 2005). The flies were raised in a 12:12 hr light-dark (LD) cycles and then analysed in constant light (LL) and 12:12 hr 25℃:16℃ temperature cycles (TC).

Initially, for the first quarter of the screen, the temperature cycles were applied in-phase compared to the previous LD entrainment (warm-phase corresponded to the light-phase and the cold-phase corresponded to the dark-phase). In the subsequent part of the screen the phase of the TC was opposite compared to the LD entrainment (cold-phase corresponded to the previous light-phase and the warm-phase corresponded to the dark-phase). The temperature entrainment regime was changed, because given the low rate of mutants isolated during the first part of the screen, we decided for a more stringent paradigm to discriminate between flies able to re-synchronize to the new temperature entrainment and those who were not (potential temperature entrainment mutants), rather than keeping the previous LD-cycle phase.

We utilized three different *per-luc* transgenic types (Figure 3.1), each of them

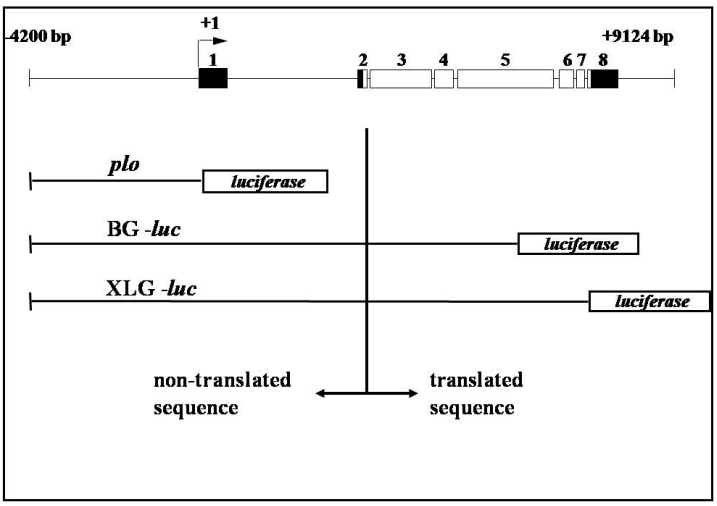

FIGURE 3.1: Structure of the *period* locus and *period-luciferase* transgenes used in this study. The structure of the 13.2 kb genomic DNA fragment containing the *per* gene is shown in the upper part (from Stanewsky et al., 1997a). White bars: coding exon. Black bars: non-coding exon. Line: regulatory and intronic sequences. Note that the *plo* construct contains only the promoter region of *per* fused with the *luciferase* cDNA sequence (modified from Stanewsky et al., 1997a).

containing genomic DNA of the *period* gene, fused with the coding sequence of the firefly *luciferase* gene (Brandes et al., 1996). One line, called *plo* (promoter luciferase only) carries only the promoter region of *period* directly fused with the *luciferase* cDNA. The *plo* construct is inserted on chromosome *2* and it was used in the EMS mutagenesis screen for testing putative mutants on chromosome *3*. Another line (called BG-*luc*) carries the promoter of *per*, the N-terminal two-third of the coding sequence of the PER protein and the *luc* gene (Stanewsky et al., 1997b). This line carries the BG-*luc* transgene on the chromosome *3* and therefore was used as background for isolating putative mutations on chromosome *2*. The third line used, XLG-*luc*, contains the same *per* and *luc* sequence as *plo*, but in addition carries the DNA encoding the entire PER protein, with the exception of the last 10 amino acids (Veleri et al., 2003). For practical reasons this line was used as read-out during the RNAi screen (see chapter 4).

Given the different nature of the two *per-luc* lines utilized in the mutagenesis

A. Generation of putative mutations on chromosome *2*

P:	☿☿	$\frac{y\ w}{y\ w}; \frac{Bl}{CyO}; \frac{+}{+}$	×	♂	$\frac{y\ w}{Y}; \frac{+}{+}; \frac{BG-luc}{BG-luc}$	(EMS-fed males)
F_1:	☿	$\frac{y\ w}{y\ w}; \frac{Bl}{CyO}; \frac{+}{+}$	×	♂	$\frac{y\ w}{Y}; \frac{+^*}{Bl/CyO}; \frac{BG-luc^*}{+}$	(single male cross)
F_2:	☿☿	$\frac{y\ w}{y\ w}; \frac{+^*}{CyO}; \frac{BG-luc^*}{+}$	×	♂	$\frac{y\ w}{Y}; \frac{+^*}{CyO}; \frac{BG-luc^*}{+}$	
F_3:	♂	$\frac{y\ w}{Y}; \frac{+^*}{+^*}; \frac{BG-luc^*}{+/BG-luc^*}$		→	bioluminescence assay	

B. Generation of putative mutations on chromosome *3*

P:	☿☿	$\frac{y\ w}{y\ w}; \frac{+}{+}; \frac{Dr}{TM3}$	×	♂	$\frac{y\ w}{Y}; \frac{plo}{plo}; \frac{+}{+}$	(EMS-fed males)
F_1:	☿	$\frac{y\ w}{y\ w}; \frac{+}{+}; \frac{Dr}{TM3}$	×	♂	$\frac{y\ w}{Y}; \frac{plo^*}{+}; \frac{+^*}{Dr/TM3}$	(single male cross)
F_2:	☿☿	$\frac{y\ w}{y\ w}; \frac{plo^*}{+}; \frac{+^*}{TM3}$	×	♂	$\frac{y\ w}{Y}; \frac{plo^*}{+}; \frac{+^*}{TM3}$	
F_3:	♂	$\frac{y\ w}{Y}; \frac{plo^*}{+/plo^*}; \frac{+^*}{+^*}$		→	bioluminescence assay	

FIGURE 3.2: Crossing scheme applied to screen for novel mutation affecting temperature entraining of the circadian clock on (A) chromosome *2* and (B) chromosome *3*. Stars indicate chromosomes with potential EMS-induced mutations. Bl/CyO and $Dr/TM3$ are balancer chromosome for autosome *2* and *3*, respectively (Lindsley and Zimm, 1992). ☿: virgin female flies, ♂: male flies .

screen, we wanted to trace both the effect of mutations on the transcriptional and post-translational level of *period*, by exposing *plo* and BG-*luc* to mutagenesis, respectively. *plo*, in fact, is lacking the translated region of PER, thus the bioluminescence readings correlates with the expression of *per* mRNA. The BG-*luc* line, instead, expresses also PER protein, therefore it gives indications of the post-transcriptional regulation of PER-LUC protein.

Figure 3.2 shows the crossing scheme we applied to generate autosomal variants specific for chromosome *2* and chromosome *3*. As visible from the crossing scheme, the line analysed in our bioluminescence assay carried only one specific autosome with homozygous EMS-induced mutations. However, also the other au-

tosome could have carried EMS-induced mutations. Let's consider for instance the crossing scheme regarding isolation of mutants for chromosome *2* (Figure 3.2A). The lines we tested in our bioluminescence assay were $\frac{y\ w}{Y}; \frac{+^*}{+^*}; \frac{BG-luc^*}{+/BG-luc^*}$, which potentially load mutations on chromosome *3*. Anyway, almost all of the lines we tested carried only one EMS-treated chromosome *3* (with orange eyes — indicating the presence of the BG-*luc* transgene) and the homologue was non-treated ($\frac{BG-luc^*}{+}$). This because for practical reason we selected in the F_2 only one parent with orange eyes. This reduced the possibility to isolate mutants on the third chromosome. In addition, eventual mutations on chromosome *3* were not balanced and would have been lost by recombination. Therefore the eventual mutant phenotype would not be seen in the following generations and the line not taken into further investigations. Analogue approach applied for chromosome *2* (Figure 3.2B).

3.2 Isolation of mutant lines

It has been shown that temperature cycles can also synchronize *per-luc* expression in isolated organs and body parts, such as legs, wings, abdomen and head (Glaser and Stanewsky, 2005). Interestingly, isolated body parts, particularly legs, exhibit a less erratic and "smoother" bioluminescence expression of *per-luc* compared to that of the intact fly, in which luminescence rhythms are relatively noisy (e.g. Glaser and Stanewsky, 2005). The small variability between isolated legs of different individuals of the same genotype, does not require the need to test a large number of flies of the same genotype to distinguish a potential mutant from a wild-type. This can be important in a big screen for mutants, since it reduces the costs of the screen, in terms of time and money.

Recordings of isolated legs during LL and 25:16°C TC

A)

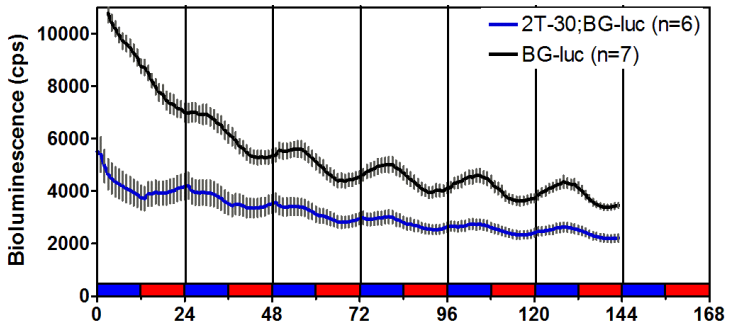

B)

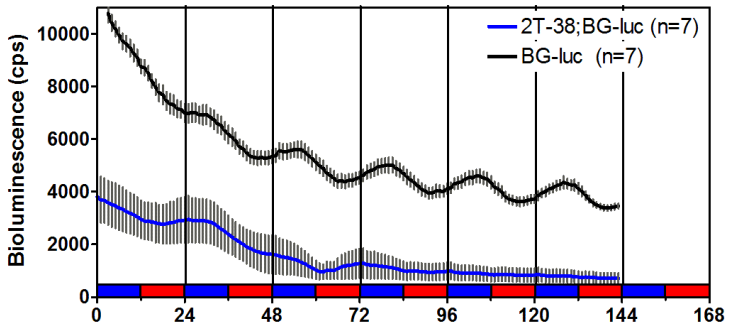

C)

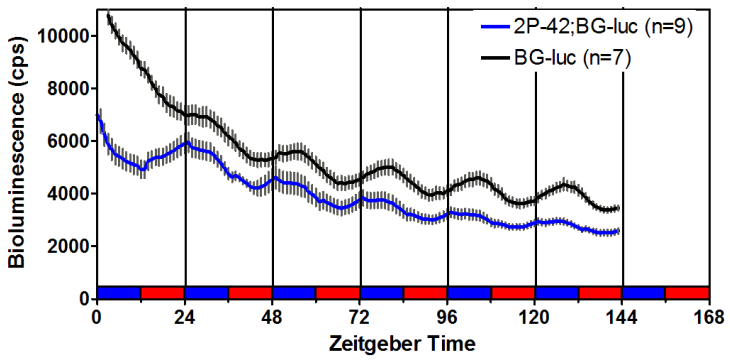

FIGURE 3.3: Average bioluminescence recordings from legs of EMS mutant and control flies (BG-*luc*) during LL and 12:12 hr 25:16°C TC. The phase of the previous LD entrainment was opposite compared to the TC applied here and this explains why control flies take up to 2 days to synchronize to the TC. Red/blue bars at bottom indicate warm-phase (25°C) and cold-phase (16°C), respectively. Error bars indicate SEM. Number of individuals is indicated.

For those reasons, we monitored the expression of *per-luc* in isolated legs, maintained in luciferin-enriched insect tissue-culture media and subjected to constant light and 12:12 hr 25℃:16℃ temperature cycle conditions (see Materials and Methods for details). We isolated 3 lines labelled *2T-30*, *2T-38* and *2P-42* that exhibited mutant phenotype, i.e. reduced rhythmicity during LL and TC conditions (Figure 3.3). In all the three lines, *per-luc* expression in isolated legs is drastically reduced compared to untreated control (BG-*luc*) and other EMS-treated lines (see Figure 3.3 and Table 3.2). There is drastic reduction of *per-luc* level of expression, together with a lower amplitude of oscillation. For line *2P-42*, the remaining *per-luc* rhythm exhibits an earlier phase (see below). The two lines *2T* were isolated in a batch originating from a single EMS treatment, which produced 82% of homozygous lethal mutant flies, suggesting a very effective mutagenesis. The origin of the two lines from the same treatment includes also the possibility that the two lines are clones, i.e. they carry the same mutation (see below). The treatment which generated the line *2P-42*, instead, produced 46% homozygous lethal mutant lines.

For unknown reasons, the BG-*luc* control did not exhibit a consistent rhythmicity between the different independent experiments. Therefore, we compared the EMS-treated lines among themselves, since almost all showed a clear and robust rhythmicity in LL and TC conditions, such as the line *2X-8* exemplified in Table 3.2, which is an EMS-treated line that shows a wild-type phenotype. We considered a line to be mutant in those conditions if it exhibited a mutant phenotype in at least three independent experiments. The three lines isolated have been the only ones to fulfil this criteria and therefore selected for further characterization.

The mutagenesis screen has been performed analysing *per-luc* expression in dissected legs. We then monitored bioluminescence expression in the whole fly

Genotype	Rhythmic (%)	n	τ (hr) ± SEM	Rel-Amp ± SEM	Phase ± SEM
LL and temperature cycle entrainment					
Isolated legs					
2T-30	26.7	15	24.7 ± 0.27	0.20 ± 1.13	20.2 ± 1.13
2T-38	37.9	29	25.1 ± 0.31	0.30 ± 1.13	20.6 ± 0.43
2P-42	47.2	36	25.1 ± 0.17	0.28 ± 0.68	21.8 ± 0.40
BG-*luc*	58.3	12	25.3 ± 0.37	0.19 ± 0.01	17.5 ± 1.02
2X-8	100	4	24.9 ± 0.10	0.23 ± 0.05	23.2 ± 0.34
Whole fly					
2T-30	26.9	26	24.5 ± 0.67	0.61 ± 0.02	18.6 ± 1.21
2T-38	25.0	8	23.9 ± n.c.	0.53 ± n.c.	20.7 ± n.c.
2P-42	22.2	9	23.1 ± n.c.	0.54 ± n.c.	20.0 ± n.c.
BG-*luc*	66.7	21	23.7 ± 0.73	0.54 ± 0.03	18.2 ± 0.97
LD entrainment and constant temperature (25℃)					
Isolated legs					
2T-30	100	12	23.9 ± 0.07	0.25 ± 0.04	23.4 ± 0.17
2T-38	100	8	24.0 ± 0.21	0.30 ± 0.04	23.1 ± 0.31
2P-42	93.3	15	23.9 ± 0.06	0.19 ± 0.02	23.2 ± 0.10
BG-*luc*	100	15	23.8 ± 0.05	0.24 ± 0.03	23.1 ± 0.13
DD and temperature cycle entrainment					
Isolated legs					
2T-30	100	23	24.3 ± 0.06	0.12 ± 0.01	19.6 ± 0.23
2T-38	100	22	24.2 ± 0.04	0.13 ± 0.01	18.7 ± 0.27
2P-42	95.6	23	24.2 ± 0.06	0.14 ± 0.01	19.9 ± 0.29
BG-*luc*	100	24	24.3 ± 0.07	0.16 ± 0.01	19.7 ± 0.30
Whole fly					
2T-30	54.5	22	24.1 ± 0.39	0.55 ± 0.03	19.2 ± 0.89
2T-38	78.5	14	24.5 ± 0.17	0.46 ± 0.03	20.0 ± 0.91
2P-42	62.5	24	24.4 ± 0.21	0.59 ± 0.04	17.8 ± 0.98
BG-*luc*	63.2	19	25.0 ± 0.41	0.51 ± 0.04	19.5 ± 1.12

TABLE 3.2: FFT-NLLS analysis of bioluminescence oscillation of EMS mutants and control (BG-*luc*). Whole adult flies or isolated legs were entrained in LL and 12:12 hr 25:16℃ temperature cycles, in 12:12 hr LD and constant temperature (25℃) or in DD and 12:12 hr 25:16℃ TC, as indicated. EMS mutant flies are weakly rhythmic compared to non-treated control (BG-*luc*) and a treated non-mutant line (*2X-8*). See text for more details. FFT-NLLS analysis was applied to calculates "period" (τ), "relative amplitude error" (Rel-Amp) and "phase" only of rhythmic flies. Flies were considered rhythmic if rel-amp error was$\leqslant$0.7 and the period valued was in the range of 24±1.5 hr. SEM indicates Standard Error of the Mean.

(Figure 3.4 and Table 3.2). Line *2T-30* and *2T-38* show strongly reduced rhythmicity compared to control (Figure 3.4A–B). Analysis of plots of individual-fly recordings of *2T-30* and *2T-38* (Figure 3.5) reveals that *per-luc* expression of the different individuals is weakly (if at all) rhythmic and out of phase each other, explaining the overall flat bioluminescence reading when the average is plotted. Line *2P-42* (Figure 3.4C), instead, seems to cycle with an opposite phase compared to control, although with a minor amplitude. Noticeably, we observed a steep increase of LUC activity just after temperature rising and a fast decrease after temperature dropping, suggesting more a temperature response rather than synchronization to TC with an opposite phase. This is also suggested by inspection of recording from individual flies (Figure 3.5) which also shows that not all the flies exhibit the same phase. This phenotype is reminiscent of *per-luc* expression in isolated brains, which do not entrain to temperature: if a brain of a wild-type *per-luc* fly is dissected from the body, it cannot synchronize *per* expression to TC, but rather reacts to temperature step-up with an steep increase of *per-luc* expression (Sehadova et al., 2009).

Isolated legs of the three EMS mutant lines synchronize normally to LD cycles, in terms of period, phase and expression level compared to control, as shown in Figure 3.6, with a peak of *per* expression towards the end of the night (ZT 23, see Table 3.2), indicating a specific defect on temperature entrainment.

We then investigated whether the mutant phenotype was manifested also during DD and TC. Figures 3.3 and 3.8 show bioluminescence expression of BG-*luc* and the three EMS mutant lines, in DD and temperature cycles. Interestingly, isolated legs of mutants could entrain to TC with a comparable period, phase and amplitude to the control (Figure 3.3 and Table 3.2), but with a subtle reduced *per* expression level (and no differences between the different mutated lines). Note

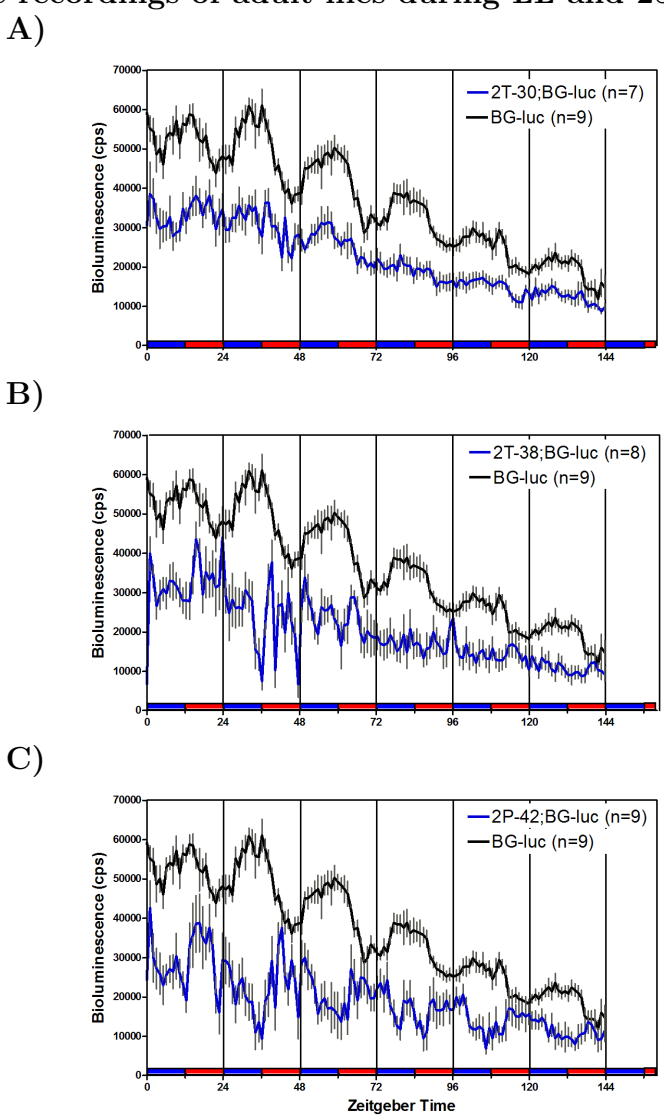

FIGURE 3.4: Average bioluminescence recordings of whole adult flies of control (BG-*luc*) and EMS mutants during LL and 12:12 hr 25:16°C TC. Conditions and coloured bars are as described in Figure 3.3. Grey error bars indicate SEM.

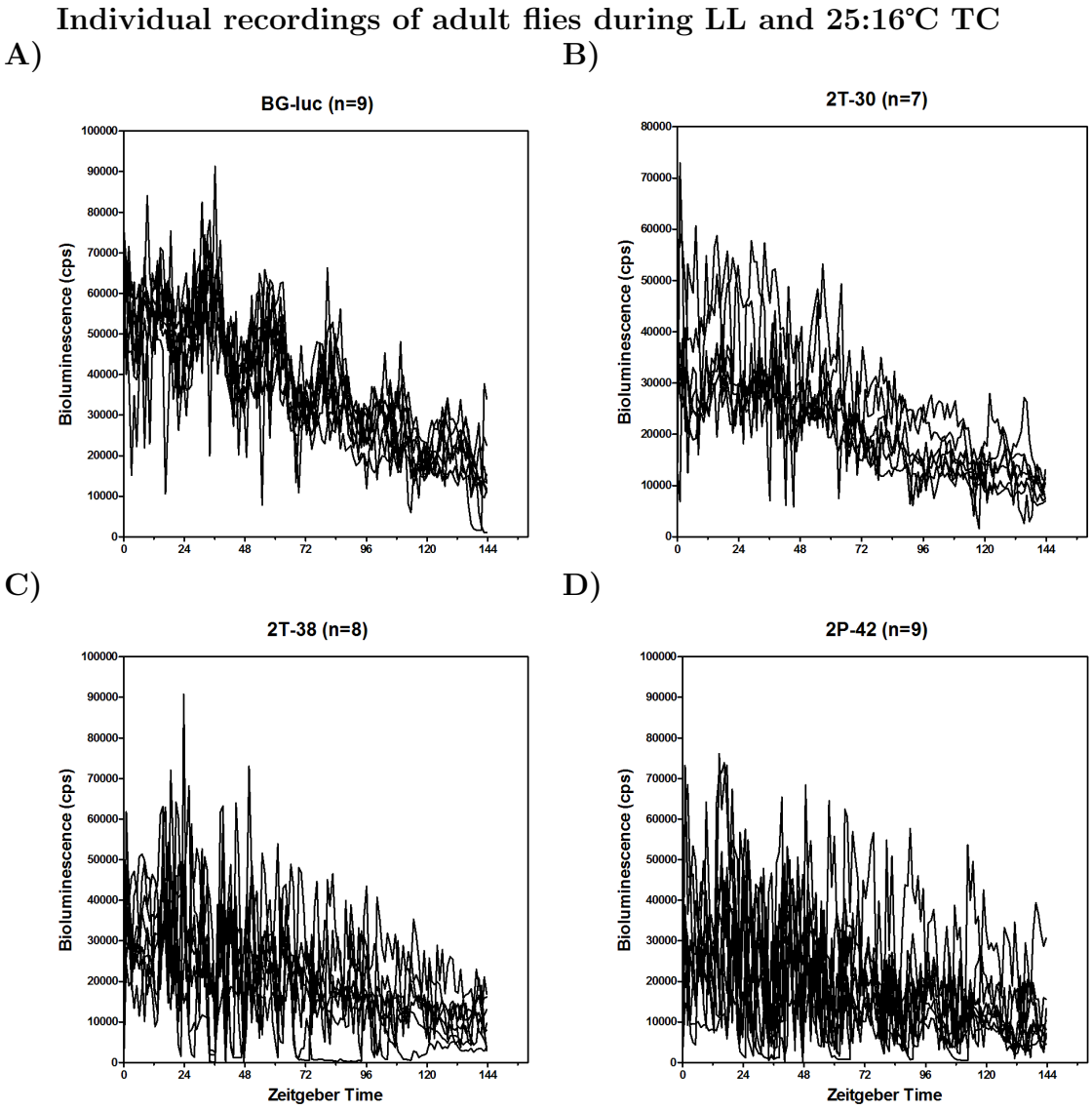

FIGURE 3.5: Individual bioluminescence recordings of whole adult flies of control (BG-*luc*) and EMS mutants during LL and 12:12 hr 25:16°C TC. Average recordings and conditions are shown in Figure 3.4.

Bioluminescence recordings of isolated legs during LD and 25°C

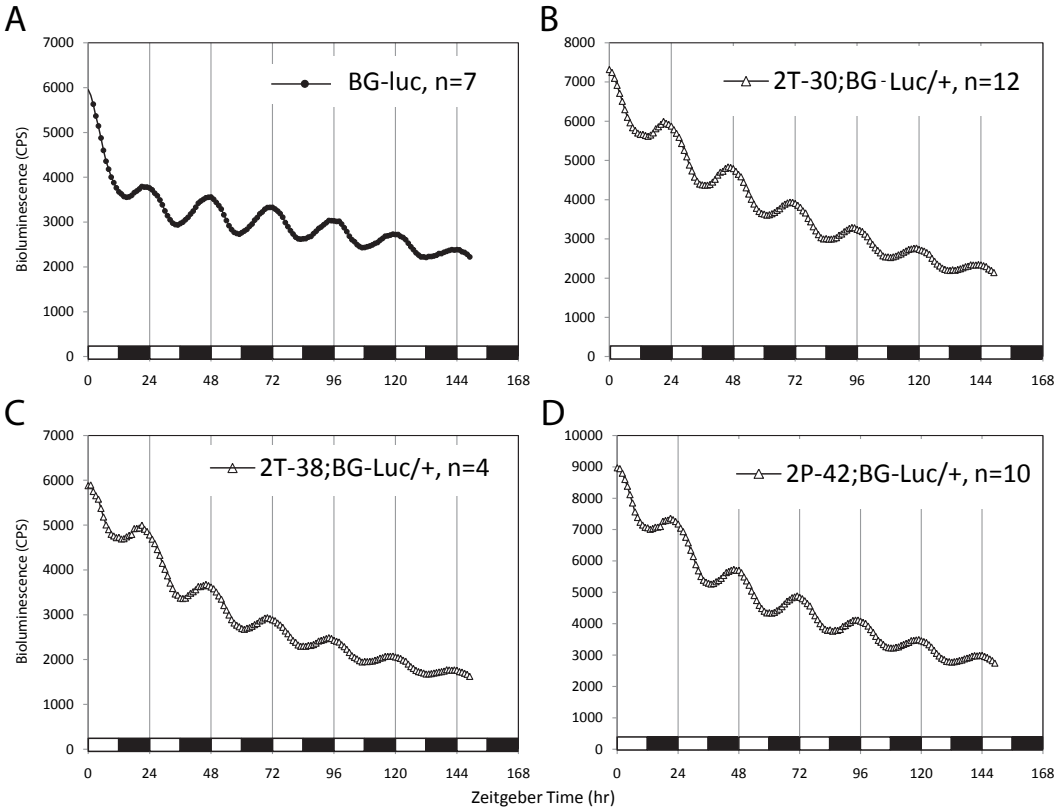

FIGURE 3.6: Bioluminescence expression of EMS mutant lines and controls in LD conditions. A) Control flies (BG-*luc*) entrain normally to LD cycles (at constant 25°C) with a peak of *per* expression towards the end of the night (ZT23). B–D) EMS mutant lines show no significant difference of *per-luc* expression during light-dark cycles compared to controls. White bars at the bottom of the plot indicate light-on. Black bars indicate light-off.

that during temperature entrainment (LL or DD) the peak of *per-luc* expression occurs 2–3 hours earlier then during LD entrainment. This observation differs slightly compared to previous reports, for instance Glaser et al (2005). The divergence can be related to different technical experimental conditions in which the flies were monitored (10:14 hr 25:18°C vs 12:12 hr 25:16°C). However, my data correlates also with an advance evening peak of locomotor activity during TC entrainment compared to LD (see below and Discussion). An explanation could be a difference in light and temperature cycles as they occur in natural environmental

conditions: light arises earlier in the morning than temperature, and the latter increases more gradually during the day and peaks later than light, generating a gap between temperature and light profile (Boothroyd et al., 2007; Currie et al., 2009; Yoshii et al., 2009a and Discussion).

PER-LUC luminescence in the whole fly revealed distinct phenotypes among the 3 mutant lines during DD and TC. Average *per* expression in line *2T-30* is flat (Figure 3.8). FFT-NLLS analysis shows that only half of the flies are weakly rhythmic (Table 3.2), and inspection of individual recordings (Figure 3.9) shows that the remaining rhythmic ones are out of phase with each other during temperature entrainment. This explains the overall flat *per-luc* reading when the average of all flies is plotted.

Line *2T-38* synchronizes to temperature cycles in DD, even if the level of *per-luc* expression is reduced (similarly as for isolated legs of the same genotype). Although not all the flies are strongly in phase with each other as visible form recordings of individual flies (Figure 3.9) and large standard error in the FFT-NLLS analysis, they appear to be in phase with the BG-*luc* control (Figure 3.8 and 3.9).

Adult *2P-42* flies exhibit the same phenotype in LL and DD and temperature cycles: flies seem synchronized with an opposite phase compared to control (Figure 3.8). Also, inspection of individual recordings (Figure 3.9) shows that most of the flies exhibit the same phase. However, the steep increase of LUC activity just after the temperature goes up, and the steep decrease after temperature goes down suggests more temperature reaction (masking effect) rather than entrainment.

The fact that isolated body parts during DD and temperature cycles entrain, while the whole fly does not, is very interesting. In fact, this is similar to the phenotype of other already described "temperature mutants", e.g. $nocte^{1}$ or $norpA^{P41}$,

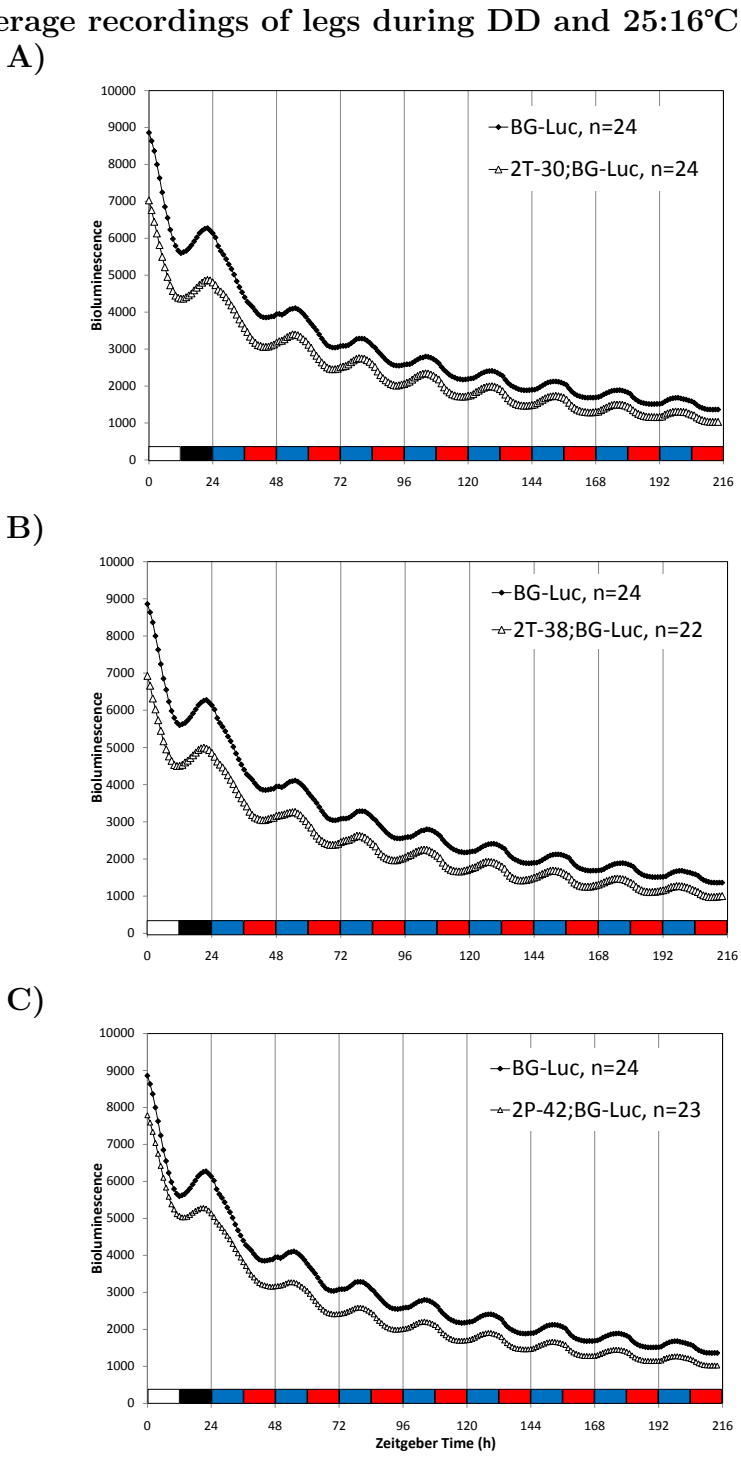

FIGURE 3.7: Average bioluminescence recordings of isolated legs of control (BG-*luc*) and EMS mutants during DD and 12:12 hr 25:16°C TC. Conditions and coloured bars are as described in Figure 3.3.

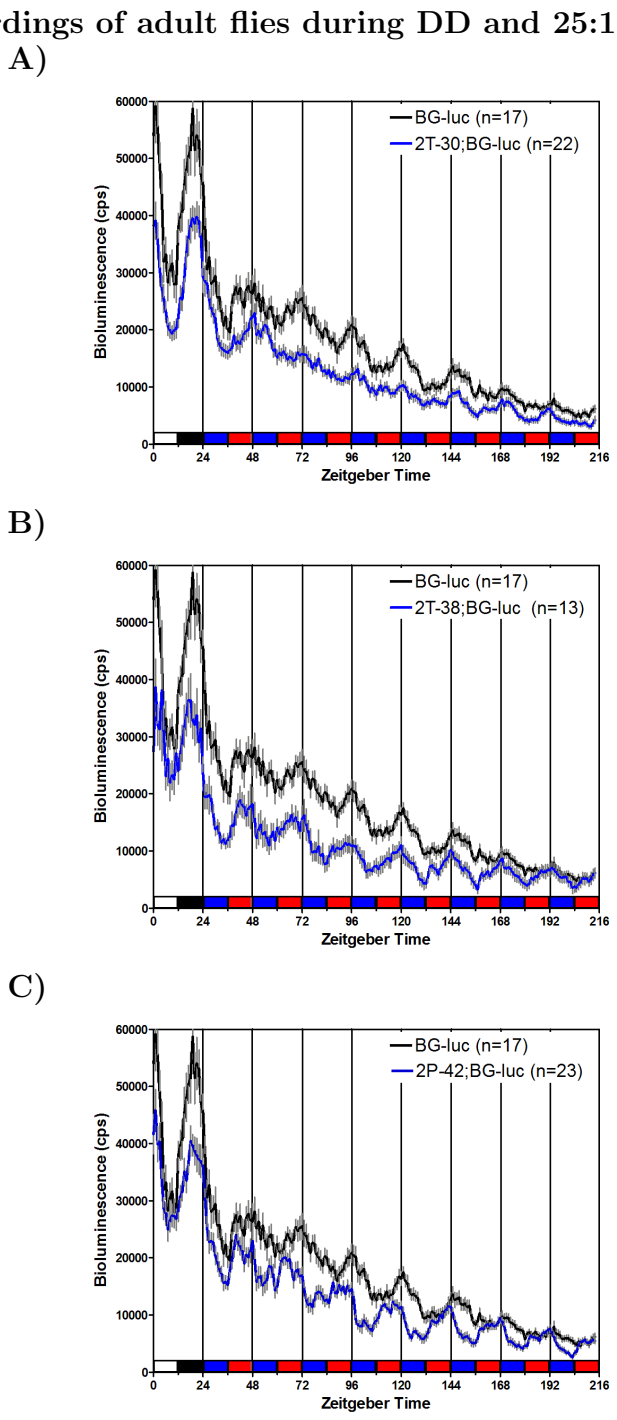

FIGURE 3.8: Average bioluminescence recordings of whole adult flies of control (BG-*luc*) and EMS mutants during DD and 12:12 hr 25:16°C TC. Conditions and coloured bars are as described in Figure 3.3.

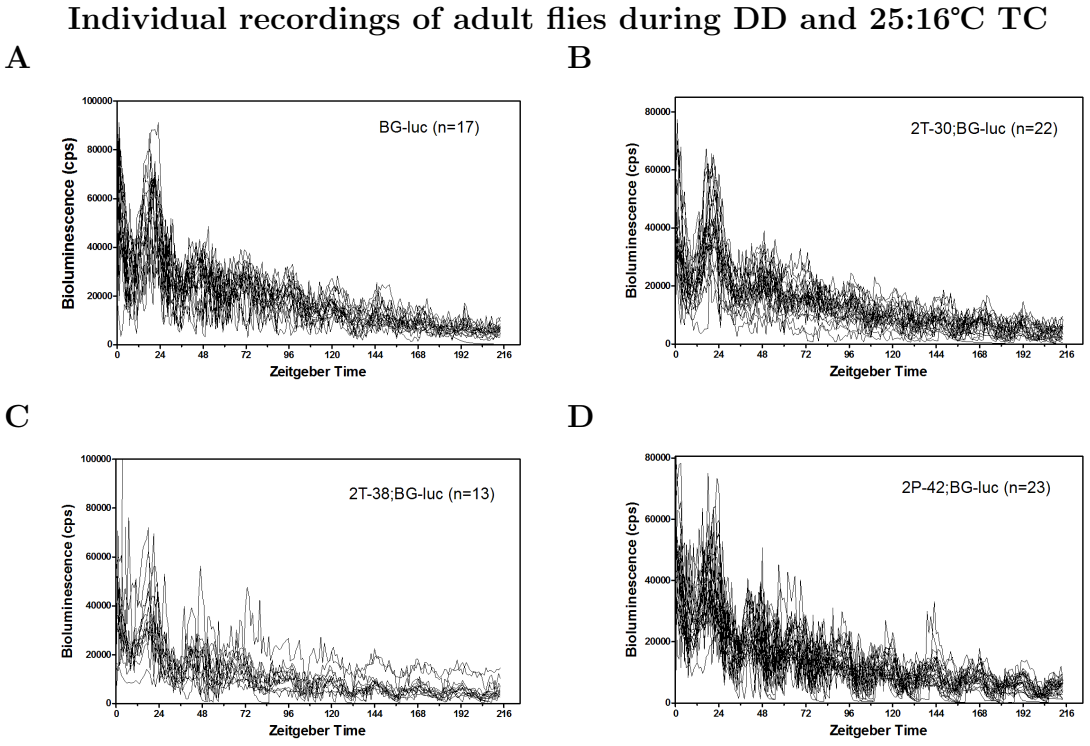

FIGURE 3.9: Individual bioluminescence recordings of whole adult flies of control (BG-*luc*) and EMS mutants during DD and 12:12 hr 25:16°C TC. Mean recordings and conditions are plotted in Figure 3.8.

in which *per-luc* expression in isolated body parts synchronise to TC, but it does not when the whole animal is considered (Gentile C., Simoni A., Stanewsky R., in preparation and see Discussion).

Because the line *2T-30* and *2T-38* were isolated from a batch of lines generated by the same EMS treatment, we performed a complementation test to rule out the possibility that they affected the same gene or that the different phenotypes observed were due to the generation of allelic variants of the same gene. This case is rare but indeed possible. In the EMS screen which led to the isolation of the first clock gene, three different mutants were isolated with different phenotypes. All mapped to the very same locus *period* (Konopka and Benzer, 1971).

We crossed the 3 mutants to each other and then tested the progeny for their

Complementation test:

Recordings of isolated legs during LL and 25:16°C TC

A)

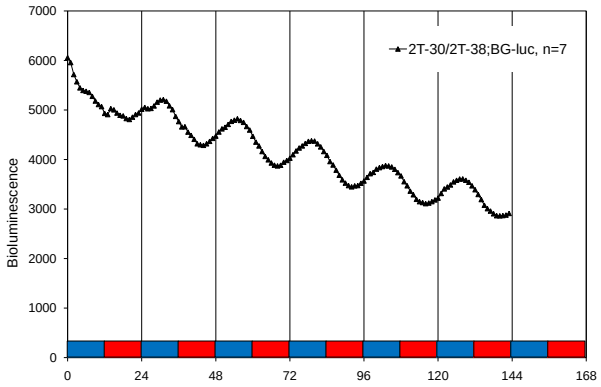

B)

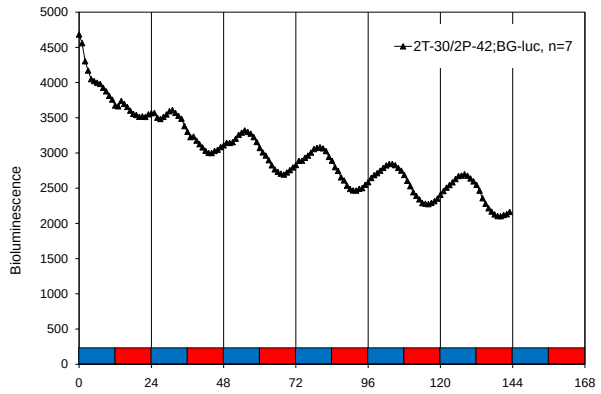

C)

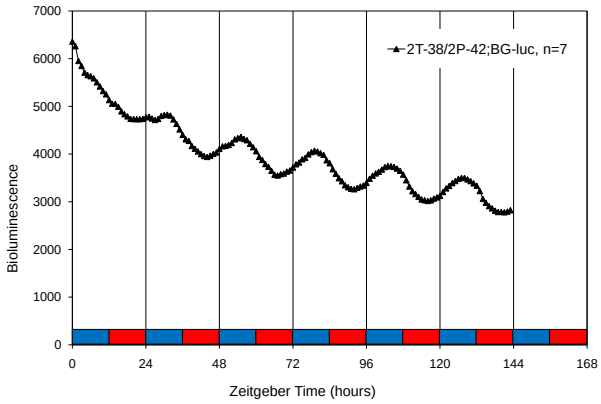

FIGURE 3.10: Complementation test of EMS mutants. Recording of PER-LUC in isolated legs from lines (A) *2T-30/2T-38*, (B) *2T-30/2P-42* and (C) *2P-42/2T-38* during LL and 12:12 hr 16:25°C temperature cycles. All the mutants complemented each other, indicating that each EMS mutant line affects a different gene. Red and blue bars indicate warm and cold, respectively. Note that the phase of TC is opposite to that of the previous LD (in which the flies have been raised, not shown). Legs take up to two days to synchronize to temperature.

ability to entrain *per-luc* expression to TC in constant light. Figure 3.10 shows that all the mutants complement and the wild-type phenotype is restored. This suggests that the 3 EMS lines affect different genes and this may explain the variety of phenotypes observed in different light/temperature conditions between the lines.

3.3 Behavioural analysis of the EMS mutants

3.3.1 Entrainment in constant light and temperature cycles

In the previous section we described that our three candidate temperature-entrainment mutants affect synchronization of *per-luc* expression to temperature cycles during constant light. Next, we addressed whether the observed molecular phenotype was also reflected at the behavioural level.

The rest-activity pattern of the fly is one of the best studied behavioural outputs of the circadian clock. The locomotor behaviour of a wild-type male under light-dark cycles displays a bimodal pattern of activity (as shown in Figure 3.11B, left column). The fly is very active in the morning, anticipating the transition from dark to light, then displays an afternoon *siesta* of very low activity before becoming again very active in the evening, again anticipating the transition from light to dark.

During constant light and temperature cycles (Figure 3.11C) locomotor activity is unimodal: the morning peak of activity disappears, flies are mainly active towards the end of the warm phase, anticipating the transition from warm to cold. In the three mutant lines we isolated the morning anticipation during LD is only weakly present (if at all, see Figure 3.11B). The reason for this can be the differ-

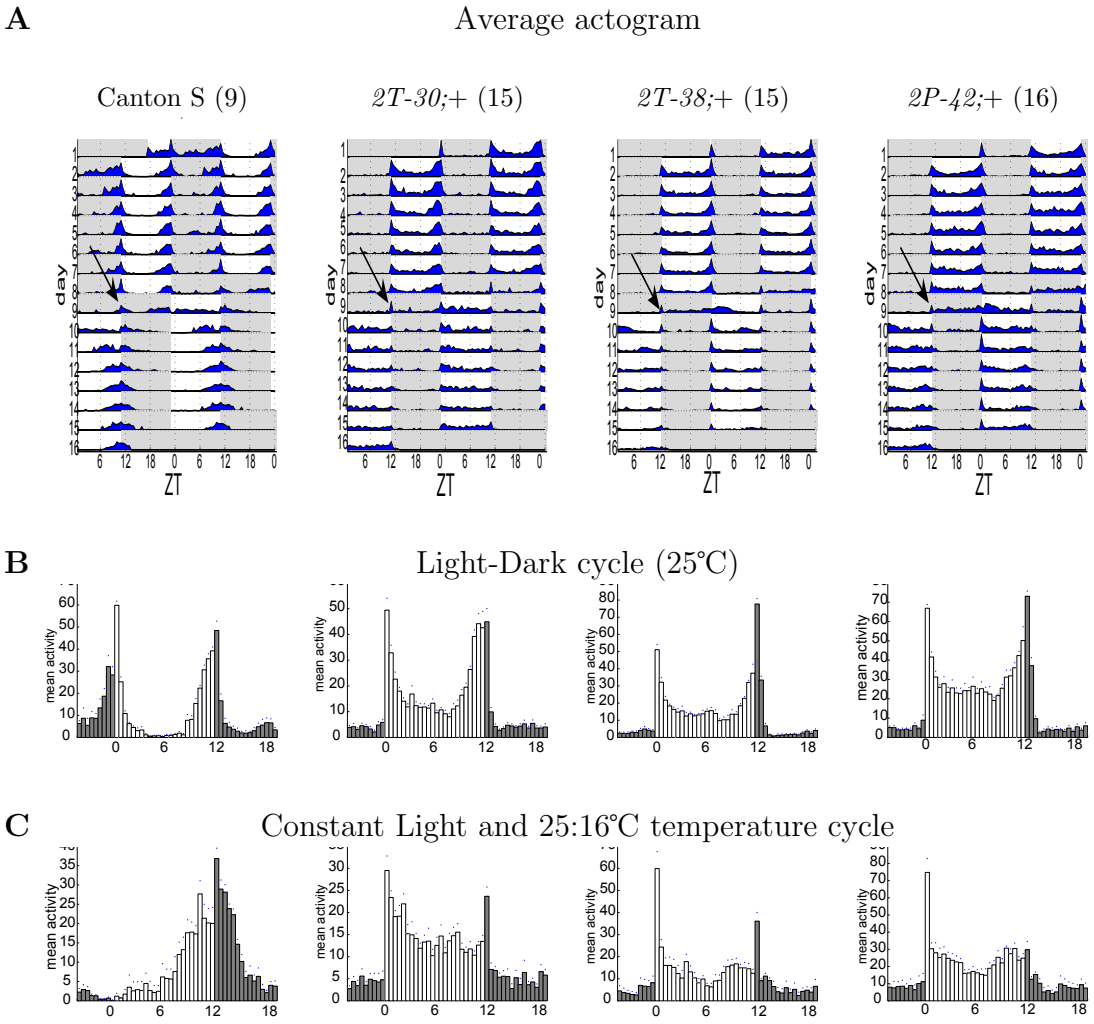

FIGURE 3.11: Rest-activity pattern of EMS mutant lines and control during LD cycles and LL & TC. **A)** Double-plot average actogram of wild-type (Canton S), *2T-30*, *2T-38* and *2P-42*. Flies were first exposed to 12:12 hr LD cycle at constant temperature for 7 days and then to constant light (LL) and 12:12 hr 25:16°C temperature cycles (arrows) for the following 7 days, in which the phase of temperature was opposite compared to the previous LD (warm corresponding to dark phase and cold corresponding to the previous light phase). **B)** Average histograms showing daily average activity of flies during the LD entrainment days. **C)** Daily average activity of flies during the subsequent entrainment to LL and TC. Shaded areas in the background correspond to the dark-phase (during LD entrainment) or the cold-phase (during TC entrainment). Dots above bars in the histograms represent SEM. Number of individuals analysed is indicated in brackets.

ent genetic background of the EMS-treated lines. BG-*luc* flies lack the morning anticipatory activity (see Figure 5 in Glaser and Stanewsky, 2005).

The mutant flies have a less pronounced *siesta* but show a robust anticipation

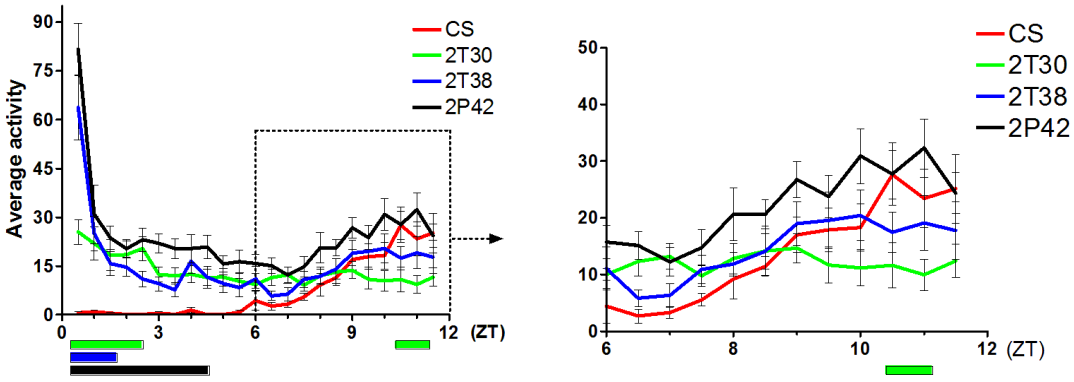

2T-30: $F_{(22,506)}$=6.75, $P< 0.0001$
2T-38: $F_{(22,391)}$=8.36, $P< 0.0001$
2P-42: $F_{(22,506)}$=7.23, $P< 0.0001$

2T-30: $F_{(11,252)}$=3.90, $P< 0.0001$
2T-38: ns
2P-42: ns

FIGURE 3.12: Daily average activity of controls (red line) and EMS mutants (green, blue and black, as indicated) during the warm-phase only of LL and TC of the histograms depicted in Figure 3.11C. Activity of the different genotypes is overlapped to see the effect of the mutation pattern and on the activity level. Two-way Anova was performed to determine overall statistical interaction between Canton S and EMS mutants for the range ZT 0–12 (left) and ZT 6–12 (right). Coloured bars underneath represent the time points in which each mutant shows significant difference compared to Canton S control (Bonferroni posttest $P< 0.05$). Error bars indicate SEM.

of the lights-off transition in the evening. In contrast, the mutants behaviour looks drastically different during temperature entrainment (Figure 3.11C and 3.12). Analysis of behaviour was performed first by inspection of actograms and histograms of daily average activity (Figure 3.11) and then by determining statistical interactions between activity of each mutant lines with the wild-type control (Figure 3.12). Anova was performed on the warm-phase only of temperature entrainment. We considered both the whole warm phase (ZT 0–12, left plot) and the second half of the warm phase (ZT 6–12, right plot), independently. In this way, we could monitor both the effects of the mutations on the overall activity (included the startle response induced by the steep increase of temperature) and the effect specifically on the peak of activity which anticipates the transition from warm to cold.

Unlike Canton S, all three mutant lines show a sharp increase of activity after

A

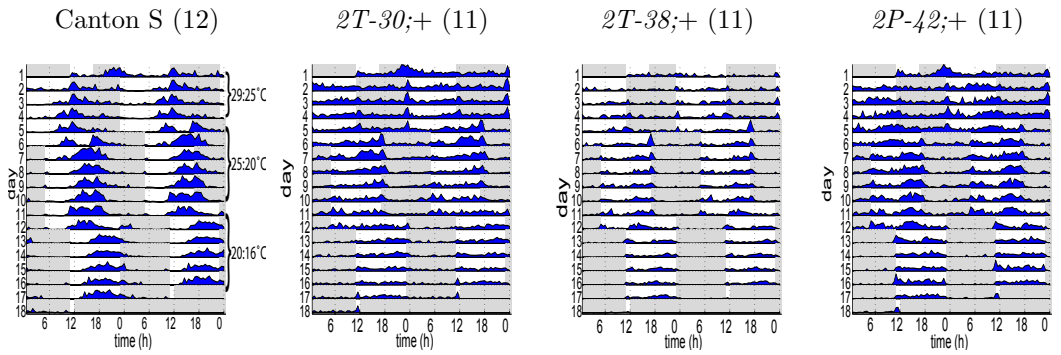

B

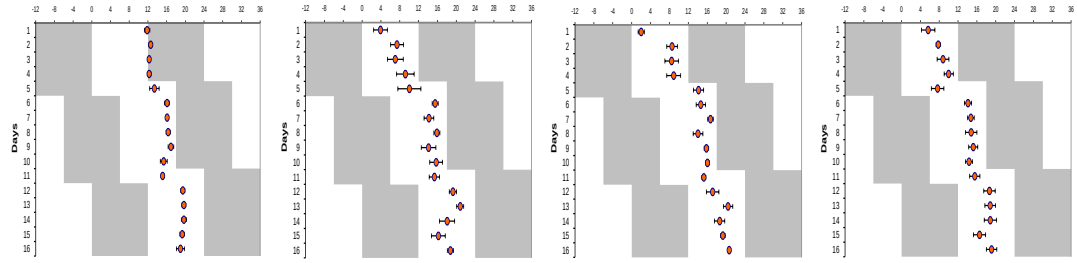

C Daily average activity at 29:25°C Temperature cycles

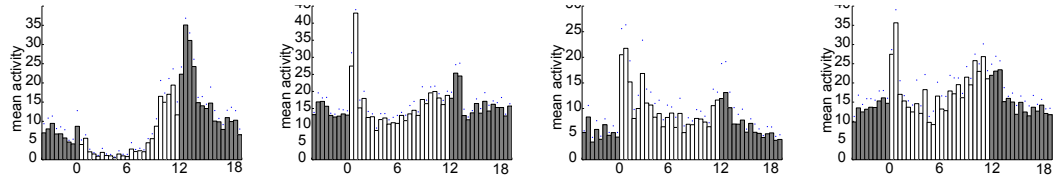

D Daily average activity at 25:20°C Temperature cycles

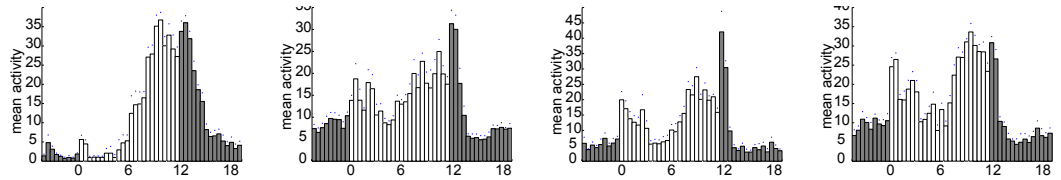

E Daily average activity at 20:16°C Temperature cycles

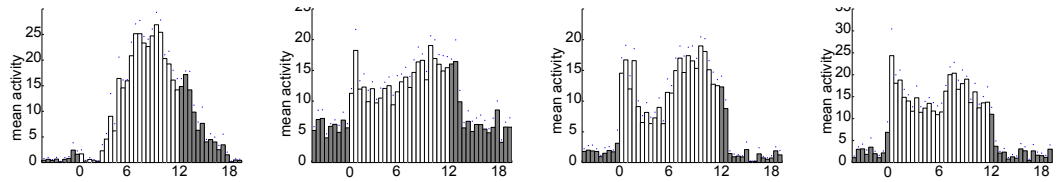

temperature rise and they remain active for the whole warm phase (Figure 3.12). Line *2T-30* does not show any anticipation of the transition warm-cold, with highly significant interaction with control ($F_{(11,252)}$=3.90, $P<$ 0.0001, Two-way Anova). Interestingly, when we consider only the second half of the warm phase (ZT6–12), mutant *2T-38* and *2P-42* do not differ from control (interaction not significant, Anova) in term of activity level and pattern. However, the three mutants interact with Canton S (in the range ZT 0–12), indicating an overall effect on the activity pattern.

The temperature cycles applied in this study to elicit entrainment were 25:16℃. We wondered if mutant flies were responding in a different way at different temperature intervals. This was also done in the light of the poor, but visible, ability of *2T-38* ad *2P-42* to entrain to 25:16℃. It is known that a temperature cycle as little as 2–3℃ is enough to synchronize behaviour in wild-type flies (Wheeler et al., 1993). We monitored the behaviour of flies at three different temperature intervals (in LL) to try to understand if distinct mutant lines were able to synchronize specifically to a certain temperature range, but fail to entrain when a wide temperature range was applied. Figure 3.13 shows the behaviour of the EMS mutant

---

FIGURE 3.13 *(preceding page)*: Behaviour activity of EMS mutant lines and control in LL and different temperature intervals.
A) Average actogram of wild-type control (Canton S), *2T-30*, *2T-38* and *2P-42* putative mutant lines. Flies were first entrained in LD cycles at 25℃ (not shown) followed by 5 days of LL and 12:12 hr – 29:25℃ temperature cycles which was 6 hr delayed compared to the previous LD (warm phase delayed compared to the previous light phase). This was followed by 6 days of LL and 12:12 hr – 25:20℃ temperature cycles again delayed by 6 hr compared to the previous TC. Finally, the flies were exposed to 6 days of LL and 12:12 hr – 20:16℃ temperature cycles, delayed 6 hr compared to the previous TC. B) Activity peak phase of control and mutant flies. Conditions are the same as in (A). C–E) Daily activity plot of control and mutant lines during LL and 29:25℃ (C), 25:20℃ (D) and 20:16℃ (E). Grey shadows (A, B) and grey bars (C–E) represent cold-phase (in any different temperature intervals) while white areas/bars indicate warm phase. Error bars in (B) indicate SEM. Number of individuals is indicated in brackets.

Daily average activity at 29:25℃ TC

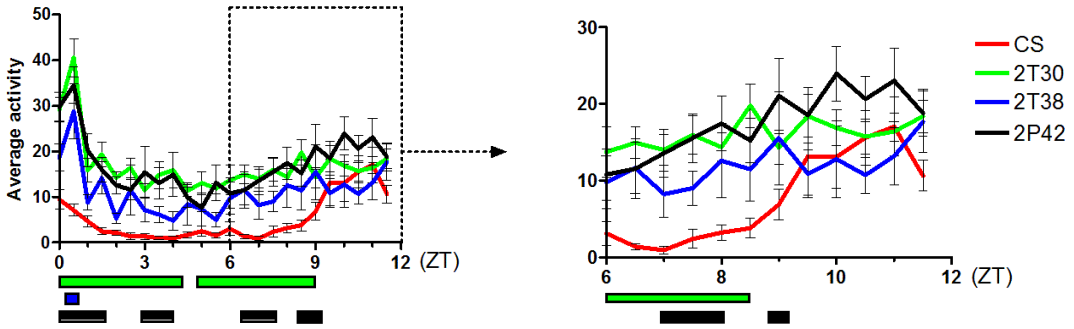

2T-30: $F_{(23,432)}=4.60$, $P< 0.0001$
2T-38: $F_{(23,480)}=1.71$, $P< 0.05$
2P-42: $F_{(23,432)}=1.65$, $P< 0.05$

2T-30: $F_{(11,216)}=2.26$, $P< 0.05$
2T-38: ns
2P-42: ns

Daily average activity at 25:20℃ TC

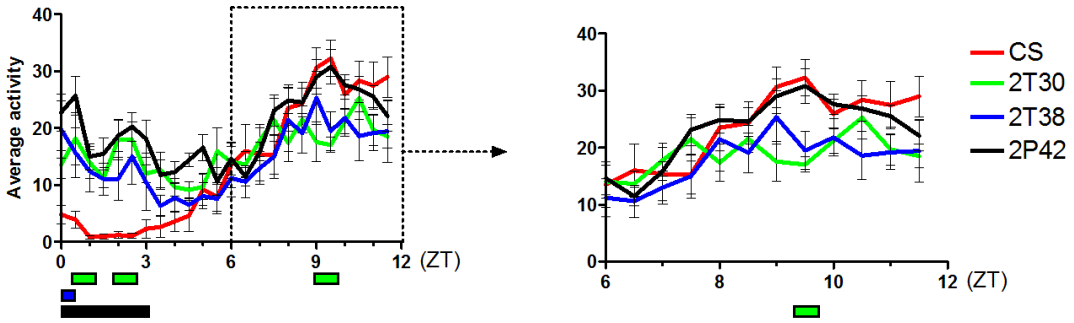

2T-30: $F_{(23,432)}=4.96$, $P< 0.0001$
2T-38: $F_{(23,480)}=2.87$, $P< 0.0001$
2P-42: $F_{(23,432)}=4.41$, $P< 0.0001$

2T-30: ns
2T-38: ns
2P-42: ns

Daily average activity at 20:16℃ TC

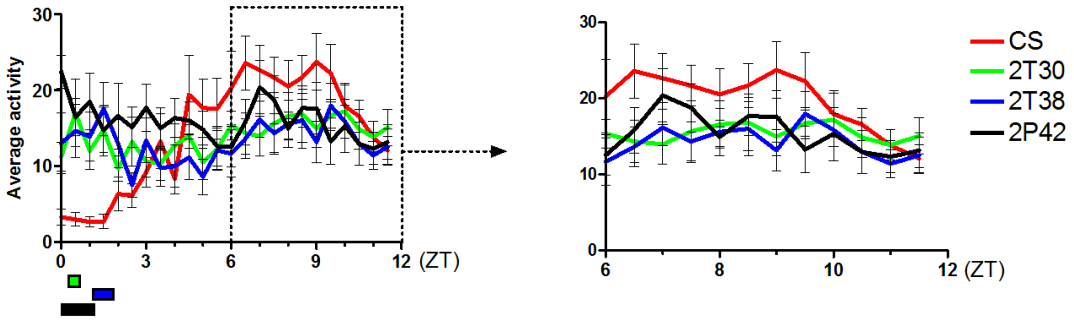

2T-30: $F_{(23,432)}=3.27$, $P< 0.0001$
2T-38: $F_{(23,480)}=1.71$, $P< 0.0001$
2P-42: $F_{(23,432)}=3.89$, $P< 0.0001$

2T-30: ns
2T-38: ns
2P-42: ns

lines and controls at constant light and 29:25℃, 25:20℃ and 20:16℃ temperature intervals. As before, activity was plotted in form of actograms and histograms of the individual genotypes (Figure 3.13) and by overlapping the activity of the all genotypes for each condition in single plots, where statistical analysis was performed (Figure 3.14). Wild-type flies strongly entrain to all three temperature intervals. Note also the effect of "seasonal adaptation" of the clock (Majercak et al., 1999; Collins et al., 2004; Stoleru et al., 2007): The phase of evening activity is moving towards the centre of the day (i.e. warm phase in a temperature entrainment regime) during a cold interval (20:16℃), the equivalent of an autumn day. In a warm range (29:25℃), like a summer day, the fly's activity is shifted more to the end of the day (see Figure 3.13B, first column). The advantage of this behaviour pattern could be to avoid the hottest part of the day during summer, preventing excessive dehydration, while in colder seasons activity mainly occurs during mildest hours before dusk.

The overall pattern of activity of the three mutants is significant different form Canton S control in any temperature intervals (Figure 3.14). All the mutants, in contrast to Canton S, exhibit a strong peak of activity after the transition from cold to warm (morning) and a less pronounced anticipation of the transition from warm to cold (evening), indicating defective entrainment to temperature. However, when a Two-way Anova is restricted to the second half of the warm phase (ZT 6–12, i.e. the evening anticipation peak), we found statistical difference from

FIGURE 3.14 *(preceding page)*: Daily average activity of controls (red line) and EMS mutants (green, blue and black, as indicated) during the warm-phase only of LL and different temperature intervals of the histograms depicted in Figure 3.13C–E. Two-way Anova was performed to determine statistical interaction between Canton S (CS) control and each EMS mutant lines in the range ZT 0–12 (left) and ZT 6–12 (right). Coloured bars underneath indicate the time points in which each mutant shows significant difference compared to Canton S (Bonferroni posttest $P < 0.05$).

control only for the mutant line *2T-30* during LL and 29:25℃ TC ($F_{(11,216)}$=2.26, $P< 0.05$, Figure 3.14). Therefore, the lines *2T-38* and *2P-42*, although exhibiting a stronger reaction peak in response to the temperature increase, are able to entrain to the different temperature intervals, in terms of exhibiting a clear evening anticipation peak of activity comparable to control (Two-way Anova interaction not significant). In addition, from overlapped daily activity plots in Figure 3.14 it is visible that at 29:25℃ the activity level of the mutants is higher compared to control, whereas at 20:16℃ the activity level is lower (with statistical significance, Anova, data not shown), suggesting again that the passive response to temperature is more pronounced in the mutant than in control flies.

We thus observed a clear difference of activity at different temperature intervals in LL. The clearest effect is observed for *2T-30* at 29:25℃ TC. Interestingly, all the lines which exhibit a mutant phenotype at 25:16℃ entrain (weakly) at 25:20℃ and 20:16℃ (which are "part" of 25:16℃). This indicates, surprisingly, that mutants fail to synchronize to higher temperature cycles than to lower ones.

3.3.2 Entrainment in constant darkness and temperature cycles

It is known that temperature cycles can entrain locomotor activity in constant darkness (Wheeler et al., 1993). We first entrained flies to LD cycles and then applied 12:12 hr 25:16℃ TC in constant darkness in phase with the previous LD. Subsequently, a new temperature regime was applied, which was 6 hour delayed compared to the previous and then flies were released to DD and 25℃ where free run activity was monitored. In addition to plot the activity in form of average actograms and daily activity histograms (Figure 3.15), the behaviour analysis software calculates also the average peak phase of activity, which have been reported

in Table 3.3. Then, Two-way Anova was performed to determine statistical interaction between the mutants and control. During the first temperature regime, Canton S flies move the evening activity earlier during the warm phase, compared to the previous LD, stabilizing to ZT7.8 (Figure 3.15B and Table 3.3 "pre-shift"). A minor peak of activity occurs just after temperature-up (ZT0.3), probably induced by the steep increase of temperature. A similar "temperature response" was observed in the same conditions also in per^{01} flies (Tomioka et al., 1998), suggesting that it is clock-independent. After a 6-hr temperature shift, the main peak of activity in wild-type flies stabilizes at ZT3.6, much earlier compared to LL (compare Figures 3.15 to 3.11). The activity take 3–4 days to reach a stable phase, indicating that in DD flies synchronize their behaviour to TC more slowly compared to LL (in which they take 2–3 days). A burst of activity still occurs just after the temperature increase (Figure 3.15C), but it is not considered by the phase analysis, which apply a 4-hr low-pass filter to the data (Table 3.3). When flies are released in DD (and 25℃) the phase of free-running activity follows the previous temperature entrainment, indicating that the flies are fully synchronized (Figure 3.15D and Table 3.3).

The mutant line *2T-30* is unable to synchronize its behaviour to TC in DD (Figure 3.15). As soon as the flies are subjected to TC, their activity is characterized by a strong reaction to temperature just after the cold to warm transition (ZT0.8) and an overall low activity during the warm phase. Although the "reaction" peak of mutants and control is comparable, both before and after the temperature shift (Figure 3.16), in case of the mutants a second "entrainment" peak exhibited by control flies does not follow. Before the temperature shift, the analysis of variance revealed not significant difference compared to control in term of statistical interaction when the second half of the warm phase only is consid-

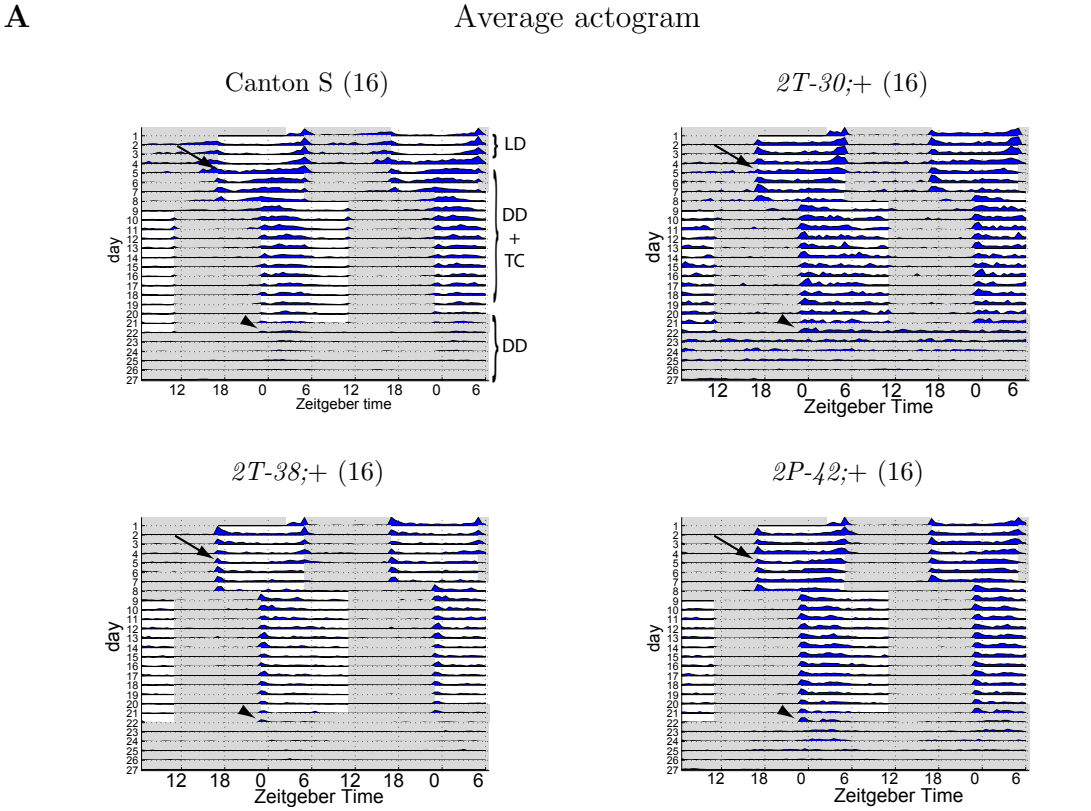
A
Average actogram
Canton S (16)
2T-30;+ (16)
2T-38;+ (16)
2P-42;+ (16)
LD
DD
+
TC
DD
day
Zeitgeber time
Zeitgeber Time
B
DD and 25:16°C TC
Canton S (16)
2T-30;+ (16)
2T-38;+ (16)
2P-42;+ (16)
mean activity
C
DD and 25:16°C TC after 6 hr temperature shift
D
DD and 25°C (Day 1-3)

ered, but a clear difference of activity level is visible (Figure 3.14). After the temperature shift (Figure 3.15C) the "temperature mutant" phenotype is even clearer (and highly significant). Subsequent free-running activity of *2T-30* flies in DD is mainly arrhythmic (Figure 3.15D, Table 3.4 and see below).

2T-38 exhibits a main peak of activity just after the cold to warm transition, before and after the shift (Figure 3.15 and Table 3.3), suggesting a reaction to temperature, rather than synchronization. The peak of entrained activity which characterize Canton S flies, is barely visible, but not significant (Figure 3.16). Mutant flies subsequently released to constant conditions free-run with a phase at CT0.8 (Figure 3.15D and Table 3.4), 3 hours earlier than Canton S, and a second peak of free-running activity occurs in the same position as in controls.

Activity of line *2P-42* is comparable to controls, in terms of activity pattern and number of days required to reach a stable phase (Figure 3.15 and Table 3.3). Before the temperature shift, the activity is synchronized to temperature cycles, it peaks two hour later than control (ZT9.8 vs 7.8) and although the activity level of the "entrainment" peak is lower than Canton S it is not statistically different

FIGURE 3.15 *(preceding page)*: Rest-activity pattern of EMS mutant lines and controls during DD and TC. **A)** Double-plot average actogram of wild-type (Canton S), *2T-30*, *2T-38* and *2P-42*. Flies were first entrained to 12:12 hr LD cycle at constant temperature (25℃) for 4 days and then exposed to DD and 12:12 hr 25:16℃ TC (arrows) for the following 4 days in which the phase of temperature was the same as the previous LD (warm corresponding to previous light phase and cold corresponding to the dark phase). Subsequently, a new temperature regime was applied 6 hr delayed compared to the previous TC, followed by release to DD and 25℃ (arrowheads), where free-running activity was analysed. Note that the evening activity during TC is advanced compared to LD. **B)** Histogram showing daily average activity of flies during the first DD and TC entrainment (4 days). **C)** Daily average activity of flies during the subsequent entrainment to DD and TC (13 days). D) Average free-running activity during the first 3 days of DD and 25℃. Shaded areas in the background correspond to the dark/cold phase and white areas to light/warm phase. In (D) light- and dark-grey shadings represent subjective day (warm) and night (cold), respectively. Dots above bars in the histograms represent SEM. Number of individuals analysed is indicated in brackets.

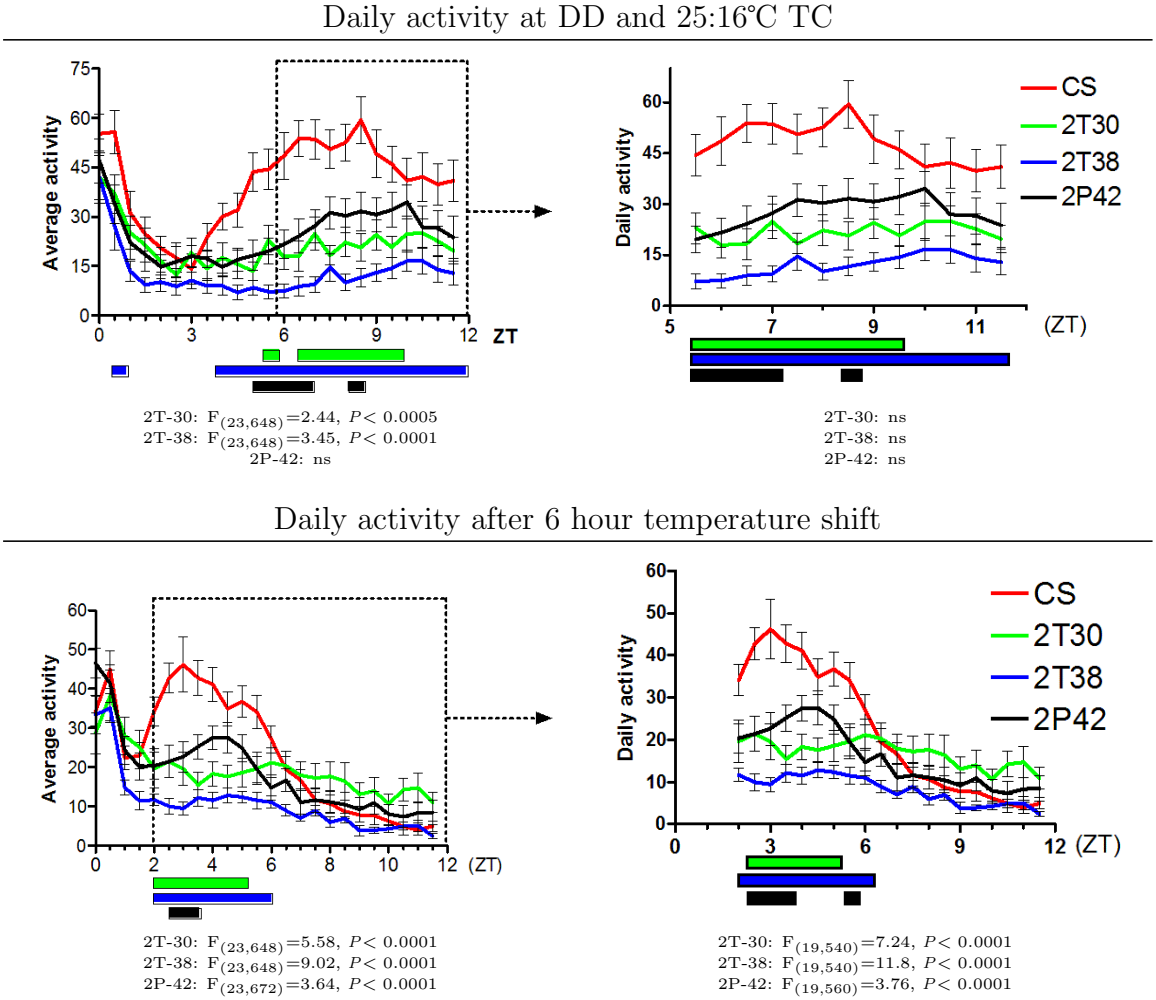

FIGURE 3.16: Daily average activity of controls (red line) and EMS mutants (green, blue and black, as indicated) during the warm-phase only of DD and TC histograms depicted in Figure 3.15B–C. Two-way Anova was performed to determine statistical interaction between Canton S (CS) control and each EMS mutant lines in the range ZT 0–12 (left) and ZT 2–12 or ZT 6–12 (right), as indicated. Coloured bars underneath represent the time points in which the respective mutants show significant difference compared to Canton S (Bonferroni posttest $P< 0.05$).

	Peak phase (ZT)[a]					
Genotype	LD	DD + TC pre-shift		DD + TC post-shift		DD
Canton S	12.3	7.8[b]	0.3 (77)[c]	3.6	–	3.8
2T-30	11.8	0.8	10.3 (82)	1.3	6.8 (72)	1.3
2T-38	12.3	0.3	10.8 (54)	0.8	5.8 (51)	0.8
2P-42	11.8	9.8	0.8 (89)	0.8	4.8 (84)	4.3

TABLE 3.3: Peak phase analysis of EMS mutants and controls during DD and TC entrainment. Peak phase (in hr) are calculated from 4-hr lowpass filtered versions of the histograms depicted in Figure 3.15. During LD entrainment, only the evening peak is considered, which occurs at the transition between light and dark (around ZT12). During temperature entrainment, before and after the temperature shift (pre- and post-shift, respectively), two main activity peaks are present and the respective values are reported. The phase of the major peak (relative amplitude of 100%) is displayed in the first column. The phase of a minor, secondary peak, is displayed in the second column (and relative peak amplitude is shown in brackets). Note that Canton S flies display only one activity peak after the temperature shift.

[a] Phase relative to the entrainment regime: 0 = lights-on or temperature-up. 12 = lights-off or temperature-down. For DD conditions, CT values relative to the previous temperature regime are considered. Phase calculated only for rhythmic flies.

[b] Major peak. Relative peak intensity 100%

[c] Minor peak. Relative peak intensity is indicated in brackets (%)

(Figure 3.16). After the temperature shift (Figure 3.15C) the peak of activity is even lower than control and occurs 1.2 hr later, determining a statistically significant difference from Canton S (Figure 3.16). However, analysis of actogram and histogram reveals that a synchronized activity peak is indeed visible, and free-running activity phase after temperature entrainment follows the previous TC (Table 3.3 and Figure 3.15D), suggesting that *2P-42* flies are synchronized to temperature in DD.

3.3.3 Free-run rhythmicity of EMS mutants

Wild-type flies strongly entrain to LD, as well as to TC. After any entrainment condition, be it light or temperature, the rhythm persists in constant conditions. We proceed by monitoring the free-running activity of the EMS mutants compared

Genotype	**n**	**% rhythmic**	**τ (h) ± SEM**	**RI ± SEM**	**RS ± SEM**
After LD entrainment					
Canton S	42	97.6%	24.4 ± 0.1	0.38 ± 0.02	3.2 ± 0.2
2T-30	59	42.4%	24.0 ± 0.8	0.26 ± 0.02	2.2 ± 0.2
2T-38	47	51.1%	24.8 ± 0.2	0.29 ± 0.02	2.0 ± 0.2
2P-42	37	81.1%	24.3 ± 0.2	0.28 ± 0.02	2.4 ± 0.2
After LL + 25:16℃ temperature entrainment					
Canton S	23	82.6%	24.7 ± 0.2	0.25 ± 0.01	2.2 ± 0.2
2T-30	22	36.4%	24.0 ± 0.3	0.24 ± 0.02	1.8 ± 0.2
2T-38	15	66.7%	24.1 ± 0.5	0.16 ± 0.02	1.8 ± 0.1
2P-42	16	43.8%	23.7 ± 0.8	0.21 ± 0.03	1.6 ± 0.2
After DD + 25:16℃ temperature entrainment					
Canton S	36	91.7%	24.2 ± 0.21	0.29 ± 0.02	2.30 ± 0.18
2T-30	31	16.1%	24.0 ± 1.19	0.21 ± 0.03	1.62 ± 0.23
2T-38	33	69.7%	24.4 ± 0.24	0.28 ± 0.02	2.27 ± 0.18
2P-42	40	87.5%	23.7 ± 0.20	0.27 ± 0.02	2.20 ± 0.15

TABLE 3.4: Free-running locomotor activity of EMS mutant and wild-type control. Flies were entrained in light or temperature conditions (as indicated) and then released in DD and constant temperature (25℃). Free-running period (τ) of rhythmic flies is calculated and autocorrelation values are shown. RI (Rhythmicity Index) and RS (Rhythmicity Statistic) determines the statistical significance and strength of the rhythm. RI and RS > 0.1 and 1.0 respectively, indicate statistical significance (based on autocorrelation). See Materials & Methods for details. SEM: Standard Error of the Mean.

to wild-type control, after light and temperature entrainment. The phase of the clock can be reset by the LL to DD transition and we did not address this possibility for our EMS mutants. However, we calculated free-running rhythmicity after LD, LL and TC and DD and TC conditions.

Line *2T-30* exhibits a very low rhythmicity in DD after any entrainment conditions. After LD cycles, 42% of flies are still rhythmic; after LL and TC, only 36% shows rhythmicity and the percentage drop to 16% after DD and TC (Table 3.4).

50% of *2T-38* mutant flies are not rhythmic after LD entrainment, while more than 65% free-run after temperature entrainment (both in LL or DD). In contrast to *2T-30* this allows determination of the phase of the free-running activity peak

after TC. Although the flies do not look synchronized during temperature cycles, the free-running phase follows that of the previous warm phase, suggesting that the clock is actually entrained and it free-runs in phase with the previous temperature cycle (see Figure 3.15A and Table 3.3).

Mutant line *2P-42* is weakly rhythmic (44%) after LL and TC, while it free-runs after LD and DD & TC (more than 80% of flies are rhythmic). The free-running phase is synchronized to the previous regime, and the rest-activity pattern during TC resembles that of wild-type (Figure 3.15), indicating that *2P-42* can entrain to temperature only in DD and not in LL.

Free-running period is slightly longer than 24 hours for all the genotypes (after any entrainment conditions), with no significant difference among control and mutants. The only exception is *2P-42* after LL and TC, which free-runs with a 23.7 hr period. Note, though, a low rhythmicity and a large SEM (Table 3.4).

Circadian clocks are temperature compensated. This means that free-running period is almost invariant over a wide range of physiological temperatures and the "temperature factor" (Q_{10}) is about 1 (see Introduction and Pittendrigh, 1954). The mechanism underlying temperature compensation is not known. However, mutations in the *period* gene compromise temperature compensation: per^L, for instance, in addition to exhibiting a very long free-running period (27–30 hr) also has impaired temperature compensation (Konopka et al., 1989 and Figure 3.17).

We investigated whether the EMS mutants exhibited a different free-running behaviour at different constant temperatures. We first entrained mutant and control flies to LD and then released them in DD, at three different temperatures: 18°C, 25°C and 29°C. All EMS-mutants tested show similar period length compared to the wild-type control (Figure 3.17) and they are all temperature compensated. Line *2T-30* has a slightly longer period at 29°C but this is probably reflecting

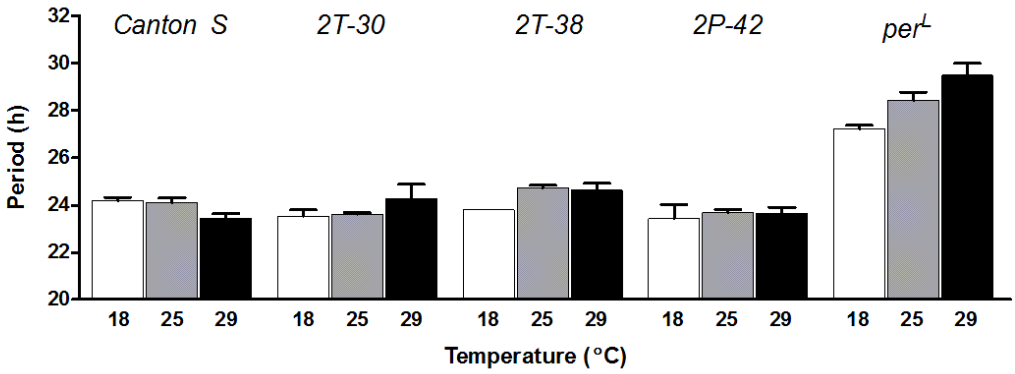

n	10	8	9	12	12	9	9	9	8	10	7	10	4	4	4
Rhythmic	10	8	9	9	5	3	1	7	7	7	7	8	4	3	2

FIGURE 3.17: Average free-running period length of controls and EMS mutants at different constant temperatures. EMS mutant and wild-type (Canton S) flies are temperature compensated. per^L in addition to exhibiting a long free-running period also lacks temperature compensation (27.2 hr at 18°C, 28.4 hr at 25°C and 29.5 hr at 29°C). White columns indicate free-running period of rhythmic flies at 18°C, grey columns at 25°C and black columns indicate period at 29°C. Error bars indicate SEM. Number of individuals tested and of rhythmic flies are shown in the table underneath the graph.

the lower number of rhythmic flies at that temperature. Interestingly, the *2T-30* mutant decreases DD rhythmicity with an increase of temperature, while mutant *2T-38* shows the opposite effect (aperiodic behaviour at 18°C). per^L mutants, instead, consistently free-run with a long period, which increases with temperature (27.2 hr at 18°C, 28.4 hr at 25°C and 29.5 hr at 29°C), i.e. it is not temperature compensated (Konopka et al., 1989).

3.4 *2T-30* is a locomotor output mutant

Given that line *2T-30* is largely arrhythmic in DD after any entrainment condition (Table 3.4 and Figure 3.18B), we wondered if this mutation affects the central clock mechanism.

Together with locomotor activity, a different behavioural output of the clock

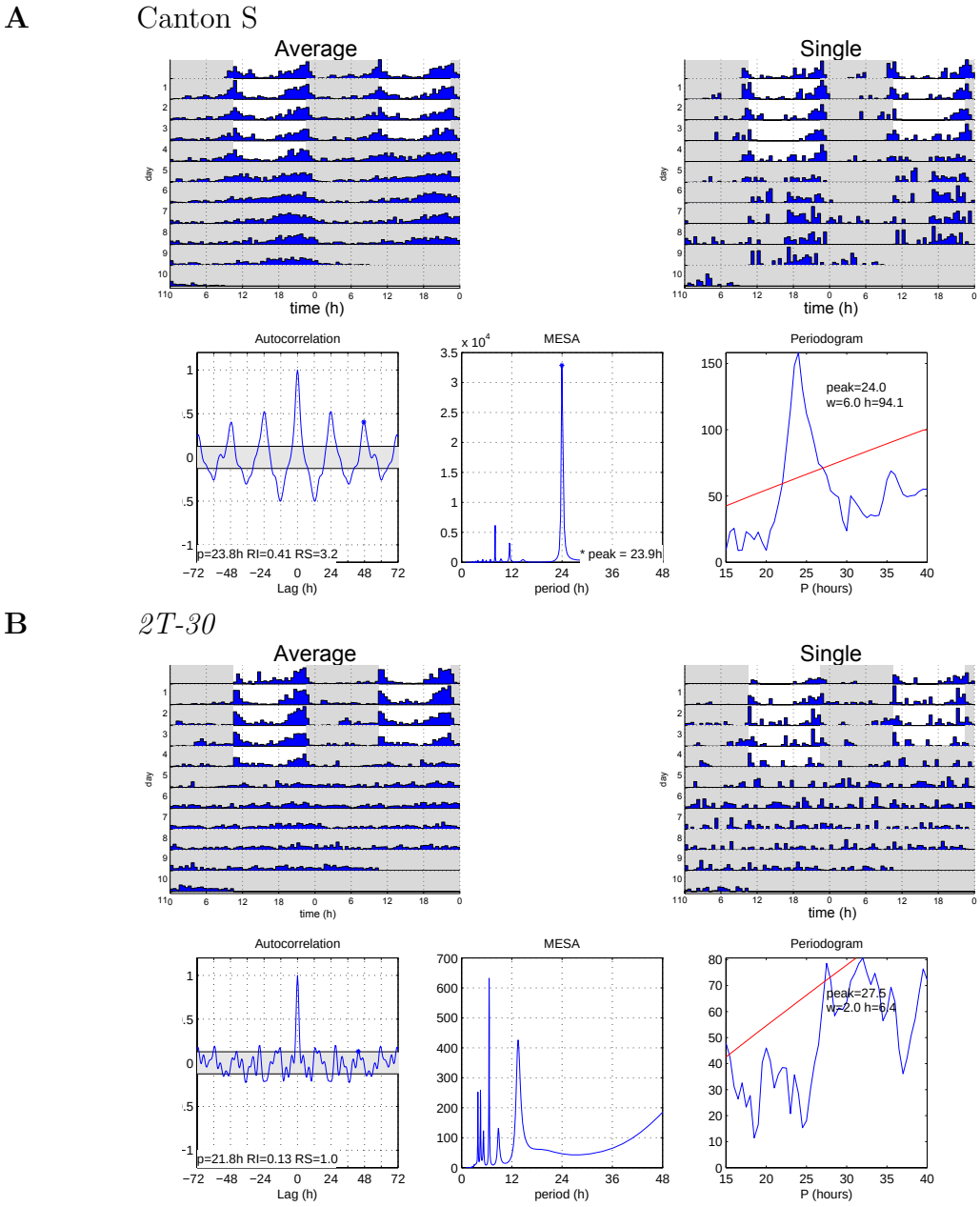

FIGURE 3.18: Locomotor activity of *2T-30* and controls. Average actogram (n=16), single-fly actogram, autocorrelation, MESA and χ^2-periodogram of (A) Canton S and (B) the *2T-30* mutant. Flies were entrained in 5 LD cycles and then released to DD (25°C). Autocorrelation, MESA and periodogram are calculated during the DD part of the experiment only. Data of one representative fly are shown.

is the eclosion rhythm, i.e. the adults emergence from the pupal case. Eclosion exemplifies a population rhythm that is equally affected by clock mutants (per^L,

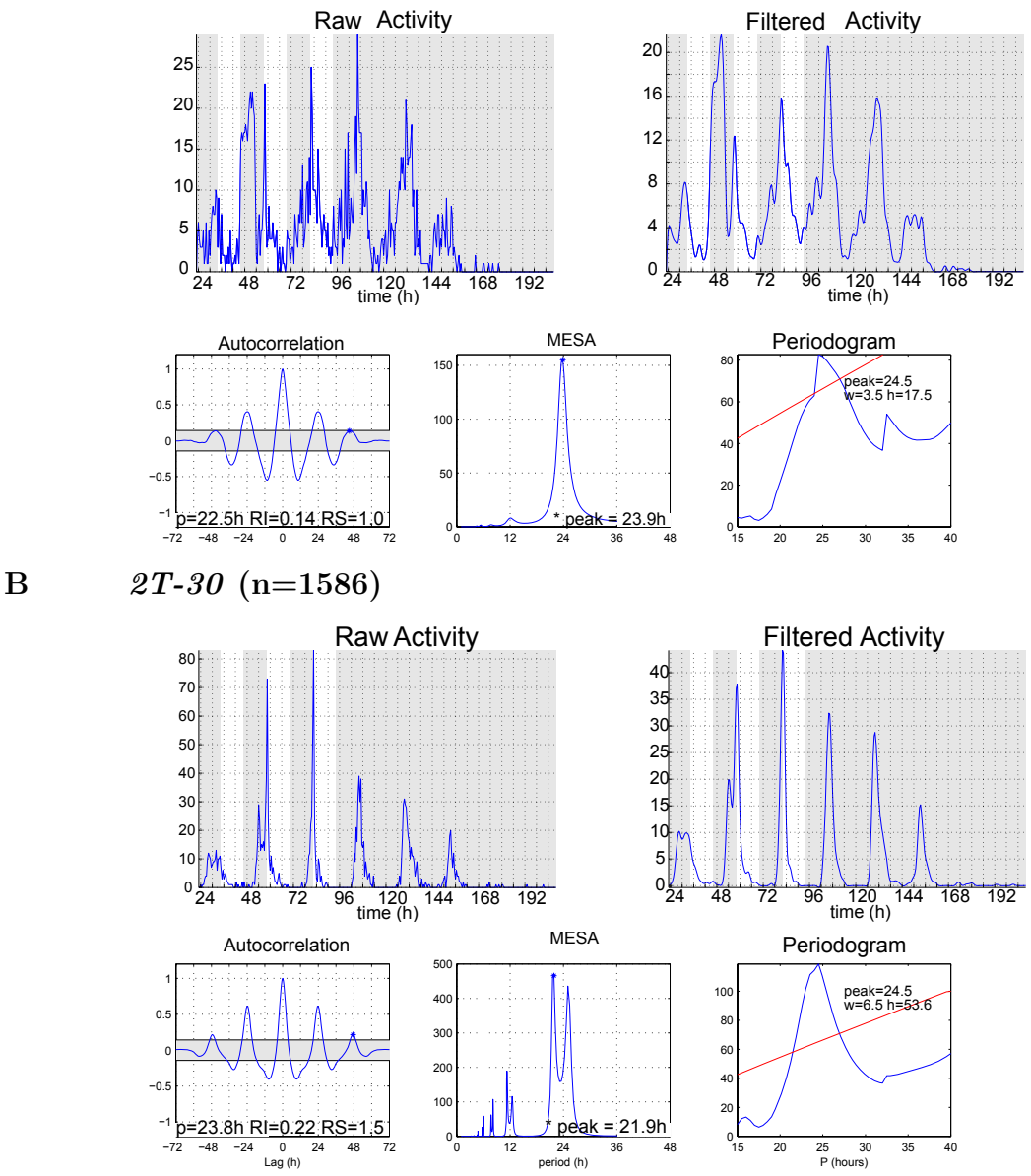

FIGURE 3.19: Eclosion profile of (A) Canton S and (B) *2T-30* during 3 days of a LD cycle, followed by 4 days in DD (20°C). The ordinates of the two upper plots depict number of emerging adults per 30 min bin. The total number of eclosed flies is indicated next to the genotype. Left-hand panel (raw activity) displays the actual number of eclosed flies, and the right-hand panel displays 4-hr low-pass filtered version of the left plot (filtered activity). The lower plots show analysis of eclosion rhythms performed in the same way as that for locomotor activity (see Figure 3.18).

per^{s} and *per*^{01}) as locomotor rhythms (Konopka and Benzer, 1971). Figures 3.18 and 3.19 shows a comparison of locomotor and eclosion behaviour of *2T-30* and wild-type control in a LD to DD experiment. As described above, locomotor behaviour of adult *2T-30* flies is largely arrhythmic in DD. The left-hand panel (in 3.18B) shows an average actogram in which the typical locomotor activity during LD to DD is visible; the activity becomes arrhythmic as soon as the mutant flies are released to DD. The right-hand panel shows an actogram of a single representative fly (compare to wild-type control in A). We then investigated free-running adult-emergence profiles of *2T-30* in the same condition. In a LD cycle, wild-type flies mainly eclose in the morning, before the dark-to-light transition (Figure 3.19). This rhythm persists in constant conditions, with a period of circa 24 hours (Pittendrigh, 1954). Both Canton S and *2T-30* exhibited eclosion rhythmicity (Figure 3.19A–B), and interestingly, *2T-30* exhibited a even "sharper" emergence peak than Canton S (probably due to different genetic backgrounds. See Chapter 6 for more details about eclosion). The eclosion rhythm of *2T-30* is strong and persists for several days in DD, with a period of 23.8 hours. The eclosion rhythm is generated by the central clock located in the brain and in the prothoracic gland (PG), and particularly the LN neurons and the PG are required to maintain rhythmicity in DD (Blanchardon et al., 2001; Myers et al., 2003 and Introduction). The *2T-30* mutation also does not alter rest-activity pattern in LD. Taken together, these data indicate that the mutation, which characterizes line *2T-30*, does not affect central oscillator genes. The gene mutated reveals a new component of the locomotor output pathway, in addition to being defective in temperature entrainment.

3.5 Uncoordination phenotype

A previous genetic screen led to the isolation of a temperature mutant, named *nocte*, affecting temperature entrainment (Glaser and Stanewsky, 2005, 2007). It has been recently shown by our group that chordotonal (ch) organs are involved in synchronization of the circadian clock of *Drosophila melanogaster* to temperature cycles (Sehadova et al., 2009). In this paper we reported that *nocte* mutants exhibit an "uncoordinated" phenotype when exposed at 37°C for 90 minutes (for more details see Chapter 7 and Cook et al., 2008), likely caused by fluid loss from ch organs due to structural defects.

We questioned whether the *2T-30* mutants exhibit a similar phenotype. Figure 3.20 shows that *2T-30* flies lose the ability to walk properly if exposed to 37°C for 90 minutes and exhibit an "uncoordinated" phenotype. After increasing environmental humidity in parallel to temperature (37°C) — by introducing a filter paper soaked with water in the chamber where the flies were monitored — we were able to rescue completely their uncoordinated phenotype. Given that the same phenotype is observed in *nocte* (Sehadova et al., 2009) and *spam* mutants (Cook et al., 2008), and that both genes are affecting the structural function of the chordotonal organs, it is possible that *2T-30* also has an effect at the structural level of the ch organs. Further studies investigating morphological and structural alterations of ch organs will shed light on a possible ch role of this mutant to the temperature signalling pathway.

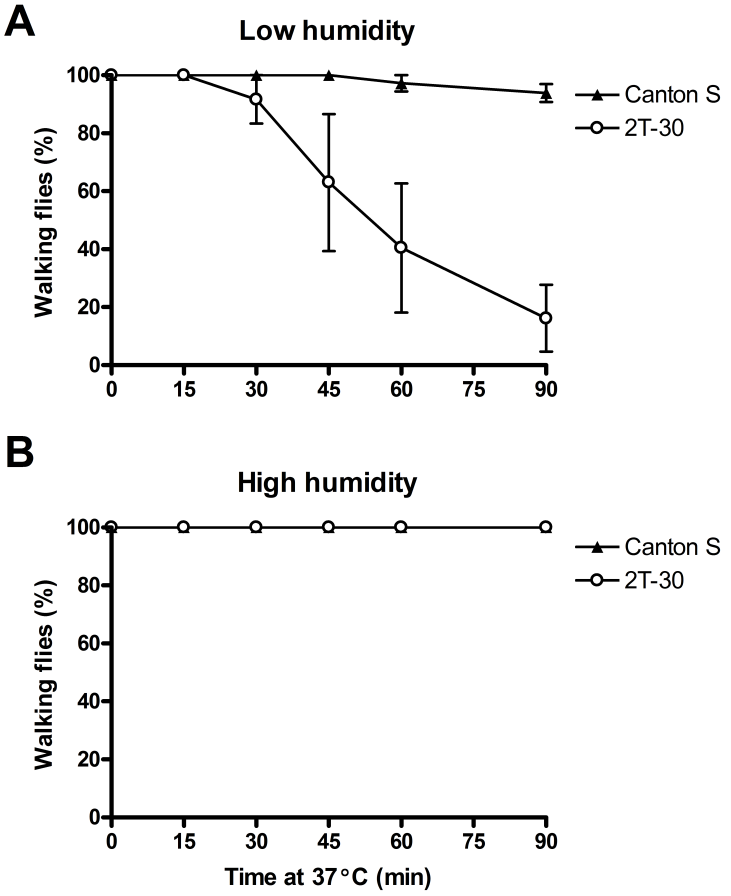

FIGURE 3.20: Uncoordination phenotype of EMS mutant *2T-30* and control (Canton S). Flies were raised at 25℃ and then transferred to 37℃ where they were monitored every 15 minutes for their ability to walk. The percentage of normal walking flies compared to the uncoordinated ones is shown. A) Mutant flies exposed to heat and low relative humidity became quickly uncoordinated. B) The uncoordination phenotype can be completely rescued by exposing the flies to high temperature with high humidity. At least 3 independent experiments (of 10 flies per genotype each) have been performed. Error bars indicate SEM. In (B), Canton S and *2T-30* data overlap.

3.6 Mapping of mutant line *2T-30*

3.6.1 Complementation test

The EMS mutagenesis screen led to the isolation of three mutants with impaired *per-luc* synchronization to temperature cycles and defects on entrainment of the locomotor activity to TC. To reveal which genes are affected and elucidate the molecular basis of temperature entrainment it is crucial to map the mutations.

Given that the chemical-induced mutant line *2T-30* exhibited the strongest phenotype among the three lines isolated in term of aperiodic *per-luc* expression, arrhythmicity of locomotor behaviour in constant conditions and inability to entrain rest-activity pattern to TC, we decided to initiate our mapping experiments with this mutation.

The mutagenesis and crossing scheme applied have been performed in order to isolate putative mutations linked to chromosome *2* and *3* (see Figure 3.2). According to this scheme, *2T-30* is located on chromosome *2*. We first investigated whether the mutation complemented the other 2nd-chromosome mutants, known to affect circadian clock. tim^{01} and $vrille^{1}$ are central clock mutants (Sehgal et al., 1994; Blau and Young, 1999) and were our first candidates.

Homozygous *2T-30* flies were crossed with homozygous tim^{01} and $vrille^{1}$ flies. The heterozygous progeny for *2T-30* and *tim* (or *vri*) mutations were tested for their ability to entrain to TC. If *2T-30* affected the same gene as, for instance, tim^{01}, the progeny would not possess a normal copy of the gene and therefore would exhibit the mutant phenotype as the parental lines. In contrast, if the gene affected in line *2T-30* is different from *tim* (or *vri*), complementation would occur resulting in a wild-type phenotype. We also tested a range of 2nd chromosome *transient receptor potential* (*trp*) channel mutants, because they are candidates

for mediating temperature entrainment (see Chapter 5).

Figure 3.21A–H shows complementation test between *2T-30* with two clock genes (*tim* and *vri*), a TRP channel mutant (*trpM*) which exhibits temperature entrainment defects (see Section 5 for more details) and three more TRP channel mutants which do not show temperature entrainment defects (*painless*, *nompC* and double mutant *trp* trp^{l}). The wild-type phenotype of the transheterozygous tim^{01}/*2T-30* was only partially restored in this condition (LL and TC). We then repeated the complementation test and assayed the progeny *2T-30*/tim^{01} in a LD to DD experiment (Figure 3.21I–K), since tim^{01} and most of the *2T-30* mutants are arrhythmic in DD (Sehgal et al., 1994 and Table 3.4). All the tested flies showed strong rhythmicity in DD conditions, indicating that the two genes complemented each other and therefore *2T-30* does not affect *timeless*.

Genetic complementation analysis of 4 *trp* genes suggests that *2T-30* does not affect *trpM*, *painless*, *trp* trp^{l} nor *nompC* (Figure 3.21E–H). Although *2T-30*/$pain^{3}$ is not completely normal, complementation to the the allele $pain^{1}$ restores completely the wild-type phenotype. Both the *pain* alleles are induced by *P*-element insertion in the start region of the *pain* gene and they are both null mutation (Tracey et al., 2003).

The attempt to map the mutation by meiotic recombination with second multiple-marked chromosome which carry recessive mutations associated with morphological markers in known positions, failed. At the moment of writing a finer localization of the mutation is being carried out by deficiency mapping covering all the left arm of chromosome *2*.

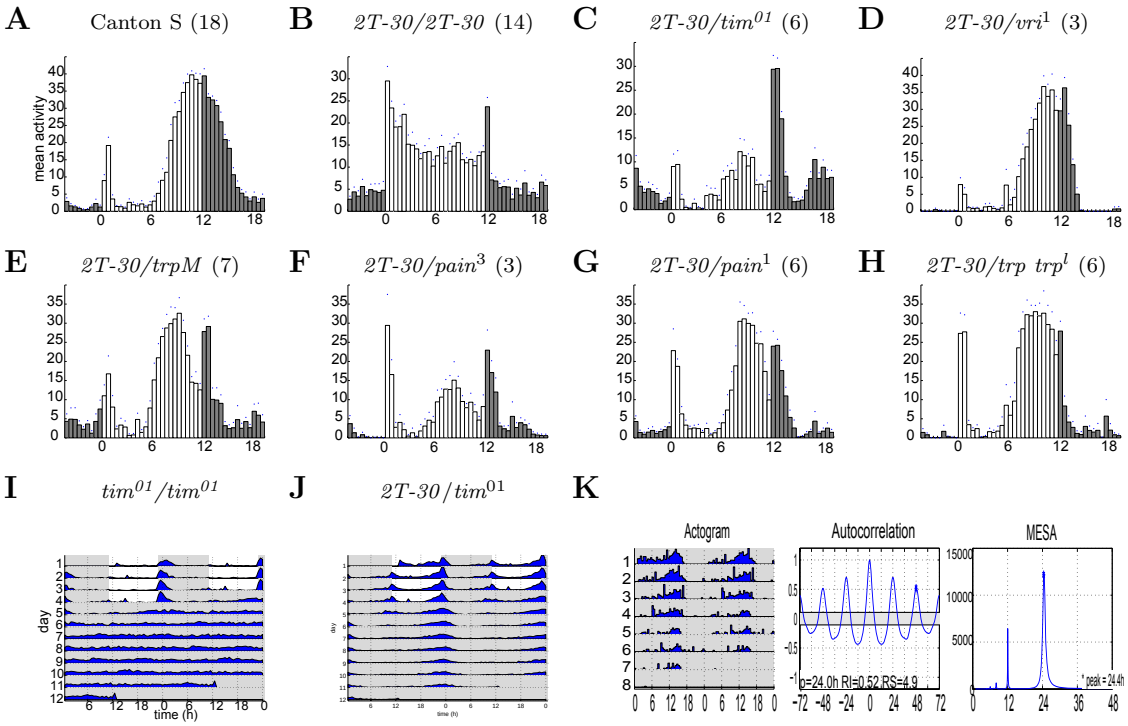

FIGURE 3.21: Complementation test between *2T-30* and 2nd-chromosome mutants during LL and 12:12 hr – 25:16℃ TC. Rest-activity pattern of (A) Canton S, wild-type control, (B) *2T-30* mutant control, (C) *2T-30* over tim^{01}, (D) *2T-30* over $vrille^{1}$, (E) *2T-30* over *trpM*, (F) *2T-30* over $painless^{3}$, (G) *2T-30* over $painless^{1}$ and (H) *2T-30* over *trp* trp^{l}. White bars represent average activity during warm (25℃) and grey bars activity during cold phase (16℃). Number of individual is indicated in brackets. I,J) Average actogram of *y w;* tim^{01}/tim^{01} (n = 12) and *y w;* tim^{01}*/2T-30* (n = 16), respectively, for 4 days in LD followed by 7 days in DD (25℃). Note that DD rhythmicity is rescued in the heterozygous flies (100%, $\tau = 24.1 \pm 0.05$, RI=0.51±0.02, RS=4.8±0.20). K) DD analysis of a representative *y w;* tim^{01}*/2T-30* fly.

3.7 Summary

- Screen of 1637 EMS-induced mutant lines analysing *per-luc* expression in isolated legs during LL and 12:12 hr 25:16℃ TC.
- Isolation of three lines, *2T-30*, *2T-38* and *2P-42*, which have impaired *per-luc* expression specifically during TC (both in LL and DD) and normal in LD conditions.
- Locomotor activity of the three mutant lines is affected specifically during

25:16℃ TC and normal during LD conditions. In particular, they all exhibit a sharp peak of activity after the increase of temperature and a less pronounced peak of activity in the second half of the warm phase. Statistical analysis at different and smaller temperature intervals revealed that all mutants exhibit overall defects of entrainment to temperature, but only mutant line *2T-30* fail to synchronize at 29:25℃ TC when considering the evening anticipation peak only. In DD and TC, *2T-30* mutants do not synchronize their locomotor activity to temperature and they are mainly arrhythmic in constant conditions. *2T-38* flies exhibit mainly a reaction peak to temperature and the entrainment peak is barely visible (and not significant). Line *2P-42*, instead synchronize to TC in DD but not in the same extent as controls.

- Locomotor activity of *2T-30* mutants is mainly arrhythmic in constant conditions, while adult emergence is normal, suggesting that the mutation affects the locomotor output pathway in addition to the temperature entrainment one.

- The mutant line *2T-30* exhibit an "uncoordinated" phenotype when exposed to high temperature and low humidity, suggesting involvement of the chordotonal organs for the gene affected.

- *2T-30* complement with *tim*, *vri*, *trpM*, *pain* and double mutant *trp trpl* in LL and TC, suggesting that the mutation does not hit any of those second chromosome genes.

Chapter 4

Role of the *forkhead domain 3F* gene in the circadian clock

4.1 Screen of 148 RNAi lines for defects in the temperature synchronization of the circadian clock

In parallel to the chemical mutagenesis screen, we screened a library of RNAi lines generated by the National Institute of Genetics Fly Stock Center (Japan) and generously provided by François Rouyer's group (CNRS, Paris, France).

We combined the UAS-GAL4 system (Brand and Perrimon, 1993) with the bioluminescence assay monitoring real-time *per-luc* expression in living flies. Driven by GAL4, the RNAi flies produce double-stranded RNA which induces knockdown of the specific target gene *in vivo*. We used a *tim-gal4* (line 27) driver line in order to down-regulate the expression of targeted genes in all clock cells (*tim*-expressing cells, see Kaneko and Hall, 2000).

In Appendix A are listed the 148 lines we screened, which covered 96 different genes (for most of the genes, 2 independent insertion lines were available). Figure 4.1 shows the crossing scheme we applied to generate flies in which we could assay the RNAi lines for their ability to entrain XLG-*luc* expression to temperature cycles in constant light. For reasons described in the previous chapter, we monitored *per-luc* expression in isolated legs, kept in an insect-tissue culture media. The XLG-*luc* transgene encodes for the full PERIOD protein (except for the last 10 aa) fused to LUCIFERASE (see Figure 3.1). This construct can partially rescue rhythmicity and restore *per* spatial distribution in a per^{01} background (Veleri et al., 2003).

Among the 148 lines screened we isolated one which failed to synchronize *per* expression to temperature in isolated legs. *tim-gal4* down-regulation of *12632-R2* led to misexpression of *per-luc* during LL and TC and during LD cycle (Figure 4.2). The line *12632-R2* affects the gene *CG12632* (Flybase annotation symbol) which encodes the FORKHEAD DOMAIN 3F transcription factor, or FD3F (see below for more details on the gene). In both LD and TC conditions, XLG-*luc* expression is drastically reduced in isolated legs of *tim*-driven RNAi flies, in terms of cycling amplitude and overall expression level. The two upper graphs of Figure 4.2 show the bioluminescence readings of control and *fd3F*-RNAi-R2, respectively. In TC

Screen of UAS-RNAi library driven by *tim-gal4*

P: ♀♀ UAS-RNAi × ♂ $\frac{y\,w}{Y}; \frac{tim-gal4}{CyO}; \frac{XLG-luc}{TM3}$

F_1: ♂ $\frac{+}{Y}; \frac{tim-gal4}{UAS\text{-}RNAi}; \frac{XLG-luc}{+}$ or $\frac{+}{Y}; \frac{tim-gal4}{+}; \frac{XLG-luc}{UAS\text{-}RNAi}$ → to test

FIGURE 4.1: An UAS-RNAi library was crossed to *tim-gal4* (line 27), in order to knock-down specific genes in all the clock cells. Driver line carries also a *per-luc* transgene (XLG-*luc*, line 1:1). *CyO* and *TM3* are balancer chromosome for autosome *2* and *3*, respectively. ♀: virgin female flies, ♂: male flies.

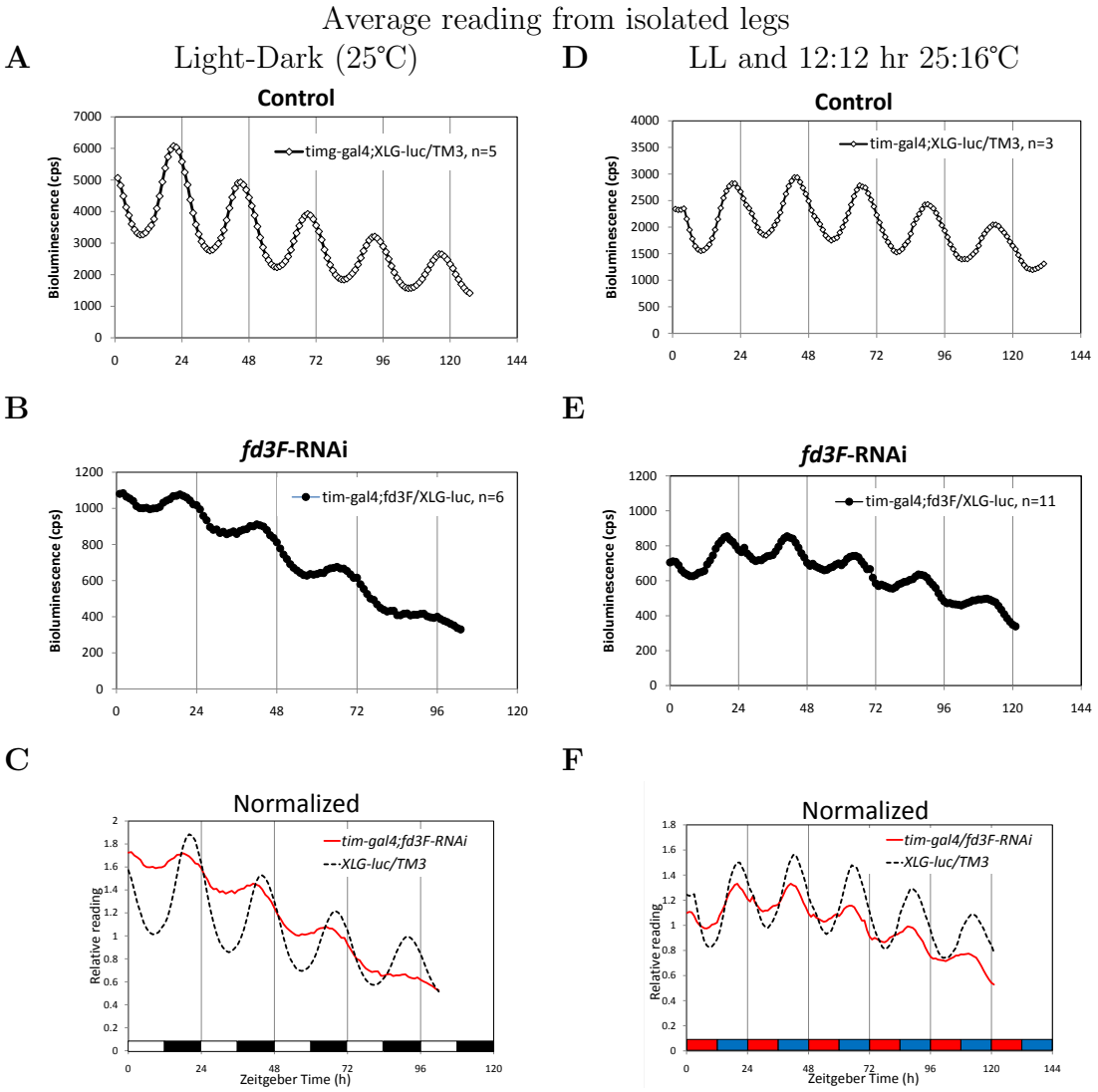

FIGURE 4.2: XLG-*luc* bioluminescence expression from isolated legs of *fd3F*-RNAi-R2 and control flies in light and temperature entrainment. A–B) LUC readings of controls and flies in which *fd3F* is down-regulated by the *tim-gal4* driver (line 27), respectively, during LD cycles (25°C). D–E) *per-luc* expression during LL and 12:12 hr 25:16°C temperature cycles. In both conditions, the level of *per-luc* expression and the cycling amplitude is drastically reduced in the RNAi line compared the control (which carries the same XLG-*luc*). (C, F) To better visualize the effective down-regulation of the *period-luciferase* gene caused by the RNAi line, we plotted the same graphs as above normalizing the bioluminescence reading to the average value for each genotype . Control XLG-*luc*: black dashed line. *fd3F*-RNAi-R2: red solid line. Number of individuals tested is indicated in each graph with the genotype. In LD graphs, white/black bars at the bottom indicate light and dark phase, respectively. In TC graphs, red/blue bars indicate warm and cold phase, respectively. cps: counts per second. ZT: Zeitgeber Time (ZT0 = lights-on or temperature-up. ZT12 = lights-off or temperature-down).

conditions, the expression levels are between 1500 and 3000 counts per second (cps) for the control and between 400–800 cps for the RNAi line. During LD conditions, the difference is similar, if not even higher: 2000–6000 cps for control versus 400–1000 cps of the RNAi. Given the very low level of LUCIFERASE activity in the RNAi flies compared to controls (which carry the same XLG-*luc* transgene), we normalized the expression values to the average values for each genotype (Figure 4.2C,F). This allows a better visualization of the effects of *fd3F* down-regulation not only on the overall *per-luc* expression levels, but also on the amplitude of *per-luc* cycling. The amplitude of *fd3F*-RNAi is 2-fold reduced in LD and 1.5-fold in TC conditions, compared to control. Note also that the phase of *per-luc* expression during LL and TC is 2–3 hours advanced compared to LD conditions, as we already observed in the previous chapter (Section 3.2).

Analysis of *per-luc* expression of *tim-gal4;fd3F*-RNAi-R2 in the whole intact fly was not performed because *tim-gal4:27*-driven *fd3F*-RNAi expression induces adult lethality (flies die 2–3 days after hatching, see below).

A second RNAi line targeting the same gene is available, *12632R-1* (Table A.1). When driven by *tim-gal4*, it induces adult lethality in the same way as the line *12632R-2*. Analysis of *per-luc* expression in legs in LL and 12:12 hr 25:16°C TC gives comparable results, in term of reduction of *per-luc* expression level and 2-fold decrease of cycling amplitude (Figure 4.3). This suggests specificity of the phenotype of the line *12632R-2*, rather than insertional effects due to the presence of the RNAi transgene. Given the reproducibility of the phenotype between the 2 lines, the line *12632R-1* was not investigated further.

Hereafter, all the results of this section refer to the line *12632R-2*, which we will call *fd3F*-RNAi.

A LL and 12:12 hr 25:16°C

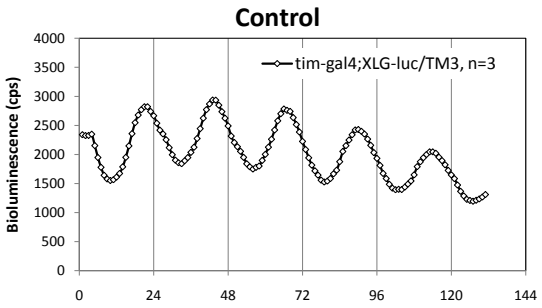

B

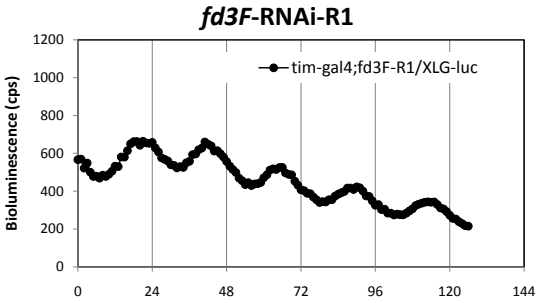

C

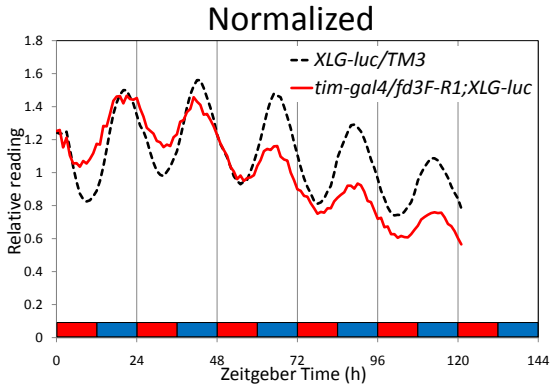

FIGURE 4.3: XLG-*luc* bioluminescence expression of *fd3F*-RNAi-R1 and controls in LL and 12:12 hr 25:16°C temperature entrainment. *per-luc* expression level is drastically reduced and the cycling amplitude is 2-fold decreased. For description of plots, see Figure 4.2

4.2 Behavioural analysis of *fd3f*-RNAi

Driver	Lethality (stage)
tim-gal4:27	Adult day 2–3
tim-gal4:16	Adult day 4–5
tim-gal4:67	Adult day 2–3
nocte-gal4	Pupae
repo-gal4	Pupae
elav-gal4	n.l.
cryBN-gal4	n.l.
Pdf-gal4	n.l.
F-gal4	n.l.

TABLE 4.1: Different lethality effects on *fd3F*-RNAi caused by several driver lines. n.l.: no lethality

When the *fd3F* gene is down regulated with the *tim-gal4:27* driver, flies do not survive the third day of adult stage, suggesting severe defects induced by the RNAi. Light-microscopy inspection did not reveal any gross morphological abnormalities. We tested the effect of several *tim-gal4* lines, which only differ for the insertional position on the chromosomes but not for spatial distribution of *timeless* expression (Kaneko and Hall, 2000). As stated in Table 4.1, there is a slight difference between the onset of lethality induced by line 16 (4–5 days) and lines 27 and 67 (2–3 days). Kaneko and Hall (2000) showed that the *tim-gal4* lines applied in this study have the same spatial expression both in larvae and in the adult. However, there could be some slight spatially differences not detected by Kaneko and Hall and also differences in the expression level (caused by insertion site).

Since *tim-gal4*-induced lethality, locomotor activity of *tim-gal4*/*fd3F*-RNAi flies is difficult to be analysed and we could monitor only 4 days of activity in LD conditions. Although it looks as if the morning peak, which anticipates the transition from dark to light, is missing (or not very pronounced), the LD activity looks normal and comparable to control (Figure 4.4F).

Expressing *fd3F*-RNAi with other drivers, which express in different tissues than *tim-gal4*, does not induce adult lethality and therefore the rest-activity pat-

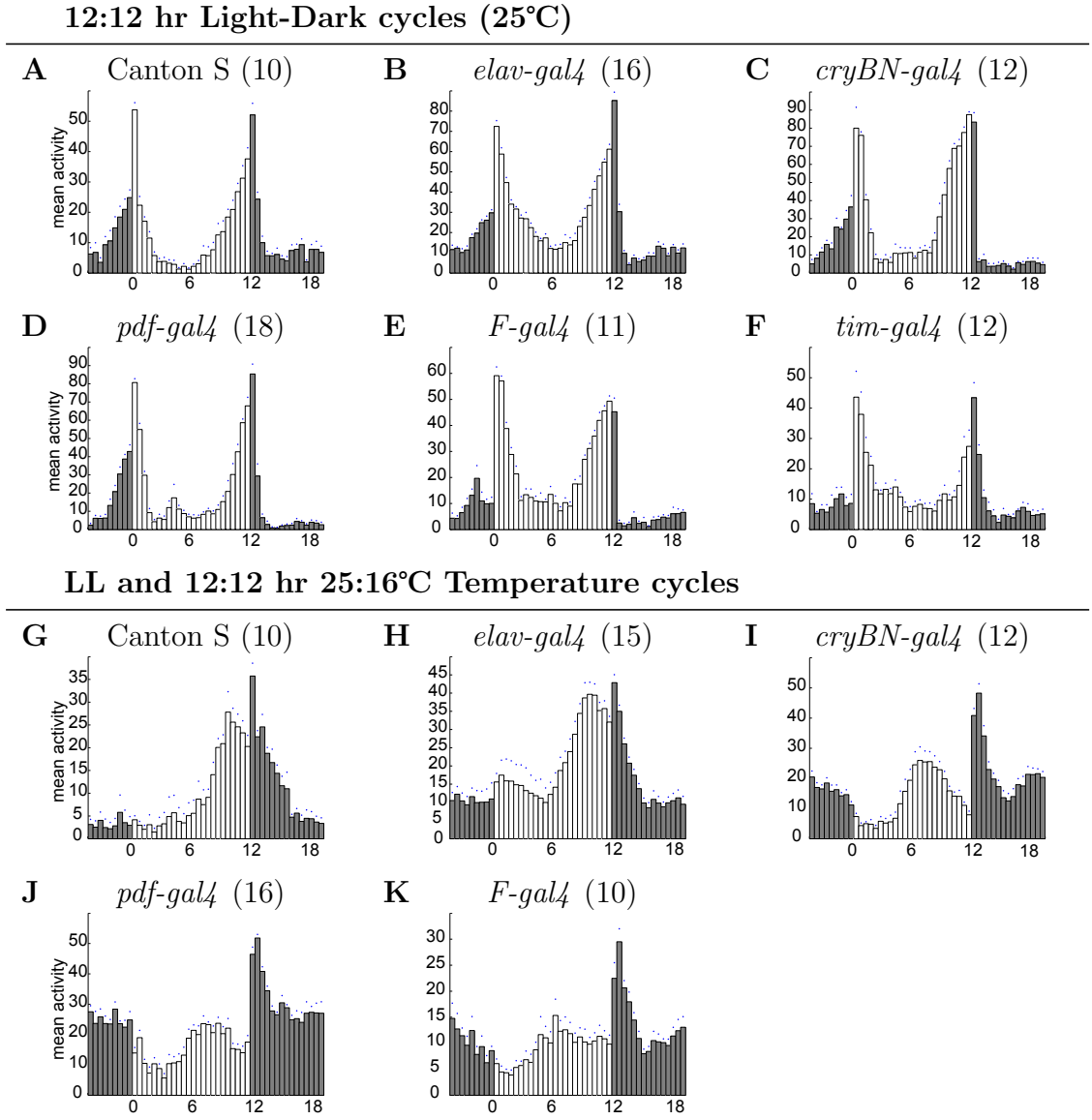

FIGURE 4.4: Rest-activity patterns of *fd3F*-RNAi driven by different GAL4 driver lines, as indicated. Flies were first synchronized to LD cycles for 5–7 days at 25°C (A–F), then subjected for 7 days to constant light and 12:12 hr 25:16°C temperature cycles which was in opposite phase compared the previous LD (G–K). F) *tim-gal4*-driven silencing of *fd3F* induces lethality. However, when line 16 is used, flies survive until day 4–5 of adult stage, so it is possible to monitor rest-activity pattern up to 4–5 days. Only activity during LD entrainment has been analysed and it is normal. Number of individuals tested is indicated in brackets.

terns could be monitored (Figure 4.4 and Table 4.1). When we used the neuronal-specific driver *elav-gal4*, which express GAL4 in the CNS and PNS (Luo et al., 1994), *fd3F*-RNAi flies can synchronize both to LD and LL and TC with no difference compared to control (4.4B,G).

Interestingly, a driver widely expressed like *elav-gal4* does not kill the flies, while *tim-gal4* does (Table 4.1). This suggests either that FD3F executes essential functions in non-neuronal *tim*-expressing cells or that *elav-gal4* is not as strongly expressed as *tim-gal4*. Moreover, when we silenced *fd3F* with the *nocte-gal4* driver, which is broadly expressed in the fly, including neurons and glia cells in CNS (Sehadova et al., 2009), *fd3F* flies do not hatch (flies die at the pupal stage). Given that the glia-specific driver *repo-gal4* (Sepp et al., 2001) also induces *fd3F*-RNAi pupal lethality, we could speculate an essential role for FD3F in glia cells.

We then investigated locomotor behaviour of *fd3F*-RNAi when down-regulated by drivers specific to subgroups of clock neurons. CRY is expressed in small- and large-LN_vs, 3 LN_ds and some DN_1 neurons (Yoshii et al., 2009b). If *fd3F* down-regulation is restricted to *cry* expressing cells using a *cry-gal4* line (Emery et al., 2000), flies entrain normally to LD cycles (Figure 4.4C) and to temperature cycles: the evening peak of activity is advanced and flies are more active during the cold phase compared to controls (Figure 4.4I). The mean activity during the cold phase (per 30 minutes interval) is 20.3 for *cry-gal4*/*fd3F*-RNAi versus 9.0 for the wt control. The overall pattern of activity, in particular if we consider the anticipation from warm to cold, is normal. We observed similar results when we crossed *pdf-gal4* to UAS-*fd3F*-RNAi. In this case, *fd3F* is silenced in the PDF-positive LN_vs (Park et al., 2000). Locomotor activity in LD cycles is again normal but in TC flies do not exhibit a clear and pronounced evening anticipation of the transition to 16℃ and flies are more active during the cold phase (mean activity

28.9).

A more severe temperature entrainment phenotype was seen when we silenced *fd3F* with *F-gal4* (Figure 4.4K), a chordotonal (ch) organ driver line (Kim et al., 2003; Sehadova et al., 2009). LD entrainment is not affected (Figure 4.4E) but, interestingly, temperature entrainment in LL is compromised (Figure 4.4K). There is no evening anticipatory peak but a gradual increase of activity towards the middle of the day (as in *Pdf-gal4*) but not a clear reduction afterwards. The overall level of activity in the cold phase is comparable to the controls (mean activity 12.6) but flies exhibit mainly a reaction to temperature changes, typical phenotype of "temperature mutants" (Glaser and Stanewsky, 2005; Sehadova et al., 2009). Although these are preliminary results, and analysis of *F-gal4*-driven *fd3F*-RNAi need to be addressed more in details and in different conditions, this is very intriguing. Our group already reported the importance of ch organs for temperature entrainment (see further sections and Sehadova et al, 2009). This data suggest a good potential candidate (a forkhead transcription factor) for TC-dependent transcription regulation in ch organs (see below and Discussion).

However, it is important to mention that *F-gal4* is not expressed exclusively in neurons of ch organs as reported by Kim et al. (2003), but also in a number of putative chemoreceptive and mechanoreceptive external sensory organs located in the legs, labial and maxillary pulpus, wings, haltere and antennae. It is also expressed in the retina and neurons of the central brain, most prominently within the antennal lobes (Sehadova et al., 2009). I mention this because the function of FD3F could be executed in different structures than — or not only in — ch organs.

Finally we examined whether the down-regulation of the forkhead transcription factor has any effects on the free-running locomotor activity in constant conditions.

Genotype	n	% rhythmic	τ (h) ± SEM	RI ± SEM	RS ± SEM
+;fd3F-RNAi	11	90.1%	24.1 ± 0.2	0.45 ± 0.02	4.3 ± 0.3
cry-gal4/fd3F-RNAi	18	94.4%	24.5 ± 0.1	0.45 ± 0.02	4.3 ± 0.2
Pdf-gal4;fd3F/+	18	100%	24.4 ± 0.1	0.47 ± 0.03	4.9 ± 0.3

TABLE 4.2: Free-running locomotor rhythmicity of control (non-driven RNAi line) and *fd3F*-RNAi driven by *cry-gal4* and *Pdf-gal4*. Flies were entrained in LD (for at least 3 days) then released to DD and constant temperature (25℃). The free-running period (τ) of rhythmic flies is calculated and autocorrelation values are shown. RI: Rhythmicity Index. RS: Rhythmicity Statistic. SEM: Standard Error of the Mean.

When we silenced FD3F with *cry-gal4* or *Pdf-gal4* and monitored activity in constant conditions, flies free-run with a strong rhythm and normal period (Table 4.2). This suggests that FD3F does not execute essential clock function in *Pdf*- and *cry*-cells. Since *Pdf*-expressing ventro-lateral neurons (LN_vs) are necessary to generate DD free-run activity (Frisch et al., 1994; Blanchardon et al., 2001), we can speculate that FD3F function is not required to generate free-running activity driven by the *Pdf* cells.

4.3 FD3F affects PERIOD accumulation in LL and TC

We showed that *tim-gal4*-driven down-regulation of *fd3F* compromised *period-luciferase* expression, both during LD and during LL and temperature cycles. We wondered whether this is reflected at the protein level, i.e. if temporal PER accumulation is normal or not, as suggested by the abnormal *per-luc* expression. For this, we quantified PERIOD protein levels isolated from head-extracts of individuals that have been previously entrained in LD or LL and TC, at 4 hr intervals.

We showed that *tim-gal4:16* driven knocked-down of *fd3F* induces adult lethality at day 4–5, thus we entrained flies to different environmental conditions from

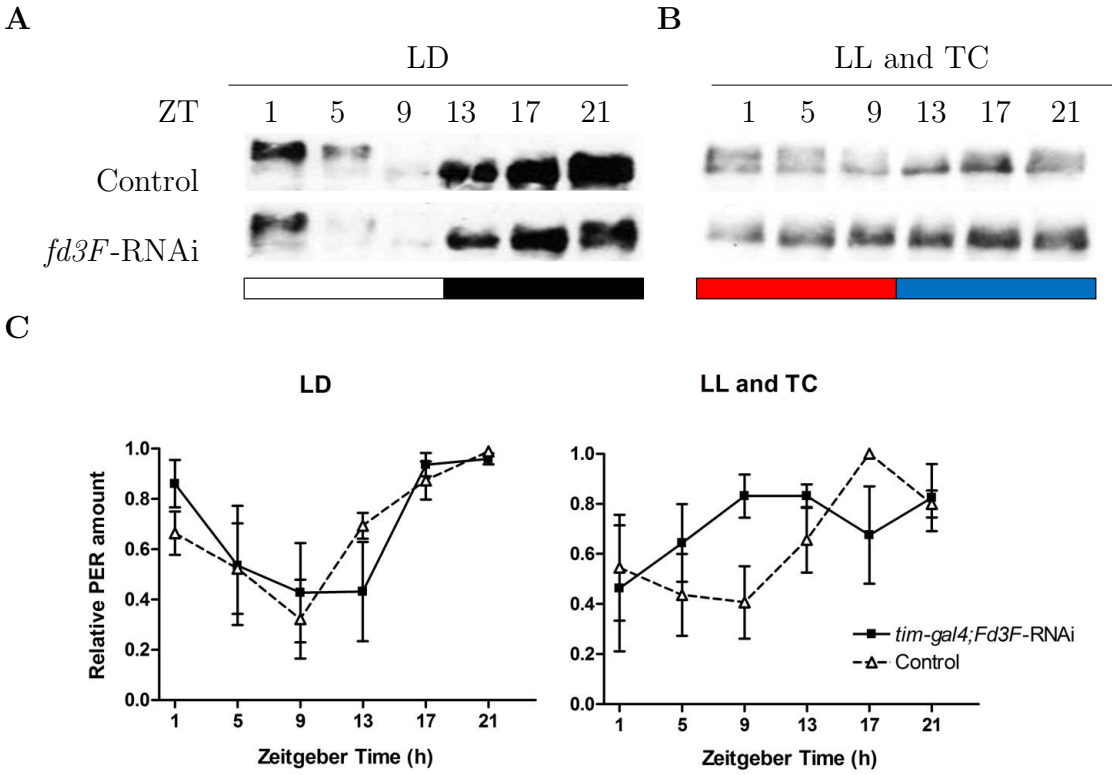

FIGURE 4.5: Quantification of PERIOD amount in head-extracts of *fd3F* flies and controls. Western blot of PER protein extracted from equal amount of heads from flies entrained for 4 days in LD (A) or LL and 12:12 hr 25:16°C temperature cycles (B). *tim-gal4* line 16 was used to silence *fd3F* in clock cells. *tim-gal4/fd3F*-RNAi flies have been entrained since eclosion, due to early lethality in adult stage (see Table 4.1). C) Quantification of PER in *fd3F*-RNAi and control flies from 3 independent experiments of 20-25 individuals each. Error bars indicate SEM. "Control" is the non-driven parental line *fd3F*-RNAi. ZT: Zeitgeber Time (ZT0 is lights-on or temperature-up. ZT12 is lights-off or temperature-down).

the time of eclosion, in order to have enough days of entrainment before the flies died.

During LD entrainment, PER protein oscillates with a peak at ZT21 and trough at ZT9, both in control and in *tim-gal4/fd3F*-RNAi flies (Figure 4.5). In the RNAi flies, we observed a slight extension of the PER trough (until ZT13), even though with a prominent error, indicating non-continuity between independent experiments. These data are conflicting with the previously described *per-luc*

oscillation results, which indicated defects on *per* expression also in LD conditions. However, *per-luc* expression has been monitored in isolated legs, while the PER protein has been quantified from head-extracts.

During LL and TC entrainment, PER protein in wild-type heads oscillates with a smaller amplitude compared to LD conditions (Figure 4.5B–C), and the protein peaks 2–3 hours earlier (compare also Glaser and Stanewsky, 2005). This fits well with the advanced peak of *per-luc* expression and the earlier evening peak of locomotor activity in LL and TC compared to LD entrainment, described in the previous chapter (Section 3.2). PER in *fd3F*-RNAi flies, is highly accumulated and it seems to weakly oscillate with opposite phase compared the control, but with no statistical significance ($p > 0.05$, 1-way Anova). It is also difficult to distinguish different PER bands corresponding to the different forms of the phosphorylated protein (compare control at ZT1, for instance, and Edery et al., 1994), suggesting defects in PER phosophorylation and subsequent degradation during the warm phase of TC.

4.4 *fd3F* alters the phase of eclosion

RNAi-mediated down-regulation of *fd3F* in all clock cells (via *tim-gal4*) induces early lethality and therefore behavioural analysis of the knocked-down flies is restricted to a few days only. Therefore, we opted to investigate another circadian rhythmicity to complement the limited locomotor rest-activity pattern analysis.

We investigated the eclosion activity of *fd3F*-RNAi flies driven by *tim-gal4* during LL and TC conditions. Pupae of Canton S wild-type cultures synchronize their eclosion rhythm to TC in 2 days and the peak of emergence occurs towards the end of the cold phase (Figure 4.6A–B). We silenced *fd3F* with 3 different

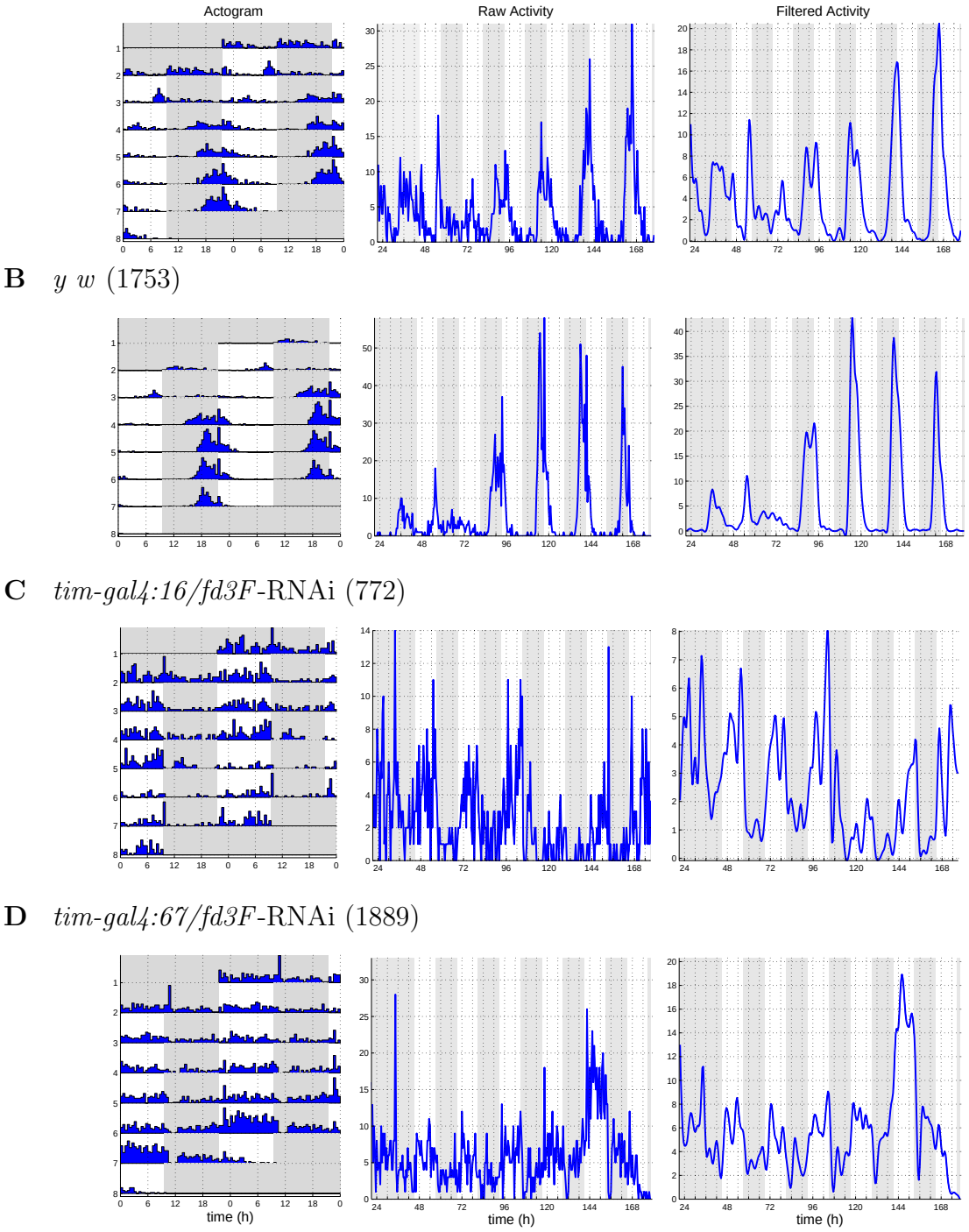
Constant light and 25:16°C Temperature cycles
A Canton S (1332)
Actogram
Raw Activity
Filtered Activity
B *y w* (1753)
C *tim-gal4:16/fd3F*-RNAi (772)
D *tim-gal4:67/fd3F*-RNAi (1889)
time (h)
time (h)
time (h)

FIGURE 4.6

E *tim-gal4:27;fd3F*-RNAi (1205)

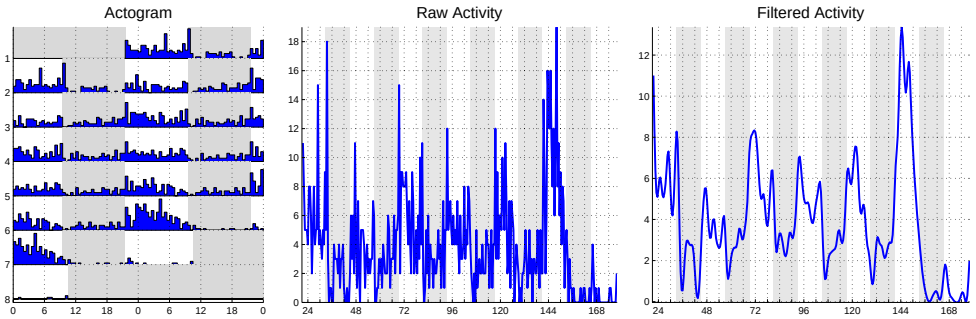

F *tim-gal4/fd3F*-RNAi (3753)

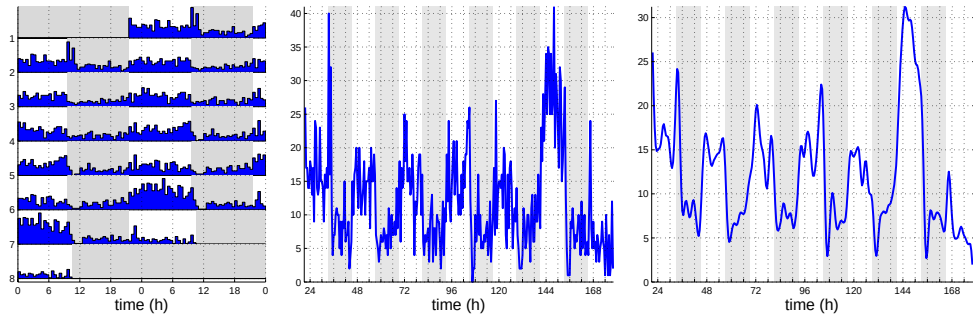

G

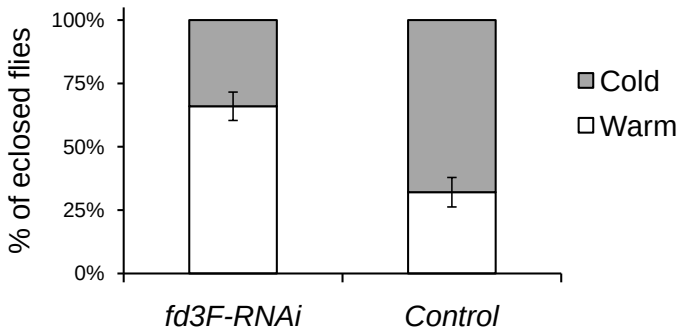

tim-gal4 driver lines (16, 67 and 27, see M&M), and then monitored the eclosion activity during LL and TC entrainment. The eclosion occurs rhythmically, synchronized with TC, but with a different phase compared the control. The flies eclose mainly during the warm phase (25℃) and no distinct eclosion peak is visible (Figure 4.6C–E). We did not observe any difference of eclosion activity when different *tim-gal4* lines were used to silence *fd3F*. Therefore, we could combine the results of the 3 independent experiments in a single plot in which the phenotype was even more prominent (Figure 4.6F). Control cultures move their eclosion phase from the previous "LD-entrained" to the "TC-entrained" in the first 2 days, and they stabilize their phase with the temperature cycles from day 3. In contrast, *fd3F*-RNAi cultures always (and immediately) hatch in the warm-phase. Although this might be interpreted as lack of entrainment, analysis of the clock mutant per^{01} suggests that *fd3F*-RNAi exhibits a difference of eclosion phase rather than lack of synchronization (see chapter 6, Figure 6.2 and Discussion).

FIGURE 4.6 *(preceding page)*: Eclosion profiles of control and *fd3F*-RNAi cultures in LL and TC. A–F) The left columns show double-plot actograms of flies emerged during LL and 12:12 hr 25:16℃ TC, which was in opposite phase compared to the previous LD entrainment. Only the last dark cycle of the previous LD entrainment is indicated (in A–D). The two right-hand columns depict, respectively, the total number of flies emerged as a function of time ("raw activity", middle plot) and 4-hr low-pass filtered versions of the middle plots ("filtered activity", right-hand plot, see M&M for more details). The total number of flies emerged is indicated in brackets next to the genotype. Shaded areas refer to temperature conditions (grey shading: 16℃; white shading: 25℃). A–B) Canton S and *y w* control flies synchronize eclosion to TC in 2 days and, once synchronized, exhibit peak of emergence during the last part of the cold phase (ZT22–23). C–E) *fd3F*-RNAi driven by *tim-gal4* eclose with a different phase, emerging mainly at 25℃, regardless of the *tim-gal4* line used (16, 67 and 27, respectively). We thus combined the 3 independent experiments (F) to better visualize this phenomenon. G) Quantification of number of flies eclosed during the warm phase (white bar) compared the cold phase (grey bar). There is a statistically significant preference ($F_{(1,2)}$=26.88, P<0.05, two-way ANOVA) in *fd3F*-RNAi to emerge during the warm phase compared to control flies. Plot generated from average of 3 independent experiments. Error bars indicate SEM.

To support the idea that *tim-gal4/fd3F*-RNAi has a different eclosion phase, we calculated the number of flies eclosed during the warm phase, compared to the ones emerged in the cold. Figure 4.6G shows a striking difference between the number of *fd3F*-RNAi flies which eclose during the warm phase (66 ± 5.6%) compared the control (32 ± 5.8%). The analysis of variance between the RNAi line and control reveals statistical significance ($F_{(1,2)}$=26.88, P<0.05, Two-way Anova).

The eclosion profile of *fd3F*-RNAi, induced by *tim-gal4* (line 67) has been monitored in free-running conditions (Figure 4.7). After LD entrainment, control flies (Canton S and *y w*, in our case) emerge rhythmically in DD with a strong period of circa 24 hours (24.5 and 23.8 hours, respectively). *fd3F*-RNAi flies also eclose rhythmically in constant conditions, with a period of 24.3 hours, although the rhythm is not as strong as in the control flies: the profile is "noisier" and the peak less "sharp" compared to control, which is also indicated by the lower RS values.

The eclosion peak of wt cultures is centred to the transition between the subjective dark- to light-phase, following the pattern of eclosion during LD cycles, where the majority of flies emerge at dawn (Figure 4.7 and Qiu and Hardin, 1996). Interestingly, *fd3F* knocked-down flies eclose mainly during the whole part corresponding the subjective day, and the peak is "broader" and centred at the middle of the subjective light-phase. This correlates with the eclosion activity during TC, which is phase-shifted (towards the warm phase) compared to the controls (Figure 4.7 and 4.6).

It has been shown previously that mutants can affect the phase of eclosion. Mutants for the RNA-binding protein LARK, for instance, exhibit an early-eclosion phenotype: *lark* mutant eclose several hours earlier than control both during LD

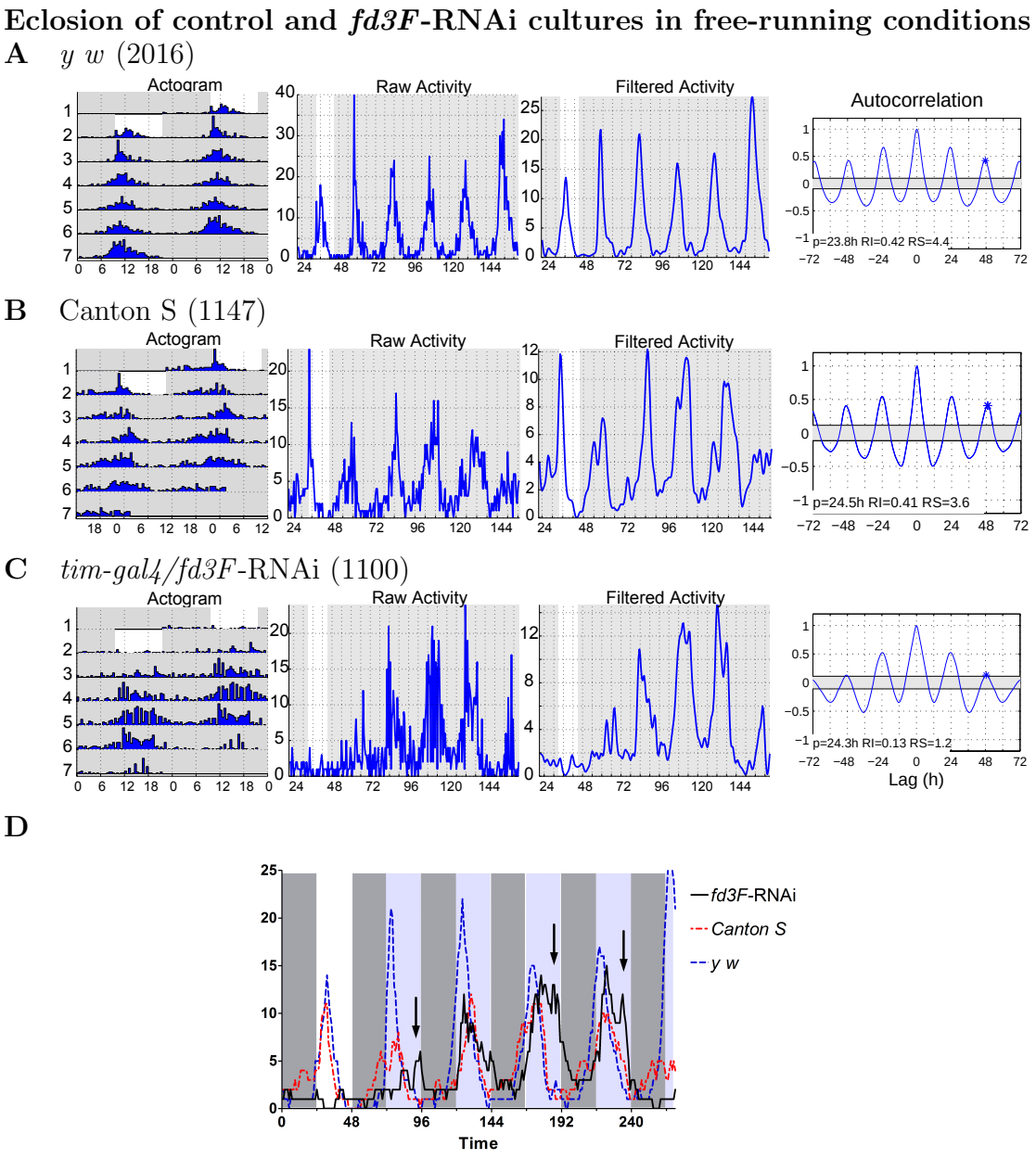

FIGURE 4.7: Flies were entrained in LD and then released to DD (at 20°C). Only the last cycle of LD is included in the plot. The 3 left-hand columns are as described in Figure 4.6. The most right-hand plot depicts the autocorrelation values calculated for the DD part only. A) *y w* and (B) Canton S flies exhibit free-running rhythm with a period of 23.8 and 24.5 hr, respectively. C) *tim-gal4/fd3F*-RNAi (line 67) eclosed rhythmically with a period of 24.3 hr. Number of flies eclosed is indicated in brackets. D) Eclosion activity of the cultures depicted in (A–C) to which a 5-point moving average has been applied. *fd3F*-RNAi flies eclose with a later phase compared to controls (arrows). Light- and dark-grey areas indicate subjective days and nights, respectively.

and TC entrainment (Newby and Jackson, 1993). Accumulation of the clock proteins PER and TIM in *lark* mutant is normal as well as locomotor activity, suggesting that LARK acts specifically on the "eclosion output pathway" of the clock (McNeil et al., 1998; Schroeder et al., 2003). Our data, however, indicate abnormal PER-LUC expression and PER accumulation in *fd3F*-RNAi adults, together with the delayed-phase of eclosion and abnormal behaviour of adults during TC (when driven by *F-gal4*). The transcription factor nature of the gene, suggests more a role on clock gene expression, rather than on the output pathway (see Discussion).

4.5 Role and function of forkhead transcription factors

In the RNAi screen, monitoring real-time *per-luc* expression in tissue cultures kept in LL and TC, we isolated the line *CG12632* as showing impaired *period* synchronization. The line affects the gene *forkhead domain 3F* (or *fd3F*) which encodes a forkhead domain containing protein. What are forkhead proteins?

Forkhead domains, known also as "winged helix", are a family of DNA-binding domains highly conserved between different eukaryotic transcription factors, from yeast to humans (Lai et al., 1993). They were first discovered in *Drosophila* as proteins required for the proper development of the terminal structures of the anterio- and posterio-gut. *forkhead* mutants fail to develop correctly and the embryo shows a "spiked head" — hence the name (Weigel et al., 1989). While the detailed temporal and spatial expression of forkhead domain proteins differ, they are expressed in many, if not all, tissues (Lai et al., 1993). The mammalian counterparts of *Drosophila*'s forkhead proteins are Hepatocyte Nuclear Factor-3 (HNF-

3), named because they are required to activate specifically expression of genes in the rat and mouse liver (Clark et al., 1993). Interestingly, mammalian HNF-3 transcription factors are under the control of the circadian clock and their expression is regulated by clock-controlled gene (CCG) promoters (Bozek et al., 2009). HNF-3 mRNA expression is reduced by the *Clock* mutation and up-regulated in *Cry*-deficient mice (Oishi et al., 2003).

In *Drosophila* there are 17 forkhead domain protein encoding genes. Only 6 of them are characterized and studied; Those include *forkhead* (*fkh*), *sloppy paired 1* (*slp1*), *sloppy paired 2* (*slp2*), *crocodile* (*croc*), *jumeaux* (*jumu*) and *biniou* (*bin*) (reviewed by Kaufmann and Knochel, 1996; Lee and Frasch, 2004). Phylogenetic analysis with each other and with mouse orthologues allows classification of 13 members (out of 17) to 10 subgroups (Figure 4.8). The classification considers sequence comparison with forkhead domain in mouse and rat rooted with the forkhead domain sequence from the yeast protein Fhl1p as an outgroup (Lee and Frasch, 2004). The remaining 4 genes cannot be grouped within any subclass that are known in chordates, and are named according their cytological position (Lee and Frasch, 2004). One of these 4 is *fd3F* which maps to position *3F* on chromosome *X* (*3F2*), and it does not have a mouse homologue.

fd3F mRNA expression is broadly distributed during early embryonic stages (until stage 12, see Figure 4.9, taken from Lee and Frasch, 2004). Interestingly, after stage 12, *fd3F* expression is restricted to a subgroup of cells which, based upon their position and arrangements, corresponds to chordotonal sensory organs and their precursor (Lee and Frasch, 2004). These observations are in good agreement with our findings, which showed that *F-gal* (ch organ-specific) down-regulation of *fd3F* exhibits defects of synchronization of locomotor behaviour to temperature cycles (Figure 4.4K).

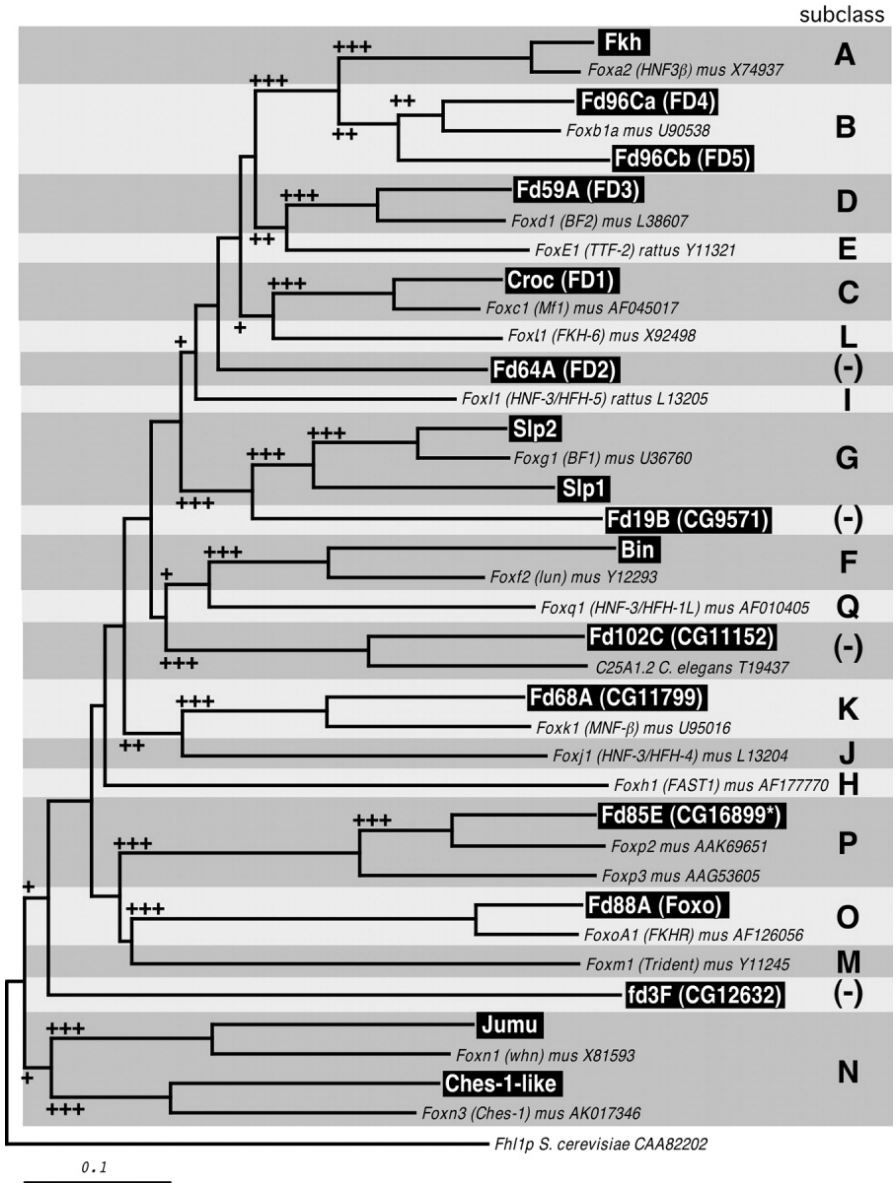

FIGURE 4.8: Phylogenetic tree of *Drosophila* and mouse forkhead domains. The tree is constructed from sequence alignment of all *Drosophila* forkehaed domains with each other and and with mouse orthologs, using the forkhead domain sequence from the yeast protein Fhl1p as an outgroup. *Drosophila* proteins are shown in black boxes. CG numbers refer to Computed Gene Products as predicted by the Berkeley Drosophila Genome Project (BDGP). The bar denotes 10% divergence. Nodes with a bootstrap value of $< 50\%$ are unmarked, those at 50–75% are marked +, 77-95% ++, and 95-100% +++. This figure is taken from Lee and Frasch (2004).

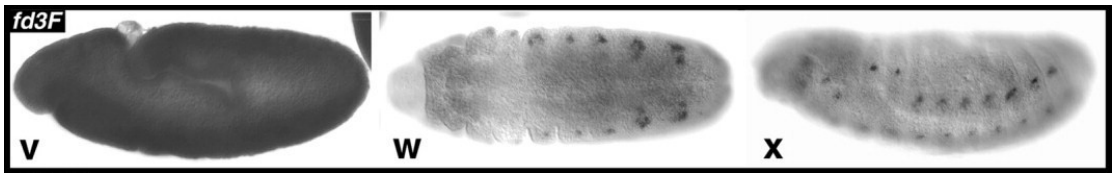

FIGURE 4.9: mRNA expression pattern of *fd3F* gene in *Drosophila* embryos. v) Stage 10 embryo with uniform *fd3F* mRNA expression, w) ventral view of early stage 12 embryo with *fd3F* mRNA expression in chordotonal sensory precursor cells and (x) lateral view of stage 15 embryo with expression in chordotonal organs. Figure taken from Lee and Frasch (2004).

Given that ch organs are required for clock entrainment to TC (Sehadova et al., 2009), we can speculate that *fd3F* plays a role in this mechanism and in these structures. The transcription factor nature of the protein suggests a possible regulation of important target genes required for temperature entrainment (*nocte*?), which, so far, are mainly unknown.

It has been reported that a gene related to the class of forkhead domain transcription factors is involved in circadian rhythm. *Circadianly Regulated Gene 1* (*Crg-1*) is circadianly expressed with the same phase as *per* and *tim* and its spatial distribution overlaps with that of *per* — at least in *Drosophila* heads (Rouyer et al., 1997). Interestingly, genomic sequence analysis of different *Drosophila* species showed that *Crg-1* is a chimeric gene originating from a genomic duplication and fusion of the *fd3F* and *Tousled-like kinase* (*tlk*) genes (Hogan and Bettencourt, 2009 and Figure 4.10). *fd3F* is present in all the *Drosophila* species according to this study, while *Crg-1* is absent in evolutionary related species like *D. simulans* and *D. yakuba* and appears only in *D. melanogaster* (which originated ∼2.3 million years ago) (Hogan and Bettencourt, 2009). This explains why *Crg-1* exhibits high sequence similarity with *fd3F*. However, even if *Crg-1* probably acquired the novel function as circadian regulator only after the duplication event (Hogan and Bettencourt, 2009), we can not exclude a possible circadian regulation for *fd3F* as

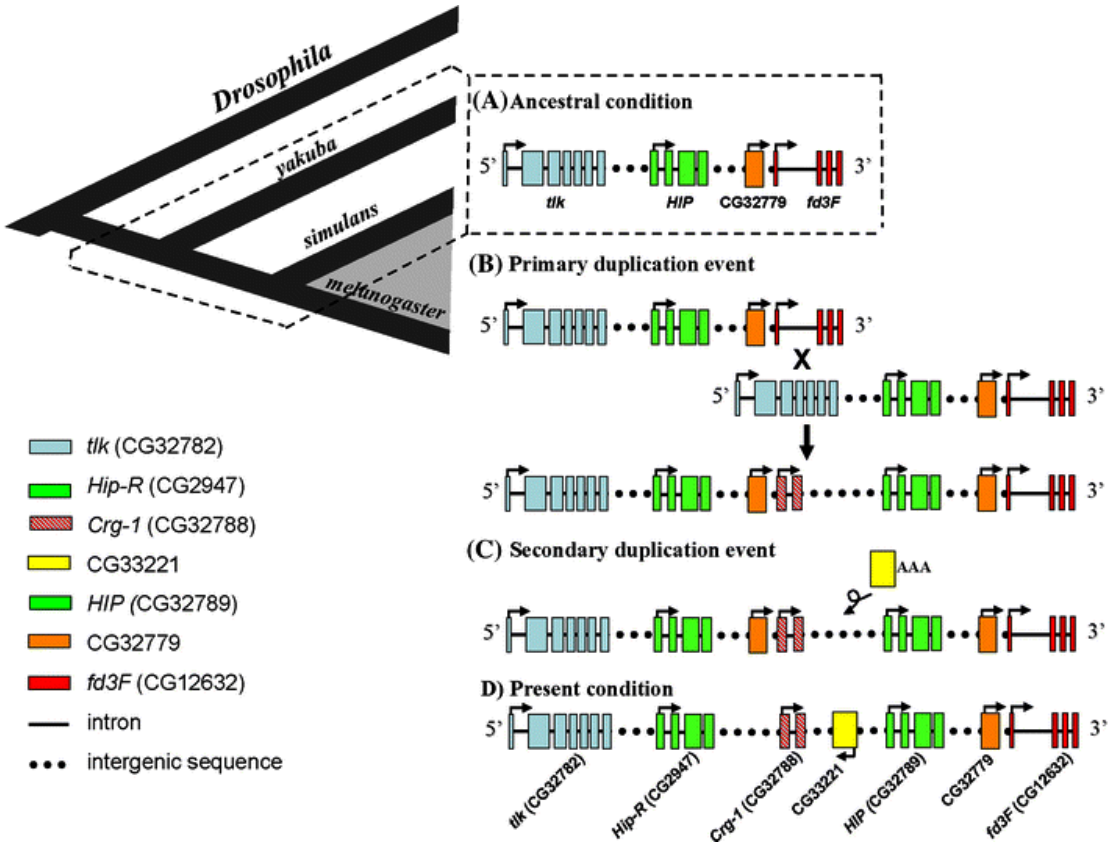

FIGURE 4.10: Schematic of the duplication model for the *fd3f* locus. Ancestral condition of closely related *Drosophila* species contain single copies of *tlk*, *HIP*, *CG32779*, and *fd3F*. Only *D. melanogaster* possesses the duplication. An unequal crossover event gave rise to a region composed of seven genes through the complete duplication of *HIP* and *CG32779* and the formation of a new gene, *Crg1*, through the fusion of portions of *tlk* and *fd3F*. This figure is taken from Hogan and Bettencourt (2009).

well.

Analysis of protein interaction libraries based on genome-wide yeast 2-hybrid data, reveals putative interactions of FD3F with 2 proteins: NINAE and X11L. We considered three independent *Drosophila* interaction databases, BioGrid (Stark et al., 2006), IntAct (Hermjakob et al., 2004) and Mint (Zanzoni et al., 2002): the three of them indicated identical putative interactions.

The *neither inactivation nor afterpotential E* (*ninaE*) gene encodes the major visual pigment protein (Rhodopsin 1) contained in *Drosophila* photoreceptor cells

R1–R6 (O'Tousa et al., 1985). *ninaE* mutants lack the rhodopsin protein Rh1 and although the light-sensitivity of the mutant is reduced in circadian context (Stanewsky et al., 1998), it does not affect the light-dependent degradation of TIM (Yang et al., 1998).

The *Drosophila* X11L is homologue to the mammalian X11L proteins, which interact with the cytoplasmic domain of the amyloid precursor protein (APP) and act as adapter proteins during the regulation of neural function (Hase et al., 2002). X11L plays an important role in the preservation and/or degeneration of neuronal functions (Hase et al., 2002). In *Drosophila*, the expression of the X11L is neural tissue-specific, and its overexpression results in destruction of the eye morphology probably due to enhanced developmental apoptosis (Hase et al., 2002; Vishnu et al., 2006).

Based on these observations, it is difficult to speculate a role for FD3F, in particular, it is not known whether *fd3F* is co-expressed with *ninaE* and/or *x11l*. Furthermore, the interactions are suggested by databases which are based on the yeast system and thus the interactions may not occur *in vivo*.

4.6 Summary

- *tim-gal4*-driven knock-down of *fd3F* reduces the expression level and cycling amplitude of *per-luc* both during LD and TC conditions.
- PER protein during TC is not cycling and is highly expressed throughout the day, while it is normal in LD conditions.
- Adult *tim-gal4* down-regulated flies do not survive more than 4–5 days after hatching and display a normal locomotor activity in LD.

- *F-gal4*-driven down-regulation compromises the ability of the flies to synchronize their rest-activity pattern to TC.

- *fd3F* embryonic expression is restricted to ch organs suggesting an active role for the transcription factor in development of the ch organs, supporting the observation of locomotor synchronization defects of the RNAi line when driven by *F-gal4*.

- Eclosion activity is rhythmic in DD conditions, and therefore the central oscillator is not affected. However, *tim–gal4*-driven *fd3F*-RNAi flies eclose mainly during the warm phase in temperature entrainment conditions with implications to the regulation of eclosion phase.

Chapter 5

Involvement of TRP channels in temperature synchronization of the circadian clock

5.1 Background

In the previous chapters, we described two screens we performed in order to isolate novel components playing a role in the entrainment of the circadian clock of *Drosophila melanogaster*. The screens were based on random chemical mutagenesis and screen of RNAi library, respectively. These two approaches, although different, share very similar principles, i.e. "forward genetics". This means that we started inducing mutants (or making use of available RNAi libraries) and screen for a phenotype — in our case, defects of entrainment of the circadian clock to TC. The mutation responsible for the mutant phenotype is then identified (step unnecessary in the case of the RNAi screen) and further analyses are conducted to determine the role of the gene affected and the function being studied.

The work described in this chapter made use of a "reverse genetics" approach. Instead of searching for the genetic basis of a particular phenotype (defect of temperature entrainment), we used a candidate gene approach. For this, we utilized the RNAi technique (and the availability of genomic RNAi libraries), and specific mutants to knock-out (or knock-down, in case of RNAi) genes which we thought might be possible candidates for playing a role in the temperature entrainment mechanism.

The transient receptor potential (TRP) family of cation channels are ubiquitously involved in sensory physiology. They are highly conserved between organisms, from nematodes to human and they respond to light, temperature, touch, pain, sound, humidity and mechanical stress (reviewed by Clapham, 2003; Montell, 2005; Minke and Parnas, 2006; Hardie, 2007).

In *Drosophila* there are 13 *trp* channel encoding genes, belonging to 7 different subgroups, or classes (Table 5.1). Most of them have been implied to function in several physiological sensory responses (Table 5.1).

Although the mechanisms underlying the temperature synchronization of the circadian clock is only poorly understood, it is reasonable to imagine the requirement of temperature sensors, able to "sense" and transmit the temperature information from the external, environmental world, to the internal, physiological environment (and thereafter, to the central clock). Given the distribution and variety of TRP channels in sensory physiology, they were our first candidates as putative components for the temperature input pathway to the circadian clock.

Class	Gene	Mutant alleles	RNAi	Described function	References
TRPM	*trpM*	$trpM^{EY01618}$ †, $trpm^{1}$, $trpm^{2}$	2+2*	Mg^{2+} homeostasis	Hofmann et al. (2010)
TRPV	*nanchung*	nan^{dy5} †, nan^{36a} †	2	hearing, hygrosensation, geotaxis	Kim et al. (2003); Gong et al. (2004); Liu et al. (2007); Sun et al. (2009)
	inactive	iav^{1}	2	hearing, geotaxis	Gong et al. (2004); Sun et al. (2009)
TRPA	*TrpA1*	$TrpA1^{ins}$ †	1	warm avoidance, chemical nociception	Hamada et al. (2008); Rosenzweig et al. (2005, 2008); Kang et al. (2010)
	painless	$pain^{1}$ †, $pain^{3}$ †	1+1*	nociception, geotaxis	Tracey et al. (2003); Sun et al. (2009)
	pyrexia	pyx^{2} †, pyx^{3} †	1	high temperature tolerance, geotaxis	Lee et al. (2005); Sun et al. (2009)
	water witch	RNAi dominant negative transgenes	n.a.	hygrosensation	Liu et al. (2007)
TRPC	*trp*	trp^{P343} †	3+1*	vision, cold avoidance	Montell and Caterina (2007); Rosenzweig et al. (2008)
	trpl	$trpl^{302}$ †	1	vison, cold avoidance	Montell and Caterina (2007); Rosenzweig et al. (2008)
		$trpl^{302}$;trp^{P343} †		vision, cold avoidance	Montell and Caterina (2007); Rosenzweig et al. (2008)
	trp-γ	*trp-γ*^{MB06664}	2	vision	Xu et al. (2000)
TRPN	*nompC*	$nompC^{3}$, $nompC^{4}$	n.a.	mechanoreception	Walker et al. (2000)
TRPP	*Pkd2*	$Pkd2^{1}$ $Pkd2^{MB06703}$	2	sperm motility, smooth muscle function	Gao et al. (2003, 2004)
TRPML	*CG8743*	$CG8743^{PL00182}$	2	autophagy	Venkatachalam et al. (2008)

TABLE 5.1: List of the 13 *trp* channel encoding *Drosophila* genes. TRP channels are classified in 7 subgroups or classes. The function of TRP channels (if known) is indicated. Several mutants targeting *trp* genes are available and only the one marked with daggers (†) have been assayed in this study. RNAi lines used in this Thesis were provided by the VDRC, except the ones marked with an asterisk which were provided by the NIG Fly Stock Center (and the number of insertion lines indicated). "n.a.": not available.

5.2 Analysis of RNAi targeting *trp* genes

Our "reverse genetic" approach involved the use the RNAi technique of available lines (see Table 5.1) combined with the biolominescence assay, monitoring real-time expression of *per-luc* transgenes in living flies. We silenced *trp* channel genes in all clock cells, crossing RNAi lines with a *tim-gal4* driver (line 27, Kaneko and Hall, 2000). Flies were monitored in our automated bioluminescence assay for their ability to synchronize *per-luc* (XLG-*luc*) in LL and 12:12 hr 25:16℃ TC. Initially, we restricted our analysis to monitoring *per-luc* expression in isolated legs. Among the 23 RNAi lines available (covering 11 different genes) we did not observe any major defects of *per-luc* expression during LL and TC (data not shown).

We wondered if this was a false negative determined by the nature of the RNAi technique with the combination of the *tim-gal4* driver line. RNAi does not induces null mutation of targeted genes and the expression pattern of many TRP channels is not known. It is possible that a more comprehensive driver might be more useful. We extended out investigation to several mutants available against *trp* channel encoding genes (Table 5.1). To our knowledge, there is not so far any study which connects the TRP channels family to the circadian clock, with the exception of *trp* and *trpl* in the phototransduction cascade required for the *Drosophila* visual system (Niemeyer et al., 1996; Yang et al., 1998).

5.3 Behavioural analysis of *trp* mutants

5.3.1 Behaviour analysis in constant light and TC

We analysed 12 mutant lines, targeting 7 *trp* encoding genes, for their ability to entrain locomotor activity to TC. Flies were entrained in LD first and then released

in LL and TC, which were in opposite phases compared the previous LD cycles (Figure 5.1). One line exhibited entraining defects in LD cycles. nan^{36a} does not synchronize to LD but rather reacts to lights-on and lights-off: High peaks of activity arise just after the change of conditions, with a lack of typical anticipatory patterns both in the morning and in the evening (Figure 5.1B). Interestingly, during LL and TC the activity looks more "normal"(Figure 5.1O), although the evening peak of activity arises later and persists more during the cold phase, compared to control (Figure 5.1N). A second allele affecting the same *nanchung* gene (nan^{dy5}) also lacks the anticipatory activity from dark to light, whereas the evening peak of activity is normal in both LD and LL and TC (Figure 5.1C, P). *nan* has been identified as a TRP channel required for hearing, and is expressed in larval and adult chordotonal organs (Kim et al., 2003). nan^{36a} and nan^{dy5} were generated by *P*-element imprecise excision and lack the first intron, and the first four introns, respectively (Kim et al., 2003). The two mutants alleles have been reported to be sedentary and mildly "uncoordinated" (Kim et al., 2003), and this might explain the inability of nan^{36a} to properly synchronize to LD cycles. However, this is not the case for the allele nan^{dy5}, which is normal.

Another line exhibits minor entrainment defects both during LD and TC conditions. The double mutant $trpl^{302}; trp^{P343}$ affects the 2 related TRP channels *trp* and *trpl* genes, which are components required for the visual phototransduction cascade (Niemeyer et al., 1996). During LD conditions, $trpl^{302}; trp^{P343}$ flies anticipate the light-dark transitions but their behaviour lacks a pronounced siesta and flies are instead very active during the whole day (Figure 5.1M). Also during LL and TC the activity is not normal, the flies are more active during the warm phase and the peak of activity that usually anticipates the transition from warm to cold is (if present at all) advanced (Figure 5.1Z).

12:12 hr Light-Dark cycles (T=25°C)

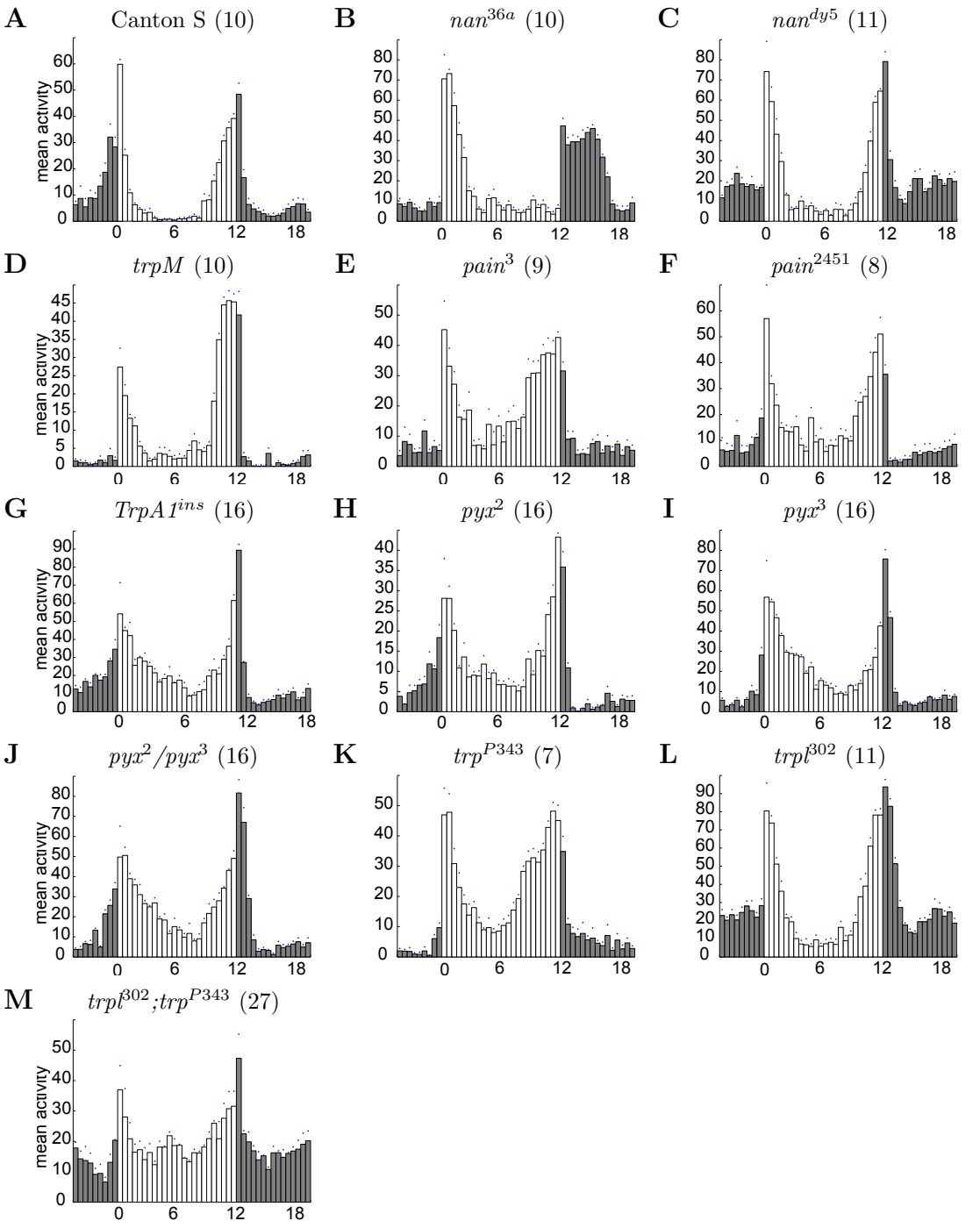

LL and 12:12 hr 25:16℃ Temperature Cycles

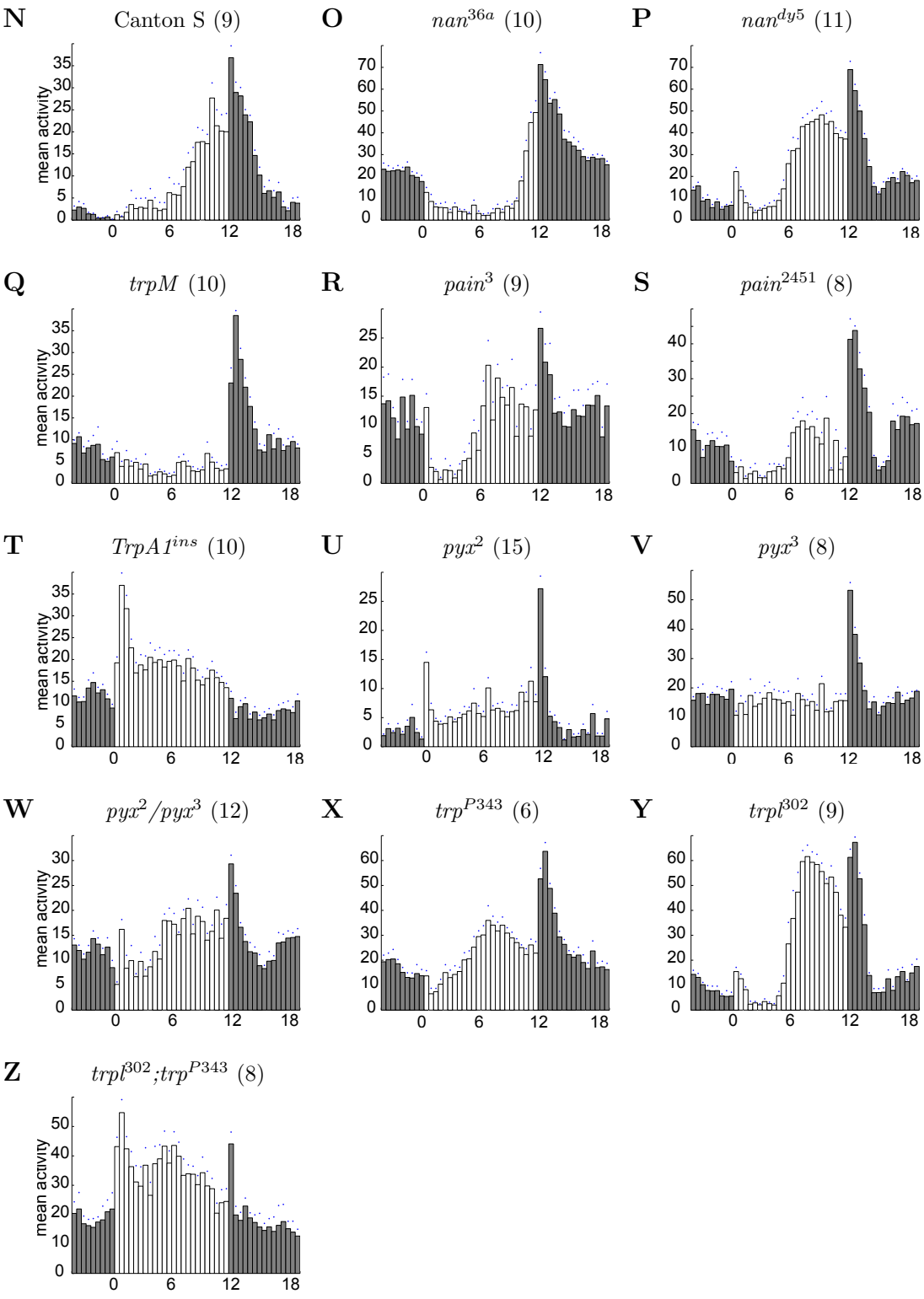

The *trpl;trp* double mutant is visually blind but the circadian clock can still be reset by light (through non-visual light signalling, i.e. CRY) but the light-induced TIM degradation is attenuated (Yang et al., 1998). It has been reported that the $trpl^{302}; trp^{P343}$ double mutants have impaired cold avoidance behaviour, when mutant larvae are let to choose between room-temperature and cold-temperature (15°C) in a thermal gradient (Rosenzweig et al., 2008).

Among the lines tested, we found 4 mutant lines (affecting 3 genes) which showed abnormal locomotor activity specifically during TC conditions. Mutants for *pyrexia* (*pyx*), *trpM* and *TrpA1* have normal LD behaviour but fail to synchronize to TC: no anticipatory activity for the transition from warm to cold and a pronounced startle response after temperature step-up (*TrpA1*) or step-down (*pyx* and *trpM*). For *pyrexia*, two different alleles show very similar results, together with the transheterozygous line pyx^2/pyx^3, indicating that the phenotype is specific to the *pyrexia* gene.

The *pyx* mutants have been isolated in a screen aimed to isolate thermopreference mutants (Lee et al., 2005). The channel is made of two isoforms, PYX-PA and PYX-PB, resulting from alternative transcripts. pyx^2 is characterized by a *P*-element inserted 538 bp upstream from the first translation codon which greatly decreases the expression of the PYX-PB transcript and increases that of the PYX-PA. pyx^3, which has been induced by *P*-element hopping, is a null allele, and it

FIGURE 5.1 *(preceding page)*: Daily average profiles of TRP channel mutants during LD cycles and LL and TC. Flies were first synchronized in 12:12 hr LD cycles at 25°C (A–M) and then subjected to LL and 12:12 hr 25:16°C TC (N–Z) which were in opposite phase compared to the previous LD. All the genotypes included in the figure have been tested at least twice, with reproducible results. *trpM* (D, Q), *TrpA1* (G, T) and *pyx* (H–J, T–W) lines display mutant phenotype specifically in LL and TC (and not in LD conditions). See text for more details. Grey shading represents activity during dark-phase in LD or cold-phase in TC. Number of individuals is indicated in brackets next to the genotype.

does not express any of the two PYX transcripts (Lee et al., 2005). *pyx* mutant flies do not distribute normally when they are subjected to a temperature gradient, they are less responsive to heat stress and they paralyse faster than wild-type if exposed to noxious warm temperature (40℃) (Lee et al., 2005). It has also been shown by Lee et al. (2005) that PYX channels are gated by temperature, at least when expressed in *X. leavis* oocytes or HEK cells. *In vivo* studies of PYX distribution revealed that it is widely expressed in larval central and peripheral nervous system (Lee et al., 2005). In the adult, it is expressed in both multidendritic (type II) and nonmultidendritic (type I) sensory neurons innervating bristles, in the maxillary palps, proboscis, and antennae (Lee et al., 2005). A more recent paper (Sun et al., 2009), studying the function of different TRP channels in geotaxis within the chordotonal neurons of Johnston's organ (which is the specialized organ for hearing, located in the antennae, see Introduction), revealed the expression of *pyx* in the cap cells of the scolopidium.

The *trpM* mutant is caused by a *P*-element insertion (Flybase symbol *P-{EPgy2}CG34123^{EY01618}*) in the coding region of the *CG34123* gene, or *trpM*. TRPM has been recently described as required for magnesium (Mg^{2+}) intake in the Malpighian tubules (Hofmann et al., 2010). Given that two mutants alleles generated by Hofmann et al. (2010) are pupal lethal, the allele we used (named *trpM*) is presumably hypomorphic. In our assay, *trpM* exhibits a very similar phenotype to the *pyx* mutants. It belongs to the TRPM class and *trpM* mutant flies are normal in a thermopreference assay (Rosenzweig et al., 2005). The mammalian ortholog to *trpM* is TRPM3, which is activated by cell swelling (reviewed by Kraft and Harteneck, 2005). The other six members of the mammalian TRPM class are associated with taste transduction, sensation of cool temperatures and Mg^{2+} absorption in the intestine (Hofmann et al., 2010).

TrpA1 has been already described as a TRP channel required for warm avoidance in *Drosophila* larvae (Rosenzweig et al., 2005, 2008) and adults (Hamada et al., 2008). $TrpA1^{ins}$ null mutant has been generated via site-directed insertional disruption which change its reading frame resulting in a truncated protein (Hamada et al., 2008). *TrpA1* is expressed in three groups of cells in the adult brain, the anterior cells (AC), the ventral cells (VC) and the lateral cells (LC) neurons, but only the AC neurons (which projects to the antennal lobe) seem to be necessary and sufficient to restore normal thermopreference in *TrpA1* mutants and to act as "internal" thermosensors (Hamada et al., 2008) in addition to the "external" one, located in the third antennal segment (Sayeed and Benzer, 1996). Recently, TRPA1 has been proposed to be required for chemical nociception and *TrpA1* mutants fail to respond to reactive electrophiles, i.e. allyl isothiocyanate, *N*-methylmaleimide or cinnamaldehyde (Kang et al., 2010).

5.3.2 Behaviour analysis at different temperature intervals

The different TRP channels can be activated and respond to warm and cold in a wide range of temperatures (Montell and Caterina, 2007). To address whether certain genes or mechanisms operate in restricted temperature intervals, and to identify the specific role that each isolated *trp* mutant plays in the process of temperature entrainment of the circadian clock, we investigate the locomotor behaviour at different and smaller temperature intervals than the one utilized previously. We first entrained the flies to 12:12 hr LD cycles and then monitored their activity in LL and three different TC: 29:25℃, 25:20℃ and 20:16℃.

Figure 5.2 shows the locomotor activity of the four TRP channel mutants and controls in LL and different temperature intervals. Flies were first entrained in LD (25℃) then transferred to LL and 12:12 hr 29:25℃ TC for 5 days. Subsequently,

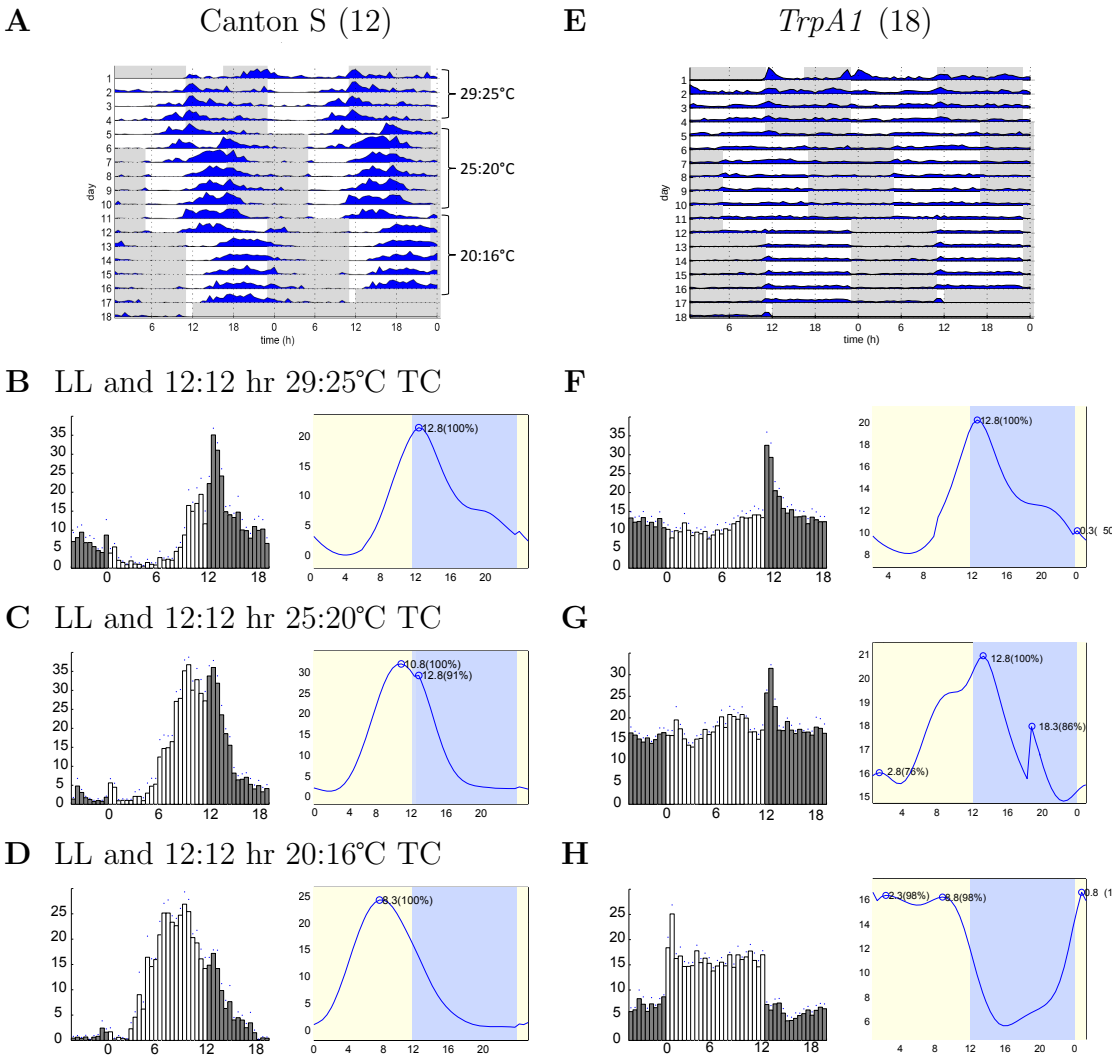
A
Canton S (12)
E
TrpA1 (18)
29:25°C
25:20°C
20:16°C
day
time (h)
B LL and 12:12 hr 29:25°C TC
F
12.8(100%)
C LL and 12:12 hr 25:20°C TC
G
10.8(100%)
12.8(91%)
18.3(86%)
2.8(76%)
D LL and 12:12 hr 20:16°C TC
H
8.3(100%)
8.3(98%)
8.8(98%)

FIGURE 5.2

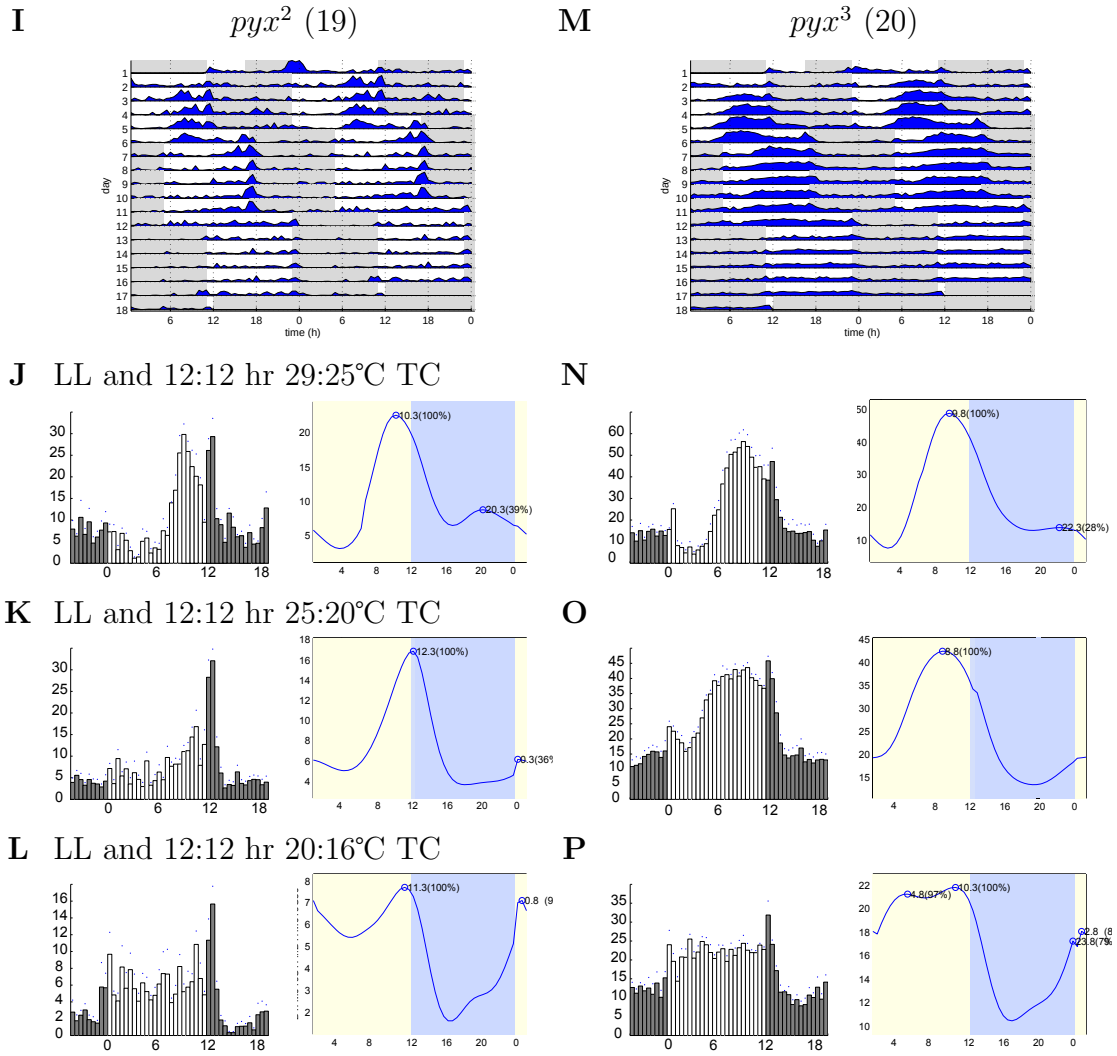
I
pyx^2 (19)
M
pyx^3 (20)
day
time (h)
J LL and 12:12 hr 29:25°C TC
N
10.3(100%)
20.3(39%)
9.8(100%)
22.3(28%)
K LL and 12:12 hr 25:20°C TC
O
12.3(100%)
6.8(100%)
L LL and 12:12 hr 20:16°C TC
P
11.3(100%)
10.3(100%)

FIGURE 5.2

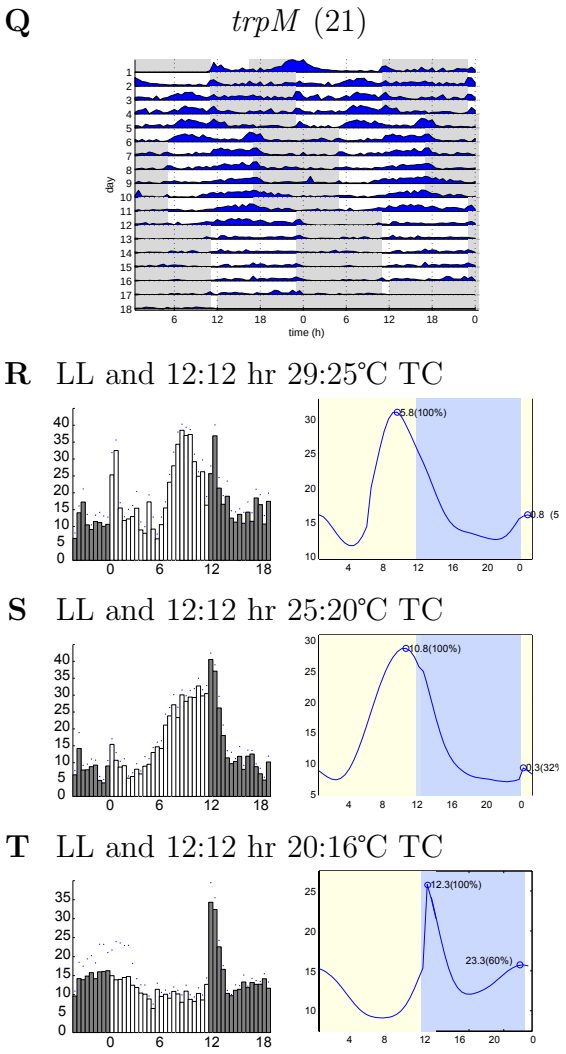

FIGURE 5.2: Locomotor activity of TRP channel mutants and controls in LL and different temperature intervals. The plot on top depicts average actograms. The lower plots depict daily average activity (left) and a low-pass filtered version of the same plot (right) from which the average peak phase (in ZT) has been extrapolated (and depicted in Table 5.2), in LL and 12:12 hr 29:25°C, 25:20°C and 20:16°C TC, respectively (as indicated). Flies have been entrained in LD first and then subjected to LL and the different temperature intervals, each of those were 6-hr phase delayed compared to the previous conditions (see shaded areas in the actogram). LD part is not shown. The experiment has been performed twice. In the second repetition, the TC intervals have been applied in the reverse order, i.e. from 20:16°C to 29:25°C. The results were similar, excluding that ageing effects caused the failure of entrainment during the cold interval (data not shown). Shaded areas (grey in the actograms and daily average or blue in the peak-phase plots) represent activity during the cold-phase. Number of individuals tested is indicated in brackets.

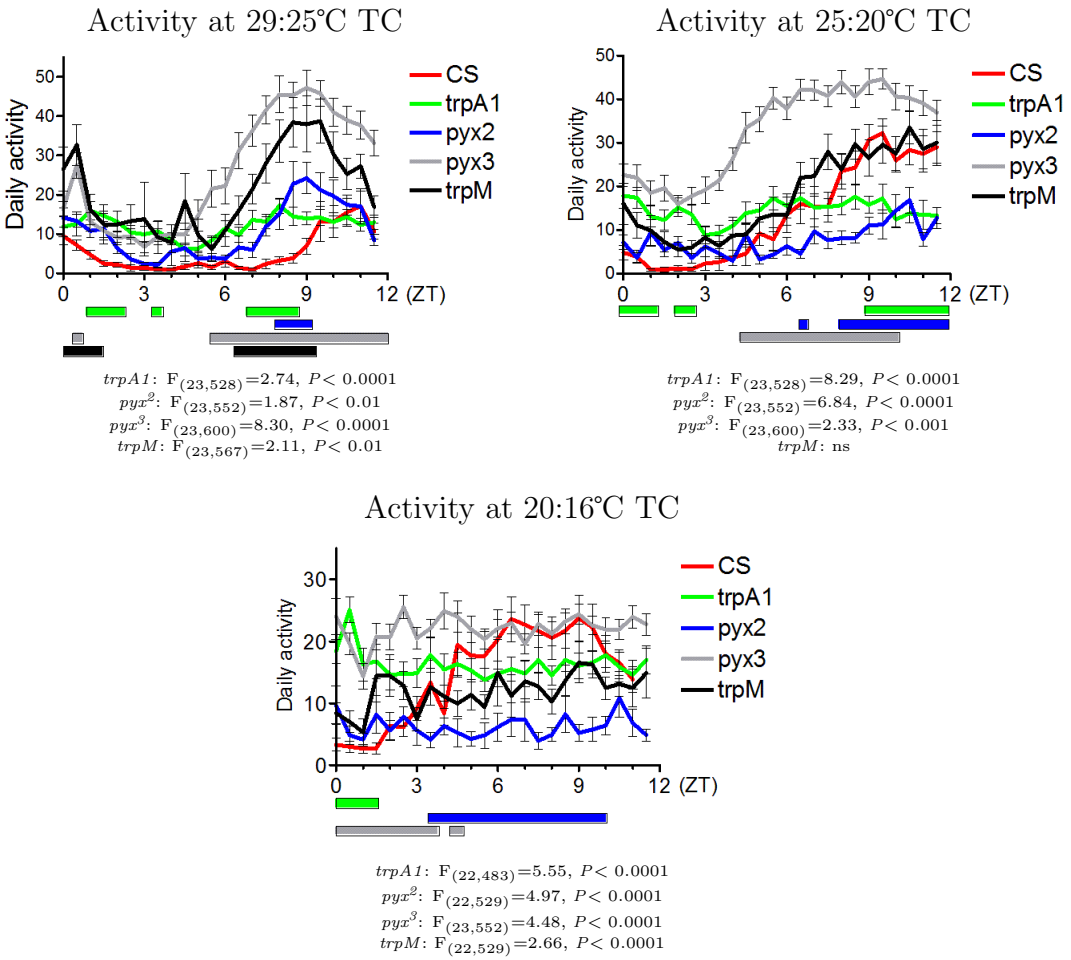

FIGURE 5.3: Daily average activity of controls (red line) and TRP mutants (green, blue, grey and black, as indicated) during the warm-phase only in LL and different temperature intervals of the histograms depicted in Figure 5.2B–D, F–H, J–L, N–P, R–T. Two-way Anova was performed to determine statistical interaction between Canton S (CS) control and each TRP mutant lines in the range ZT 0–12. Coloured bars underneath represent the time points in which the respective mutants show significant difference compared to Canton S control (Bonferroni posttest $P< 0.05$).

the temperature regime was then changed to 25:20°C and delayed by 6 hr compared the previous regime. After 6 days, the temperature cycles regime was shifted again by other 6 hr (delay) and changed to 20:16°C. Activity was first analysed by monitoring both actograms and histograms (Figure 5.2). Subsequently, by overlapping the daily activity of the mutants and control in the same plot and performing a Two-way Anova to determine statistical interactions of each mutant

with the controls in the warm phase only (Figure 5.3). In addition, the phase of the activity peak and amplitude of the rhythm were calculated (Table 5.2).

Canton S flies entrain their locomotor activity to any of the three temperature intervals. As described in the previous chapter (Section 3.3.1) Canton S flies nicely display the effect of "seasonal adaptation" of behaviour to different temperature intervals (Figure 5.2A–D, Figure 5.3 and Table 5.2).

TrpA1^{ins} flies do not entrain at 20:16℃ TC and 25:20℃ TC and very weakly, if at all, at 29:25℃, but not in a way comparable to controls (Figure 5.2E–H). Two-way Anova finds highly significant interaction with Canton S at any temperature intervals (Figure 5.3) and the pattern of activity during the warm phase is weakly cycling (amplitude 2.8) only at 29:25℃, whereas it is not rhythmic at 25:20℃ and at 20:16℃ TC (Table 5.2). To support this observation, note that the main peak of activity occurs just after temperature changes (phase values in Table 5.2).

Analysis of actograms and histograms of *pyx*^{2} flies revealed that they synchronize their rest-activity pattern to temperature cycles in the warm range (29:25℃), very weakly in the mid range (25:20℃) and not in the cool (20:16℃). Two-way Anova suggests significant difference from control at any temperature intervals and this can be explained by the different phase of activity: the peak of evening activity during 29:25℃ occurs 2.5 hours earlier than in controls and 1.5 hours later during 25:20℃ TC (Table 5.2). In the cold range, *pyx*^{2} activity is flat (amplitude not significant) and flies do not exhibit any peak of activity in terms of anticipation of the warm-cold transition (Figure 5.2L Figure 5.3 and Table 5.2).

The behaviour of *pyx*^{3} mutants resembles very much that of *pyx*^{2}: entrainment in 29:25℃ and 25:20℃ intervals, but not at 20:16℃ TC. The phase of activity in the two higher temperature intervals occurs two hours earlier than control, resulting in an significant difference of the overall activity compared to control

when Anova is performed (Figure 5.3). This is supported also by the overall higher level of activity of the mutants compared to Canton S in all the three temperature intervals. Activity in the cold range (20:16℃) is flat (amplitude not significant), and flies are not synchronized. The PYX channel is required for warm avoidance and the mutants lack the ability to react to noxious warm (Lee et al., 2005), so one would expect inability to entrain in a warm temperature interval. Yet our results reveal the opposite effect on temperature entrainment: both *pyrexia* mutant alleles we assayed entrain to 29:25℃ TC but not at all at 20:16℃.

trpM mutants entrain normally to LL and 25:20℃ TC, in a way comparable to control (Figure 5.2 and Figure 5.3). Similarly to pyx^2 and pyx^3, the shape of the daily average activity during 29:25℃ TC is similar to that of wild-type control, but the phase is 2 hours earlier and the activity level higher, resulting in an overall statistically significant interaction with control. *trpM* mutants fail to synchronize their activity to the cold interval 20:16℃: the activity pattern is flat (amplitude not significant, Table 5.2) and it exhibits only a sharp increase when temperature drops to 16℃ (Figure 5.2 and Figure 5.3).

Looking at the actograms in Figure 5.2, one could argue that the mutants inability to synchronize their behaviour in the cold interval 20:16℃ could be consequence of ageing effects, since the cold temperature interval occurs at the end of the experiment. To address this question, the same experiment was performed with opposite temperature regimes, i.e. starting with the cool range 20:16℃ and increasing up to 29:25℃. The results were comparable and the mutant lines showed the same activity patterns, regardless of the order in which the temperature intervals had been applied (data not shown).

	LL and Temperature cycles						
	Phase				Amplitude		
	25:16°C	29:25°C	25:20°C	20:16°C	29:25°C	25:20°C	20:16°C
Canton S	10.8	12.8	10.8	8.3	18.4	38.2	8.9
$TrpA1^{ins}$	1.3	12.8	12.8	0.8	2.8	ns	ns
pyx^{2}	12.3	10.3	12.3	11.3	11	0.7	ns
pyx^{3}	12.8	9.8	8.8	10.3	7	2.8	ns
trpM	13.3	9.8	10.8	12.3	6.2	6.1	ns

	DD and Temperature cycles						
	Phase				Amplitude		
	25:16°C	29:25°C	25:20°C	25:20°C	29:25°C	25:20°C	20:16°C
Canton S	3.3	1.8	1.8	3.8	16.5	16.4	8.8
$TrpA1^{ins}$	1.8	1.3	2.3	2.3	7.9	12.5	8.5
pyx^{2}	2.3	0.3	9.8	2.3	6.9	3.6	23.9
pyx^{3}	1.8	0.3	1.3	1.8	3.6	2.1	2.8
trpM	2.3	1.3	2.8	4.3	14.1	16.9	26.7

TABLE 5.2: Summary of peak phase and amplitude of locomotor activity in LL or DD and different temperature intervals. The phase values (in ZT) are calculated from 4-hr low-pass filtered versions of daily average histograms depicted in Figure 5.1, 5.2, 5.4 and 5.6. When more than one peak of activity was observed, only the main one is considered (100% relative intensity). Colour backgrounds summarize the behaviour of flies which were entrained (green), not entrained (red) or weakly entrained (hypomorphic behaviour, yellow) in the different conditions. Amplitude was calculated by dividing the the maximum and minimum activity level of daily average activity. One-way Anova was used to calculate whether the activity oscillation between peak and trough was significant ($P<0.05$. ns: $P>0.05$).

5.3.3 Behaviour analysis in constant darkness and TC

All the behavioural analysis shown so far has been performed in constant light (and TC). It is known that at least some TRP channels are involved in the phototransduction cascade, for instance, TRP and TRPL (Niemeyer et al., 1996). Both are not directly activated by light, but through a phospholipase C (PLC)-mediated signalling pathway (reviewed by Katz and Minke 2009). We therefore wondered if the constant presence of light could have some direct effects on the channels that may alter behaviour, in spite of the putative role on the temperature synchronization of the clock. We thus monitored the ability of the *trp* mutants to entrain to temperature cycles in DD.

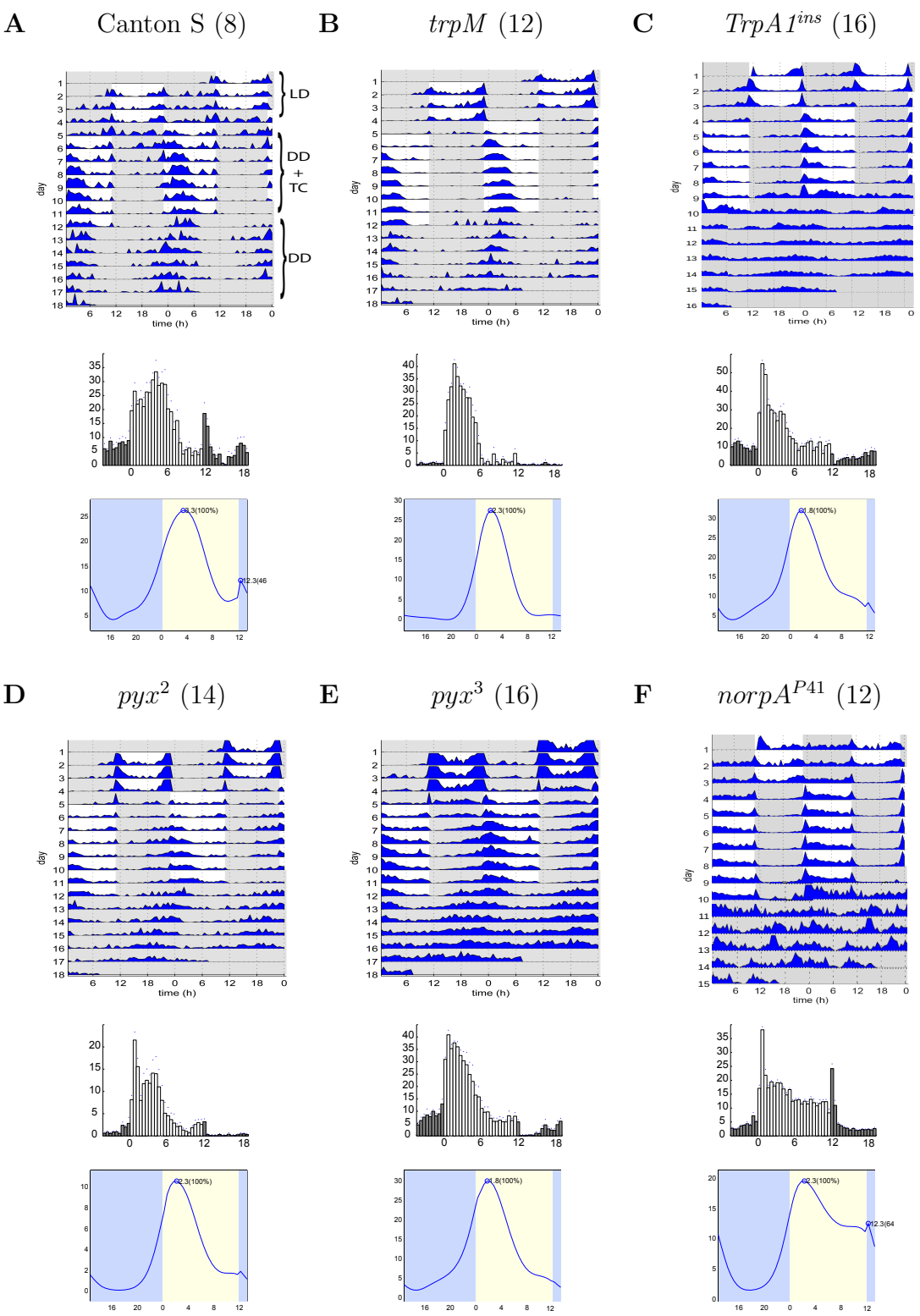
A
Canton S (8)
B
trpM (12)
C
TrpA1ins (16)
LD
DD
+
TC
DD
day
time (h)
D
pyx2 (14)
E
pyx3 (16)
F
norpAP41 (12)

The locomotor activity pattern of wild-type flies in DD and TC resembles in shape the activity pattern during LL and TC, exhibiting a unimodal pattern (and not a bimodal one as in LD entrainment) but with a different phase. The peak of activity does not occur towards the end of the warm phase (around ZT10), but at beginning of the thermo-phase, soon after the raise of temperature (around ZT3, Figure 5.4A). During DD and TC conditions, temperature-entrainment mutant flies, such as $norpA^{P41}$ (Glaser and Stanewsky, 2005), exhibit a so called "startle response", which occurs just after the temperature increases (ZT0–1) (see Figure 5.4F). In LL and TC conditions, the circadianly-regulated peak (at around ZT10) is far apart from the startle response at ZT0 so it is "easier" to discriminate mutant flies from wild-type. In DD and TC, the situation is different, since the circadianly-regulated peak partially overlaps the startle response peak at the beginning of the day (warm-phase). For this reasons, it can be misleading to judge the behaviour of a fly only on the position of the activity peak of histograms (during TC conditions). However, careful inspection of the activity pattern, gives in many cases the possibility to discriminate whether the activity is reaction to temperature or (in addition) circadianly regulated. One way to test if the locomotor activity is synchronized to temperature is to monitor the transients from one condition to another and to check free-running phase when the flies are released to constant conditions.

Figure 5.4 shows actograms, histograms and peak phase analysis of *trp* mu-

FIGURE 5.4 *(preceding page)*: Locomotor activity of TRP channel mutants and controls during DD and TC. Average actograms (top plot), daily average (middle plot) and activity peak phase (bottom plot) during 12:12 hr 25:16°C TC. Flies were first entrained in LD conditions (3 days are included in the actograms) and then moved to DD and TC which was in opposite phase compared to the previous LD (warm-phase corresponding to previous dark and cold-phase corresponding to light). Subsequently, flies were released to constant conditions (DD and 25°C).

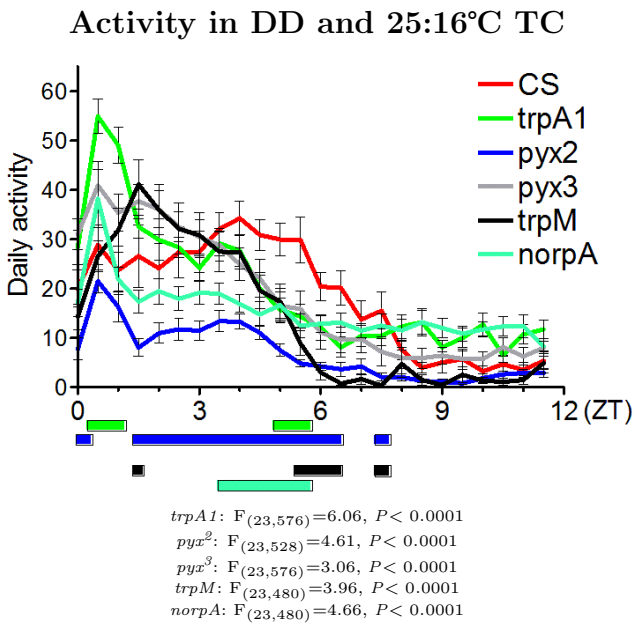

FIGURE 5.5: Daily average activity of controls (red line), TRP mutants (green, blue, grey and black) and *norpA* (light blue), as indicated, during the warm-phase only in DD and 25:16°C TC of the histograms depicted in Figure 5.4. Two-way Anova was performed to determine statistical interaction between Canton S (CS) control and each mutant lines in the range ZT 0–12. Coloured bars underneath represent the time points in which the respective mutants show significant difference compared to control (Bonferroni posttest $P< 0.05$). Error bars indicate SEM.

tants and controls during (25°C) to DD and 12:12 hr 25:16°C TC (after initial LD entrainment) and subsequent release to constant conditions. The activity peak of wild-type flies occurs 3 hours after the transition from cold to warm and it takes 2–3 transition cycles to stabilize. When wild-type flies are then released to constant conditions, the initial phase of free-running activity follows the phase observed during entrainment.

trpM flies exhibit a very similar behaviour to Canton S controls, although their peak phase during TC occurs one hour earlier (ZT2.3 versus ZT3.3 of control, see Table 5.2), resulting in significant interaction with control in an Anova test (Figure 5.5). *trpM* behaviour exhibits transients before reaching a stable phase and it is distinct from a pure temperature-reaction activity, which mainly occurs

just after the cold-warm transition (compare with $norpA^{P41}$, Figure 5.6F). Also, free-running activity after TC follows the behaviour peak observed at the end of entrainment (Figure 5.4B), suggesting the *trpM* flies entrain their activity to 25:16℃ TC. This result indicates a striking difference of behaviour during TC between LL and DD for the *trpM* mutant flies.

$TrpA1^{ins}$ activity is very similar to a "temperature mutant": a prominent behavioural activity peak just after temperature increase from the first day of the new regime and no clear transients are observed (Figure 5.4C). Two-way Anova revealed highly significant interaction with Canton S, and the main peak of activity occurs 1.5 hours earlier then control. Also free-running activity after TC is not clearly synchronized with the behaviour during TC (Figure 5.4C). These results are consistent with the inability of $TrpA1^{ins}$ mutants to synchronize their behaviour to LL and TC (Figure 5.1).

Similar to *trpM*, pyx^2 flies are able to entrain to TC during DD (Figure 5.4D). This is particularly evident if considering the free-running activity after TC entrainment (see below and Figure 5.4D). pyx^3 shows a similar synchronization to temperature than pyx^2: the activity peak during TC follows the temperature and the free-run activity after TC conditions is dampened but in phase with the previous activity. For both mutants, Two-way Anova revealed significant difference form control (Figure 5.5), probably because they exhibit an higher response to temperature increase, an overall higher activity level and an earlier phase of activity peak (1 and 1.5 hours, respectively, Table 5.2).

Interestingly, *pyx* and *trpM* mutants do not entrain locomotor behaviour to 25:16℃ TC in LL but they do in DD. We had also observed different behaviour among the mutants assayed in LL when smaller temperature intervals were applied, so we investigated if this was the case also in constant darkness.

Figure 5.6 and Figure 5.7 show rest-activity patterns of TRP mutants and controls in DD and different temperature intervals.

Canton S flies entrain to any of the three temperature intervals we applied. The activity shows clear transients when flies are subjected to the different TC and they persist longer than in LL. Interestingly, the seasonal adaptation of the behaviour is also less pronounced compared to LL and TC condition (figure 5.2A–D). Those observations are in agreement with previous results of "stronger" entrainment in LL compared to DD (see Tomioka et al., 1998; Yoshii et al., 2002; Glaser and Stanewsky, 2005 and Discussion).

Analysis of variance between $TrpA1^{ins}$ flies and Canton S exhibit statistical interaction at any temperature intervals (Figure 5.7). By inspection of the actograms and histograms (Figure 5.6), *TrpA1* flies do not exhibit the same activity pattern as controls. In particular, we did not observe any transients and the activity peak of $TrpA1^{ins}$ flies occurs just after the temperature raise.

trpM mutants entrained to 25:20℃ and 20:16℃ temperature interval and weakly at 29:25℃ TC. Interestingly, *trpM* entrain to the cold 20:16℃ TC (a condition to which it does not entrain in LL, compare Figure 5.2T). Anova analysis restricted to the warm-phase only shows interaction with Canton S at 29:25℃, probably as a consequence of the lower activity level and the slightly earlier activity phase (0.5 hour). However, the pattern of activity (Figure 5.7) and the amplitude of oscillation (Table 5.2) is comparable to control suggesting *trpM* flies are weakly entrained (but not in the same extent as controls).

pyx^2 flies exhibit a different activity profiles compared to control in the 29:25℃ and 25:20℃ intervals, while it is comparable to control (P>0.05, Two-way Anova) in the cold interval (Figure 5.7). Interestingly, in the 29:25℃ and 25:20℃ ranges, the activity peak is shifted towards the end of the warm phase (ZT10), the activity

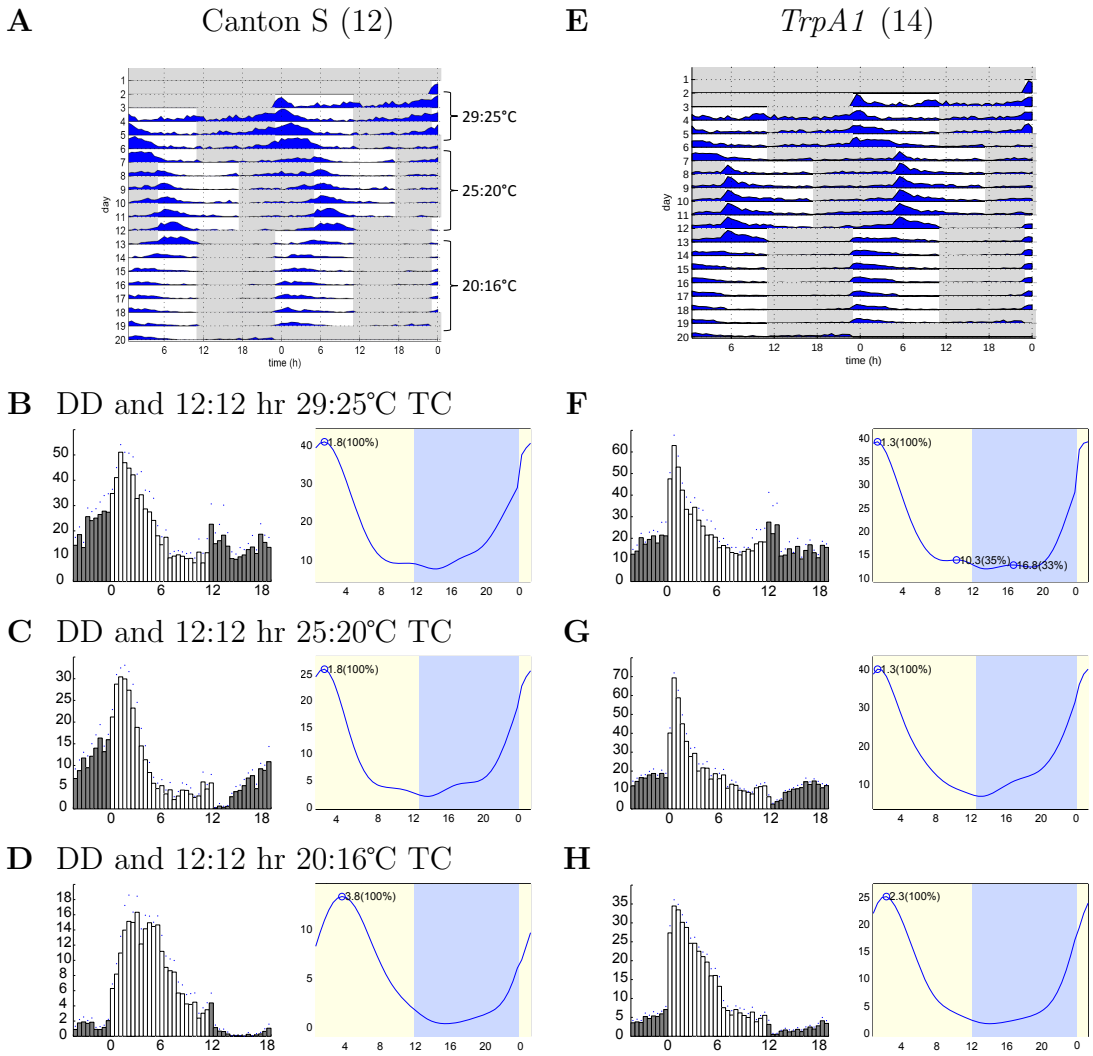
A
Canton S (12)
E
TrpA1 (14)
29:25°C
25:20°C
20:16°C
day
time (h)
B DD and 12:12 hr 29:25°C TC
F
C DD and 12:12 hr 25:20°C TC
G
D DD and 12:12 hr 20:16°C TC
H
1.8(100%)
1.3(100%)
10.3(35%)
16.8(33%)
3.8(100%)
2.3(100%)

FIGURE 5.6

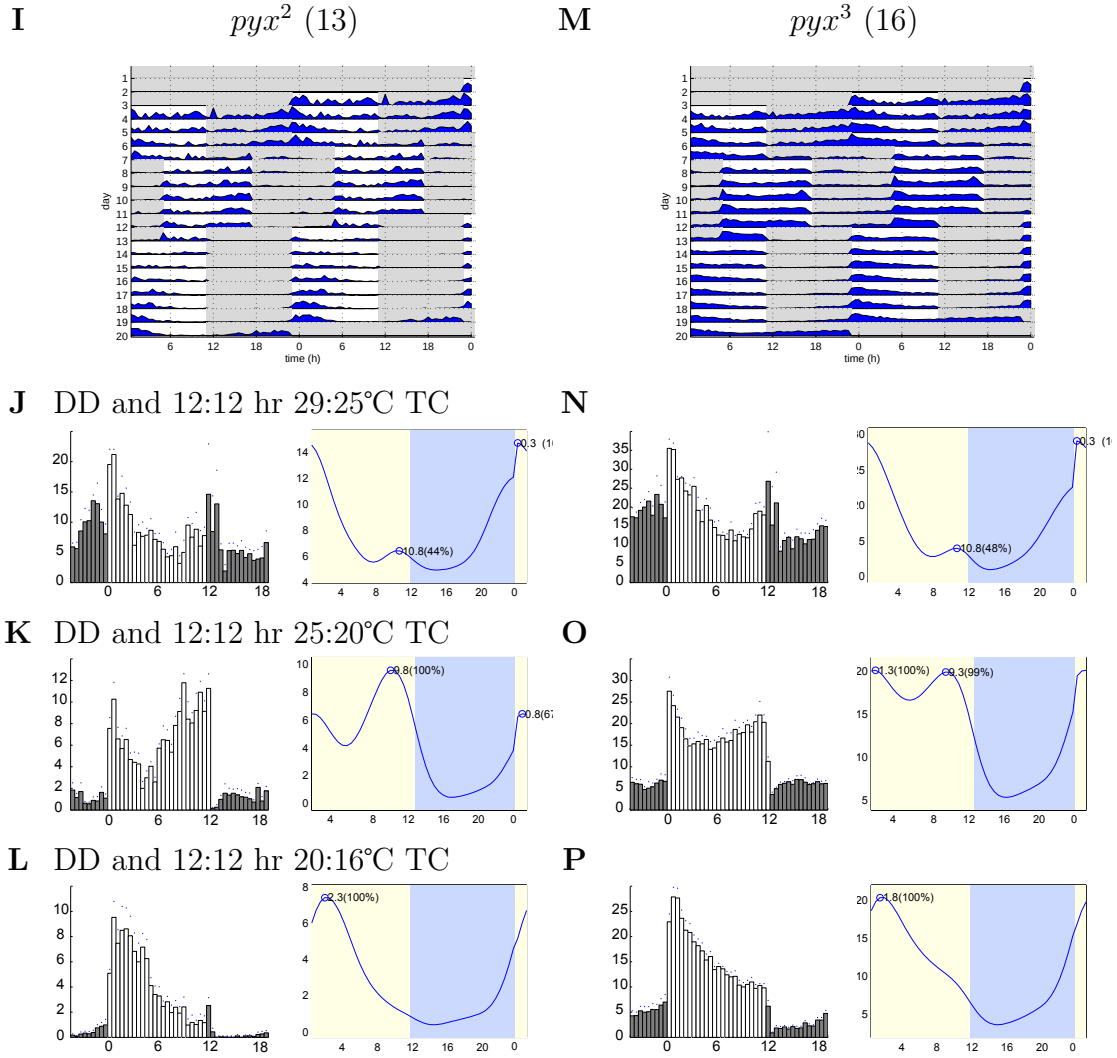
I
pyx^2 (13)
M
pyx^3 (16)
day
time (h)
J DD and 12:12 hr 29:25℃ TC
N
10.8(44%)
10.8(48%)
K DD and 12:12 hr 25:20℃ TC
O
9.8(100%)
11.3(100%)
9.3(99%)
L DD and 12:12 hr 20:16℃ TC
P
12.3(100%)
11.8(100%)

FIGURE 5.6

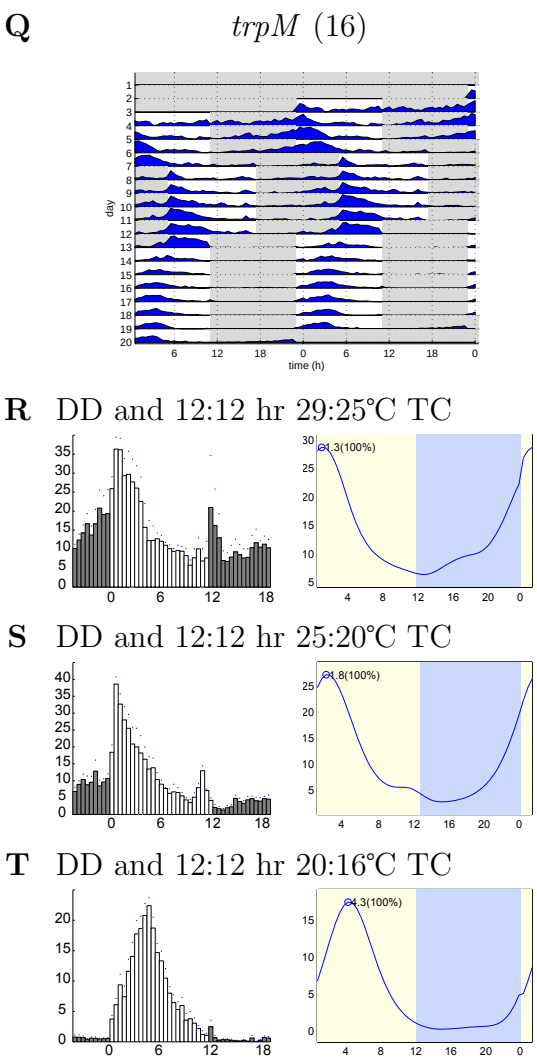

FIGURE 5.6: A–T) Locomotor activity of TRP channel mutants and control in DD and different temperature intervals. The plots have been described in Figure 5.2. Flies were entrained in 12:12 hr LD cycle (not included in the graphs) and then subjected to DD and different TC (29:25°C, 25:20°C and 20:16°C respectively, as indicated) which were 6-hr phase delayed and advanced, respectively, compared to the previous entrainment regime (see shading). Note that in DD and TC, the main peak of activity seats at the beginning of the warm phase. See text for more details. Average phase values of the main activity peak (100% relative intensity) are summarized in Table 5.2.

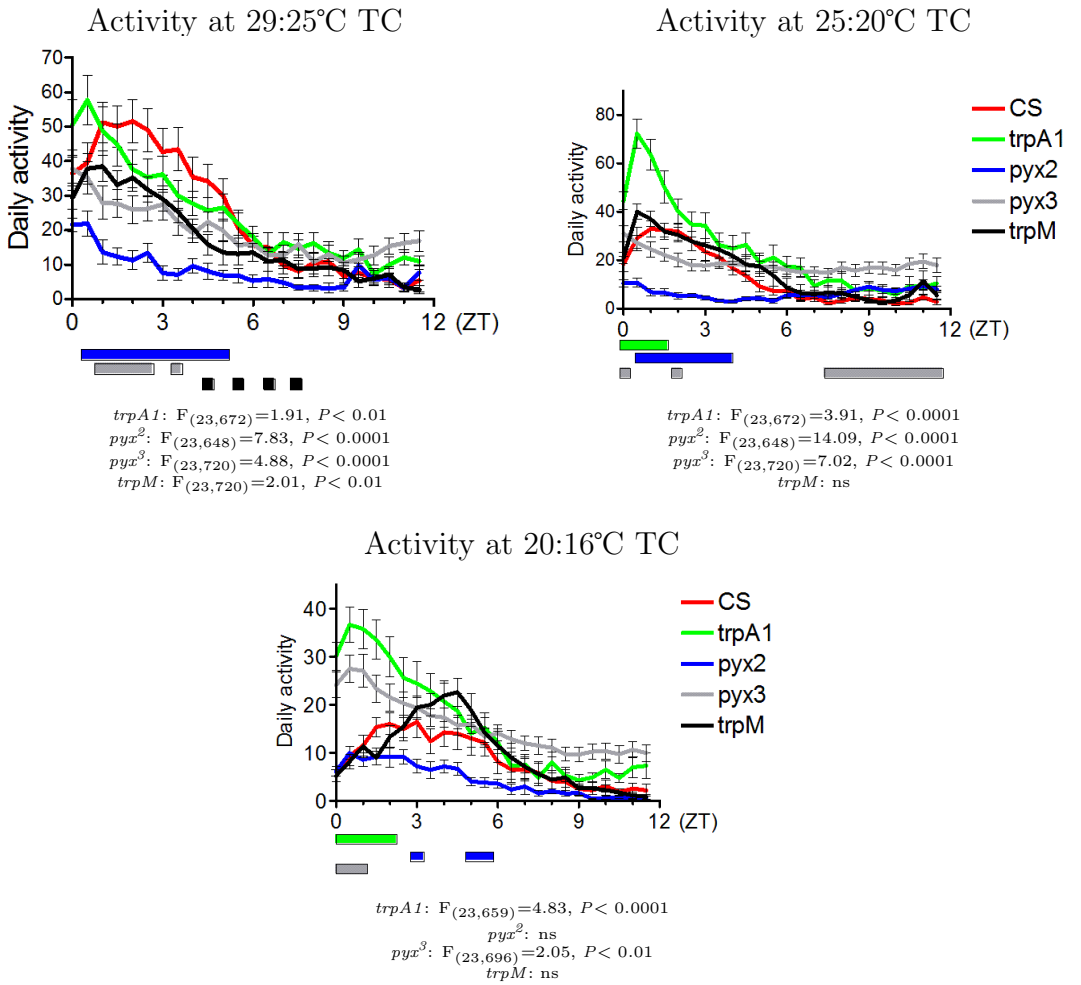

FIGURE 5.7: Daily average activity of controls (red line) and TRP mutants (green, blue, grey and black, as indicated) during the warm-phase only in DD and different temperature intervals of the histograms depicted in Figure 5.6B–D, F–H, J–L, N–P, R–T. Two-way Anova was performed to determine statistical interaction between Canton S (CS) control and each TRP mutant lines in the range ZT 0–12. Coloured bars underneath represent the time points in which the respective mutant shows significant difference compared to Canton S (Bonferroni posttest $P< 0.05$). Error bars indicate SEM.

profile is relatively noisy, the cycling amplitude is lower than control as well as the overall activity level. A similar behaviour is observed for pyx^3 in the same ranges. Instead, the behaviour of the pyx^3 allele at 20:16℃ seems more a reaction to the temperature increase, rather than synchronization (Figures 5.6 and 5.7). In fact, the activity is more concentrated during the warm-phase (and the level higher than control), and we did not observe transients between the different temperature intervals.

Among the TRP channel mutants we analysed, $TrpA1^{ins}$ exhibits the most severe phenotype of defective temperature entrainment. In addition, from my observations it emerges a very complex picture in which it is challenging how to classify mutations affecting *trp* genes that also affect aspects of temperature entrainment of the circadian clock. It appears that it is crucial to consider the conditions in which the flies are assayed, in terms of light or darkness and interval of temperature cycles in order to judge how a TRP channel affects temperature entrainment. Some mutant lines can exhibit the phenotype in certain conditions, but not in other, and *vice versa*. These observations could also help to understand the functions that a specific channel plays. For instance, the ability to entrain only in one specific temperature range, could mean the non-requirement of that particular channel in that specific range. In other words, the different behaviour of *trp* mutants could help to generate a "temperature map" where different channels respond to different temperature cycles, thereby allowing the fly to sense, react, and ultimately entrain to different environmental conditions.

5.4 *per-luc* expression in *trp* mutants

I next investigate if *trp* mutants affect directly the expression of the *period* gene and its product when assayed in temperature cycles conditions. I first assayed *per-luc* expression in RNAi lines against *TrpA1*, *trpM* and *pyx* driven by *tim-gal4*, both in isolated legs and in the whole adult fly. Four independent RNAi lines are available against *trpM*, and one each against *TrpA1* and *pyx* (see Table 5.1).

Flies were first entrained to LD (25℃) and then subjected to LL and 12:12 hr 25:16℃ TC in opposite phase compared the previous LD regime. Note that wild-type adult flies take up to 2 days to entrain to the new temperature regime, while isolated legs are fully synchronized to temperature after 1 day of transition (Figure 5.8). Overall *per-luc* (XLG-*luc*) expression appeared normal in isolated legs during LL and TC in all the RNAi lines we assayed (Figure 5.8, left column), as already discussed in Section 5.2. Expression levels in legs of *tim-gal4*-driven *TrpA1*-RNAi and *pyx*-RNAi were slightly lower than in controls, but similar in terms of rhythmicity, amplitude and phase. Interestingly, when we monitored *per-luc* expression in the whole adult fly, we observed that PER-LUC in *trpM*-RNAi (line R4) is not cycling at all, while it is normal in *pyx*-RNAi and *TrpA1*-RNAi. We tested 4 different RNAi lines against *trpM* and only one (line R4) shows the phenotype (reproducible among different experiments). This can be interpreted in 2 different ways. The first explanation is that the other 3 RNAi lines are not efficient or they do not knock-down the *trpM* gene enough in order to manifest the phenotype. Secondly, it could be that the phenotype induced by *trpM*-RNAi (line R4) is not due to silencing the *trpM* gene, but due to insertional effects of the RNAi line itself, and this would be supported by the results obtained with the XLG-*luc* transgenic mutant line (see below). However, the observation that *per-luc* expression synchronizes to temperature in legs but not in the context

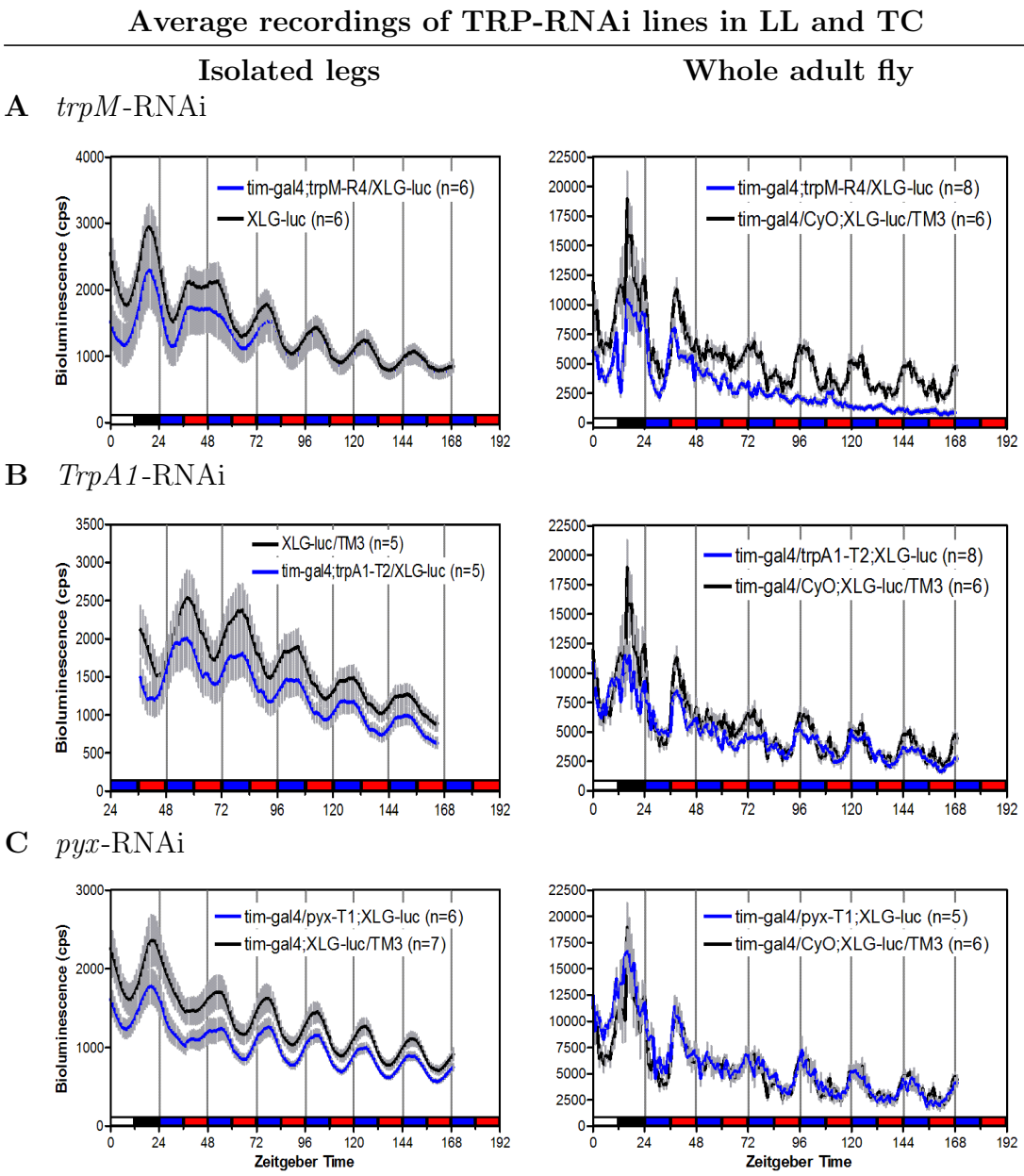

FIGURE 5.8: Flies were first entrained in LD and then subjected to LL and 12:12 hr 25:16℃ TC which was in opposite phase compared the previous LD regime. The last day of LD is included in the plots (except in (B) left column, were only LL and TC part is included). Black line represents bioluminescence readings from control flies. Blue line represents reading from *tim-gal4*-driven RNAi lines. White/black bars indicate light and dark phase. Red/blue bars indicate 25℃ and 16℃ phase, respectively. Error bars (grey) indicate SEM. Number of individuals tested (n) is indicated.

of the whole animal is reminiscent of the phenotype of the known "temperature mutants" *nocte*^{1} and *norpA*^{P41} (Glaser and Stanewsky, 2005; Sehadova et al., 2009 and C. Gentile, A. Simoni, R. Stanewsky, in preparation). It is interesting to note that this phenotype appears in several different mutants, as for example in the EMS mutants (in DD and TC, described in the Section 3), *nocte*, *norpA* and now *trpM*. At the moment, the explanation for this phenomenon remains unknown, but further investigation will hopefully help to understand the underlying mechanism.

The RNAi technique is an extremely powerful genetic tool, however it is not free from drawbacks. RNAi knock-down may be not sufficient to induce a phenotype (in particular when dealing with potential signal transduction events that can be amplified) or RNAi may be driven in the wrong cells (see Discussion). To solve those problems, we also generated transgenic flies carrying the XLG-*luc* transgene in the *TrpA1*^{ins}, *trpM* and *pyx* mutant backgrounds.

In order to compare the results obtained with the RNAi lines with results of chromosomal mutation in the same genes we monitored TRP channel mutants for their ability to synchronize *per-luc* expression in LL and 12:12 hr 25:16°C TC. *trpM*;XLG-*luc* flies entrain PER-LUC expression to temperature. Expression in isolated legs is equivalent to wild-type controls, and in adult flies the *per-luc* expression reaches a stable and synchronized phase to TC one day earlier than controls (Figure 5.9). *trpM* mutants exhibit a small (and bigger than control) rise in PER-LUC expression directly after the temperature increase (particularly evident at ZT12 of day 3 of TC, Figure 5.9A, right). Two-way Anova performed in the range ZT 48–144 (i.e. for four days after the moment *per-luc* expression is synchronized to TC) revealed not statistical interaction between the genotypes, indicating no significant difference between *trpM* XLG-*luc* and control both in isolated legs and in the whole adult flies.

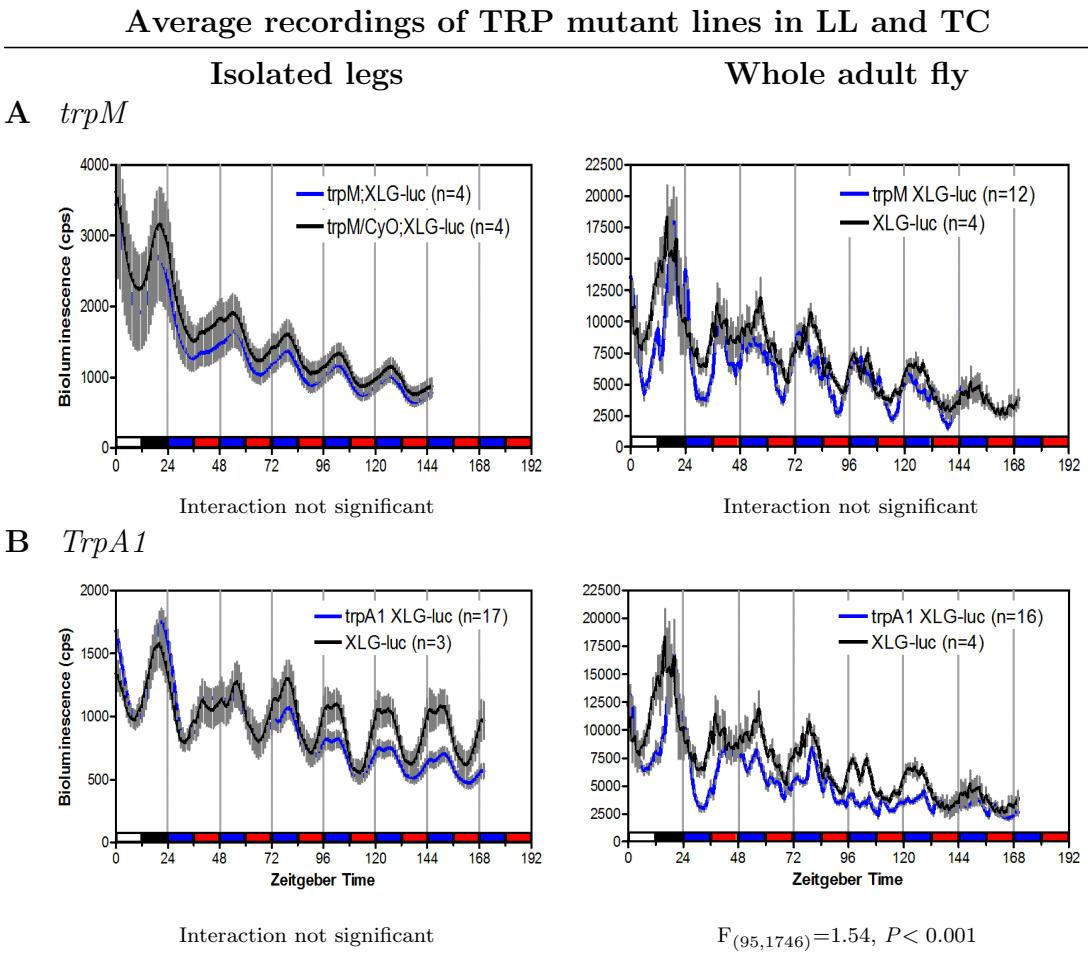

FIGURE 5.9: Average bioluminescence recordings of (A) TRPM and (B) TRPA1 mutant lines in LL and TC. Flies were first entrained to LD and then subjected to LL and 12:12 hr 25:16℃ TC which was in opposite phase compared the previous LD regime. The last day of LD is included in the plots. Black line represents bioluminescence recordings from control flies (XLG-*luc*). Blue line represents XLG-*luc* in TRP channel mutant backgrounds, as indicated. Number of individual tested is indicated next to the genotype. White/black bars indicate light and dark phase. Red/blue bars indicate 25℃ and 16℃ phase, respectively. Error bars (grey) indicate SEM. Two-way Anova was performed in the range ZT 48–144 to determine statistical interaction of each mutant with control (results reported under each plot).

The *TrpA1*^{ins} XLG-*luc* flies entrain to TC, but not in the same extent compared to control. *per-luc* expression in isolated legs is strongly reduced in terms of amplitude only during LL and TC and not in LD (Figure 5.9B). Analysis of variance revealed interaction not significant but an highly significant genotype effect ($F_{(1,1746)} = 66.4$, $P< 0.0001$), as a results of the lower amplitude of cycling, but not an overall effect on the rhythmic *per-luc* expression and phase (Figure 5.9). PER-LUC expression in the whole adult flies of *TrpA1* mutant is lower compared to control in terms of cycling amplitude. It is instead comparable with the wild-type control in terms of overall bioluminescence levels, suggesting defects in synchronization rather than generally repressing PER expression. Two-way Anova performed in the range ZT 48–144 shows highly significant interaction between the mutant and control ($F_{(95,1746)}$=1.54, $P< 0.001$). Interestingly, we noticed also a 2-hr phase delay of *per-luc* expression in the *TrpA1* mutant compared to wild-type control during LD conditions. This is noticeable only in adult flies, but not in isolated legs (Figure 5.9B).

The defects in *period* expression during TC for *TrpA1*^{ins} mutant correlates well with the observation that this mutant shows the most severe "temperature phenotype" at the behavioural level in many temperature conditions we assayed, suggesting an important role for this TRP channel in the temperature entrainment pathway. We also generated transgenic lines carrying XLG-*luc* in *pyx*^{2} and *pyx*^{3} mutant backgrounds. At the moment it is not possible to present any results from those lines. For time reasons the experiments have not been completed and further investigation will determine whether *per-luc* expression in *pyrexia* mutants is affected. Additional experiments monitoring *per-luc* expression in the *TrpA1*, *pyx* and *trpM* mutant backgrounds are also needed under the conditions in which they exhibited a phenotype in our behaviour assays.

5.5 Summary

- Analysis of *trp* channel encoding genes in LL and 25:16℃ TC revealed that *pyrexia*, *TrpA1* and *trpM* exhibit impaired synchronization of locomotor activity specifically to TC and normal activity in LD conditions.

- *tim-gal4*-driven knock-down of TRP-RNAi lines did not give any results.

- Behavioural analysis at different temperature intervals in LL shows that *pyx* and *trpM* have entrainment defects specifically at cold interval (20:16℃) and normal entrainment at 25:20℃ and 29:25℃ TC. *TrpA1* mutants entrain weakly (if at all) at 29:25℃ TC and do not at 25:20℃ and 20:16℃.

- pyx^2 and *trpM* synchronize their behaviour in DD to 25:16℃ TC and even to small temperature intervals (29:25℃, 25:20℃ and 20:16℃). Similarly, pyx^3 entrain at 29:25℃ and 25:20℃ but not in the range 20:16℃. *trpA1* flies weakly entrain to all temperature intervals but not in the same extent as control (statistical interaction highly significant).

- *tim-gal4*-driven RNAi lines against *pyx* and *trpA1* do not induce any effect on *per-luc* expression in LL and TC. On the opposite, *per-luc* expression in *tim-gal4*-induced *trpM*-RNAi is not rhythmically cycling in LL and TC when the whole adult flies are analysed and normal in isolated legs.

- XLG-*luc* expression in *trpM* mutant background is comparable to control. *TrpA1* mutant flies exhibit a down-regulation of XLG-*luc* expression both in isolated legs and in the context of the whole fly (in terms of cycling amplitude).

Chapter 6

Circadian regulation of eclosion

6.1 Eclosion profile of "temperature mutants"

In the previous chapters, we discussed the isolation of new components which play a role in the temperature synchronization of the circadian clock. We examined the isolation of three mutants from an EMS mutagenesis screen, of three *trp* channel encoding genes (*pyx*, *trpM* and *trpA1*) and of one forkhead transcription factor encoding gene (*fd3F*) which show defects in temperature entrainment. The isolation of the mutant lines was based on the analysis of adult locomotor activity or monitoring real-time expression of *period-luciferase* transgenes in temperature entrainment regimes. In the past, similar approaches led to the isolation of two other "temperature mutants", *nocte* and *norpA* (Glaser and Stanewsky, 2005, 2007; Sehadova et al., 2009).

In my Ph.D. I also investigated whether the novel "temperature mutants" exhibited defects in the synchronization of the circadian clock that regulates the emergence of adult flies from the pupal stage.

Eclosion rhythms can be entrained, not only by light-dark cycles, but also by

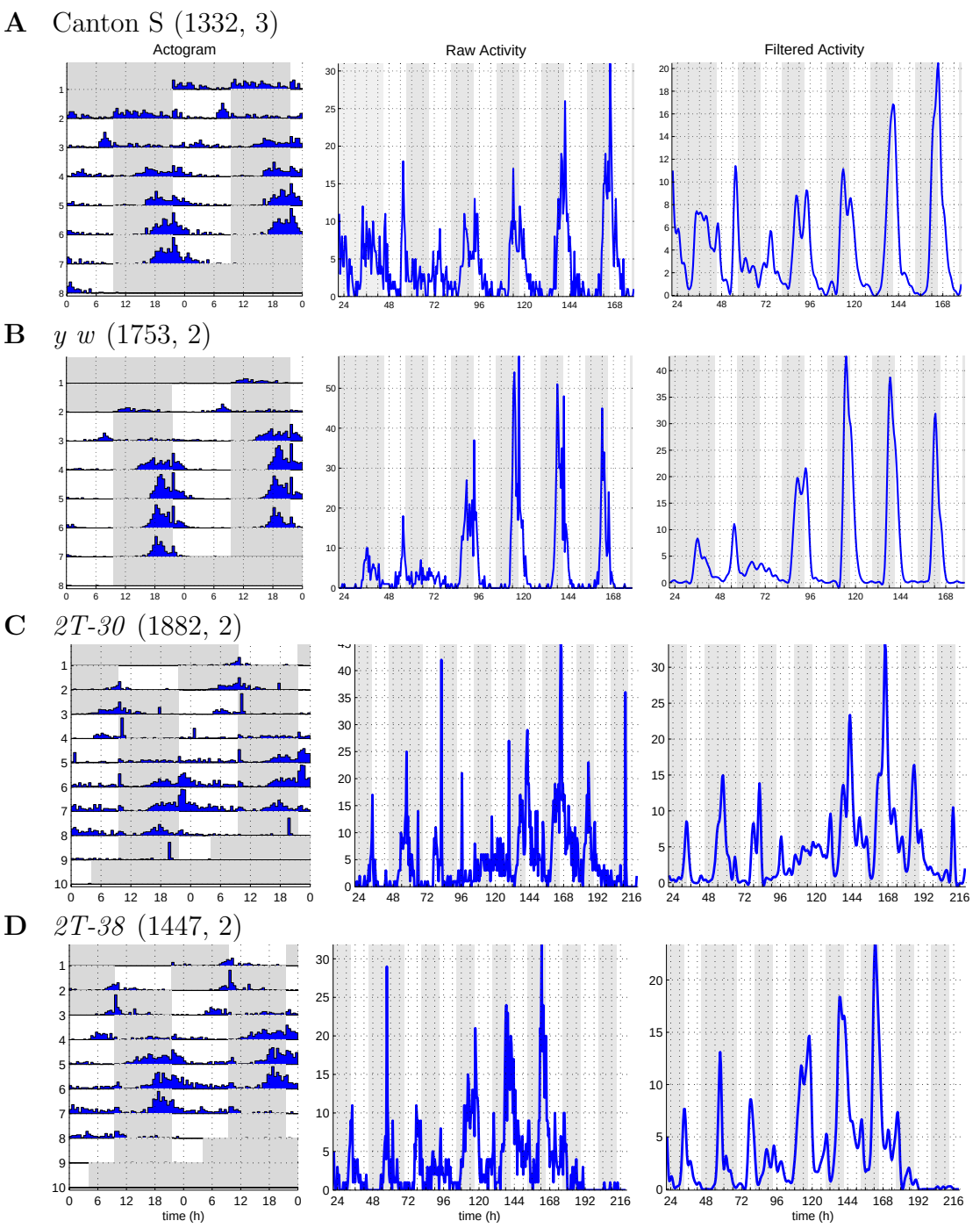
Constant light and 25:16°C Temperature cycles
A Canton S (1332, 3)
Actogram
Raw Activity
Filtered Activity
B y w (1753, 2)
C 2T-30 (1882, 2)
D 2T-38 (1447, 2)
time (h)
time (h)
time (h)

FIGURE 6.1

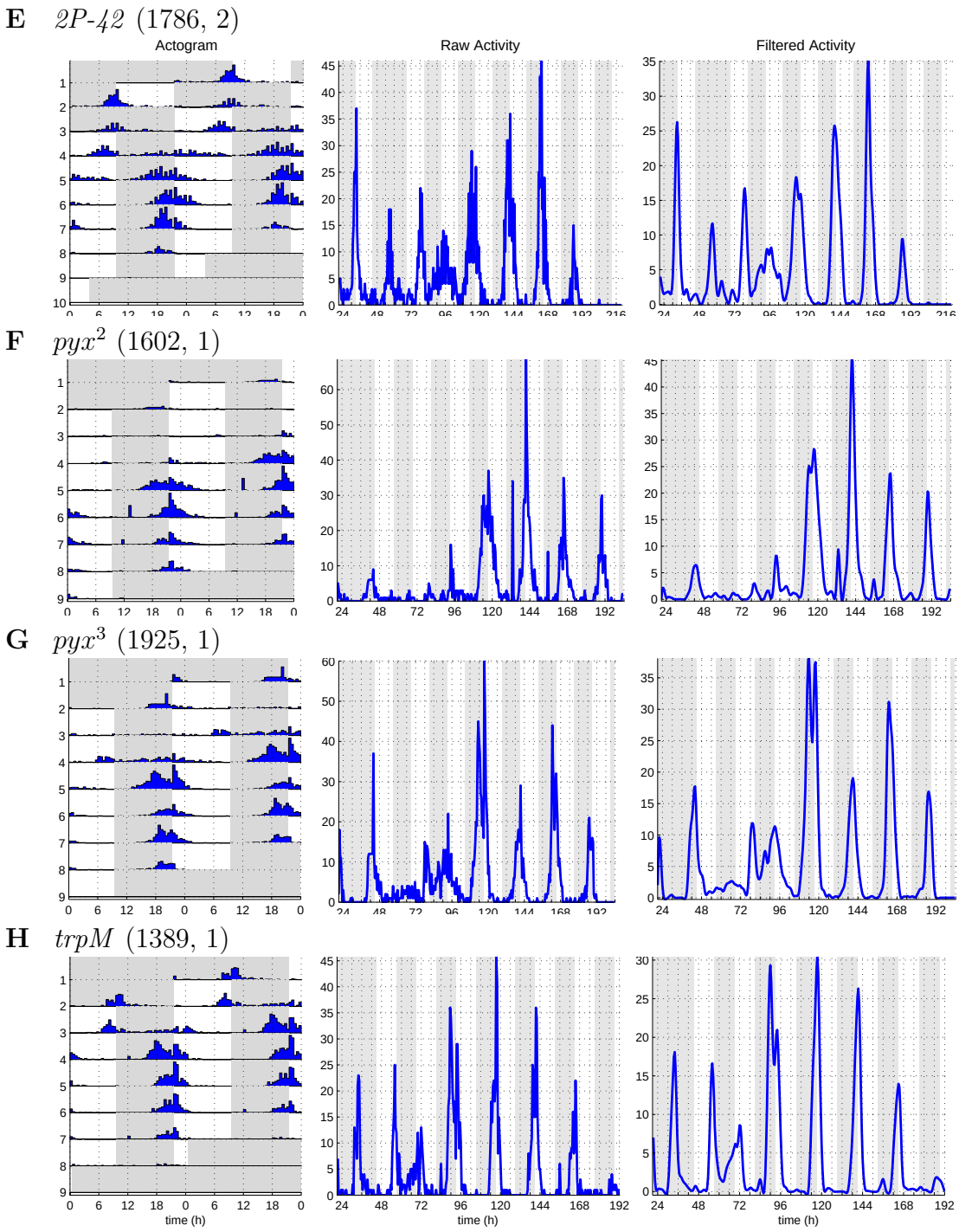
E 2P-42 (1786, 2)
Actogram
Raw Activity
Filtered Activity
F pyx2 (1602, 1)
G pyx3 (1925, 1)
H trpM (1389, 1)
time (h)
time (h)
time (h)

FIGURE 6.1

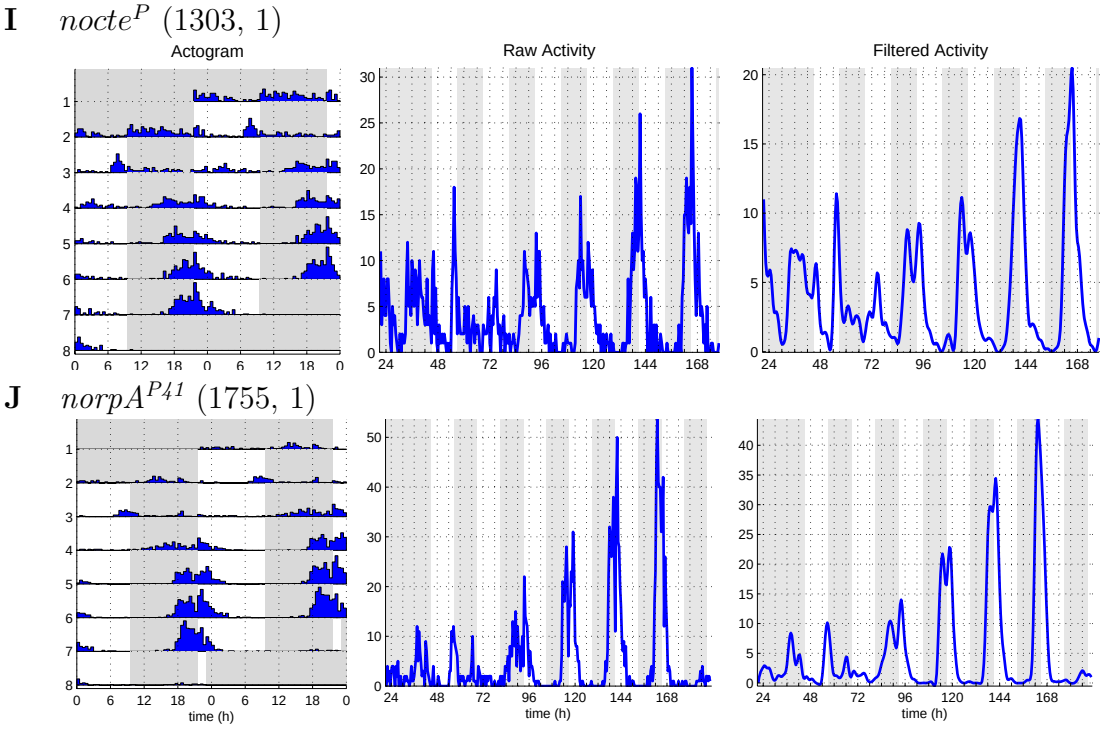

FIGURE 6.1: Eclosion profile for control and "temperature mutant" cultures during LL and TC conditions. The left-hand column shows double-plotted actograms of flies that emerged during a LL and 12:12 hr 25:16℃ TC, which was in opposite phase compared to the previous LD entrainment. Only the last dark cycle of the previous LD entrainment is indicated (except in C–E, where the full last LD cycle is included). The two right-hand columns depict, respectively, the total number of flies emerged as a function of time ("raw activity") and 4-hr low-pass filtered versions of the left plots ("filtered activity", see M&M and Levine et al., 2002a for more details). The total number of hatched flies and the number of experiment repetitions are indicated in brackets with the genotypes. Shaded areas refer to temperature conditions (grey shading: 16℃; white shading: 25℃). A–B) Canton S and *y w* control cultures synchronize eclosion to TC in 2 days and exhibit peak of emergence during the last part of the cold phase (ZT22–23). C–J) All the "temperature mutant" lines we tested show similar synchronization to TC compared to the control. Note the presence of a secondary peak, notably in day 3 and 4 of temperature entrainment, just after the transition cold-warm, which is probably a gating response induced by steep rise of temperature (see text). Repetitions showed reproducible results.

temperature cycles (Zimmerman et al., 1968). However, not many studies focus on the regulation of eclosion entrainment during temperature cycles, particularly in constant light conditions. In order to correlate the eclosion results with our locomotor behaviour data, I investigated eclosion in LL under temperature cycles.

Cultures for the desired genotype were raised in 12:12 hr LD cycles (at 20℃) and monitored for eclosion after exposing the cultures to LL and 12:12 hr 25:16℃ TC which was in the opposite phase compared to the previous LD. The eclosion profile under TC conditions, after establishing a stable phase, exhibits a clear 24 hour rhythm, and flies emerge in a 6–8 hour window which occurs shortly before the cold to warm transition. The timing of eclosion is controlled by the circadian clock, which imposes a "gate" that opens only during certain time of the day (Qiu and Hardin, 1996).

Wild-type control cultures (Canton S and *y w*) synchronize their eclosion rhythm to the TC after 2 transient days (Figure 6.1A–B), stabilizing the peak of emergence at the end of the cold phase after day 3. A second eclosion peak occurs just after the temperature rise (particularly noticeable in day 3 and 4 of temperature entrainment). This second peak occurs probably in response to the steep increase of temperature, inducing the pupae developmentally mature enough, to hatch. This second temperature-induced eclosion peak has been mentioned previously in the same conditions (Newby and Jackson, 1993).

We monitored the eclosion activity of 8 different mutant lines: *2T-30*, *2T-38*, *2P-42*, pyx^2, pyx^3, *trpM*, $nocte^P$ and $norpA^{P41}$(*fd3F* was analysed in the chapter 4). All of them exhibited a mutant phenotype (to different extents) when adult locomotor activity was monitored during temperature entrainment regime (see chapters 3, 5, Sehadova et al., 2009 and Glaser and Stanewsky, 2005, respectively). Surprisingly, all lines eclose with a normal pattern, synchronizing emergence after 2 days of TC and stabilizing the eclosion peak at the end of the cold phase (Figure 6.1). The only exception might be line *2T-30* (Figure 6.1C), which displays a "noisier" pattern of eclosion, pupae take one day longer to be synchronized with temperature and the gating window is wider then wild-type control (up to 12

hours). *2T-30* cultures exhibit also a more pronounced rise in eclosion directly after temperature rise (see day 4 and 5 of TC in Figure 6.1C). Although the pattern appears nosier, *2T-30* cultures can entrain to TC (see also Figure 6.2B).

The only mutant line we observed having defects on entrainment of eclosion to TC has been described in the previous chapter (4.4). When the transcription factor *fd3F* is down-regulated in all the clock cells (via a *tim-gal4* driver line), the phase of eclosion is shifted towards the warm phase.

To determine eclosion we utilize an automated monitor which counts the number of flies that hatch as a function of time (see M&M for details). For this reason, we could test only true breeding (not balanced) cultures, since we could not select the desired genotype from the eclosed progeny. Thus, we could not test genotypes like $nocte^{1}$, in which heterozygous females do not express the phenotype. Here I report the eclosion data from $nocte^{P}$, a hypomorphic *nocte* allele (Sehadova et al., 2009).

It was surprising that all genotypes we assayed exhibited a clear entrainment of eclosion — lines which had manifested a distinct mutant phenotype at the behavioural and molecular level in the adult. Our data suggest that entrainment of the clock that regulates eclosion involves different components and/or pathways compared to the adult clock.

To challenge further the ability to synchronize to TC even more than in the previous regime, I subjected *2T-30* and control cultures to a temperature shift (in LL) and monitored the ability to re-synchronize the eclosion clock.

Cultures were raised in LD conditions and the pupae were transferred to LL and 12:12 hr 25:16℃ TC. After 3 days, the temperature regime was advanced for 6 hours and eclosion was monitored. Canton S (control) and *2T-30* (mutant) cultures shift the peak of eclosion according to the temperature cycles, exhibiting

two days of transients and resynchronizing the emergence peak to the end of the cold phase (Figure 6.2). Clock mutant per^{01} cultures, on the contrary, are unable to synchronize to temperature cycles: they do not eclose with a 24-hr period but instead manifest bursts of emergence after any temperature transitions (Figure

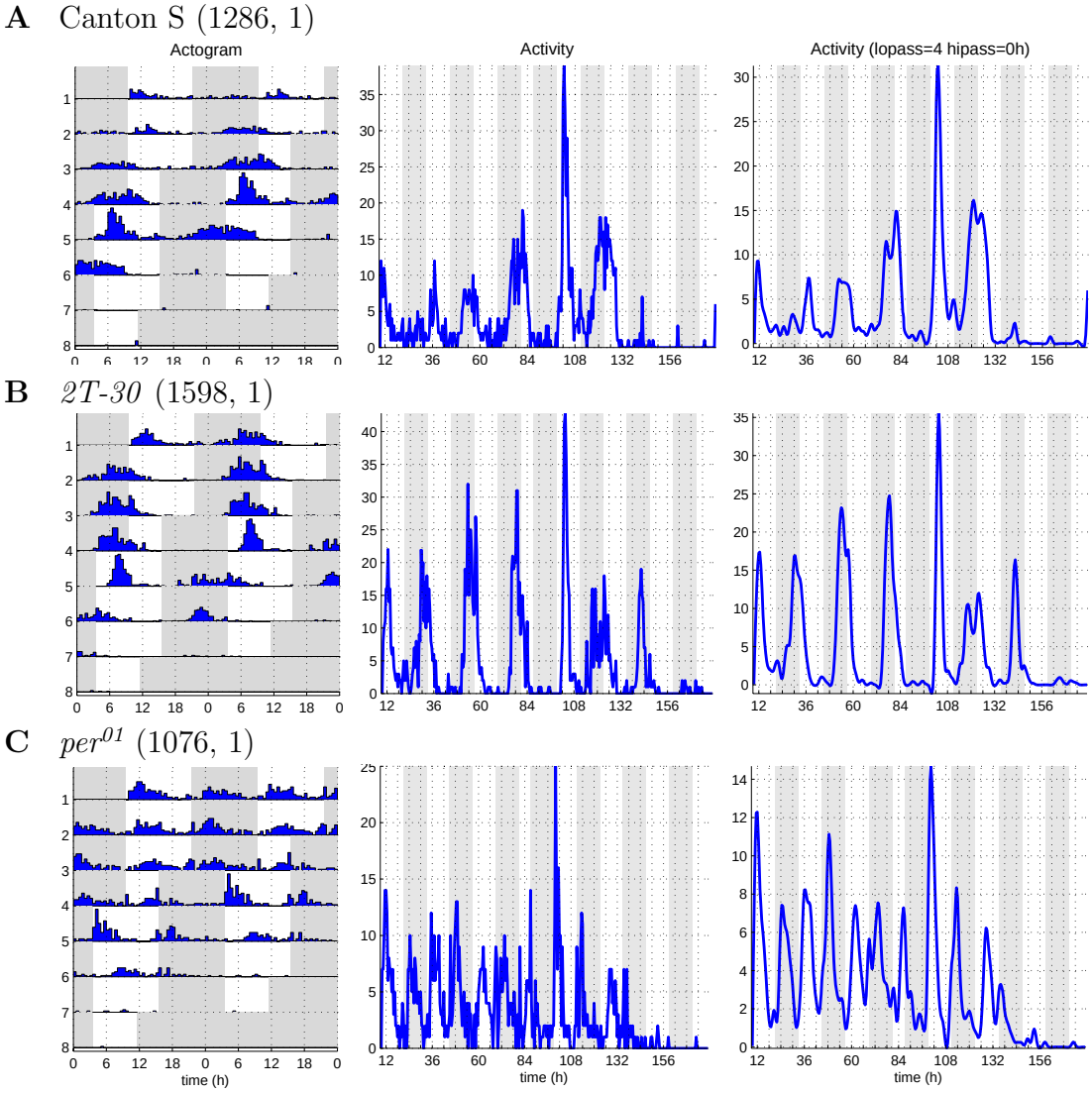

FIGURE 6.2: Re-synchronization of eclosion rhythms after 6-hr advanced temperature shift in LL. For description of the plots see Figure 6.1. Shift occurred at day 4, as shown by the shaded area in the actograms. A) Canton S and (B) EMS mutant *2T-30* cultures re-synchronize eclosion emergence to temperature cycles in 2 days. C) Eclosion of per^{01} cultures is not synchronized to TC: flies emerge mainly after all temperature changes most likely as a reaction to temperature increase and decrease.

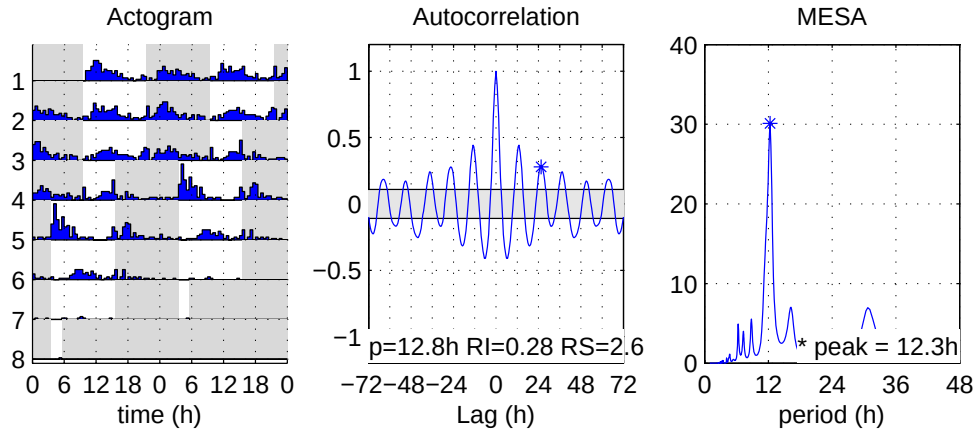

FIGURE 6.3: *per*^{01} cultures eclose with a 12-hour period. Flies emerge mainly after all temperature changes most likely as a reaction to temperature increase and decrease.

6.2C), therefore exhibiting a 12-hr period (Figure 6.3).

6.2 Effects of TC on the eclosion period

Given that adult "temperature mutants" do not exhibit eclosion phenotypes during LL and 25:16°C TC, I investigated in more detail the regulation of the circadian clock to TC, by monitoring the eclosion rhythm after temperature entrainment in constant conditions.

I raised cultures of Canton S and *2T-30* in LD and exposed them to LL and 12:12 hr 25:16°C TC (which was 6 hr delayed compared to the previous LD) for 3 days at the early pupal stage, and then released them in DD and constant temperature to monitor the eclosion rhythm. As shown in Figure 6.4A,B, the two different cultures synchronize eclosion to temperature and, when released in DD, they display a clear rhythm, which persists for several days, and is in phase with the previous temperature regime. Very surprisingly, I observed that flies emerge with a short (and reproducible) period of 20–21 hour. Canton S exhibit a 20 hour period and *2T-30* a 21 hour period (Figure 6.4). Given that the short period of

eclosion is stable (i.e. persists for several days) and is a common feature between cultures of different genetic background, we assume that it is not affected by the mutant tested.

Recent work from the Rouyer group proposed a model for temperature entrainment of the larval brain (Picot et al., 2009). Monitoring PER accumulation

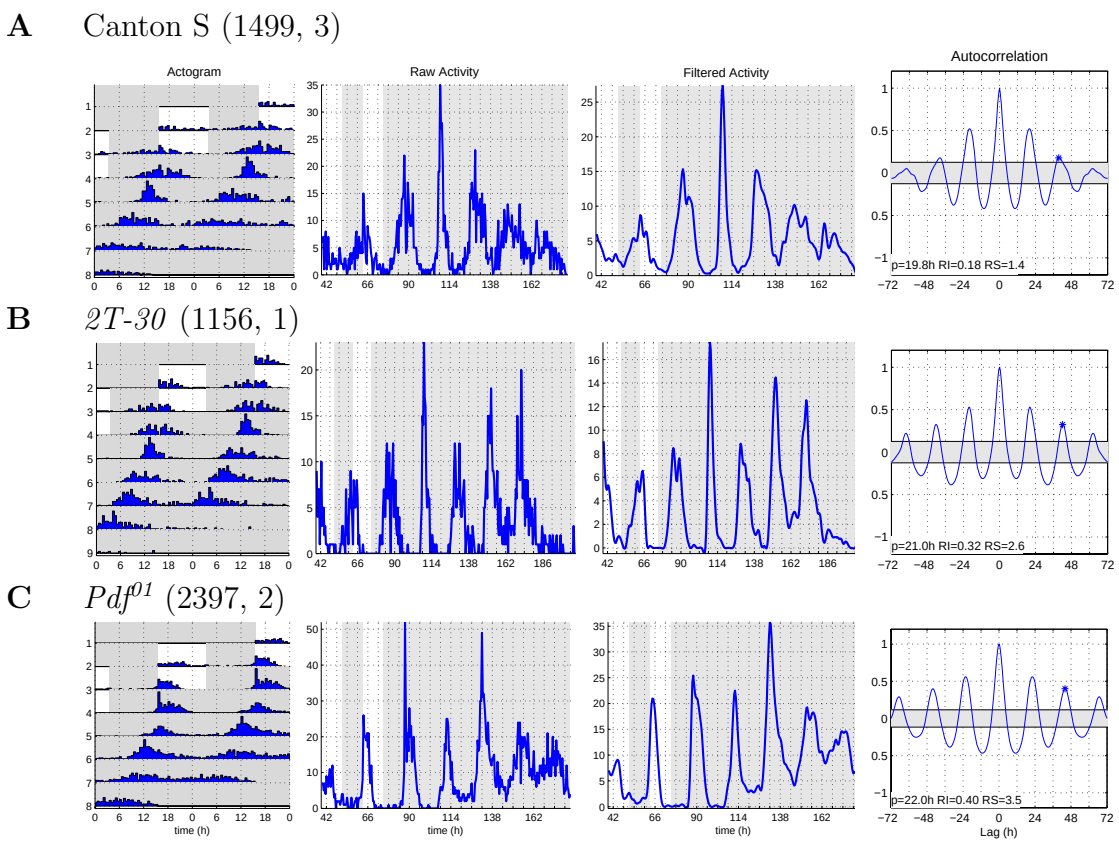

FIGURE 6.4: Free-running eclosion rhythms after 3 days of LL and TC entrainment. Cultures of Canton S, *2T-30* and Pdf^{01} flies were raised in LD (20°C) until early pupae, which were then collected and transferred to the eclosion discs. Those were subjected to 3 full 25:16°C temperature cycles in LL which were 6-hr delayed compared to the previous LD and then release in constant darkness (at 20°C). Only 2 of the 3 days of LL and TC entrainment are included in the plots. The three left-hand plots have been described in Figure 6.1. The most right-hand plot depicts autocorrelation which gives period values, calculated for the DD part only. Grey shaded areas represent 16°C (during LL and TC) or darkness (20°C). White areas represent 25°C (during LL and TC). "p", period (hr). "RI", Rhythmicity Index. "RS", Rhythmicity Statistic (RS 1.5 indicates rhythmicity, see M&M for details). Number of total emergents and experiment repetition is indicated in brackets with the genotype.

in the different groups of larval clock neurons, they described that the DN_2s can directly be entrained by TC and synchronize PER expression in the LNs through a PDF-independent (unknown) pathway. They proposed that the CRY-negative DN_2s are required to entrain the larval central clock to temperature cycles (Picot et al., 2009).

To address whether the short period was driven by the DN_2s and if *Pdf* was required in the synchronization of the eclosion to temperature cycles, we monitored Pdf^{01} mutant cultures. Surprisingly, Pdf^{01} cultures eclosed rhythmically with a short period of 22 hours, which persists for several days, comparable to wild-type (Figure 6.4C).

Short eclosion period of wild-type cultures has never been reported before. Moreover, Myers et al. (2003) reported that Pdf^{01} mutants exhibit aperiodic eclosion after LD entrainment. We wondered if the short eclosion period, and rhythmicity of Pdf^{01} cultures, were determined by the different conditions we used. Therefore, we investigated the free-running period of the same genotypes after entrainment to LD. Figure 6.5 shows free-running rhythms of Canton S, *y w*, *2T-30* and Pdf^{01} cultures. They all entrain to light-dark cycles and flies eclose with a circa 24 hour free-running rhythm, which persists for several days. Pdf^{01} cultures are strongly rhythmic for 3 days (with a 23.3 hour period) and then the rhythmicity gradually dampens, resulting in aperiodic eclosion after day 5 (Figure 6.5D). Interestingly, my observations are in disagreement with data published by the Sehgal group, which showed that eclosion of Pdf^{01} mutants (and flies lacking *pdf*-expressing cells) is arrhythmic in DD (Myers et al., 2003). Thus, we showed that *(a)* 3 days of entrainment in LL and TC during the pupal stage shortens the period of eclosion of cultures which exhibit a normal 24 period after LD entrainment and *(b)* that Pdf^{01} eclose rhythmically and comparable to control after LL

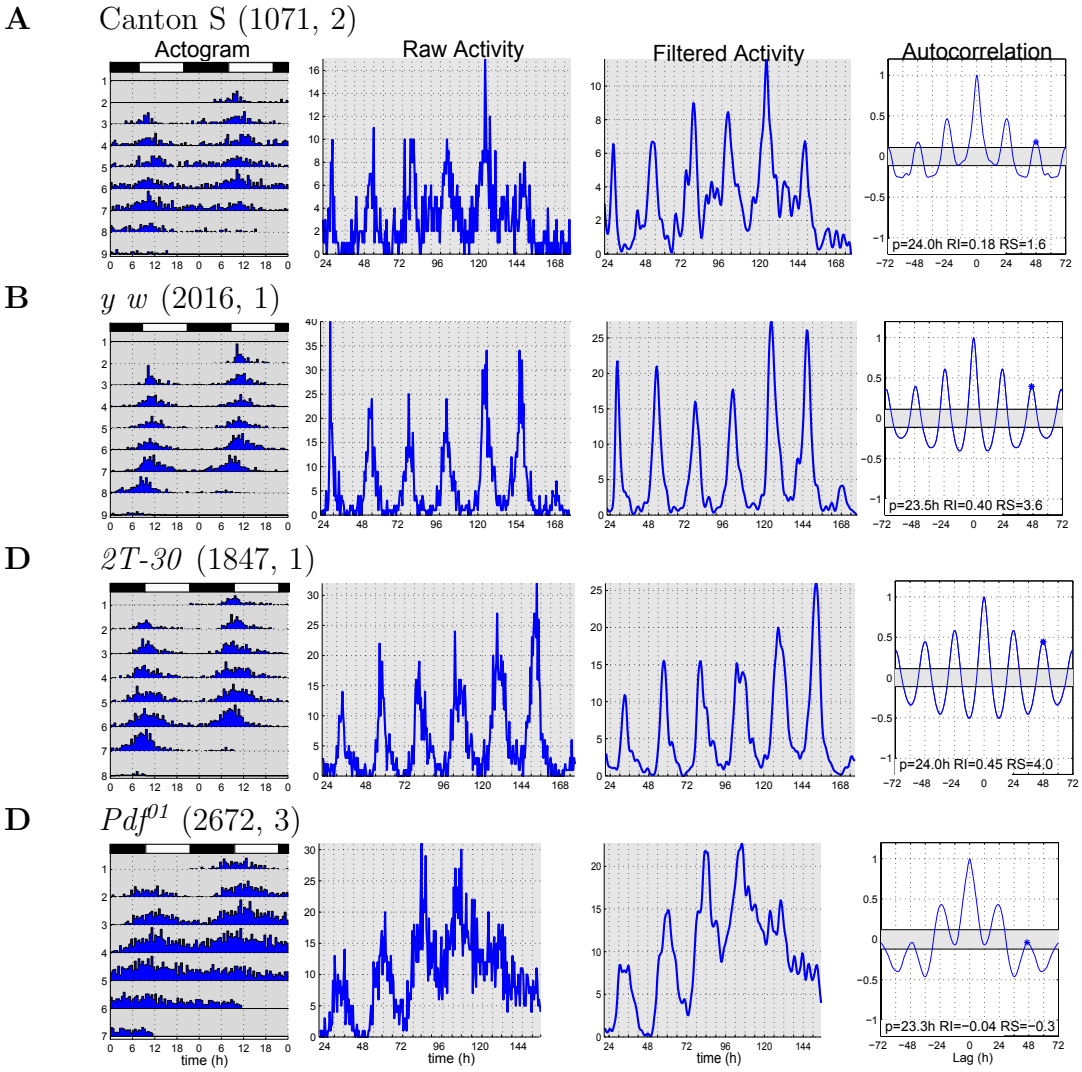

FIGURE 6.5: Free-running eclosion rhythms after LD entrainment. Cultures of Canton S, *y w*, *2T-30* and Pdf^{01} flies were raised in LD (20°C) and then released into constant conditions (DD and 20°C) where the eclosion activity was monitored. Plots have been described in Figure 6.1. Total numbers of emerged flies and experiment repetitions are indicated in brackets next to the genotypes. All the cultures eclose rhythmically with a circa 24-hr period. Pdf^{01} rhythm persists strongly for 3 days (with a 23.3 hr period) and then gradually dampens. White/black bars at top indicate subjective day and night, respectively.

and TC and that rhythmicity persist for 3–4 days in DD after LD entrainment.

Since we did not observe any gross differences in the eclosion pattern between *2T-30* and Canton S cultures (in constant conditions), we proceeded by monitoring the emergence profiles of Canton S (control) and Pdf^{01} (mutant) to address the

question on the origin of the short period observed after LL and TC entrainment.

This short period phenotype was obtained after exposing pupal cultures glued to "eclosion discs" to TC for 3 days. Since we assume that the free-running period is clock controlled, we wondered if we could observe the same short free-running period if TC entrainment was restricted exclusively to the larval stages, in order to discriminate whether the short period was generated by the larval or the pupal clock.

Thus, we restricted temperature cycle entrainment (in LL) from day 2 of development until the first pupa appeared in the cultures, and then transferred to constant darkness (at 20°C). The free-running eclosion rhythm was then monitored (Figure 6.6). Canton S flies eclosed rhythmically with a 22.8 hour period. The eclosion profile is "noisier" and the peak less sharp than in the previous conditions, probably because the cultures had been in DD for up to five days before eclosion was monitored, and therefore individuals within the population being out of phase each other. It is also interesting to note that the phase during free-run of eclosion compared to that after temperature entrainment is reversed: The peak of emergence is centred to the second half of the corresponding warm phase (CT10–12) versus ZT22–6 during temperature entrainment. This nicely correlates with the reported data that larval-only TC entrainment reverses the phase of adult locomotor activity (Picot et al., 2009 and see below). When Picot et al. restricted TC entrainment to larva only stages (in DD) and then monitored free-running adult locomotor activity, they observed that the phase of activity was opposite compared to activity of flies subjected to larval only LD entrainment (Picot et al., 2009).

Pdf^{01} cultures exhibit aperiodic eclosion in the same conditions (Figure 6.6B). The Pdf^{01} rhythm does not persist for more than 5 days in DD (after LD entrain-

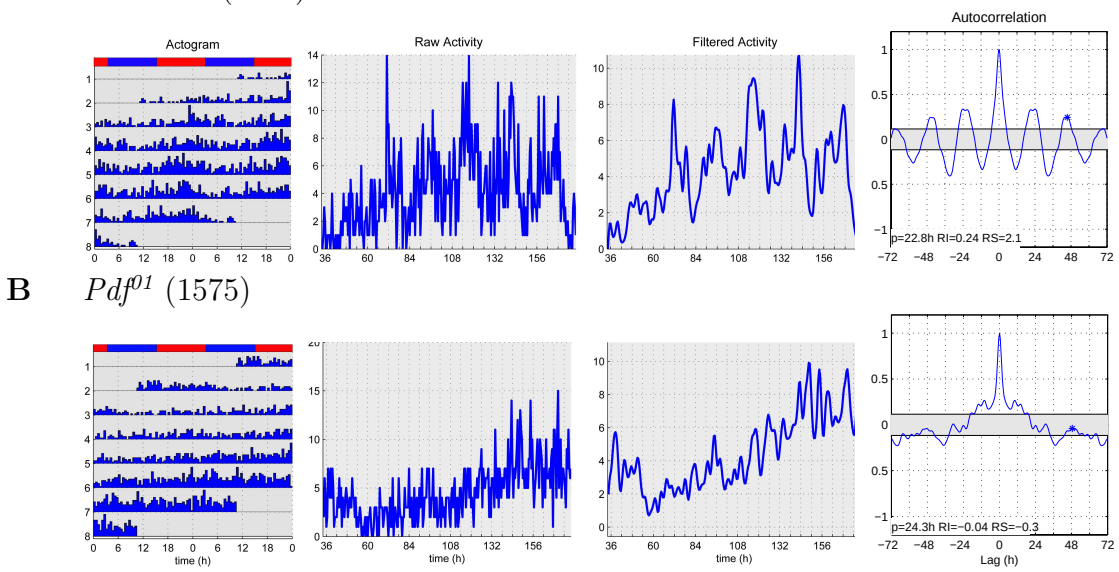

FIGURE 6.6: Free-running eclosion rhythms after LL and TC entrainment restricted to larval stages. Cultures were subjected to LL and 12:12 hr 25:16°C TC only during the three larval stages (from day 2 of development until the first pupa appeared in the culture), then were transferred to DD (20°C) where the eclosion rhythm was monitored. A) Canton S rhythms persist in DD for several days with a period of 22.8 hour. B) Pdf^{01} flies exhibit aperiodic eclosion. Red/blue bars at top indicate subjective warm- and cold-phase, respectively (relative to larval-only TC entrainment). Number of flies eclosed is indicated in brackets next to the genotype. Experiment in this conditions was performed once.

ment, Figure 6.5) and, if TC entrainment is restricted to larvae only, cultures are kept in DD for 5 days before eclosion is being monitored. Taken together, these two observations could explain why the *Pdf* mutant is arrhythmic in the current experiment. The Canton S free-running period of 22.8 hour lies in between the short period (20 hr) observed after 3 days of TC entrainment restricted to the pupal stage and the "normal" 24 hr period after LD entrainment.

Next, we asked which eclosion period cultures would exhibit when exposed to TC throughout development. We entrained Canton S and Pdf^{01} cultures to LL and 25:16°C from late embryo to pupae and then released them in DD. Canton S and Pdf^{01} cultures emerged with a short period of 22.5 and 21.8 hours, respectively

(Figure 6.7), similar to the results obtained when TC entrainment is applied to larvae or pupae only. This observation suggests that the timing at which the TC is applied during development does not determine the period of free-running eclosion, but are rather the conditions (LL and TC) themselves.

Figure 6.9 summarizes the experiments described above and illustrates free-running period of Canton S and Pdf^{01} cultures after LL and TC entrainment applied at different times during development. It appears that there is no clear correlation between the developmental stage at which TC is applied and the resulting free-running eclosion period in DD. TC restricted to larval stage only, pupae only or during all developmental stages result in a short period of 22.5, 21 and 22.5 hours, respectively, for Canton S cultures. Similarly, temperature entrainment restricted to pupae or during all developmental stages induces a period of 21.5 and 21.8 hours, respectively, for Pdf^{01} mutants, whereas eclosion is arrhythmic in larva-only temperature entrainment.

To address whether the short free-running period of eclosion after TC during the pupal stage was induced by the continuous exposure to light we also monitored free-running activity after entraining cultures to DD and TC. Canton S and Pdf^{01} cultures were entrained in DD and 12:12 hr 25:16℃ TC throughout development before being transferred to the eclosion disc (see Figure 6.9) and then released to constant conditions (at 20℃). As depicted in Figure 6.8, Canton S eclosion is rhythmic, but the free-running period is not stable and seems to change over the days. From day 1 to day 3 (of DD) flies eclose with a short, 22.5 hr period (Figure 6.8A,C). During the subsequent days, the eclosion activity exhibits a 24 hr rhythm, and the rhythmicity dampens gradually over the days. Pdf^{01} cultures also exhibit rhythmic eclosion, with a stable short period of 20.8 hr (Figure 6.8B). The rhythm is strong for the first 3 days (with a 20.5 hr period, Figure 6.8D) and

then gradually dampens and becomes very "noisy".

The short period exhibited by Canton S flies is quite surprising, since previous reports have shown a strong and stable eclosion rhythm with a 24 hr period after DD and temperature cycle entrainment (Zimmerman et al., 1968). However, Zimmerman and Pittendrigh's observation were based on experiments conducted on *D. pseudoobscura* and not on *D. melanogaster*.

For the time being, it is difficult to speculate which components of the circadian clock contribute to generate the short period of free-running eclosion after entrainment to TC. It is also largely unclear which contribution each group of neurons plays in regulating locomotor behaviour in the adult fly during temperature entrainment. Even more unclear (and less studied) is which different neuronal group drives eclosion rhythms. Nevertheless, the short eclosion period after TC

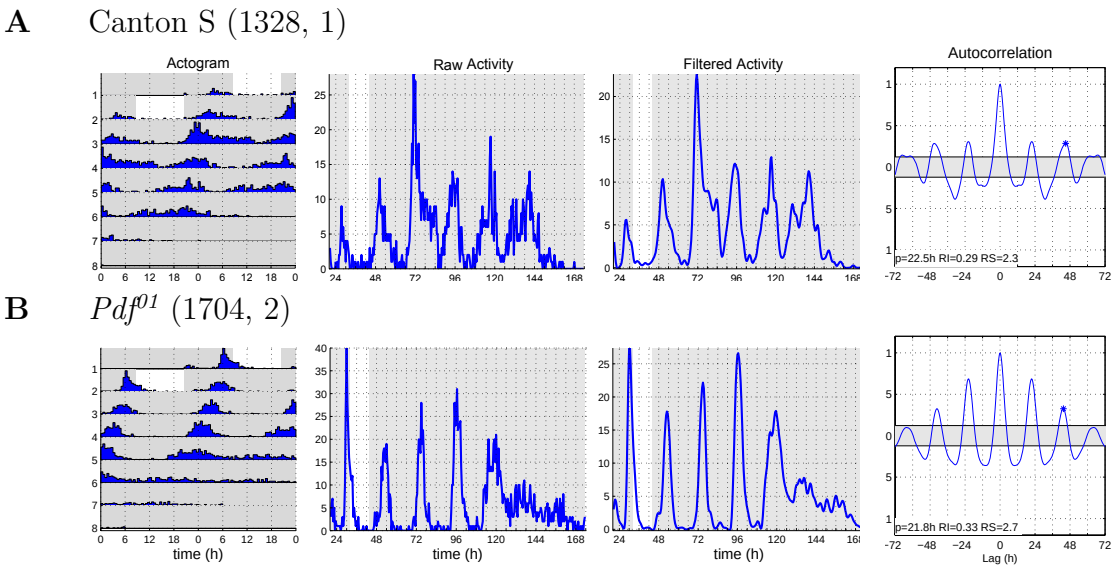

FIGURE 6.7: Free-running eclosion rhythms after 9 days of LL and TC entrainment. Cultures of Canton S and Pdf^{01} flies were raised in LL and 25:16°C TC since day 2 of development then were transferred to DD and 20°C where free-running periods were calculated. The last cycle in LL and 25:16°C is included in the plots (white/grey shading in day 0). For description of plots, see Figure 6.1. Both Canton S (A) and Pdf^{01} (B) flies eclose with a short rhythm of 22.5 and 21.8 hours, respectively. Numbers of flies eclosed and experiment repetitions are indicated in brackets next to the genotype.

A Canton S (1269)

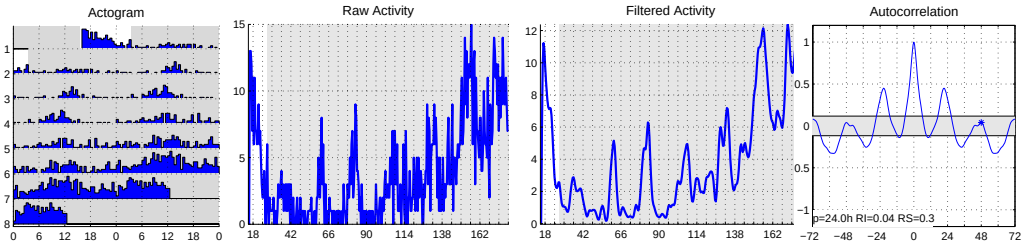

B *Pdf*^{01} (3306)

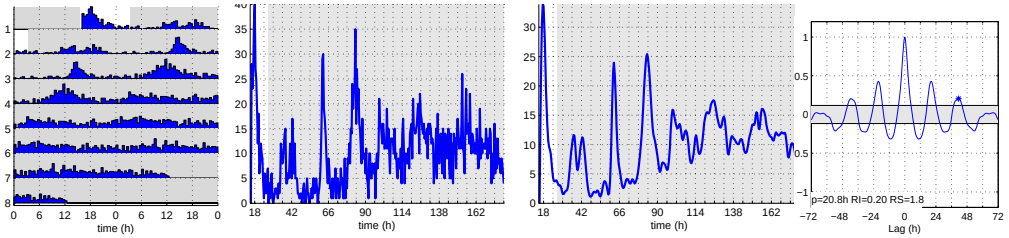

C Canton S

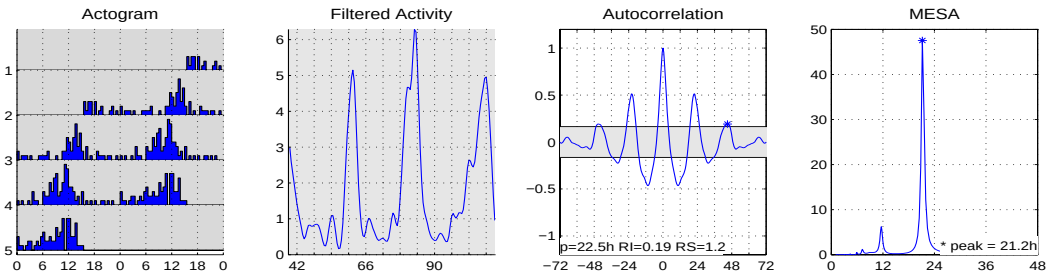

D *Pdf*^{01}

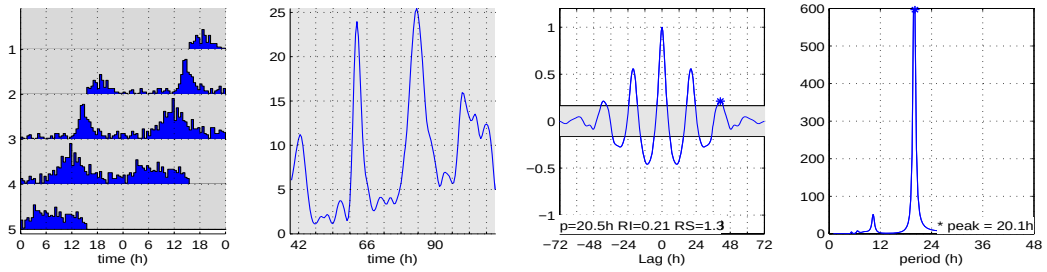

entrainment, the *pdf*-independence of the rhythms, and indications from published work (Picot et al., 2009) suggested an important role for the DN_2 neurons in the temperature entrainment of eclosion.

We can speculate a role for the larval DN_2s in setting the period of eclosion. We observed that TC applied to larval stages only reverse the eclosion phase and this is not the case for pupal-only TC entrainment. It has been reported that the larval DN_2s have an opposite phase of PER expression (compared to the LNs) in LD (Kaneko et al., 1997; Picot et al., 2009) and that they reverse their PER-expression phase during metamorphosis (Kaneko et al., 1997). Larval LNs are required to generate eclosion rhythms (Blanchardon et al., 2001) — they are the only clock-gene expressing neurons during pupation (Kaneko et al., 1997; Helfrich-Förster et al., 2007) — and we propose here that the eclosion phase is determined by the temperature sensitive DN_2s.

6.3 Summary

- Components required for entrainment of the adult locomotor activity to TC do not affect the ability of cultures to synchronize their eclosion rhythms to temperature. This suggests the involvement of different structures and

FIGURE 6.8 *(preceding page)*: Free-running eclosion rhythms after DD and TC entrainment. A–B) Cultures of Canton S and Pdf^{01} were entrained in DD and 12:12 hr 25:16°C since day 2 of development until pupae were loaded on the "eclosion disc". Then, cultures were released in DD (and 20°C), where free-running emergence was monitored. The last day of TC is included in the plots (white/grey areas indicate 25°C and 16°C, respectively). C–D) Analysis of rhythmicity considering only the first 3 days after TC entrainment. A) Canton S flies eclose rhythmically with a period of 24 hours. The rhythmicity is very noisy and dampens quickly. The free-running period changes from 22.5 the first 3 days (C) to 24 hours during subsequent days. B) Pdf^{01} cultures eclose with a stable rhythm of 20.8 hr (20.5 hr in the first 3 days, D). After 3–4 days, the eclosion profile of both genotypes becomes "noisier" and the peak less "sharp". Number of flies eclosed is indicated in brackets with the genotype. Experiment performed once.

1	2	3	4	5	6	7	8	9	10	11	12	13	14	15	τ *CS*	τ
LD										DD					24	23.3
LD									LL+TC			DD			21	21.8
LD	LL+TC								DD						22.5	n.r.
LD	DD+TC									DD					22.5	21
LD	LL+TC									DD					22.5	21.8

FIGURE 6.9: Summary of free-running eclosion periods after different light and temperature entrainment conditions. Top 2 rows depict a visual representation of the *Drosophila* life cycle and a rough estimation of the days it takes to go through the different stages (during TC). See text for more details of the precise number of days in which the cultures have been exposed to the different Zeitgebers. Arrow indicates the moment when the cultures were transferred from bottles to the "eclosion discs" and when data collection started (grey background days: duration of data collection). Cultures were entrained in different entrainment conditions, as indicated, and the period calculated after release to DD. LD is 12:12 hr light-dark and 20°C. TC is 12:12 hr 25:16°C. DD refers to constant darkness and 20°C. The period of eclosion (τ, in hr) is calculated for the last 4 or 5 days of DD. Images of the *Drosophila* life cycle are taken from the cover of *Science*, Vol. 297, Issue 5590 (2002) "n.r." indicates not rhythmic.

pathways for temperature entrainment of eclosion clock compared to the adult clock.

- pdf^{01} mutants exhibit rhythmic eclosion in DD, after light and temperature entrainment.
- TC applied at different times during development modulate the free-running period of eclosion, in a largely PDF-independent manner. Pupal TC entrainment drastically shortens free-running eclosion period of wild-type cultures, and similarly of pdf^{01} mutants.
- Larval-only temperature entrainment reverse the phase of eclosion compared to light-dark entrainment.
- We propose that the free-running phase and period of eclosion after TC are determined by the DN_2s

Chapter 7

nocte and peripheral sensory tissues

7.1 Background

In a previous EMS mutagenesis screen, aimed on the isolation of novel factors involved in the temperature entrainment of the circadian clock, a new genes has been isolated. *no circadian temperature entrainment* (*nocte*) shows impaired *per-luc* synchronization as well as abolished entrainment of the locomotor behaviour to temperature cycles (Glaser and Stanewsky, 2005). Later, the mutation has been mapped on the X chromosome and the gene identified (Glaser, 2006).

In this chapter, the following work is discussed, which led to the publication of the article "Temperature entrainment of *Drosophila*s circadian clock involves the gene *nocte* and signaling from peripheral sensory tissues to the brain" in the journal *Neuron* (Sehadova et al., 2009).

7.2 My contribution to the paper

The contribution I had for the publication of the paper was the behavioural analysis of the two *nocte* alleles and of chordotonal organ mutants in LL and TC (Figure 4). In particular, I analysed the behaviour of $nocte^{1}$, $nocte^{P}$, eys^{395}, eys^{734}, $spam^{1}$, $tilB^{1}$ and *smetana* (the transheterozygous *smet/Df(smet)* and double mutant $nocte^{P}$;*smet/Df(smet)*). All those mutants lines showed defects of temperature entrainment in LL and 25:16℃ TC. Similarly, analysis of the several *nocte*-RNAi lines driven by *F-gal4* have been tested in LL and TC, and quantification of behaviour is depicted in Figure S5. We observed that lines from both types of RNAi constructs can results in either normal or mutant phenotype, indicating that positional effects of the insertion sites influence the efficiency of the RNAi effect.

Next, I showed that both *nocte* alleles exhibit an uncoordinated phenotype, similar to *spam* mutants, after prolonged exposure to high temperature (37℃). The uncoordination phenotype is rescued when flies are exposed to to the same high temperature at >90% humidity (Figure 7).

I also showed that stopping the clock in the ch organs neurons by over-expressing a dominant negative form of *cycle* (*cyc*-Δ, Tanoue et al., 2004), under the F-gal4 promoter, does not prevent the flies to entrain to TC in LL (Figure 8). This suggests that temperature entrainment does not require a functional clock in ch organ to take place. Finally, I demonstrated that removal of either the 3rd antennal segment, or the whole antenna results in "entrained" behaviour (Figure S5). This demonstrates that ch organs located in the antennae are not required for temperature entrainment

Neuron
Article

Temperature Entrainment of *Drosophila*'s Circadian Clock Involves the Gene *nocte* and Signaling from Peripheral Sensory Tissues to the Brain

Hana Sehadova,[1,5] Franz T. Glaser,[2,5] Carla Gentile,[1,5] Alekos Simoni,[1] Astrid Giesecke,[1,4] Joerg T. Albert,[3] and Ralf Stanewsky[1,2,*]
[1]School of Biological and Chemical Sciences, Queen Mary College, University of London, Mile End Road, London, E1 4NS, UK
[2]Institut für Zoologie, Universität Regensburg, Universitätsstrasse 31, 93040 Regensburg, Germany
[3]The Ear Institute, University College London, 332 Gray's Inn Road, London, WC1X 8EE, UK
[4]Present address: MRC Laboratory of Molecular Biology, Structural Biology Division, Hills Road, Cambridge CB2 0QH, UK
[5]These authors contributed equally to this work
*Correspondence: r.stanewsky@qmul.ac.uk
DOI 10.1016/j.neuron.2009.08.026

SUMMARY

Circadian clocks are synchronized by the natural day/night and temperature cycles. Our previous work demonstrated that synchronization by temperature is a tissue autonomous process, similar to synchronization by light. We show here that this is indeed the case, with the important exception of the brain. Using luciferase imaging we demonstrate that brain clock neurons depend on signals from peripheral tissues in order to be synchronized by temperature. Reducing the function of the gene *nocte* in chordotonal organs changes their structure and function and dramatically interferes with temperature synchronization of behavioral activity. Other mutants known to affect the function of these sensory organs also interfere with temperature synchronization, demonstrating the importance of *nocte* in this process and identifying the chordotonal organs as relevant sensory structures. Our work reveals surprising and important mechanistic differences between light- and temperature-synchronization and advances our understanding of how clock resetting is accomplished in nature.

INTRODUCTION

Circadian clocks regulate many biological processes so that they occur at beneficial times for the organism. Although these clocks are self-sustained and continue to run under constant conditions, they are synchronized with the environment by so called "Zeitgebers" (Dunlap et al., 2004). Two prominent Zeitgebers are the natural light-dark and temperature cycles that are able to synchronize the circadian clock of *Drosophila* and other organisms (see Boothroyd and Young, 2008; Dubruille and Emery, 2008; Glaser and Stanewsky, 2007 for recent reviews). Although our knowledge regarding light entrainment of both fly and mammalian clocks is quite advanced, relatively little is known about temperature synchronization. Light is generally considered to be the more powerful Zeitgeber, but a temperature cycle with only 2°C–3°C amplitude robustly synchronizes *Drosophila* behavioral rhythms (Wheeler et al., 1993). In mammals, chick, and zebrafish, similar low-amplitude temperature rhythms (equivalent to body-temperature rhythms) are able to synchronize clock gene expression in the suprachiasmatic nucleus (SCN) and peripheral clock cells (Barrett and Takahashi, 1995; Brown et al., 2002; Herzog and Huckfeldt, 2003; Kornmann et al., 2007; Lahiri et al., 2005; Prolo et al., 2005), exemplifying the potential strength of this Zeitgeber. Moreover, as shown for *Drosophila* (Glaser and Stanewsky, 2005), temperature synchronization of clock gene expression in these organisms occurs in tissue- or cell-autonomous manners, indicating that similar mechanisms are involved in ectothermic and endothermic animals.

Drosophila's daily locomotor rhythmicity profile is bimodal, exhibiting major activity peaks in the morning and evening (e.g., Wheeler et al., 1993). This bimodality is regulated by several groups of clock neurons in the fly brain (see Sheeba et al., 2008 for a recent review). Recent work has revealed that a group of ventrally located neurons controls mainly the morning activity peak of fly behavior (M-cells), whereas more dorsally located cells regulate evening activity (E-cells) (Sheeba et al., 2008). These neurons control locomotor rhythms, and cyclically express several clock genes and proteins in synchrony with light-dark or temperature cycles (e.g., Yoshii et al., 2005; Zerr et al., 1990).

While clock neurons are mainly cell autonomously synchronized by light via Cry, it is not known how temperature signals reach the brain clock. It is formally possible that temperature sensitive neurons express a circadian temperature receptor that is able to synchronize the molecular clock within the pacemaker neurons (Hamada et al., 2008). Alternatively, temperature could be sensed by other neurons in the brain or by sensory structures in other parts of the fly, which then signal to the clock neurons. Two mutations that interfere with temperature entrainment, both molecularly and behaviorally, have been identified and could therefore shed light on the temperature entrainment mechanism (Glaser and Stanewsky, 2005). Mutants in the *norpA*

gene, which encodes for the enzyme phospholipase C, are not able to synchronize to temperature cycles (Glaser and Stanewsky, 2005), indicating that a G protein-coupled signal transduction cascade might be involved. The mutated gene of the other temperature-entrainment-deficient variant (*nocte*) was not known until now.

Here we demonstrate that isolated *Drosophila* brains are not able to synchronize to temperature cycles. Since they do synchronize to light-dark cycles, these findings indicate that the brain requires temperature input from the periphery. We further reveal the molecular identity of the *nocte* gene, which encodes a large glutamine-rich protein with unknown function. Downregulation of *nocte* in peripheral tissues, including neurons of specific sensory structures (chordotonal [ch] organs), thoroughly disrupts temperature entrainment of behavioral rhythms. Similarly, other mutants known to affect the structure and function of ch organs also interfere with temperature entrainment, and mutant *nocte* alleles exhibit structural as well as physiological defects of sensory organ function. Moreover we show that a functional clock within these sensory structures is not required for behavioral temperature entrainment to occur, indicating that temperature information must be interpreted in a temporal fashion by downstream clock neurons in the thoracic central nervous system (CNS), or by the brain pacemaker neurons themselves. Our findings demonstrate the existence of a periphery-to-brain signaling pathway, identify the responsible sensory structures, and uncover fundamental differences between the light- and temperature-entrainment pathways of the fly circadian clock.

RESULTS

Tissue-Autonomous Synchronization to Temperature Cycles Is Restricted to Peripheral Organs

The *Drosophila* circadian clock can easily be entrained by temperature cycles (or steps), both in constant darkness (DD) and constant light (LL) (Busza et al., 2007; Glaser and Stanewsky, 2005; Matsumoto et al., 1998; Stanewsky et al., 1998; Wheeler et al., 1993; Yoshii et al., 2002, 2005, 2007). We previously showed that molecular synchronization can occur on a tissue-autonomous level. Isolated body parts of flies expressing two different *period-luciferase* (*per-luc*) constructs showed entrained bioluminescence oscillations when kept in LL and temperature cycles (Glaser and Stanewsky, 2005). When we performed these experiments, we noticed that isolated brains showed a 12 hr phase-advanced bioluminescence peak compared to all other isolated tissues (Figure 1A and Glaser and Stanewsky, 2005). This phase advance was not observed in LD cycles at constant temperature (Figure 1A), perhaps indicating a prominent role of the brain in synchronizing the phase of other tissues during temperature cycles. Alternatively, because the rise in *luc*-reported *per* expression occurs immediately after the temperature increase, it could reflect a mere response to the environmental transition, rather than bona fide synchronization of clock gene expression.

To address this issue we next analyzed brain *per-luc* expression in various mutant backgrounds known to interfere with temperature entrainment. We applied the *BG-luc* and *XLG-luc* transgenes, encoding 2/3 or the entire Per protein fused to Luc, respectively; both expressed under control of a 4.2-kb DNA fragment from the *per* promoter (Stanewsky et al., 1997; Veleri et al., 2003). Both the *norpA* and *nocte* mutations, previously shown to abolish molecular and behavioral synchronization by temperature (Glaser and Stanewsky, 2005), did not prevent the increase in brain *per-luc* expression after the temperature rise (Figure 1B). Next, we analyzed *per-luc* oscillations in the clock mutant backgrounds of tim^{01} and Clk^{Jrk} (Allada et al., 1998; Sehgal et al., 1994). Both mutations were previously shown to disrupt temperature entrainment at behavioral and molecular levels (Glaser and Stanewsky, 2005, 2007; Yoshii et al., 2002, 2005, 2007). Although temperature-induced oscillations were strongly suppressed in most clock mutant tissues analyzed, the brains again showed sharp increases of expression immediately after the change to the warm temperature (Figure 1B).

Because the rise in Luc activity occurred in clock-less mutant genetic backgrounds, the increase in reported *per* expression reflects a response to the temperature increase, rather than meaningful entrainment (which is read out as a cyclical phenomenon requiring an underlying oscillator). To address if this temperature-induced rise in Per-Luc expression occurs in clock neurons within the brain or in ectopic locations, we imaged brain bioluminescence signals using a highly sensitive imaging system (Figure 2). Brains were kept in cell culture medium in LL and temperature cycles and imaged at a time corresponding to the peak of *luc*-reported *per* expression (ZT8, Figures 1A and 1B). In a control experiment, brains were kept in LD cycles and constant temperature and imaged at ZT0, a time of high bioluminescence levels in brains (and other tissues) kept in LD (Figure 1A). In the LD control brains, luminescence signals could be detected in regions corresponding to various groups of clock neurons, presumably large and small Lateral Neurons ventral (LNvs), the dorsal Lateral Neurons (LNds), and two groups of the Dorsal Neurons (DNs) (Figure 2A, upper panel). Expression was also found in the ocelli and in the retina (Figure 2A, upper panel), previously shown to express *per* (Hall, 2003).

Surprisingly, brain expression in temperature cycles was not confined to cells that usually express clock genes. In a clock-normal genetic background, bioluminescence signals were restricted to the dorsal brain (Figure 2A). Compared to the LD expression pattern, the dorsal expression domain appeared broader, indicating that in addition to the DN located in this region, other cells now express the *XLG-luc* construct. Moreover, signals were clearly absent from brain regions where the lateral clock neurons are usually located. This cannot be explained by the constant presence of light (LL) (cf. Zerr et al., 1990), because Per is expressed in these clock neurons under LL and temperature cycling conditions in the intact animal (Yoshii et al., 2005). Strikingly, an almost identical expression pattern was observed in the tim^{01} genetic background, further indicating the non-clock-related nature of *luc*-reported *per* expression (Figure 2A). Similarly, in a Clk^{Jrk} mutant background, *BG-luc* expression occurred in a central brain region corresponding to the calyces of the mushroom bodies not known to contain any clock-gene-expressing cells (Figure 2A). Note that both *XLG-luc* and *BG-luc* transgenes are expressed in clock neurons

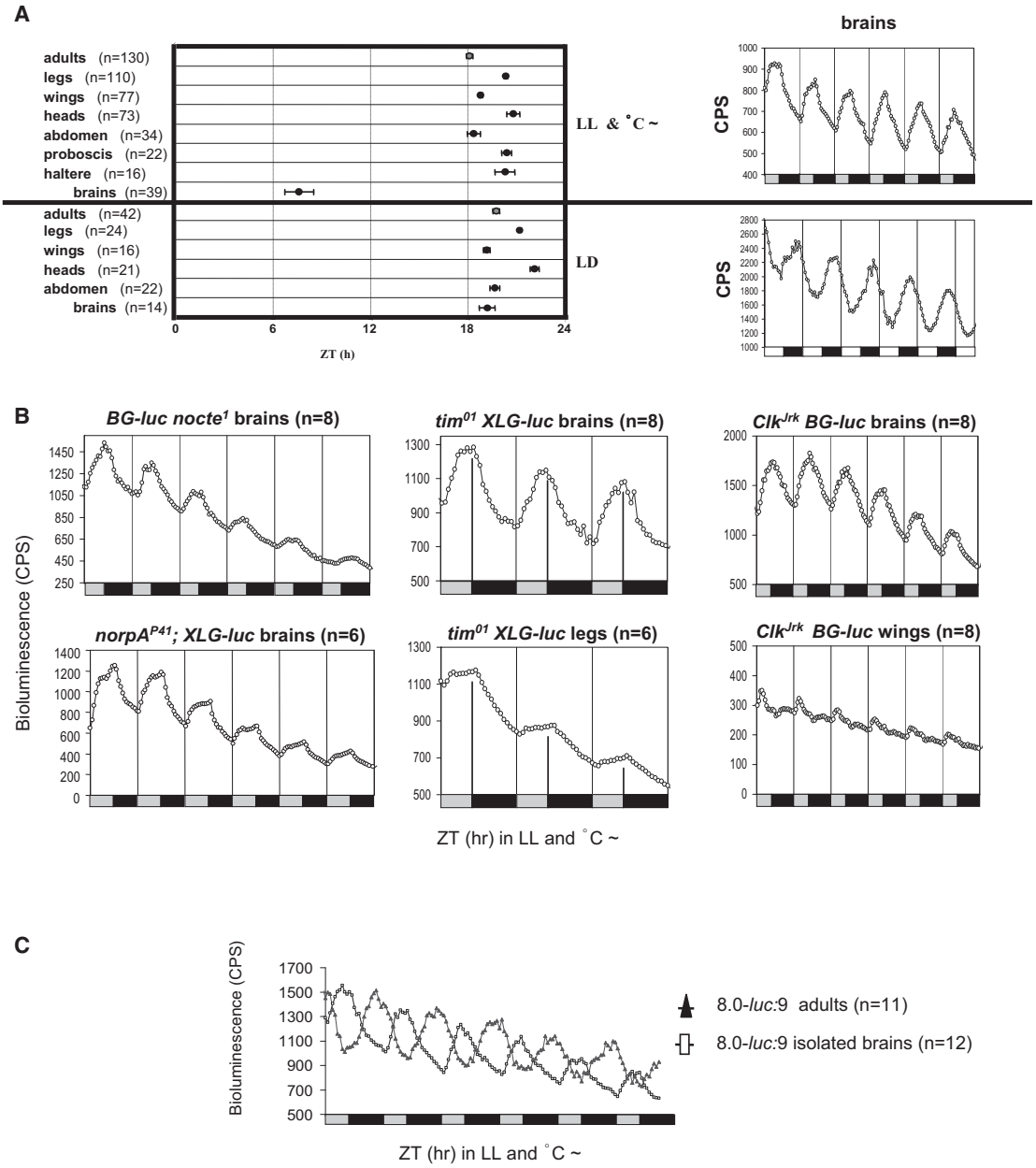

Figure 1. Cultured Brains Synchronize to Light-Dark, but Not to Temperature, Cycles

Isolated body parts or whole flies were either kept in light-dark cycles (LD) at 25°C or in constant light and 25°C:16°C temperature cycles (LL & °C~) as indicated in the figure.

(A) (Left) Phase comparison of bioluminescence peaks obtained from *XLG-luc* transgenic flies, in which the entire *period* (*per*) gene is fused to the *luciferase* (*luc*) cDNA. (Right) *XLG-luc* brains kept in LL & °C~ (top) or LD (bottom). Error bars indicate SEM. See Experimental Procedures for details about phase determination.

(B) Averaged bioluminescence recordings of different body parts from *XLG-luc* and *BG-luc* (containing a transgene encoding for two-thirds of the Per protein fused to *luc*) flies in different mutant backgrounds.

(C) Bioluminescence recordings from the *8.0-luc:9* transgenic type. This promoter-less *per-luc* construct encodes the entire Per protein and is predominantly expressed in dorsal clock neurons. White/gray and black bars indicate light/warm or dark/cold phase of the LD or temperature cycle, respectively.

during LD cycles (Stanewsky et al., 1997; Veleri et al., 2003; Figure 2A), indicating that the dramatic difference of spatial signal distribution between the two transgenic types observed in isolated brains during temperature cycling conditions depends more on the transgenic insertion site than on regulatory *per* sequences contained within the transgene. Importantly, in neither case does the spatial expression pattern significantly overlap with that of clock-gene-expressing cells under LD

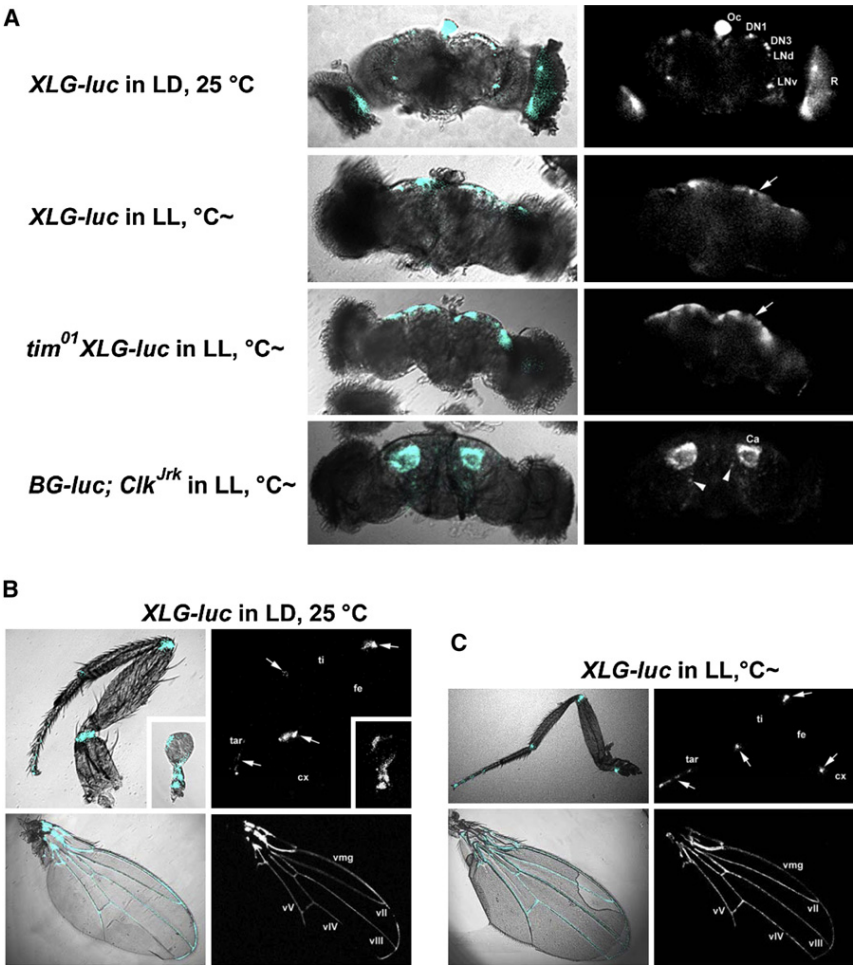

Figure 2. Spatial Per-Luc Expression in Brains Dramatically Differs after Light-Dark and Temperature Entrainment

(A) Brains dissected from *XLG-luc* flies and kept in LD at 25°C show bioluminescence signals in regions corresponding to the location of the clock neurons (DN1, DN3, LNd, LNv) and in the retina (R) and ocelli (Oc). In LL and temperature cycles (25°C:16°C), ectopic Per-Luc expression occurs in clock-normal and mutant genetic backgrounds (arrows) (see text for details). (B and C) Bioluminescence signals in peripheral tissues of *XLG-luc* flies kept in LD and 25°C or in LL and temperature cycles (25°C:16°C), respectively. Signals were detected in the joints of all leg segments, at the wing base, in ventral wing margin (vmg), in longitudinal wing veins (vII–vV), and in the scabellum, pedicel, and capitellum of the haltera (insets in B). cx, coxa; fe, femur; ti, tibia; tar, tarsus. (A–C) Left panels represent merged bioluminescence and bright-filed images; right panels show bioluminescence images.

conditions, pointing to a complete lack of spatial regulation of *per* under these conditions.

The ectopic Per-Luc expression observed in cultured brains—along with the lack of such signals from clock neurons—raised the possibility that spatial clock gene expression is generally altered in LL and temperature cycles compared to LD cycles at constant temperature. To test this, we imaged tissues known to synchronize under these conditions as well as in LD cycles (Glaser and Stanewsky, 2005; Figure 1A). Both legs and wings showed very similar spatial Per-Luc bioluminescence expression patterns under the two entrainment regimes, showing that peripheral clock tissues can be synchronized by light and temperature (Figure 2B).

In agreement with an earlier study describing *per-gal4*-driven GFP expression (Plautz et al., 1997), we also observe Per-Luc expression in potential mechanosensory and chemosensory cells along the wing margin and veins. In addition to what has been reported, we detected strong Per-Luc signals originating from the base of the wing, from the joints of the various leg segments (Figure 2B), and from segments of the haltere (inset in Figure 2B).

The *8.0-luc:9* line contains a promoterless *per-luc* fusion gene, which is expressed within a subpopulation of the DNs and occasionally in some LNd cells, but not in peripheral clock cells (Veleri et al., 2003). When *8.0-luc:9* adults were tested in LL and temperature cycles, bioluminescence peaks (presumably reflecting Per expression in brain clock neurons only) occurred late in the cold phase, similar as for the other Per-Luc transgenics tested (Figure 1C). When isolated brains were analyzed, we again observed a 12 hr phase shift, indicated by increased bioluminescence levels immediately following the temperature step up (Figure 1C).

Our results show that the brain has to be in the context of the intact fly in order for clock-neuronal gene expression to be synchronized by temperature cycles, and implies that in whole flies temperature entrainment involves signaling from peripheral tissues to the brain. As we will show below, this involves the gene *nocte*, a locus previously identified to play a role in temperature entrainment (Glaser and Stanewsky, 2005).

The *nocte* Gene Encodes a Large Glutamine-Rich Protein

In order to learn more about the function of *nocte* in temperature entrainment, we cloned the gene. Using meiotic mapping involving visible marker mutations and single nucleotide polymorphisms (SNPs), *nocte* was mapped to the 9A2–9D3 interval on the X chromosome (Experimental Procedures). Fine mapping using deficiencies placed *nocte* within the 9C1–9D2 interval containing 12 genes, flanked by the proximal breakpoint of $Df(1)c52,flw^{c52}$ (which removes 8E3-5;9C1; Tweedie et al., 2009) and the distal breakpoint of *Df(1)ED7010* (removing 9D3;9D4; Ryder et al., 2004) (Experimental Procedures). A chromosomal duplication covering this region ($Dp(1;2)v^{+75d}$ 9A2;10C2) rescued the

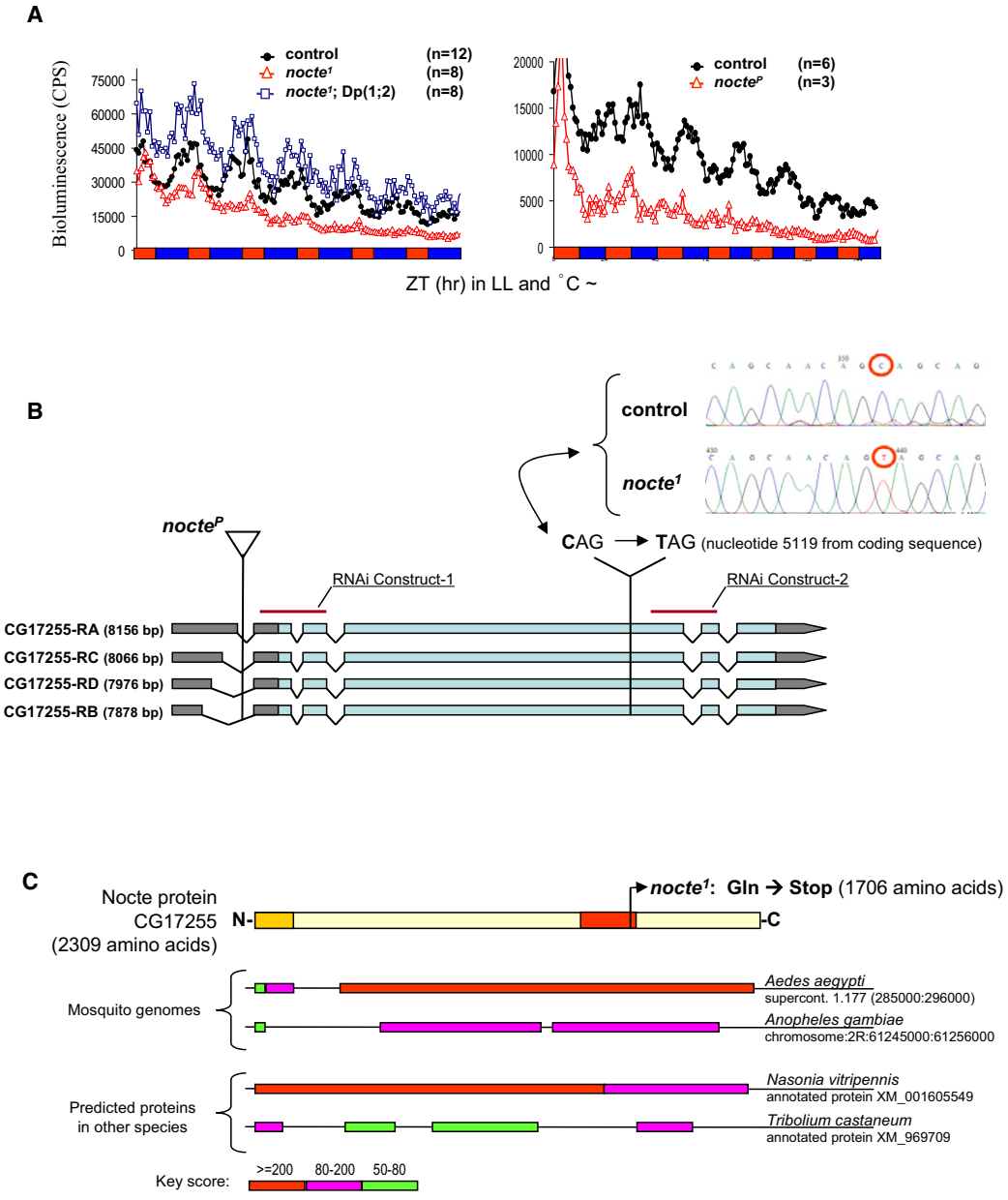

Figure 3. The *nocte* Gene Encodes a Large Glutamine-Rich Protein

(A) Bioluminescence recordings of *BG-luc* (left) and *XLG-luc* (right) adults in wild-type and *nocte* mutant flies. The *Dp(1;2)v*$^{+75d}$ (Dp(1;2)) covers the X chromosomal region 9A2–10C2 and rescues the phenotype of the EMS-induced *nocte*^{1} mutant.

(B) *nocte* gene structure, mRNA transcripts (gray: noncoding regions, blue: coding regions), location of the two mutant alleles, and the target regions of two *nocte* RNAi constructs (brown bars). In addition to the two transcript types reported in flybase (*CG17255-RA* and *RB*), we identified two additional transcripts by RT-PCR (*RC* and *RD*). All transcripts encode the same predicted protein and differ only in regard to the 5′-UTR (see also Figure S2).

(C) The predicted *Drosophila* Nocte protein has weak homology to the mammalian GRP-1 protein (red) and to the BAT2 domain of MHCIII genes (orange). *nocte*^{1} results in a truncated protein as indicated. In addition to other Drosophilidae, potential Nocte homologs were found in the mosquitoes *Aedes aegytpi* and *Anopheles gambiae* (Diptera), in the wasp *Nasonia vitripennis* (Hymenoptera), and in the beetle *Tribolium castaneum* (Coleoptera) (see Experimental Procedures for details).

molecular temperature entrainment defects of the original *nocte* mutant (Figure 3A), which confirmed the results of our mapping experiments. Next, we analyzed available mutations for the 12 candidate genes (Tweedie et al., 2009). One *P* element insertion line exhibited a temperature entrainment phenotype comparable to that observed in the original *nocte* mutant (Figures 3A, 4B, and 4C): wild-type flies anticipate the transition to the cold phase by an increase of their activity levels, which usually peak

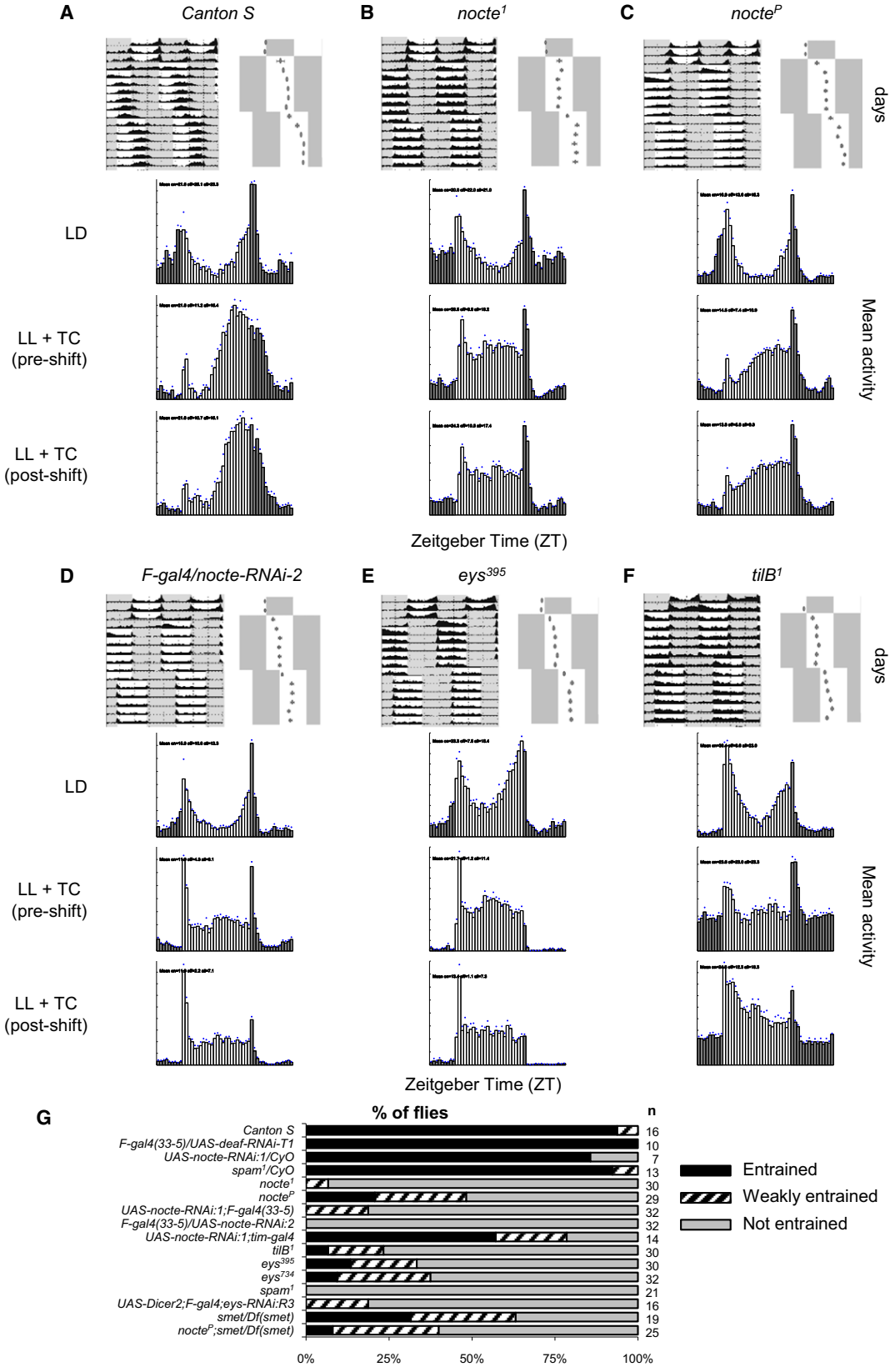
A
Canton S
B
nocte1
C
nocteP
days
LD
LL + TC
(pre-shift)
LL + TC
(post-shift)
Mean activity
Zeitgeber Time (ZT)
D
F-gal4/nocte-RNAi-2
E
eys395
F
tilB1
days
LD
LL + TC
(pre-shift)
LL + TC
(post-shift)
Mean activity
Zeitgeber Time (ZT)
G
% of flies
n
Canton S
F-gal4(33-5)/UAS-deaf-RNAi-T1
UAS-nocte-RNAi:1/CyO
spam1/CyO
nocte1
nocteP
UAS-nocte-RNAi:1;F-gal4(33-5)
F-gal4(33-5)/UAS-nocte-RNAi:2
UAS-nocte-RNAi:1;tim-gal4
tilB1
eys395
eys734
spam1
UAS-Dicer2;F-gal4;eys-RNAi:R3
smet/Df(smet)
nocteP;smet/Df(smet)
16
10
7
13
30
29
32
32
14
30
30
32
21
16
19
25
0%
25%
50%
75%
100%
Entrained
Weakly entrained
Not entrained

several hours before the actual transition (Busza et al., 2007; Glaser and Stanewsky, 2005), while flies carrying the chemically induced *nocte* allele do not show this anticipation, and simply react to temperature changes (Figure 4B) (Glaser and Stanewsky, 2005). Similarly, 80% of the flies carrying the insertion *P{lacW}CG17255*^{d07154}, or females heterozygous for the insertion and the original *nocte* allele, do not synchronize properly to temperature cycles, though they do entrain to LD (Figures 4C, 4G, and S1 available online). The insertion associated with this line is located in the first intron of the gene *CG17255* (Tweedie et al., 2009) (Figures 3B and S2) and results in the generation of abnormally spliced *CG17255* transcripts (Figure S2). We sequenced the open reading frame (ORF) of this gene in the original *nocte* mutant and in the background strain used to induce the original mutation (Experimental Procedures) and found that this mutant contains a single base pair change at nucleotide 5119 of the *CG17255* cDNA. This alteration introduces a premature stop codon (CAG → TAG) at position 1707 of the predicted protein, which normally is 2309 amino acids long (Figure 3C). Both mutations interfere with molecular and behavioral temperature entrainment, fail to complement each other, and affect the same transcription unit (Figures 3A, B, 4B, 4C, and S1). We therefore conclude that disruption of *CG17255* causes the observed phenotypes and named this gene *nocte*. The original ethyl methanesulfonate (EMS)-induced allele will from now on be referred to as *nocte*^{1}; the *P* element insertion as *nocte*^{P}. The *nocte*^{1} mutation maps to a portion of the gene's ORF that encodes one of several poly-glutamine stretches of Nocte. Apart from this feature and several poly-alanine stretches, Nocte has no apparent homologies to any other protein in the databases, except for a small region of similarity to the mammalian BAT2 domain at its N terminus (the overall similarity to the 70 N-terminal residues is weak, but it includes 11 identical amino acids). The BAT2 protein is encoded by a gene belonging the MHCIII class genes, but its function is unknown (Banerji et al., 1990). Nocte does not contain any cysteine residues, suggesting that it is an intracellular protein. Although Nocte has no apparent DNA binding domain, the presence of poly-Q and poly-A stretches also suggests that Nocte may function as transcription cofactor (Riley and Orr, 2006), which is further supported by a stretch of 268 amino acids showing weak homology to the mammalian Glutamine Rich Protein 1 (GRP-1) (Figure 3C; Cox et al., 1996). Comparison with available genome sequences revealed that *nocte* is distributed among insects (i.e., not only Drosophilidae; Figure 3C), but no obvious vertebrate homolog was identified (Experimental Procedures).

Downregulation of *nocte* in Peripheral Cells Interferes with Temperature Synchronization

Based on our finding that isolated peripheral tissues robustly synchronize to temperature cycles, but isolated brains do not (Figures 1 and 2), we wondered if *nocte* function in peripheral tissues may be required for temperature entrainment of the whole animal. For this, we generated two *nocte UAS-RNAi* transgenes (1 and 2) (Figure 3B, Experimental Procedures), and combined them (separately) with several *gal4*-containing transgenes that drive expression in various regions of the peripheral nervous system (PNS). Both *UAS-nocteRNAi* lines result in substantial downregulation of *nocte* mRNA in third-instar larvae, when crossed to *tim-gal4* or *nocte-gal4* (see below) driver lines, reducing mRNA levels to 20%–35% of peak levels (Figure S3). Synchronization to temperature cycles was analyzed by monitoring locomotor activity first in a 12 hr: 12 hr LD cycle at constant 25°C, followed by exposure to an out-of-phase 12 hr: 12 hr temperature cycle in LL for 1 week (previous light phase corresponded to the cryophase [16°C] and previous dark phase to the warm temperature [25°C]). This was followed by another such cycle, in which the onset of the warm phase was delayed by 6 hr compared to the initial temperature cycling regime (Figure 4). In this regime wild-type flies require 2–3 days to synchronize to the first temperature cycle and about the same number of days to resynchronize to the shifted temperature cycle. These "transients" are especially obvious when the activity peak phase plot (next to the actograms) is inspected (see Experimental Procedures and Figure S4 for how these plots were generated and how the ability to synchronize was determined and classified). In the daily average plots below the actograms, wild-type entrained behavior is characterized by a robust and defined activity peak in the second half of the warm phase, reflecting an anticipation of the transition to cold temperature (Figure 4A; Glaser and Stanewsky, 2005). Strikingly, the *F-gal4* transgenic (two independent insertion lines; Experimental Procedures), which is predominantly expressed in the neurons of the ch organs (Kim et al., 2003; Figures 5J–5R), produced a severe temperature entrainment defect (Figures 4D and 4G) when used to drive *nocte* RNAi-1 or 2. In the mutant plots the characteristic transients are missing or reduced and the animals largely react to the new temperature cycle. Apart from the reaction to the temperature change, the mutants remain rather constitutively active during the warm phase, not exhibiting the distinct anticipatory peak in the second half of the warm phase.

Interestingly, ~25% of the *nocte*^{P} mutant animals showed normal entrainment to temperature cycles, and another 25%

Figure 4. Downregulation of *nocte* in Peripheral Sensory Structures and Ch Organ Mutants Interferes with Behavioral Synchronization to Temperature Cycles

(A–F) Average actogram (left panels), activity peak phase (right panels), and daily activity plots (lower three panels) of flies that were entrained to 12 hr: 12 hr LD cycles for 3 days (LD) followed by 6 days of LL and 12 hr: 12 hr temperature cycles (25°C:16°C; LL + TC preshift) in which the warm and cold phase were in antiphase to the previous LD cycle. Subsequently, the onset of the warm phase was delayed by 6 hr compared to the initial regime (LL + TC postshift). Number of individual flies tested is indicated in (G). Note that all flies, except *Canton S* controls, show abnormal entrainment to temperature cycles but normal synchronization to LD. White bars or areas indicate light or warm phase and gray bars (areas) indicate dark or cold phase in LD and temperature entrainment conditions, respectively. Dots above the daily average bars indicate SEM. (G) Summary and quantification of behavior in temperature cycles for all genotypes tested. For *nocte-RNAi* lines *2:1b* and *1:3* are shown (Figure S3); for *tim-gal4* line, *16* was used. For classification criteria and methods see Experimental Procedures and Figure S4.

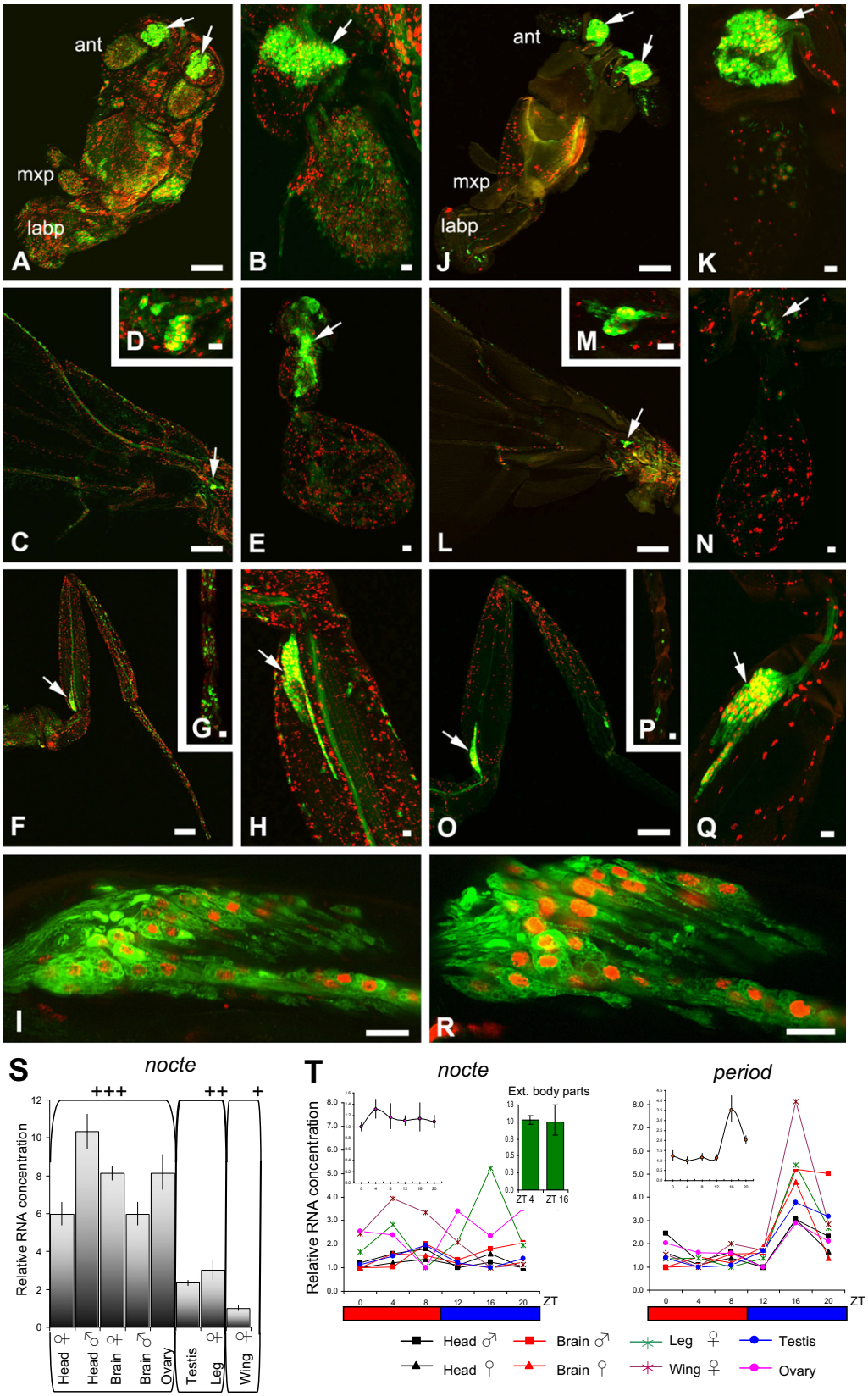
ant
mxp
labp
A
B
ant
mxp
labp
J
K
D
C
E
M
L
N
G
F
H
P
O
Q
I
R
S
nocte
+++
++
+
Relative RNA concentration
Head
Head
Brain
Brain
Ovary
Testis
Leg
Wing
T
nocte
Ext. body parts
ZT 4
ZT 16
Relative RNA concentration
ZT
period
ZT
Head
Head
Brain
Brain
Leg
Wing
Testis
Ovary

were weakly entrained (Figure 4G). This indicates that the *nocte*^{P} allele is a hypomorph, which is not surprising given that normally spliced *nocte* mRNAs can be detected in *nocte*^{P} flies (Figure S2).

As in *nocte* mutants, entrainment to LD cycles was not affected in *F-gal4/nocte-RNAi* flies, indicating a specific defect in temperature synchronization (Figures 4B–4D). Some *nocte* RNAi insertion lines (from both types) resulted in only mild temperature entrainment defects or even wild-type behavior (Figures S5A and S5D), indicating that positional effects of the transgene insertion site influence expression levels and RNAi efficiency (although levels of downregulation mediated by such "weak" RNAi lines were not assessed molecularly). These latter results, along with another control in which *F-gal4* was used to drive *deaf1*-RNAi (*deaf1* encodes a DNA binding protein unrelated to circadian clocks and ch organ function) (Veraksa et al., 2002; Figure 4G), also demonstrate that the temperature entrainment defects are not elicited by the *F-gal4* driver line alone.

F-gal4 Is Expressed in Ch and External Sense Organs

Adult ch organs are located at the joints between limb segments and are internally attached to the cuticle. They function as stretch receptors and the ch organs in adult legs and wings have been implicated in proprioception, whereas the one in antennae mediates hearing (Kernan, 2007). Neurons in larval body wall ch organs exhibit temperature-dependent calcium changes (Liu et al., 2003), but no connection between adult ch organs and temperature reception has been reported so far.

Careful analyses of *UAS-mCD8gfp* and *UAS-rfp* expression driven by the *F-gal4* transgene revealed that in addition to neurons of the ch organs (Figures 5Q and 5R), *F-gal4* is also expressed in a number of putative chemoreceptive and mechanoreceptive cells (external sense [es] organs) located in the labial and maxillary palpus (Figure 5J), first antennal segment (Figure 5K), wing (Figure 5L), haltere (Figure 5N), and leg (Figures 5O–5Q). Within the wing, *F-gal4*-positive cells were detected in the wing base, the ventral wing margin, and all wing veins, particularly in the regions close to the wing base. In the haltere and leg, *F-gal4*-positive cells are located in the cortex of every segment: marker signals were especially abundant in the capitellum of the haltere, the distal part of the femur, and the proximal part of the tibia. We also detected limited *F-gal4* expression in the brain (Figures S6 and S8).

Mutations Affecting the Ch Organs Show Deficits in Temperature Entrainment

To confirm the potential role of ch and es organs in temperature entrainment, we analyzed mutants affecting the *eyes shut* (*eys*) a.k.a. *spacemaker* (*spam*) gene that encodes a proteoglycan expressed in the interrhabdomeral space within the eye as well as within the luminal space of ch and es organs (Husain et al., 2006; Zelhof et al., 2006; Figure 6G). *eys* mutants lack the interrhabdomeral space, and as a consequence rhabdomeres are in close contact, leading to visual impairment, but no mechanosensory defects have been described (Husain et al., 2006). We tested three *eys/spam* alleles: *eys*^{734} and *eys*^{395} behave as loss-of-function mutants with respect to the rhabdomere phenotype, although Eys protein was detected in both mutants (Husain et al., 2006). The *spam*^{1} allele is protein null and exhibits the same rhabomere phenotype as the other two *eys* alleles (Zelhof et al., 2006). All three alleles showed wild-type behavior under LD conditions (Figure 4E and data not shown). Strikingly, in temperature cycles, 80% to 100% of the *eys/spam* mutant flies were mainly active during the warm phase, did not show the typical transients after transfer to a new temperature regime, and did not anticipate the temperature decrease, whereas the *spam*^{1} protein null allele showed the most severe phenotype (Figures 4E and 4G). The temperature synchronization defects observed for all three *eys/spam* alleles again indicate that ch and/or es organs are required for synchronization to temperature cycles and suggest that this function can be separated from their role in mechanoreception. Importantly, reducing *eys/spam* function in the ch and es organs using *F-gal4/eys-RNAi* also resulted in severely impaired behavioral synchronization to temperature in a manner similar to that as observed with *nocte-RNAi* (Figure 4G).

To specifically address the role of ch organs in temperature synchronization, we applied mutations of genes that are known to play a role in mechanoreception mediated by these organs and also retained normal es organ function. *touch insensitive larvaeB* (*tilB*) mutants have normal bristle receptor potentials but lack adult ch organ function, at least that of Johnston's organ (Eberl et al., 2000; Kernan, 2007). *tilB* encodes a protein conserved in ciliated eukaryotes that is required for ciliar structure and function (Kavlie, 2007; Tweedie et al., 2009). In *tilB*-mutant spermatids the axonemal structures of the cilia are disrupted, indicating that ciliary motility is impaired—the likely

Figure 5. Spatial and Temporal Expression Pattern of *nocte*

(A–R) Expression of *UAS-mCD8gfp* and *UAS-rfp* driven by *nocte-gal4* (A–I) and *F-gal4* (J–R) in potential chemoreceptors and mechanoreceptors and in neurons of the ch organs. (A and J) Signals in the labial (labp), maxillary palpus (mxp), antenna (ant), and antennal ch organs (arrows). (B and K) Larger magnification of the antenna. Arrow depicts neurons of the ch organ that project into the antennal nerve. (C and L) GFP and RFP signals in the wing base, ventral wing margin, all wing veins, and wing ch organ (arrow). (D and M) Wing ch organ. (E, F, N, and O) Signals in all segments of the haltere and leg. Arrows point to the ch organs. (G and P) Close-up of the last tarsal segments. (H, I, Q, and R) Leg ch organ (arrow). With *nocte-gal4*, both GFP and RFP signals were more abundant in all external organs tested. Intensity of GFP signals varied between "strong" in the ch organs and "weak" or "undetectable" in the chemoreceptors and mechanoreceptors, while RFP signals in all positive cells appear uniform. Scale bar for (A), (C), (F), (J), (L), and (O), 100 μm; for (B), (D), (E), (G–I), (K), (M), (N), and (P–R), 10 μm. (S) Comparison of the relative RNA expression of *nocte* in different body parts (normalized by *rp49*). ANOVA indicated highly significant differences of relative expression levels of *nocte* in the different body parts (ANOVA, $F_{7,88} = 55.11$; $p < 0.001$). According to LSD post hoc test ($p < 0.05$), they can be clustered in three groups of higher (+++), medium (++), and lower (+) *nocte* expression. (T) Temporal RNA expression of *nocte* (left panel) and *per* (right panel) in different body parts, under LL and temperature cycles (12 hr: 12hr, 25°C:16°C). Expression levels were normalized to *rp49*. Insets show the average of all body parts. Note that the apparent peak expression of *nocte* in the legs at ZT16 was not significant, nor could it be reproduced in an independent experiment in which mRNA levels in legs and wings were estimated at ZT4 and ZT16 (green histogram bars). Error bars in (S) and (T) indicate SEM. See Experimental Procedures for details.

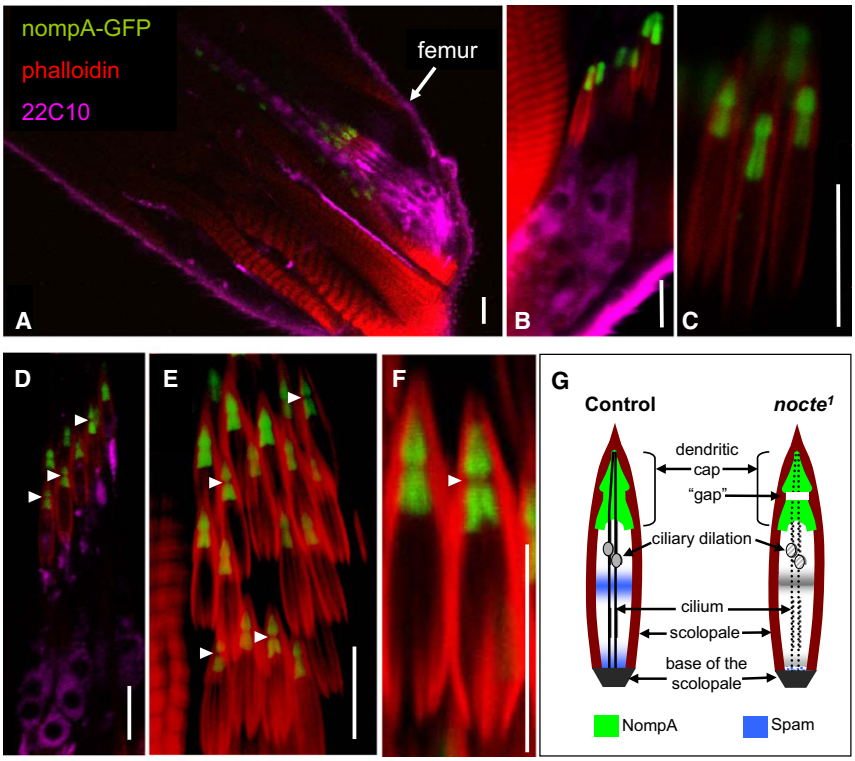

Figure 6. Altered Dendritic Caps or NompA Expression in the Femoral Ch Organs of *nocte*^{1} Flies

(A–C) Femur dissected from legs of *FM6* control and (D–F) *nocte*^{1} flies expressing the *gfp-nompA* construct. GFP-NompA (green) reports NompA expression in the dentritic cap of the scolopale. Cell bodies of ch organ neurons are visualized by 22C10 (magenta) and the scolopale actin capsule by phalloidin (red). Note that the ch organ neurons are the same as those expressing *F-gal4* and *nocte-gal4* in Figures 5I and 5R. Gaps detected in the NompA expression domain of *nocte*^{1} flies are indicated by arrow heads. Scale bars are 10 μm. (G) Cartoon showing structure and selected gene expression patterns in control and *nocte*^{1} mutant femoral scolopales (Kernan, 2007). Dotted structures indicate the uncertainty of the integrity of cilia, ciliary dilation (gray), and Spam/Eys distribution (blue) in *nocte*^{1}.

cause of sterility associated with this mutation (Caldwell et al., 2003). Although no such structural defect can be observed in adult ch organs at the light microscopy level, the same defect may underlie the deafness observed in *tilB* mutants (Kernan, 2007). *smetana* (*smet*) was isolated in a genetic screen for auditory mutants, and like *tilB*^{1}, causes male sterility and deafness, indicating a structural defect of the axoneme, but the mutated gene is not known (Caldwell et al., 2003). Strikingly, most *tilB*^{1} (90%) and *smet/Df(smet)* (65%) mutants show no or only weak synchronization to temperature cycles (Figures 4F and 4G). In order to determine potential genetic interactions between *nocte* and ch-organ-specific mutants, we generated a *nocte*^{P}*; smet/Df(smet)* double mutant. Interestingly, the double mutant flies exhibited a more sever temperature entrainment phenotype compared to the single mutants, indicating an additive effect and the involvement of both genes in the same process (Figure 4G). These results strongly implicate ch organs and the axonemal cytoskeleton surrounding the ch organ cilia as crucial components of the temperature input pathway.

nocte Is Expressed in Many Tissues, Including Ch and Es Organs

To determine if *nocte* is indeed expressed in the adult ch and es organs, we generated a *nocte-gal4* transgene by cloning an ~2 kb genomic DNA fragment upstream of the *nocte* transcription start into a *gal4* transformation vector (Experimental Procedures). Crossing several independently isolated *nocte-gal4* insertion lines to a reporter strain containing *UAS-mCD8gfp* and *UAS-rfp* transgenes revealed identical widespread, but not ubiquitous, activity of the *nocte* promoter fragment (Figures 5A–5I, S6, and S8). Positive tissues included those that can be synchronized by temperature cycles in isolation, but they also included the brain (Figures 5A–5I, S6, and S8). To validate the spatial expression pattern of *nocte*, we performed real-time PCR experiments on RNA isolated from different body parts, which confirmed the broad expression pattern observed with *nocte*-promoter-driven reporter expression (Figure 5S). Our expression data are also in good agreement with those reported in *FlyAtlas* for *CG17255* (Chintapalli et al., 2007). Quantitative RNA expression analysis revealed that *nocte* is neither circadianly nor temperature-dependently regulated in the tissues analyzed (Figure 5T, and data not shown).

Importantly, when we compared reporter signals in *F-gal4* and *nocte-gal4* flies, the ch and es organs of the adult legs, wings, haltere, and antennae were found to express *nocte* (Figures 5A–5R; Kim et al., 2003). In particular, strong neuronal expression in the ch organs was observed, similar to that reported for *F-gal4* (compare Figures 5I and 5R). Overall, the number of *nocte*-positive cells was larger than that obtained with the *F-gal4* driver, but they were located in the same regions (Figures 5A–5R). It therefore appears that the *F-gal4*-expressing cells are a subset of *nocte*-expressing ones. This is in good agreement with our finding that *nocte* function within *F-gal4*-expressing cells mediates temperature entrainment (Figure 4D).

Johnston's Organ Is Not Required for Temperature Entrainment

Because the antennal ch organ (Johnston's organ, located in the second antennal segment) of *Drosophila* is a highly specialized organ mediating hearing, we speculated that it is not required for temperature synchronization. On the other hand, a previous report (Sayeed and Benzer, 1996) revealed a receptor for temperature preference behavior to be located in the third antennal segment. We had already shown that the antennae

are not required for temperature-cycle-induced molecular clock gene oscillations (Glaser and Stanewsky, 2005). Here we tested flies, in which either the third antennal segments or the whole antennae (including Johnston's organ) were mechanically ablated, for their ability to synchronize behaviorally to LD and temperature cycles (Figures S5B and S5C). During both environmental cycles, behavior of the manipulated flies was very similar to that of wild-type, demonstrating that the antennae are not required for temperature entrainment. Although we cannot rule out a contribution of Johnston's organ, it seems clear that one or several of the other adult ch organs (Figures 5C–5I and 5L–5R) are sufficient for clock synchronization by temperature.

nocte Mutants Exhibit Visible Ch Organ Defects

Based on the involvement of *nocte* and ch organs in temperature entrainment, it was possible that *nocte* mutants affected ch organ structure. First we analyzed RFP expression in *F-gal4/nocte-RNAi/rfp* and *nocte^{1};F-gal4/rfp* flies and could not detect any gross structural abnormalities in the adult ch organ (Figure S7 and data not shown). In order to reveal potential alterations in the fine structure of ch organs, we crossed a *gfp-nompA* reporter gene into the genetic background of *nocte^{1}* and *nocte^{P}*. *gfp-nompA* encodes a GFP-NompA fusion protein, expressed under the control of the endogenous *nompA* promoter and recapitulating the spatial pattern of *nompA* expression (Chung et al., 2001). NompA is a transmembrane protein containing extracellular ZP domains, and is specifically expressed in the dendritic cap of ch and es organs (Figures 6A–6G; Chung et al., 2001). Inspection of GFP-NompA expression in femur ch organs revealed that between 60% (*nocte^{P}*) and 100% (*nocte^{1}*) of the *nocte* mutant flies tested contain dendritic caps that appear to have physical gaps, or spatially suppressed GFP-NompA expression (Figures 6D–6F and Table S1 available online). Since NompA is critical for transmission of mechanical stimuli from sensory structures to the sensory neuron (Chung et al., 2001), the structural defect, or the NompA expression phenotype we observed, indicates that ch organ function is also impaired in *nocte* mutants.

nocte Mutants Exhibit a Temperature-Dependent "Uncoordinated" Phenotype

The above results suggest that a structural defect in ch organs is responsible for the temperature synchronization defects observed in *nocte*, *tilB,* and *smet* mutants. Interestingly, one allele of the *eys/spam* locus (*spam^{1}*) also effects ch and es organ structure, but in a temperature- or humidity-dependent manner (Cook et al., 2008). It was shown that the Eys/Spam protein within the scolopale of ch organs conserves the shape and function of this structure after water loss induced by exposure to excessive heat or osmotic shock. In *spam^{1}* mutants this structural conservation is lost and the scolopales undergo dramatic cellular deformation, leading to flies that exhibit an irreversible uncoordinated locomotor phenotype after prolonged exposure to 37°C (Cook et al., 2008). Given that both *eys/spam* (including *spam^{1}*) and *nocte* mutants fail to entrain to temperature cycles (Figures 4B, 4C, 4E, and 4G), we wondered if *nocte* mutants also exhibit the same temperature-dependent uncoordinated phenotype. For this, we exposed control and nocte mutant flies

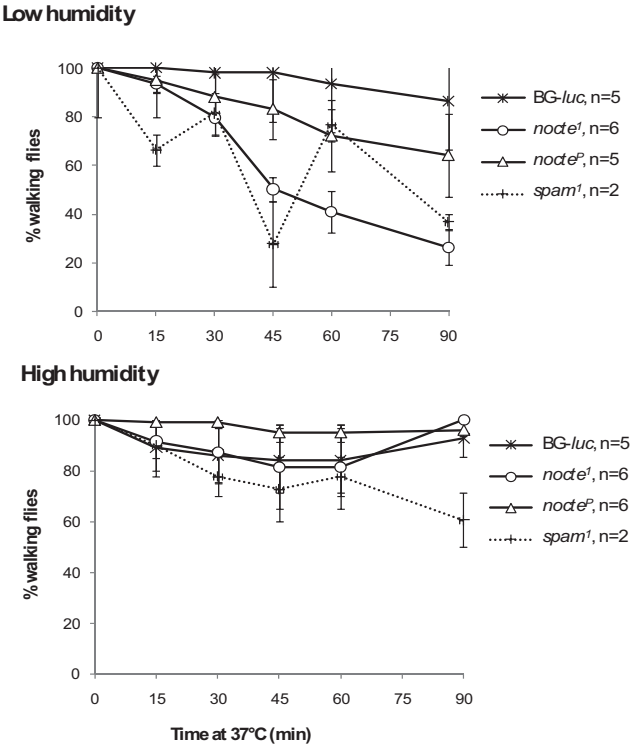

Figure 7. *nocte* Mutants Exhibit a Temperature-Dependent Uncoordinated Phenotype

Control (*BG-luc*), *nocte*, and *spam* mutant flies were raised at 25°C and transferred (in groups of 10) for 90 min to 37°C where they were observed every 15 min. The percentage of normal walking flies compared to "uncoordinated" flies is shown. The number of independent experiments (including 10 flies per genotype each) is indicated. Error bars indicate SEM.

to 37°C for 90 min and counted the number of flies that fell over during this time in 15 min intervals (Experimental Procedures; Cook et al., 2008). Both *nocte* alleles showed an uncoordinated phenotype, with more flies falling over the longer they were exposed to the high temperature (Figure 7). This phenotype was again more pronounced in *nocte^{1}* compared to *nocte^{P}*, further suggesting that the latter allele is a weak hypomorph. Interestingly, and as in the case of *spam^{1}* mutants, uncoordination was largely prevented when flies were exposed to the same high temperature at >90% humidity (Figure 7). This indicates that water loss from the scolopale also results in gross structural defects and cellular deformations of *nocte* ch organs, which may also explain why these organs fail to mediate temperature synchronization when mutated.

Temperature Entrainment Does Not Require a Functional Clock in the Ch Organs

We wanted to determine if a clock is required in the peripheral tissues expressing *F-gal4*. For this, we expressed a dominant-negative form of the *cycle* gene (*cycΔ*) in either all clock-gene expressing cells or the *F-gal4* pattern only. The *UAS-cycΔ* line causes arrhythmicity under DD and constant temperature

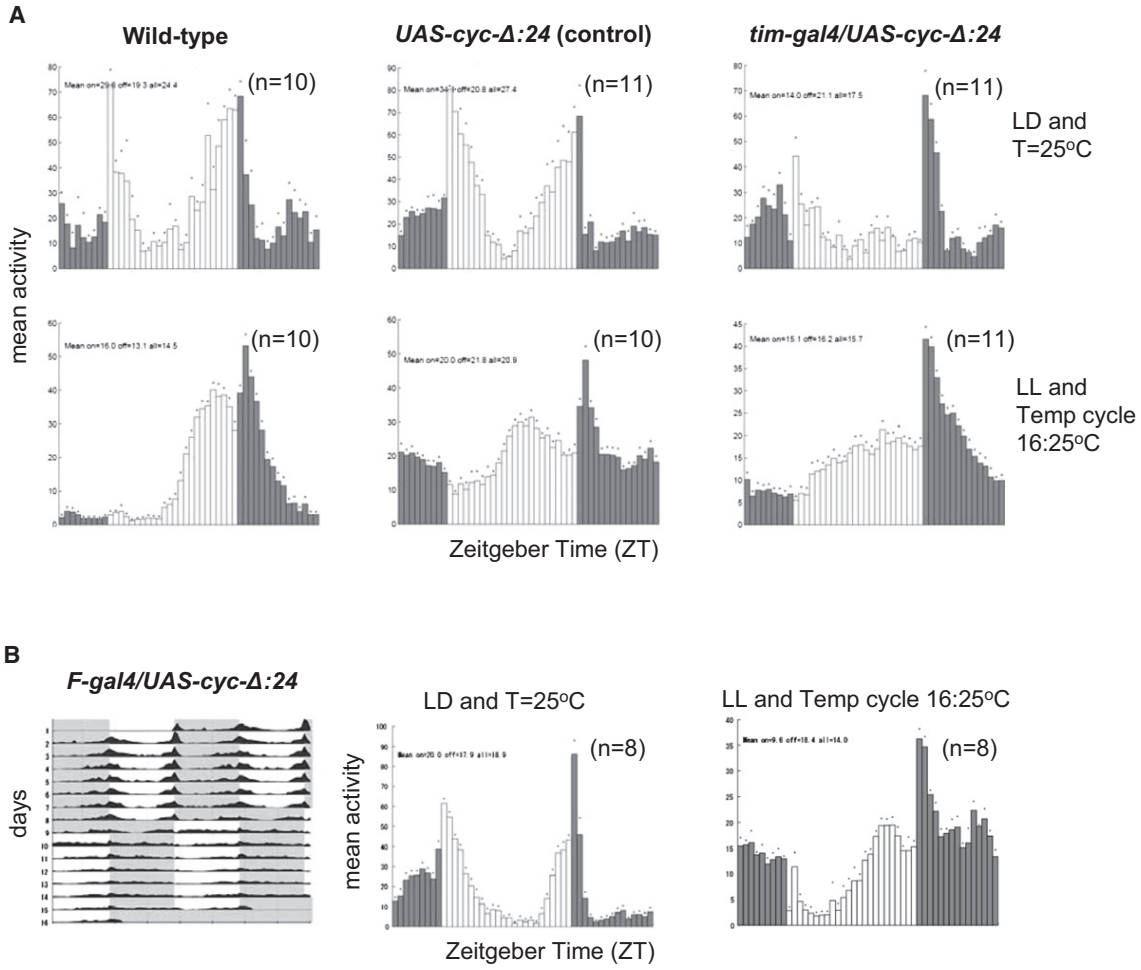

Figure 8. Peripheral Clocks in Ch Organs Are Not Required for Temperature Entrainment

Flies of the indicated genotypes were analyzed during 12 hr: 12 hr LD or temperature cycles, as indicated next to the panels.

(A) Expression of a dominant-negative form of the *cycle* gene (*cyc-Δ:24*) in all clock cells using the *tim-gal4* driver (line *27*). Wild-type (*Canton S*) and *UAS-cyc-Δ:24* flies were used as controls.

(B) *F-gal4/UAS-cyc-Δ:24* flies were entrained to LD for 3 days, followed by temperature cycles in LL, in which the warm and cold phase were in antiphase to the previous LD cycle. White and gray areas, bars, and SEM are as described in the legend to Figure 4.

conditions (Tanoue et al., 2004). As expected from the results obtained with the *tim* and *Clk* mutants (Figures 1B and 2A), *UAS-cycΔ* expression driven in all clock cells by the *tim-gal4* driver resulted in abnormal temperature entrainment (Figure 8A) (Yoshii et al., 2002, 2005). In contrast, when *UAS-cycΔ* was restricted to the *F-gal4*-expressing cells, temperature entrainment appeared normal (Figure 8B). This result is in good agreement with our failure to detect clock gene expression in ch organs (Figure S7), and also explains why *tim-gal4/UAS-nocteRNAi* flies entrain normally to temperature cycles (Figure 4G).

DISCUSSION

Temperature Entrainment of the Brain Clock Requires Signals from the Periphery

We show here unequivocally that isolated brains are not able to synchronize their circadian clock to temperature cycles, whereas they do entrain to LD. Tissue-autonomous synchronization to LD cycles is very likely mediated by the blue light photoreceptor Cry, which is expressed within a large subset of lateral and dorsal clock neurons (Benito et al., 2008; Yoshii et al., 2008). Likewise, synchronization of peripheral clock cells to light-dark and temperature cycles is tissue autonomous (Figure 1A). In contrast, brains depend on signals from the periphery for temperature entrainment to occur, indicating different temperature entrainment mechanisms for peripheral clock cells and central brain clock neurons. A possible reason for this may be that clock neurons need to be "protected" from imminent influences of temperature changes, which can occur very sporadically in nature. In fact, work from the Emery lab has shown that, even within the brain, a certain subset of light-responsive clock neurons that mainly controls the behavioral morning activity (M-cells) seems to repress temperature responsiveness of a different group of clock neurons (Busza et al., 2007).

Molecularly, this block could be mediated by Cry expression in the clock neurons, because it has been shown that the cry^b mutation enhances the amplitude of temperature-entrained clock gene expression (Glaser and Stanewsky, 2007). This suggests that some neurons are more responsive to a certain Zeitgeber than others and vice versa. For example, the Cry-negative neurons may be more important as temperature sensors as it was shown for the DN2 and Lateral Posterior Neurons (LPNs) located in the dorsal and lateral brain (Miyasako et al., 2007). These two neuronal groups do not (so far) belong to the M- and E-cell groups, and they can mediate aspects of temperature-entrained behavior in the absence of the M- and E-cells (Busza et al., 2007). In larvae the Cry-negative DN2 also play a prominent role under temperature entrainment conditions, where they seem to determine the phase of the other clock neurons in the larval brain (Picot et al., 2009).

It is conceivable that such a division of sensitivity to environmental signals, including complex protection from temperature signals in certain neurons, is required for stable synchronization to natural light-dark and temperature cycles. Since temperature cycles are a less reliable Zeitgeber compared to light-dark cycles, it would make sense that a peripheral temperature input is received only by a subset of clock neurons. These Cry-negative neurons are usually entrained by the light-responsive Cry-positive neurons, but under certain environmental conditions they could turn into the dominant neurons—now synchronizing the light-responsive neurons and activity rhythms to temperature cycles. The fact that temperature reception in these neurons occurs non-cell-autonomously (i.e., via the periphery) perhaps ensures that their input can more easily be controlled (i.e., shut off) by the clock-neuronal network.

Ch Organs as Circadian Temperature Receptors

We applied a set of PNS-*gal4* driver lines to home in on the tissues responsible for circadianly relevant temperature reception. This strategy was based on three observations: (1) PNS cells have been reported to express *per*, although a function for this expression is not known (Plautz et al., 1997); (2) isolated tissues containing these PNS cells are able to synchronize *per* expression to temperature cycles (Figures 1, 2, and Glaser and Stanewsky, 2005); and (3) *nocte* expression is also found within PNS cells of these tissues (Figure 5). We found that *F-gal4*, previously reported to be expressed specifically in ch organs, leads to disruption of temperature synchronization when crossed to *nocte-RNAi*. Although this immediately suggested that ch organs are crucial for this form of entrainment, careful inspection of the *F-gal4* expression pattern revealed that this driver is also active in es organs (Figure 5) and in a few neurons in the brain (Figures S6 and S8). Although *nocte* is also expressed in the brain, the spatial expression pattern of both genes appears to be distinct (Figures S6 and S8). Nevertheless, we cannot rule out that *nocte* and *F-gal4* are coexpressed in a few brain neurons and that *F-gal4*-mediated downregulation in brain neurons contributes to the observed temperature entrainment phenotype in *F-gal4/nocteRNAi* flies. In fact, *nocte*'s broad expression pattern in the brain does include the LNvs, and we could show that one LNv is also positive for *F-gal4* (Figure S8). But several observations strongly suggest that it is the prominent expression of *F-gal4* and *nocte* in ch organs that is mediating temperature entrainment. First, isolated brains do not synchronize to temperature cycles, indicating that *nocte* expression in the brain is not sufficient to mediate entrainment. Second, we found that mutations known to affect ch organ structure and function (*tilB*, *eys/spam*, *smet*) also interfere with temperature entrainment. Third, expression or function in the brain for any of these genes has not been described, and even if they do act in the brain it seems very unlikely that they are all expressed in the same putative "temperature entrainment cells." Fourth, if clock function is compromised in the one *F-gal4*-positive LNv via expression of the dominant-negative form of *cyc*, behavioral synchronization to temperature cycles is not affected (Figure 8B).

The *tilB* and *smet* mutants applied here are known to specifically affect ch function and leave es organ function intact (Caldwell et al., 2003; Eberl et al., 2000). Similarly, the $eys^{734/395}$ alleles retain normal mechanosensory function, but are thought to exhibit a molecular defect of the sensory dendrite of ch organs (Husain et al., 2006). All these mutations interfere with entrainment to temperature, but not to light-dark, cycles. Together with the prominent expression of *F-gal4* and *nocte* in ch organs, these findings strongly implicate ch organs as mediators of temperature entrainment, at least within the temperature interval applied in this study (25°C:16°C).

How May Ch Organs Perceive Temperature?

Ch organs can function as stretch receptors and have been implicated in mediating proprioception, gravireception, and vibration detection (Kernan, 2007). In contrast to external sensory cells, adult ch organs do not contain external bristles, and are attached to the inside of the cuticle. They consist of one to several hundred sensory units (scolopodia), and each of them contains a liquid-filled capsule (scolopale) that harbors the sensory endings of one to three neurons (Figure 6; Kernan, 2007). Interestingly, the Eys/Spam protein can be detected at the border between the ch neuron cell body and the lumen of the scolopale, and close to a characteristic dilation of the ch cilia (Cook et al., 2008; Husain et al., 2006). *spam* mutants exhibit a massive cellular deformation of the scolopale after exposure to 37°C (Cook et al., 2008). This deformation can be prevented by exposing the mutants to >90% humidity during the high temperature period. This suggests that the cellular deformation is caused by water loss from the hemolymph, which leads to water loss from the scolopale and subsequent neuronal deformation (Cook et al., 2008). *eys/spam* mutants show normal mechanoreceptor responses at room temperature, indicating that the presence of Eys/Spam protects the scolopale from excessive heat, probably by preventing water loss (Cook et al., 2008; Husain et al., 2006). *nocte* mutants exhibit the same temperature- and humidity-dependent uncoordinated phenotype as *spam* mutants, indicating a similar cellular deformation induced by excessive heat (Figure 7). Given that mutants of both genes also fail to synchronize to temperature cycles, we suspect that both phenotypes are related. As we show here, both *nocte* alleles lead to a structural defect in the dendritic cap of the ch organ (or misexpression of the dendritic cap protein NompA). It is conceivable that this defect also leads to excessive water loss at high temperatures, which would explain *nocte*'s

uncoordinated phenotype. For temperature entrainment to work properly it seems therefore absolutely crucial that the scolopale is protected from effects of extreme temperatures.

On the other hand, the ch organs must be able to sense subtle changes of temperature alterations in the fly's physiological range in order to function as circadian temperature sensors. In larvae, both ch organs and es neurons in the body wall react by increasing [Ca^{2+}] after raising or lowering the temperature (Liu et al., 2003), suggesting that they are also capable of detecting temperature changes in the adult. Considering that two other temperature entrainment mutants, *tilB* and *smet*, very likely affect the axonemal cytoskeleton structure of the ch cilia, we believe that perhaps dynamic properties of the ch cilia underlie temperature entrainment. The cilia in stimulated femoral ch organs of grasshoppers show active bending (i.e., not a passive reaction to the mechanical stimulus) close to the region where the cilia enters the scolopale (Moran et al., 1977). This ciliar bending presumably activates the ch neuron, which propagates the signal to the thoracic CNS. Interestingly, the same study showed that the femoral ch organ behaves tonically—in other words, it keeps firing at the same rate as long as the mechanical stimulation doesn't change (Moran et al., 1977). This inability to adapt to an environmental stimulus is exactly what would be required for a circadian temperature receptor, because it is necessary that it tracks subtle changes in temperature over time. Our current hypothesis therefore postulates the scolopale as an active unit for circadian temperature reception. Eys/Spam and Nocte are required to protect the unit from water loss at different temperatures, rendering the cilia able to react to subtle changes in temperature by actively changing its shape (perhaps by bending). The degree of ciliar bending then determines the firing frequency of the ch neuron, which is tightly coupled to the ambient temperature.

The Role of the *nocte* Gene Product in Temperature Entrainment

Both *nocte* alleles show similar phenotypes in regard to temperature entrainment, dendritic cap, and uncoordination phenotypes, although $nocte^{1}$ always exhibits more severe defects then $nocte^{P}$. This suggests that $nocte^{P}$ is a hypomorphic allele, a suggestion also supported by the observation that it is able to generate normally spliced transcripts in addition to aberrant ones (Figure S2). We also have evidence that $nocte^{1}$ is not a null allele, because (1) we can detect a truncated protein of the predicted size on western blots probed with an anti-Nocte serum, and (2) driving *nocte-RNAi* with broadly expressed *gal4* driver lines (e.g., *nocte-gal4, tim-gal4*) leads to adult lethality (C.G., H.S., A.S., A.G., and R.S., unpublished data).

Downregulation of *nocte* using *F-gal4* results in a severe temperature entrainment defect, confirming that this transcription unit is involved in the process. Because *F-gal4* is expressed within the neurons and cilia of ch organs, this behavioral defect indicates that *nocte* is also expressed in ch organ neurons (Kim et al., 2003). Based on the potential structural defect observed in *nocte* mutants, the Nocte protein may be required for the proper connection between the scolopale and the dendritic cap or proper expression and distribution of temperature-entrainment-relevant gene products along the cilia (Figure 6). This would also explain the structural defect or *nompA* misexpression phenotype caused by both *nocte* alleles (Figures 6D–6F and Table S1), which presumably underlies the observed temperature entrainment phenotype.

Requirement of a Functional Clock in Ch Organs

Our findings indicate that a functional clock within peripheral sensory structures important for temperature entrainment is not required (Figures 8 and S8). We therefore propose a model in which ch organ neurons, which do not possess a functional clock, send temperature information to peripheral clock neurons in the thoracic CNS, or directly to the more temperature-sensitive clock neurons within the brain (see above). A similar pathway has recently been described for sex peptide (SP) signaling, in which specific SP-receptor-expressing neurons located within the female reproductive tract signal to the CNS (Häsemeyer et al., 2009).

For daily temperature entrainment to work, temperature signals need to be interpreted by clock neurons in a time-dependent (i.e., circadian) manner in order to result in coordinated clock protein cycling and synchronized behavior controlled by these neurons. Neuronal brain clocks totally depend on these signals to become entrained by temperature, since they cannot synchronize in culture (Figures 1 and 2). Because isolated brains cell-autonomously synchronize to light (Figure 1), our findings reveal a fundamental difference between these two entrainment pathways.

EXPERIMENTAL PROCEDURES

Flies

For a detailed description of fly stocks used and generated for this study see Supplemental Experimental Procedures.

Bioluminescence Recordings and Imaging

Bioluminescence rhythms emanating from whole flies or individual body parts were recorded essentially as described (Glaser and Stanewsky, 2005) using an automated bioluminescence counter (Topcount, Perkin-Elmer). For more details, also regarding the generation of bioluminescence images shown in Figure 2 using the LuminoviewLV200 imaging system (Olympus, Tokyo, Japan), please refer to the Supplemental Experimental Procedures.

Mapping of *nocte*

By using visible markers, SNPs, chromosomal deficiencies, and insertions, *nocte* was mapped to the *CG17255* transcription unit at position 9C6–9D1 on the X chromosome. For details see Supplemental Experimental Procedures.

Generation of *nocte* Constructs

Nocte RNAi constructs were designed using fusions between *nocte* genomic and cDNA as described previously (Kalidas and Smith, 2002). For details see Supplemental Experimental Procedures.

Behavioral Analysis

Locomotor activity rhythms were recorded automatically using the *Drosophila* Activity Monitoring (DAM) system (Trikinetics, Waltham, MA) as previously described (Glaser and Stanewsky, 2005). Flies were initially synchronized and recorded in LD (12 hr: 12 hr) at a constant temperature of 25°C for 3–5 days and then released to LL and temperature cycles (12 hr: 12 hr, 25°C:16°C) in opposite phase to that of the initial LD cycle (i.e., cryophase corresponded to light, and warm phase to dark portion of the LD cycle). For the experiments shown in Figure 4, the temperature cycle was shifted after 6 days, so that the warm phase occurred in a 6 hr delay compared to the initial

temperature cycle, as indicated by the shading in the locomotor-activity plots (called actograms). For further details, please refer to the Supplemental Experimental Procedures.

Uncoordinated Assay and Quantification

The assay was performed as previously described (Cook et al., 2008). Flies were raised at 25°C and 10 young males were placed in a Petri dish and transferred for 90 min to a 37°C incubator where they were observed every 15 min. Relative humidity in the incubator was between 20%–30%. High humidity was obtained by adding a filter paper soaked in water to the Petri dish where the flies were monitored. The percentage of normal walking flies was determined by counting the number of flies walking at a certain time point and comparing it to the number of flies unable to walk or completely uncoordinated (i.e., lying on their backs or sides). High and low humidity observations were performed at the same time.

Fluorescence Microscopy and Immunohistochemistry

See Supplemental Experimental Procedures.

RNA Extractions and qPCR

Adult *Drosophila* (*y w*) were entrained for 3 days both under LD 25°C and LL 25°C:16°C (12 hr: 12 hr) conditions, and then collected at Zeitgeber Time (ZT) 0, 4, 8, 12, 16, and 20. Collection and dissection of 10 individuals started 30 min before and finished 30 min after each ZT. Wings, legs, and heads were immediately transferred to dry ice; brains, ovaries, and testis to RNA later solution (Ambion), and then stored at −80°C until RNA extraction. Two different *UAS-nocte-RNAi* transgenics (*nocte-RNAi2:1b* and *nocte-RNAi1:3*) were crossed with *tim-gal4:67* and *nocte-gal4:M3*. Crosses were kept at 18°C for 20 days and then transferred to 25°C. After four days at 25°C, five third-instar larvae were collected from each cross and from two of the parental lines (*nocte-RNAi1:3* and *tim-gal4:67*), and processed for quantitative PCR using a Reverse Transcription Reagents Kit (Applied Biossystems) (see Supplemental Experimental Procedures).

nocte Transcripts in *nocte*^{P} Mutants

Two samples of two adult female flies were collected in parallel from *Canton S* and *nocte*^{P} strains, and RNA extraction was performed as described above for samples used in qPCR and eluted in a final volume of 200 μl of H_2O. Reverse transcription reactions were performed with High Capacity RNA-to-cDNA Master Mix (Applied Biosystems) according to the manufacturer's instructions. PCR products from both strains were generated with *nocte*-specific primers and sequenced as described in the Supplemental Experimental Procedures.

Comparative Sequence Analysis to Identify *nocte* Homologs

Nocte protein sequence from *Drosophila melanogaster* was initially blasted (tblastn tool) against both the whole-genome shotgun reads on the NCBI website (http://blast.ncbi.nlm.nih.gov/Blast.cgi) and the available genomic sequences of insects on the Vector Base website (http://www.vectorbase.org/Tools/BLAST/). Several insect species were identified as potentially containing *nocte* homologs. In order to obtain a more specific blast result, the genomic regions with the best hits were downloaded and blasted (blastx tool) against the GeneBank protein sequences of *Drosophila melanogaster* in Flybase website (http://flybase.org/blast/). The most reliable candidates are presented in Figure 3C.

SUPPLEMENTAL DATA

Supplemental data for this article include eight Supplemental Figures, one Supplemental Table, and Supplemental Experimental Procedures and can be found at http://www.cell.com/neuron/supplemental/S0896-6273(09)00638-2.

ACKNOWLEDGMENTS

We thank OLYMPUS UK Ltd., namely Mr. Alan Kidger and Werner Kammerloher for their generous provision of the LuminoviewLV200, and Ko Fan Chen for help with *nocte* homology searches. We also thank C. Kim for the *F-gal4*; P. Hardin for *UAS-cyc*Δ, U. Tepass for *eys*; A. Zelhof for *spam*; D. Eberl for *tilB*, *smet*, and *gfp-nompA* flies; and P. Emery, J. Hall, and J. Levine for critical reading of the manuscript. Confocal imaging was performed with support of the Blizard Advanced Light Microscopy facility at Queen Mary. This work was supported by the Deutsche Forschungsgemeinschaft grants Sta 421/3-3 and Sta 421/6-6 given to R.S. Work in our lab is supported by EUCLOCK, an Integrated Project (FP6) funded by the European Commission and the BBSRC.

Accepted: August 19, 2009
Published: October 28, 2009

REFERENCES

Allada, R., White, N.E., So, W.V., Hall, J.C., and Rosbash, M. (1998). A mutant *Drosophila* homolog of mammalian Clock disrupts circadian rhythms and transcription of *period* and *timeless*. Cell *93*, 791–804.

Banerji, J., Sands, J., Strominger, J.L., and Spies, T. (1990). A gene pair from the human major histocompatibility complex encodes large proline-rich proteins with multiple repeated motifs and a single ubiquitin-like domain. Proc. Natl. Acad. Sci. USA *87*, 2374–2378.

Barrett, R.K., and Takahashi, J.S. (1995). Temperature compensation and temperature entrainment of the chick pineal cell circadian clock. J. Neurosci. *15*, 5681–5692.

Benito, J., Houl, J.H., Roman, G.W., and Hardin, P.E. (2008). The blue-light photoreceptor CRYPTOCHROME is expressed in a subset of circadian oscillator neurons in the *Drosophila* CNS. J. Biol. Rhythms *23*, 296–307.

Boothroyd, C.E., and Young, M.W. (2008). The in(put)s and out(put)s of the *Drosophila* circadian clock. Ann. N Y Acad. Sci. *1129*, 350–357.

Brown, S.A., Zumbrunn, G., Fleury-Olela, F., Preitner, N., and Schibler, U. (2002). Rhythms of mammalian body temperature can sustain peripheral circadian clocks. Curr. Biol. *12*, 1574–1583.

Busza, A., Murad, A., and Emery, P. (2007). Interactions between circadian neurons control temperature synchronization of *Drosophila* behavior. J. Neurosci. *27*, 10722–10733.

Caldwell, J.C., Miller, M.M., Wing, S., Soll, D.R., and Eberl, D.F. (2003). Dynamic analysis of larval locomotion in *Drosophila* chordotonal organ mutants. Proc. Natl. Acad. Sci. USA *100*, 16053–16058.

Chintapalli, V.R., Wang, J., and Dow, J.A. (2007). Using FlyAtlas to identify better *Drosophila melanogaster* models of human disease. Nat. Genet. *39*, 715–720.

Chung, Y.D., Zhu, J., Han, Y., and Kernan, M.J. (2001). *nompA* encodes a PNS-specific, ZP domain protein required to connect mechanosensory dendrites to sensory structures. Neuron *29*, 415–428.

Cook, B., Hardy, R.W., McConnaughey, W.B., and Zuker, C.S. (2008). Preserving cell shape under environmental stress. Nature *452*, 361–364.

Cox, G.W., Taylor, L.S., Willis, J.D., Melillo, G., White, R.L., 3rd, Anderson, S.K., and Lin, J.J. (1996). Molecular cloning and characterization of a novel mouse macrophage gene that encodes a nuclear protein comprising polyglutamine repeats and interspersing histidines. J. Biol. Chem. *271*, 25515–25523.

Dubruille, R., and Emery, P. (2008). A plastic clock: how circadian rhythms respond to environmental cues in *Drosophila*. Mol. Neurobiol. *38*, 129–145.

Dunlap, J.C., Loros, J.J., and DeCoursey, P.J. (2004). Chronobiolgy: Biological Timekeeping (Sunderland, Massachusetts: Sinauer Associates, Inc).

Eberl, D.F., Hardy, R.W., and Kernan, M.J. (2000). Genetically similar transduction mechanisms for touch and hearing in *Drosophila*. J. Neurosci. *20*, 5981–5988.

Glaser, F.T., and Stanewsky, R. (2005). Temperature synchronization of the *Drosophila* circadian clock. Curr. Biol. *15*, 1352–1363.

Glaser, F.T., and Stanewsky, R. (2007). Synchronization of the *Drosophila* circadian clock by temperature cycles. Cold Spring Harb. Symp. Quant. Biol. *72*, 233–242.

Hall, J.C. (2003). Genetics and molecular biology of rhythms in *Drosophila* and other insects. Adv. Genet. *48*, 1–280.

Hamada, F.N., Rosenzweig, M., Kang, K., Pulver, S.R., Ghezzi, A., Jegla, T.J., and Garrity, P.A. (2008). An internal thermal sensor controlling temperature preference in *Drosophila*. Nature *454*, 217–220.

Häsemeyer, M., Yapici, N., Heberlein, U., and Dickson, B.J. (2009). Sensory neurons in the *Drosophila* genital tract regulate female reproductive behavior. Neuron *61*, 511–518.

Herzog, E.D., and Huckfeldt, R.M. (2003). Circadian entrainment to temperature, but not light, in the isolated suprachiasmatic nucleus. J. Neurophysiol. *90*, 763–770.

Husain, N., Pellikka, M., Hong, H., Klimentova, T., Choe, K.M., Clandinin, T.R., and Tepass, U. (2006). The agrin/perlecan-related protein eyes shut is essential for epithelial lumen formation in the *Drosophila* retina. Dev. Cell *11*, 483–493.

Kalidas, S., and Smith, D.P. (2002). Novel genomic cDNA hybrids produce effective RNA interference in adult *Drosophila*. Neuron *33*, 177–184.

Kavlie, R.G. (2007). Touch insensitive larva B, a gene necessary for hearing and male fertility in *Drosophila melanogaster*, encodes a conserved ciliary protein. PhD thesis, University of Iowa, Iowa City, Iowa.

Kernan, M.J. (2007). Mechanotransduction and auditory transduction in *Drosophila*. Pflugers Arch. *454*, 703–720.

Kim, J., Chung, Y.D., Park, D.Y., Choi, S., Shin, D.W., Soh, H., Lee, H.W., Son, W., Yim, J., Park, C.S., et al. (2003). A TRPV family ion channel required for hearing in *Drosophila*. Nature *424*, 81–84.

Kornmann, B., Schaad, O., Bujard, H., Takahashi, J.S., and Schibler, U. (2007). System-driven and oscillator-dependent circadian transcription in mice with a conditionally active liver clock. PLoS Biol. *5*, e34.

Lahiri, K., Vallone, D., Gondi, S.B., Santoriello, C., Dickmeis, T., and Foulkes, N.S. (2005). Temperature regulates transcription in the zebrafish circadian clock. PLoS Biol. *3*, e351.

Liu, L., Yermolaieva, O., Johnson, W.A., Abboud, F.M., and Welsh, M.J. (2003). Identification and function of thermosensory neurons in *Drosophila* larvae. Nat. Neurosci. *6*, 267–273.

Matsumoto, A., Matsumoto, N., Harui, Y., Sakamoto, M., and Tomioka, K. (1998). Light and temperature cooperate to regulate the circadian locomotor rhythm of wild type and *period* mutants of *Drosophila melanogaster*. J. Insect Physiol. *44*, 587–596.

Miyasako, Y., Umezaki, Y., and Tomioka, K. (2007). Separate sets of cerebral clock neurons are responsible for light and temperature entrainment of *Drosophila* circadian locomotor rhythms. J. Biol. Rhythms *22*, 115–126.

Moran, D.T., Varela, F.J., and Rowley, J.C., 3rd. (1977). Evidence for active role of cilia in sensory transduction. Proc. Natl. Acad. Sci. USA *74*, 793–797.

Picot, M., Klarsfeld, A., Chelot, E., Malpel, S., and Rouyer, F. (2009). A role for blind DN2 clock neurons in temperature entrainment of the *Drosophila* larval brain. J. Neurosci. *29*, 8312–8320.

Plautz, J.D., Kaneko, M., Hall, J.C., and Kay, S.A. (1997). Independent photoreceptive circadian clocks throughout *Drosophila*. Science *278*, 1632–1635.

Prolo, L.M., Takahashi, J.S., and Herzog, E.D. (2005). Circadian rhythm generation and entrainment in astrocytes. J. Neurosci. *25*, 404–408.

Riley, B.E., and Orr, H.T. (2006). Polyglutamine neurodegenerative diseases and regulation of transcription: assembling the puzzle. Genes Dev. *20*, 2183–2192.

Ryder, E., Blows, F., Ashburner, M., Bautista-Llacer, R., Coulson, D., Drummond, J., Webster, J., Gubb, D., Gunton, N., Johnson, G., et al. (2004). The DrosDel collection: a set of *P*-element insertions for generating custom chromosomal aberrations in *Drosophila melanogaster*. Genetics *167*, 797–813.

Sayeed, O., and Benzer, S. (1996). Behavioral genetics of thermosensation and hygrosensation in *Drosophila*. Proc. Natl. Acad. Sci. USA *93*, 6079–6084.

Sehgal, A., Price, J.L., Man, B., and Young, M.W. (1994). Loss of circadian behavioral rhythms and *per* RNA oscillations in the *Drosophila* mutant *timeless*. Science *263*, 1603–1606.

Sheeba, V., Kaneko, M., Sharma, V.K., and Holmes, T.C. (2008). The *Drosophila* circadian pacemaker circuit: Pas De Deux or Tarantella? Crit. Rev. Biochem. Mol. Biol. *43*, 37–61.

Stanewsky, R., Jamison, C.F., Plautz, J.D., Kay, S.A., and Hall, J.C. (1997). Multiple circadian-regulated elements contribute to cycling *period* gene expression in *Drosophila*. EMBO J. *16*, 5006–5018.

Stanewsky, R., Kaneko, M., Emery, P., Beretta, B., Wager-Smith, K., Kay, S.A., Rosbash, M., and Hall, J.C. (1998). The *cry*^{b} mutation identifies *cryptochrome* as a circadian photoreceptor in *Drosophila*. Cell *95*, 681–692.

Tanoue, S., Krishnan, P., Krishnan, B., Dryer, S.E., and Hardin, P.E. (2004). Circadian clocks in antennal neurons are necessary and sufficient for olfaction rhythms in *Drosophila*. Curr. Biol. *14*, 638–649.

Tweedie, S., Ashburner, M., Falls, K., Leyland, P., McQuilton, P., Marygold, S., Millburn, G., Osumi-Sutherland, D., Schroeder, A., Seal, R., and Zhang, H. (2009). FlyBase: enhancing *Drosophila* Gene Ontology annotations. Nucleic Acids Res. *37*, D555–D559.

Veleri, S., Brandes, C., Helfrich-Forster, C., Hall, J.C., and Stanewsky, R. (2003). A self-sustaining, light-entrainable circadian oscillator in the *Drosophila* brain. Curr. Biol. *13*, 1758–1767.

Veraksa, A., Kennison, J., and McGinnis, W. (2002). DEAF-1 function is essential for the early embryonic development of *Drosophila*. Genesis *33*, 67–76.

Wheeler, D.A., Hamblen-Coyle, M.J., Dushay, M.S., and Hall, J.C. (1993). Behavior in light-dark cycles of *Drosophila* mutants that are arrhythmic, blind, or both. J. Biol. Rhythms *8*, 67–94.

Yoshii, T., Sakamoto, M., and Tomioka, K. (2002). A temperature-dependent timing mechanism is involved in the circadian system that drives locomotor rhythms in the fruit fly *Drosophila melanogaster*. Zoolog. Sci. *19*, 841–850.

Yoshii, T., Heshiki, Y., Ibuki-Ishibashi, T., Matsumoto, A., Tanimura, T., and Tomioka, K. (2005). Temperature cycles drive *Drosophila* circadian oscillation in constant light that otherwise induces behavioural arrhythmicity. Eur. J. Neurosci. *22*, 1176–1184.

Yoshii, T., Fujii, K., and Tomioka, K. (2007). Induction of *Drosophila* behavioral and molecular circadian rhythms by temperature steps in constant light. J. Biol. Rhythms *22*, 103–114.

Yoshii, T., Todo, T., Wülbeck, C., Stanewsky, R., and Helfrich-Förster, C. (2008). Cryptochrome is present in the compound eyes and a subset of *Drosophila*'s clock neurons. J. Comp. Neurol. *508*, 952–966.

Zelhof, A.C., Hardy, R.W., Becker, A., and Zuker, C.S. (2006). Transforming the architecture of compound eyes. Nature *443*, 696–699.

Zerr, D.M., Hall, J.C., Rosbash, M., and Siwicki, K.K. (1990). Circadian fluctuations of Period protein immunoreactivity in the CNS and the visual system of *Drosophila*. J. Neurosci. *10*, 2749–2762.

Neuron, volume *64*

Supplemental Data

Temperature Entrainment of *Drosophila*'s Circadian Clock Involves the Gene *nocte* and Signaling from Peripheral Sensory Tissues to the Brain

Hana Sehadova, Franz T. Glaser, Carla Gentile, Alekos Simoni, Astrid Giesecke, Joerg T. Albert, and Ralf Stanewsky

Figure S1: *Impaired temperature synchronization in* nocte^{1}/nocte^{P} *females.*

Group actograms, peak phase of activity (A, B upper left and right panels, respectively) and daily average activity (A, B middle and bottom panels) of flies that were entrained to 12 hr: 12 hr LD cycles for 3 days followed by two weeks of LL and 12 hr: 12 hr temperature cycles (25:16ºC) in which the warm- and cold-phase were in anti-phase to the previous LD cycle (i.e., cold-phase corresponds to the light-phase) are shown. **A)** *nocte^{1}/FM6* females were crossed to *nocte^{P}* males and locomotor rhythms of heterozygous *nocte^{1}/nocte^{P}* F1 females were analyzed. **B)** *nocte^{P}/FM6* females from the same cross served as controls. Note that control females exhibit a steep and gradual activity increase after a trough in the early morning, whereas the mutant females show high activity throughout almost the whole warm phase. Higher activity of females vs. males during the day is also typical for flies entrained to LD cycles (Helfrich-Förster, 2000). White and black areas or bars in all behavioral plots indicate light or warm and dark or cold phase, respectively. Error bars and dots in peak phase and daily average plots indicate SEM's. **C)** Quantification of ability to synchronize behavioral rhythms to temperature cycles (see Experimental Procedures for details).

Figure S2: nocte *trancripts in the* nocte^{P} *mutant.*

A) Transcripts from two independent RNA extractions (from two adult female flies each) from *Canton S* (i, ii) and *nocte^{P}* flies (iii, iv), obtained by PCR with primers that amplify a ca. 1.2 kb wild type *nocte* fragment (varies according to the different transcripts), starting from the 5'-UTR region, and spanning the insertion site of the *P*-element in *nocte^{P}*, and the start codon. **B)** Schematic representation of the *nocte* wild type transcripts cloned and sequenced from samples in (A). **C)** Abnormally spliced transcripts cloned and sequenced from *nocte^{P}*. The upper transcript contains all necessary sequences to encode a normal Nocte protein. The middle transcript encodes a predicted fusion protein between proteins encoded by *P*-element sequences and 59 out-of-frame amino acids encoded by *nocte*. The bottom example encodes short (20 amino acid) peptides initiated at an ATG upstream of the predicted *nocte* ATG, which are terminated at an out-of-frame stop codon in the *nocte* coding region.

Figure S3: *Efficiency of* nocte *downregulation by RNAi.*

Relative amounts of *nocte* RNA in larvae expressing two different *UAS-nocteRNAi* constructs (lines 2:1b and 1:3) under the control of two different drivers (*nocte-gal4:M3* and *tim-gal4:67*). *nocte* mRNA levels in two of the parental lines (*UAS-nocteRNAi:1:3* and *tim-gal4:67*) were used as control. For all samples expression was normalized to *rp49*. For both drivers, Analysis of Variance (ANOVA) indicates that the difference between larvae expressing *nocte* RNAi and the control is highly significant ($P<0.005$). Error bars indicate SEM.

Figure S4: *Examples and classification of flies with normal or impaired abilities to synchronize to temperature cycles.*

Locomotor activity plots of individual flies during the same LD and temperature entrainment regime shown in Figure 4. To classify each fly as 'entrained', 'weakly entrained', or 'not entrained' we generated an individual actogram (left column), and an average activity plot for each day of the experiment (middle and right columns, showing the activity during one day in the life of that particular fly, respectively). Flies were classified as 'entrained' if they exhibited a clear and sharp activity peak in the warm phase (arrows in the upper panel), or 'weakly entrained', if that peak appeared broader and the behavior during the warm phase was more erratic (arrows in the middle panel). For easier identification of the entrained peak, especially in more noisy records, a three-point-moving-average filter was applied to the raw data (dots connected by red line). 'Not entrained' flies did not show a behavioral peak during the warm phase but stayed active constitutively or showed erratic behavior. All flies did show a response to the temperature changes by increasing or decreasing their activity abruptly after the temperature changes (arrow heads) (see Expermiental Procedures for more details). The flies shown here were from the *Canton S* (upper panel) and eys^{395} strains (middle and lower panels).

Figure S5: *Normal temperature-entrained behavior of 'weak'* UAS-nocteRNAi *lines, and flies with impaired antennae in temperature cycles.*

A-C) Group actograms and daily average activity of flies that were entrained to 12 hr: 12 hr LD cycles for 5-7 days followed by one week of LL and 12 hr: 12 hr temperature cycles (25:16ºC) in which the warm- and cold-phase were in anti-phase to the previous

LD cycle (i.e., cold-phase corresponds to the light-phase). **A)** The *nocte-RNAi* line shown here belongs to type 2 (Figure 3B) (line 2-1a) and was crossed to the *F-gal4* insertion on chromosome *2*. **B, C)** Ablation of either the 3rd antennal segment or the whole antenna resulted in 'entrained' behavior demonstrating that the ch organ in the antenna is not required for temperature synchronization. Dots in daily average plots indicate SEM's. **D)** Quantification of behavior in temperature cycles of all *nocte-RNAi* lines after crossing to the *F-gal4* line located on chromosome *3*. Note that lines from both types of *nocte-RNAi* can result in normal or mutant behavior, indicating that positional effects of the insertion site influence the efficiency of the RNAi effect. Similarly, the *F-gal4* line located on chromosome *3* (*F-gal4-33-5*) produced stronger phenotypes compared to the chromosome *2* insertion line (compare *nocte-RNAi-2-1a* in panel A with panel D).

Figure S6: *Overview of* F-gal4 *and* nocte-gal4 *driven reporter gene expression in the brain.*

(A, B) Expression of *UAS-gfp* driven by *nocte-gal4* in the brain. GFP was detected in many neurons and glia cells within the central brain, suboesophageal ganglion (SOG), and in the optic lobes (OL). A cluster of neurons in the ventro lateral brain (arrows) corresponds to the ventral lateral clock neurons (LNvs) (see Figure S8). Dorsally from the LNvs is a group of neurons (arrowheads) from which one cell projects dorsally into the midbrain (open arrowheads). This S-shape axonal projection is typical for a subset of the dorsal lateral clock neurons (LNd) suggesting that this neuron represents an LNd (Figure S8). About 20 large neurons are clustered in the pars intercerebralis (PI). In the SOG, neurons are marked in the lateral and ventral regions. Some of them (open arrows)

are located close to the intake of the connectives to the spinal nerve cord. Extensive GFP signals were found in all compartments of the mushroom bodies including α, β, and γ lobes (α, β, γ), pedunculus (P), and calyx (Ca). **(C, D)** Brain expression of *UAS-gfp* driven by *F-gal4*. The dorsal brain harbours a group of about 3 small and 1 large neurons (arrowheads) with typical S-shape axonal projection (open arrowhead) running first to the dorsal and then to the central brain where they ramify. Varicose fibres then split in a thin nerve bundle which extents into the contralateral brain hemisphere. In the dorsal brain close to the posterior surface, a cluster of about 5 small cells (asterisks) contains GFP. Five bilateral neurons (daggers) are clustered in the anterior deutocerebrum. The most prominent signal emanates from neuronal arborisations within the antennal lobes and antennal nerves (arrows) probably originating from neurons of the antennal chordotonal organs. These arborisations form two thin nerve bundles. One interconnects the arborisation in the contralateral brain hemispheres. The second one runs dorsomedially to the brain midline where it merges with axonal projections arising from a bilateral cluster of about 4 large neurons located in the ventral area of the SOG (open arrows) and then runs parallel to the contralateral bundle into the pars intercerebralis where it vanishes. This nerve fascicle divides into two small bilateral ramifications in the wedge between the proto- and deutocerebrum. A small neuron (double arrowheads) projecting to the central brain as well as to the medulla is located in the ventral optic tract. Signals in the retina (R) can represent an autoflourescence, since in the control experiment (*UAS-gfp* flies) a signal was detected in this area. Scale bar = 100 μm.

Figure S7: *Reduction of* nocte *expression does not grossly interfere with development of chordotonal organs, which express* F-gal4 *but not* tim-gal4.

(A-G) *UAS-rfp* and *nocteRNAi:1:3* driven by *F-gal4* in external body parts. Widespread distribution of RFP was detected in nuclei of the putative chemo- and mechanoreceptors cells in the mouthpart (A), antennae (A, B), wing (C, D), haltere (E) and leg (F, G). Positive signals were also found in neurons of the chordotonal organs (arrows) in all external tissues tested. Down-regulation of *nocte* expression did not cause any significant changes in distribution of RFP, suggesting that *nocte* is not essential for development of *F-gal4*-expressing sensory organs (compare with Figure 5I-P). **(H-N)** *UAS-mCD8gfp* and *UAS-rfp* driven by *tim-gal4:62*. GFP and RFP signals were detected in mechano- and chemoreceptor cells in the mouthpart (H), antennae (H, I), wing (J, K), haltere (L), and leg (M, N). No signals were detected in the chordotonal organs (arrows). This was also the case for the other *tim-gal4* lines used in this study. labp = labial palpus; mxp = maxillary palpus; ant = antenna. Scale bar (A, C, F, H, J, M) = 100 μm, (B, D, E, G, I, K, L, N) = 10 μm.

Figure S8: nocte-gal4 *and* F-gal4 *expression in canonical clock neurons in the brain.*

Upper panel: Period expression in *nocte-gal4/UAS-rfp* flies was determined by anti-Per immunostaining (green) to identify dorsally located clock neurons co-expressing *nocte-gal4* (red). At least 4 DN1 and 1 LNd co-express Period and *nocte-gal4* (arrowheads in merged image). Middle panel: Anti-PDH signals (red) in *nocte-gal4/UAS-gfp* brains reveal that *nocte-gal4* is expressed in all ventrally located PDH-expressing clock neurons (LNvs). Lower panel: All clock neuronal groups were identified by anti-Per

immunostaining in *F-gal4/UAS-gfp* brains. Only 1 large LNv cell expresses both Period and the *F-gal4* driver (arrowhead). l-LNv, s-LNv: large and small ventral Lateral Neurons; LNd: dorsal Lateral Neurons; DN1-3: Dorsal Neurons 1-3. Scale bar: 10 μm.

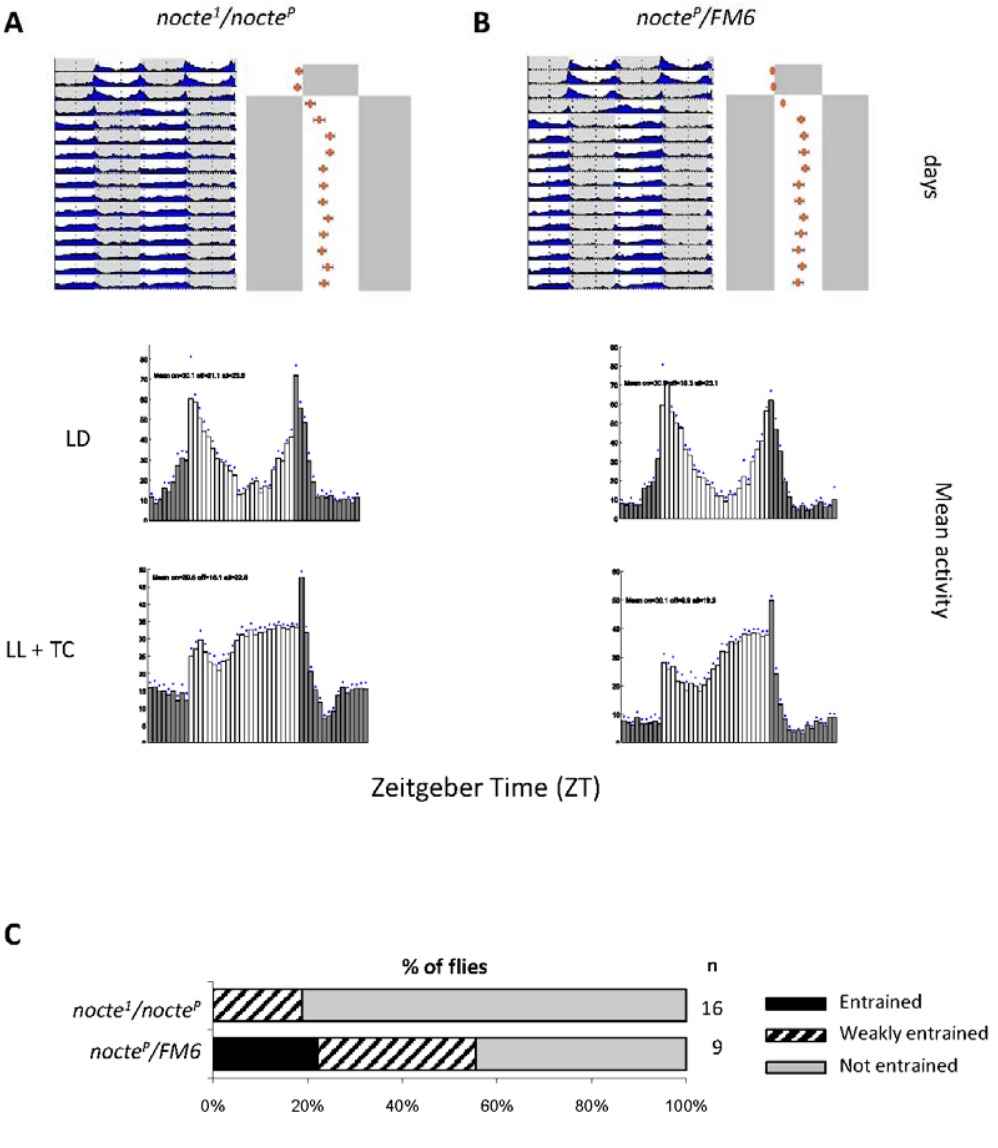
A
nocte1/nocteP
B
nocteP/FM6
days
LD
LL + TC
Mean activity
Zeitgeber Time (ZT)
C
% of flies
n
nocte1/nocteP
nocteP/FM6
16
9
Entrained
Weakly entrained
Not entrained
0%
20%
40%
60%
80%
100%

Figure S1

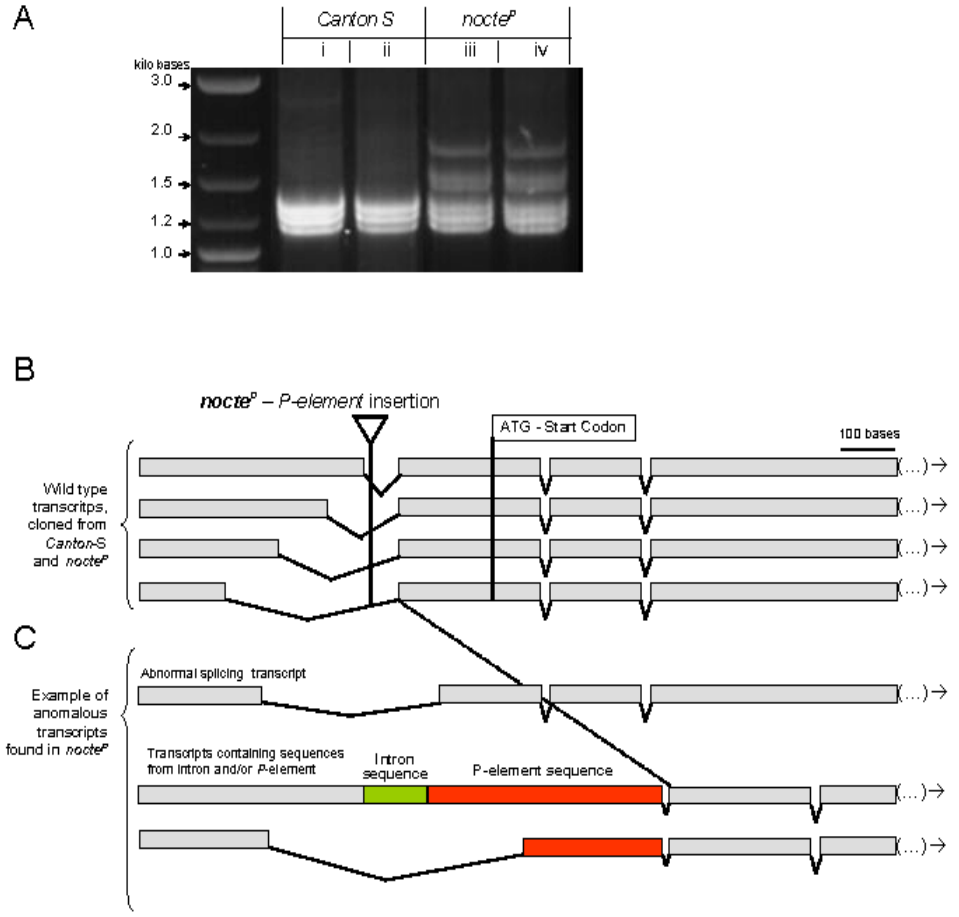
A
Canton S
nocte^P
i
ii
iii
iv
kilo bases
3.0
2.0
1.5
1.2
1.0
B
nocte^D – P-element insertion
ATG - Start Codon
100 bases
Wild type transcritps, cloned from Canton-S and nocte^P
(...)→
C
Example of anomalous transcripts found in nocte^P
Abnormal splicing transcript
Transcripts containing sequences from intron and/or P-element
Intron sequence
P-element sequence

Figure S2

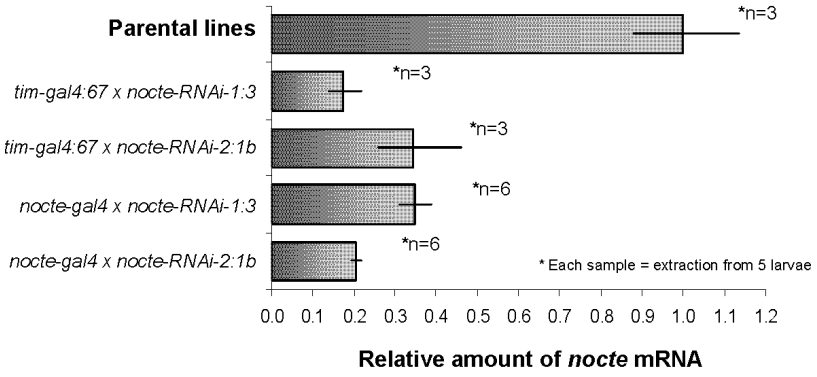
Parental lines
tim-gal4:67 x nocte-RNAi-1:3
tim-gal4:67 x nocte-RNAi-2:1b
nocte-gal4 x nocte-RNAi-1:3
nocte-gal4 x nocte-RNAi-2:1b
*n=3
*n=3
*n=3
*n=6
*n=6
* Each sample = extraction from 5 larvae
0.0 0.1 0.2 0.3 0.4 0.5 0.6 0.7 0.8 0.9 1.0 1.1 1.2
Relative amount of nocte mRNA

Figure S3

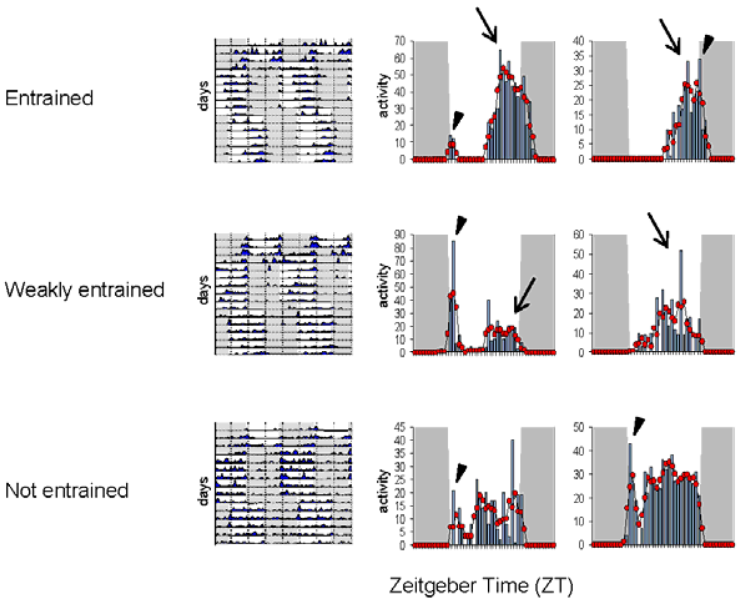
Entrained
Weakly entrained
Not entrained
days
activity
Zeitgeber Time (ZT)

Figure S4

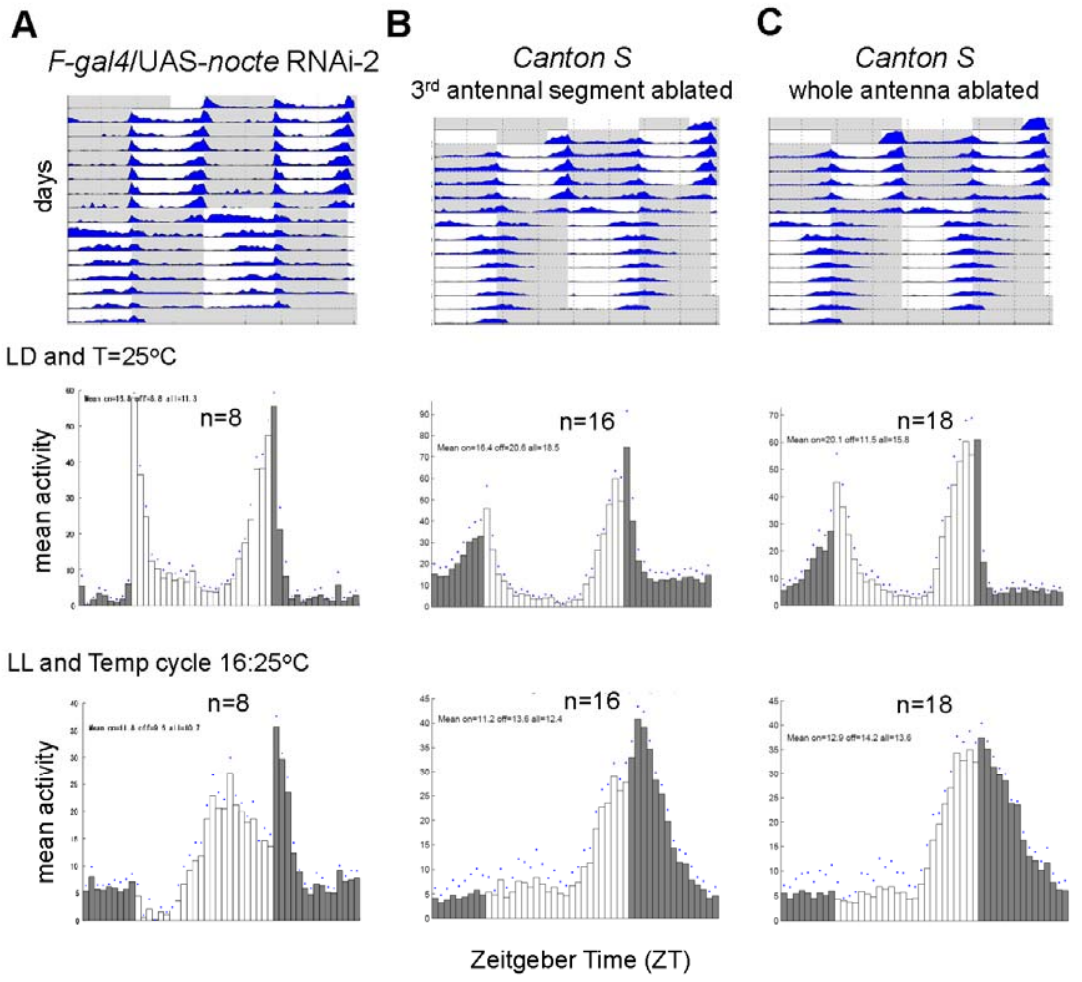
A
F-gal4/UAS-nocte RNAi-2
B
Canton S
3rd antennal segment ablated
C
Canton S
whole antenna ablated
days
LD and T=25°C
mean activity
n=8
n=16
n=18
LL and Temp cycle 16:25°C
mean activity
n=8
n=16
n=18
Zeitgeber Time (ZT)

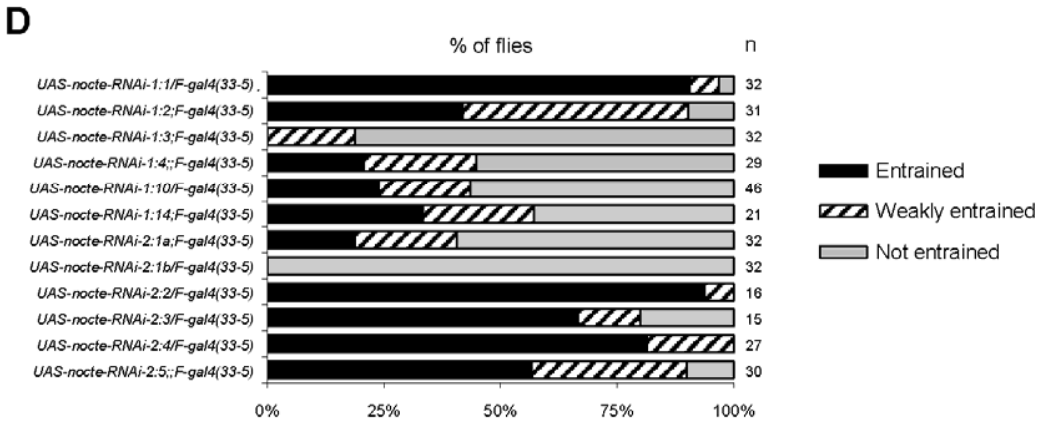
D
% of flies
n
UAS-nocte-RNAi-1:1/F-gal4(33-5)
UAS-nocte-RNAi-1:2;F-gal4(33-5)
UAS-nocte-RNAi-1:3;F-gal4(33-5)
UAS-nocte-RNAi-1:4;;F-gal4(33-5)
UAS-nocte-RNAi-1:10/F-gal4(33-5)
UAS-nocte-RNAi-1:14;F-gal4(33-5)
UAS-nocte-RNAi-2:1a;F-gal4(33-5)
UAS-nocte-RNAi-2:1b/F-gal4(33-5)
UAS-nocte-RNAi-2:2/F-gal4(33-5)
UAS-nocte-RNAi-2:3/F-gal4(33-5)
UAS-nocte-RNAi-2:4/F-gal4(33-5)
UAS-nocte-RNAi-2:5;;F-gal4(33-5)
32
31
32
29
46
21
32
32
16
15
27
30
0%
25%
50%
75%
100%
Entrained
Weakly entrained
Not entrained

Figure S5

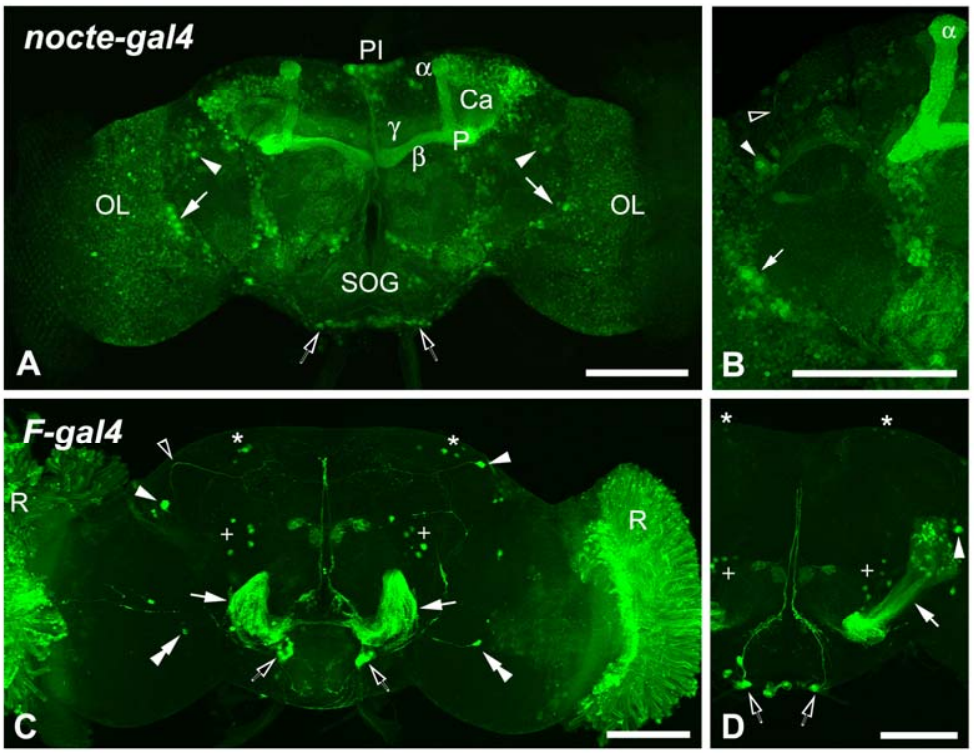

Figure S6

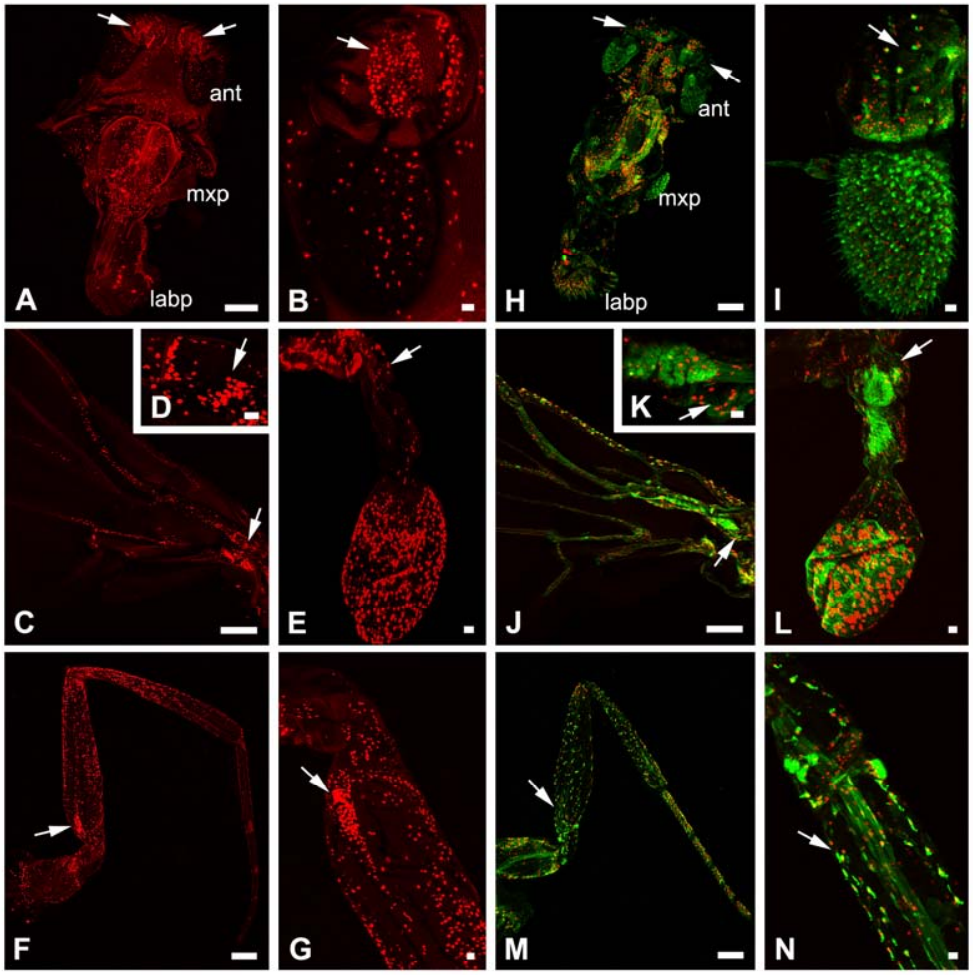

Figure S7

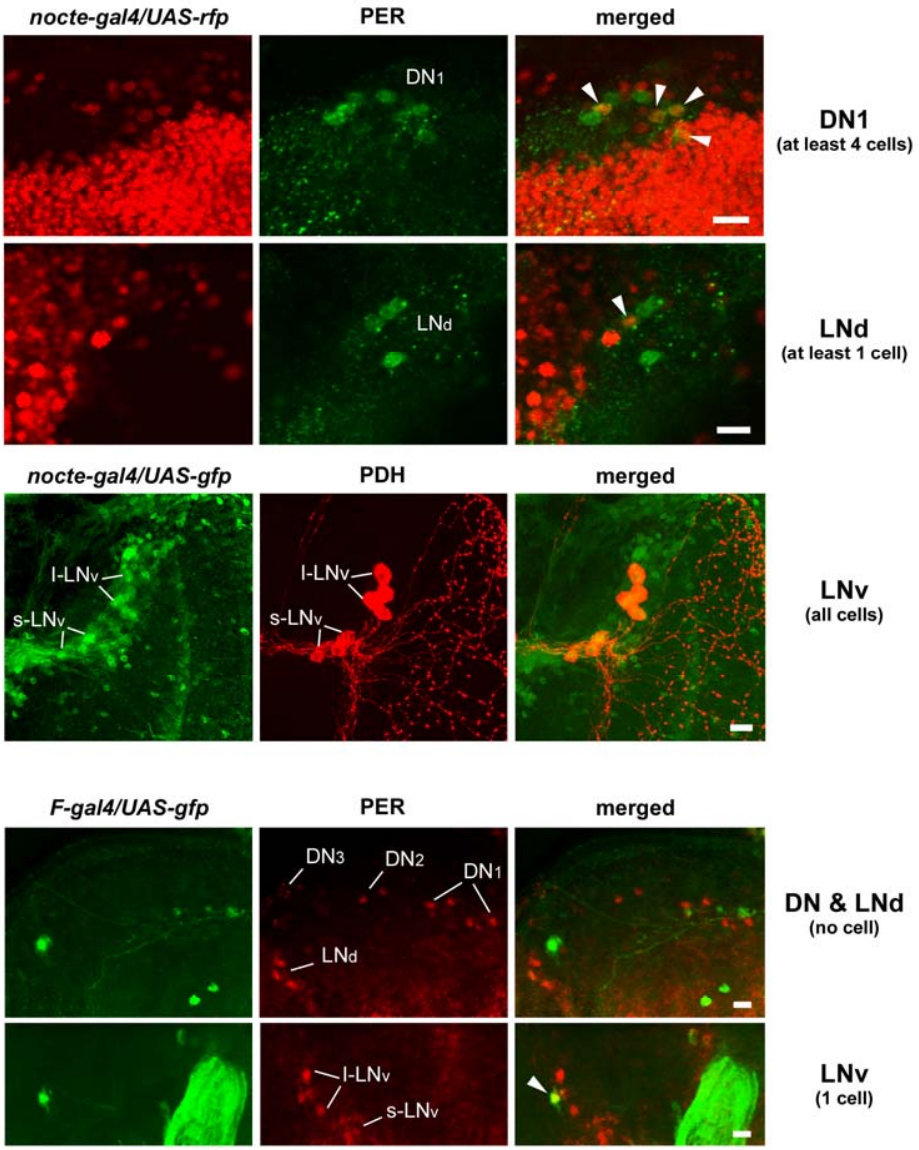
nocte-gal4/UAS-rfp
PER
merged
DN1
DN1
(at least 4 cells)
LNd
LNd
(at least 1 cell)
nocte-gal4/UAS-gfp
PDH
merged
l-LNv
s-LNv
l-LNv
s-LNv
LNv
(all cells)
F-gal4/UAS-gfp
PER
merged
DN3
DN2
DN1
LNd
DN & LNd
(no cell)
l-LNv
s-LNv
LNv
(1 cell)

Figure S8

Table S1: Quantification of dendritic cap defects or NompA misexpression in *nocte* mutants

	Genotype		
	control (*FM6*)	*nocte*^{1}	*nocte*^{P}
number of individual flies checked	10	4	5
number of flies showing defects (%)	1 (10)	4 (100)	3 (60)
average number of caps visualized per femur/average number of defective caps (%)	30/1 (3)	20/7 (35[1])	22/6 (27)

Males homozygous for the *gfp-nompA* reporter construct were crossed to *nocte*^{1}*/FM6* and *nocte*^{P}*/nocte*^{P} females. In the F1, 4-6 legs of each male individual from the indicated genotype (each carrying one copy of the *gfp-nompA* reporter) were dissected and mounted on a glass slide in a glycerol:water (2:1) solution. Freshly mounted legs were then directly inspected by confocal microscopy and one femur was scored for the presence and frequency of the dendritic cap phenotype per fly. [1]Note that although every *nocte*^{1} fly exhibited the phenotype, the frequency of defective dendritic caps within one femur varied substantially between individuals: it ranged from 15% to 70% between individual flies.

Experimental Procedures

Flies: As control flies either wild type *Canton S* or *y Df(1)w* (*y w*) were used (Lindsley and Zimm, 1992). *XLG-luc*; *8.0-luc:9* (Veleri et al., 2003), and *BG-luc* (Stanewsky et al., 1997) transgenics have been described previously as have the Clk^{Jrk} (Allada et al., 1998), tim^{01} (Sehgal et al., 1994) rhythm mutants and the $norpA^{P41}$ null mutation (Lindsley and Zimm, 1992). The original $nocte^{1}$ allele was isolated after chemical mutagenesis as described (Glaser and Stanewsky, 2005). The $P\{XP\}CG17255^{d07154}$ insertion in the first intron of *nocte* ($nocte^{P}$) was obtained from the Exelixis collection at Harvard University, Boston, MA (USA) (Thibault et al., 2004). A duplication covering the chromosomal interval 9A2-10C2 [$Dp(1;2)v^{+75d}$] was obtained from the Bloomington stock center as were the *X*-chromosomal deficiencies and multi marker chromosome bearing stocks used in the mapping tests. Two different insertion lines of *F-gal4* were applied in this study, one is inserted on chromosome *2* (*F-gal4*), one on chromosome *3* (*F-gal4-33-5*) (Kim et al., 2003). The *UAS-cycΔ:24* line was described previously (Tanoue et al., 2004) as well as eys^{395}, eys^{734}, and $spam^{1}$ mutants (Husain et al., 2006; Zelhof et al., 2006), and the $tilB^{1}$ and *smetana* mutants (Caldwell et al., 2003). The reporter strain expressing a *gfp-nompA* fusion protein under control of *nompA* promoter sequences was generated in the laboratory of M. Kernan (Chung et al., 2001). The *eys* and *deaf-RNAi* stocks were obtained from the National Institute of Genetics Fly Stock Center (Japan). A transgenic type carrying *tim-gal4* (lines 16, 27, 62, 67) (Kaneko and Hall, 2000) was used to drive *UAS-cycΔ:24*, to visualize *tim* expression in peripheral tissues (whereby *tim-gal4* drove expression of *UAS-mCD8gfp* and *UAS-rfp*), and to drive *UAS-nocte-RNAi* to determine

the efficiency of *nocte* mRNA reduction or potential effects on temperature-entrained behavior. Transgenic flies carrying either of the two *nocte-RNAi*, and the *nocte-gal4* constructs (for details see below) were generated in a *y w* genetic background by BestGene Inc. Ten independent lines were generated for each construct. Six type-1 and six type-2 *nocte*-RNAi constructs were tested, out of which four (type-1) and two (type-2) cause temperature entrainment phenotypes after crossing to *F-gal4* (Figure S5). Experiments shown in Results were performed with lines *UAS-nocte-RNAi-1:3* and *UAS-nocte-RNAi-2:1b* (except the one shown in Figure S5A, where *UAS-nocte-RNAi-2:1a* was used). For *nocte-gal4* three independent insertion lines (F10, M3, M6) were crossed to *UAS-gfp* (nuclear), *UAS-mCD8gfp,* and *UAS-rfp* (all reporter lines were obtained from the Bloomington stock center) and found to exhibit identical expression patterns in brain and peripheral clock tissues. The *nocte-gal4:M3* line was applied in the experiments shown here. To visualize nuclear and membrane expression at the same time, a true-breading stock containing *UAS-rfp* and *UAS-mCD8gfp* was generated by standard crossings.

Bioluminescence recordings and imaging: Flies or tissues were kept either in LL and temperature cycling conditions (12 hr: 12 hr, 16°C: 25°C), or in LD (12 hr: 12 hr at 25°C) for the entire duration of the experiment. Raw data was plotted and analyzed (including determining the peak phase of expression plotted in Figure 1A) using Brass software (Locke et al., 2005) as described (Glaser and Stanewsky, 2005). For the images shown in Figure 2, tissues were dissected under M3 Insect Medium (Sigma) and kept for three days in culture medium (M3 Insect Medium with fetal Bovine serum, Penicillin-Streptomycin,

Insulin and Luciferin [200 μM, Biosynth]) in light and temperature regimes as stated in Results text. The entrained tissues were imaged in the LuminoviewLV200 (Olympus, Tokyo, Japan) at a time corresponding to peak expression of PER in the Topcount luminometer (at ZT18 for brains and external tissues in LD cycles and at ZT11 and ZT18 for brains and external tissues, respectively, in LL and temperature cycles). Brains were exposed for 25 min and external tissues for 15 min at a gain of 255. Bioluminescence images were analyzed and merged with bright-field images using Cell^{M} imaging software for life science microscopy (Olympus).

Mapping of *nocte*: 118 meiotic recombinants between the *nocte* and multi marker chromosome *y w cv v f car* were established. Testing these recombinants for molecular (using bioluminescence measurements, see above) and behavioral (see below) temperature-entrainment phenotypes placed *nocte* between *cv* (cytological map position 5A13) and *v* (9F11). Further mapping using Single Nucleotide Polymorphisms (SNP's), which distinguish the *nocte* and marker chromosomes, placed *nocte* between *CG15245* (9A2) and *CG2124* (9D3). The accuracy of this mapping was confirmed by covering phenotypic effects of the *nocte* mutation with $Dp(1;2)v^{+75d}$ (9A2-10C2) (Figure 3A). For further mapping, chromosomal deficiencies with molecularly defined breakpoints were applied (Ryder et al., 2004). From five deficiencies tested [*Df(1)ED6991, Df(1)ED7005, Df(1)ED7010, Df(1)ED429,* and *Df(1)ED7042*] only *Df(1)ED7005* uncovered effects of the *nocte* mutation (both in bioluminescence and behavioral assays), placing *nocte* in the interval between 9B3 and 9D3. This region is bordered by the genes *CG15309* and *CG15296*, an interval containing 35 genes (Tweedie et al., 2009). Another deficiency

[*Df(1)c52,flw*^{c52}, which removes 8E3-5;9C1] complements *nocte* but not *flw*, thereby further reducing the interval to the 12 genes between *flw* (9B14-C1) and *CG15296* (9D3) (Tweedie et al., 2009). No obvious candidates could be identified among the 12 remaining genes so that we initiated sequence determination of all candidates along with analysis of available mutations and *P*-element insertions. This approach resulted in the identification of a *P*-element insertion (*P{XP}CG17255*^{d07154}) in the gene *CG17255*, which exhibits very similar temperature entrainment phenotypes compared to the original *nocte* mutation (Figures 3A and 4C).

Generation of *nocte* constructs: For RNAi construct 1 genomic DNA containing *nocte* exon 2, intron 2, exon 3 and intron 3 was amplified by PCR and cloned into pUAST via EcoRI and NotI. An inverted cDNA fragment encoding exons two and three was subsequently cloned as a NotI-XhoI fragment into the same vector to create a fusion between the genomic DNA and the reversed cDNA. For *nocte* RNAi construct 2 the 3' end of exon 4, intron 4, exon 5 and intron 5 were chosen and cloned into pUAST as a BglII-NotI fragment. An inverted cDNA fragment encoding the 3' end of exon 4 and exon 5 was fused to this genomic DNA fragment by cloning it subsequently into the NotI and XbaI sites of the same vector. Primer sequences for *nocte* RNAi constructs: RNAi construct 1 genomic forward: GCGGACGAATTCAAACCCACCAGAAAGACTGAAACA; RNAi construct 1 genomic reverse: CCGGCGACGCGGCCGCCTAAAATGGAAAATTCACCCAGTTAAAGG; RNAi construct 1 cDNA forward:

CCGGCGACGCGGCCGCCTTCGACTGAGACTAAGAGATTGT; RNAi construct 1 cDNA reverse: GCATCCGCTCGAGATGAGTACACTGGGGGGAAG; RNAi construct 2 genomic forward: GGCAGATCTAAAATGAATCTTTATGCGGCTCCAC; RNAi construct 2 genomic reverse: CCGGCGACGCGGCCGCCTGAAGAGGAAAGAAGGATGAATTAGG; RNAi construct 2 cDNA forward: CCGGCGACGCGGCCGCCGCGCCGTAGTTCTTGTGA; RNAi construct 2 cDNA reverse: GCGGTCTAGAATGAATCTTTATGCGGCTCCAC.

The *nocte* promoter region contained 3.646 kb of DNA upstream of the predicted start codon and was amplified from genomic DNA using primers that introduce XbaI and SpeI sites. The resulting fragment was then cloned into pPTGAL4. PCR primers to amplify the nocte promotor region were: Forward: GGCTCTAGAGGAGTCAGATTCAGATTCCGGC Reverse: TGGCGCACTAGTGCTGCCAATAGATCCTCATTAG.

Behavioral analysis: Daily average histograms and actograms were plotted using the fly toolbox and MATLab software (Levine et al., 2002). Quantification of the ability to resynchronize to temperature cycles was performed by first generating an actogram and daily histograms for individual flies. All individuals from each genotype were then scrutinized for their activity peak at each day of the experiment. To facilitate detection of peak activity a three-point moving average filter was applied to the data (red-dotted line in Figure S4) (Garnett, 1997). Wild-type flies typically show two activity peaks in the entrainment regime applied here: one peak immediately after the temperature rise, which we interpret as a ‘response’ to the environmental change, rather than entrainment (Glaser

and Stanewsky, 2005; Yoshii et al., 2005). In addition a major activity peak occurs in the second half of the warm phase. This peak is not observed in clock or temperature-entrainment mutants and is therefore referred to as the 'entrained' peak. If present, this entrained peak was determined (by eye) and assigned a numerical value for each day and each individual and tracked throughout the experiment (Phase plots in Figure 4). These animals were classified as 'entrained' (Figure 4) and examples are shown in Figure S4. Most mutant animals did not show a clear entrained peak but were either constitutively active or inactive during the warm phase. Since they did show a response to the temperature increase, this 'response' peak was tracked and plotted in Figure 4. These individuals were classified as 'not entrained' (Figure 4) and examples are shown in Figure S4. In addition, some individuals displayed an intermediate behavior. They did show characteristics of an entrained peak, which was usually less pronounced and noisier compared to wild type flies and controls. Also, these flies often displayed a more drastic response to the warm transition compared to controls. These individuals were classified as 'weakly entrained' (Figure 4) and typical examples are shown in Figure S4.

Fluorescence Microscopy and Immunohistochemistry: To observe GFP and/or RFP signals tissues of transgenic flies were dissected in *Drosophila* Ringer solution and fixed in 4% paraformaldehyde overnight at 4 ºC. Samples were then washed 3 times for 15 min in 0.1 M sodium phosphate buffer (pH 7.4) then 3 times for 10 min in phosphate-buffer saline (PBS) supplemented with 1% Triton X-100 (PBS-T) at room temperature. Following 5 min rinse in distilled water, samples were mounted in Vectashield medium (Vector laboratories, Burlingame, Calif.) and examined under a LSM-510 META

confocal microscope (Zeiss, Germany). In control assessments, the original *UAS-mCD8gfp*, *UAS-gfp*, and *UAS-rfp* lines were used to verify the absence of Gal4-independet signals (data not shown). For immunostaining with monoclonal 22C10 antibodies, samples were blocked for 2 hr in 5% normal goat serum in PBS-T after the fixation and washing steps. This was followed by incubation with the primary antibody (dilution 1:100, Developmental Studies Hybridoma Bank) in blocking solution over night (4°C) and washing steps described above. Samples were then incubated with Phalloidin-TRITC (1:1000, Sigma) and secondary Alexa 647 goat anti-mouse antibodies (Molecular Probes). Samples were then washed with PBS-T (3 x 20 min) and rinsed in water (5 min) before being mounted and inspected as described above. Control and *nocte* mutant flies expressing the *gfp-nompA* construct were obtained after crossing homozygous *gfp-nompA* males (inserted on chromosome *3*) to $nocte^{1}/FM6$ and $nocte^{P}/FM6$ females. Legs from 2-3 day old $nocte^{1}$ mutant and *FM6* control males generated by this cross (both carrying one copy of the *gfp-nompA* construct) were dissected in Ringer solution and cut at the proximal end of the femur to allow antibody penetration. For quantification of the ch organ structural defect observed in *nocte* mutants see legend to Table S1. For anti-Per and anti-PDH immunostainings (Figure S8) fixed and washed preparations were subsequently blocked with 10% normal goat serum in PBS-T for 2 h at room temperature and incubated for 2 days with anti-PER at 4°C (Veleri et al., 2003) or with affinity purified anti-crab-PDH (Hodge and Stanewsky, 2008) (both diluted 1:1000 in PBS-T). After washing, samples were incubated with AlexaFluor 488 (green) or AlexaFluor 594 (red), respectively (both diluted 1:300 in PBS-T).

RNA extraction, Reverse Transcription reaction, and qPCR: Total RNA was extracted with 0.5 ml of TRI Reagent (Ambion) followed by purification with Lithium Chloride solution (Ambion) according to the manufacturers' instructions. The volume of H_2O used for the final elution of the RNA depended on the nature of the sample, according to the potential cDNA synthesis inhibition detected for each one, which was determined as follows: standard curves of RNA dilutions from each sample were performed for every pair of primers to be used in the quantitative PCR. For 10 flies the volume of H_2O used to elute the extracted RNA from each sample (volume in which no inhibition of cDNA synthesis was observed for any pair of primers) was: heads 100 μl, brains, legs, and wings 40 μl, ovaries and testis 200 μl, and 5 3rd instar larvae in 800 μl. cDNA synthesis was performed with Reverse Transcription Reagents Kit (Applied Biosystems) in 10 μl reactions according to the manufacturer's instructions. For quantitative PCR, first, the 10 μl cDNA from each sample was diluted 10 times, and then qPCR reactions were prepared as follows: 7.5 μl Power SYBR Green PCR Master Mix (Applied Biossystems), 4.0 μl of cDNA, each primer at 0.5 μM final concentration and H_2O to a 15 μl final volume reaction. The primers used in the qPCRs were as follows (always in 5' -> 3' orientation): *rp49* sense CGATATGCTAAGCTGTCGCACA, *rp49* antisense CGCTTGTTCGATCCGTAACC, *period* sense CAACAAGTCGGTGTACACGAC, *period* antisense GTCTTGACGGATGCGCTCTG, *nocte* sense AAGAACTACGGCGCGTG, *nocte* antisense CCAAGGCGTTCATGCTC (note that the pair of primers used for *nocte* targets a region that does not overlap with any of the two *nocte-RNAi* constructs used). Reactions were performed in a Chromo4 Detector (Bio-Rad) under the following temperature conditions: hot start at 95^{o}C for 10 minutes followed by 40 cycles of 95^{o}C for 15 seconds, 60^{o}C for

30 seconds, and 10 seconds at a reading temperature (reading of the signal). The reading temperature for a pair of primers is generally ~3-5^{o}C lower than the melting temperature of the amplicon they generate, and higher than that of the potential primer dimer. The reading temperature for the pair of primers used and listed above were 77^{o}C for *rp49* and *period*, and 80^{o}C for *timeless* and *nocte*. For each sample, three replicas of the reaction were run in parallel, and the average of their Ct (threshold cycle) values (excluding outliers) was considered for quantification. The relative quantification was determined using the comparative C_T method, also known as the $\Delta\Delta C_T$ method, or the $2^{-\Delta\Delta C}{}_T$ method (Livak and Schmittgen, 2001; Pfaffl, 2001), using *rp49* as control. The Applied-Biosystems *User Bulletin #2: Relative quantification of gene expression* (1997, updated on 10/2001, available on line) was also used as support guide for the calculations, all performed in Microsoft Excel software. For the statistical analysis, analysis of variance (ANOVA) and LSD Post-Hoc test (P<0.05) were performed when possible (for details see legend of figures).

***nocte* transcripts in *nocte^{P}* mutants**: PCR was conducted with 2.0 µl of cDNA, 12.5 µl of LongAmp Taq 2x Master Mix (New England Biolabs), a pair of primers for *nocte* gene to a final concentration of 0.5 µM each (sense: 5'- GCGGCAAACTTTATGTTGGA -3'; antisense: 5'- CGTGTCCTGTGGTAATTGC -3'), and H_2O to a final volume reaction of 25 µl. The pair of primers used amplifies a ca. 1.2-kb wild type *nocte* fragment (varied slightly according to the different transcripts; see Figure 3B), starting from the 5'-UTR region, and spanning the insertion site of the *P*-element in *nocte^{P}* and the start codon of the wild-type transcripts. For each strain, the two independent PCR reactions were pooled and

purified with MicroSpin S-400 HR Columns (GE Healthcare Life Sciences), cloned in pGEM-T Easy Vector (Promega) according to the manufacturer's instructions, and used to transform XL1 Blue cells. On average 25 clones from each transformation were sequenced.

Supplemental References:

Allada, R., White, N. E., So, W. V., Hall, J. C., and Rosbash, M. (1998). A mutant *Drosophila* homolog of mammalian Clock disrupts circadian rhythms and transcription of *period* and *timeless*. Cell *93*, 791-804.

Caldwell, J. C., Miller, M. M., Wing, S., Soll, D. R., and Eberl, D. F. (2003). Dynamic analysis of larval locomotion in *Drosophila* chordotonal organ mutants. Proc Natl Acad Sci U S A *100*, 16053-16058.

Chung, Y. D., Zhu, J., Han, Y., and Kernan, M. J. (2001). *nompA* encodes a PNS-specific, ZP domain protein required to connect mechanosensory dendrites to sensory structures. Neuron *29*, 415-428.

Garnett, W. P. (1997). Chaos Theory Tamed: Taylor Francis, Inc).

Glaser, F. T., and Stanewsky, R. (2005). Temperature synchronization of the *Drosophila* circadian clock. Curr Biol *15*, 1352-1363.

Helfrich-Förster, C. (2000). Differential control of morning and evening components in the activity rhythm of *Drosophila melanogaster*--sex-specific differences suggest a different quality of activity. J Biol Rhythms *15*, 135-154.

Hodge, J. J., and Stanewsky, R. (2008). Function of the Shaw potassium channel within the *Drosophila* circadian clock. PLoS ONE *3*, e2274.

Husain, N., Pellikka, M., Hong, H., Klimentova, T., Choe, K. M., Clandinin, T. R., and Tepass, U. (2006). The agrin/perlecan-related protein eyes shut is essential for epithelial lumen formation in the *Drosophila* retina. Dev Cell *11*, 483-493.

Kaneko, M., and Hall, J. C. (2000). Neuroanatomy of cells expressing clock genes in *Drosophila*: transgenic manipulation of the *period* and *timeless* genes to mark the perikarya of circadian pacemaker neurons and their projections. J Comp Neurol *422*, 66-94.

Kim, J., Chung, Y. D., Park, D. Y., Choi, S., Shin, D. W., Soh, H., Lee, H. W., Son, W., Yim, J., Park, C. S.*, et al.* (2003). A TRPV family ion channel required for hearing in *Drosophila*. Nature *424*, 81-84.

Levine, J. D., Funes, P., Dowse, H. B., and Hall, J. C. (2002). Signal analysis of behavioral and molecular cycles. BMC Neurosci *3*, 1.

Lindsley, D. L., and Zimm, G. G. (1992). The Genome of *Drosophila melanogaster* (San Diego, California: Academic Press).

Livak, K. J., and Schmittgen, T. D. (2001). Analysis of relative gene expression data using real-time quantitative PCR and the 2(-Delta Delta C(T)) Method. Methods *25*, 402-408.
Locke, J. C., Southern, M. M., Kozma-Bognar, L., Hibberd, V., Brown, P. E., Turner, M. S., and Millar, A. J. (2005). Extension of a genetic network model by iterative experimentation and mathematical analysis. Mol Syst Biol *1*, 2005 0013.
Pfaffl, M. W. (2001). A new mathematical model for relative quantification in real-time RT-PCR. Nucleic Acids Res *29*, e45.
Ryder, E., Blows, F., Ashburner, M., Bautista-Llacer, R., Coulson, D., Drummond, J., Webster, J., Gubb, D., Gunton, N., Johnson, G.*, et al.* (2004). The DrosDel collection: a set of *P*-element insertions for generating custom chromosomal aberrations in *Drosophila melanogaster*. Genetics *167*, 797-813.
Sehgal, A., Price, J. L., Man, B., and Young, M. W. (1994). Loss of circadian behavioral rhythms and *per* RNA oscillations in the *Drosophila* mutant *timeless*. Science *263*, 1603-1606.
Stanewsky, R., Jamison, C. F., Plautz, J. D., Kay, S. A., and Hall, J. C. (1997). Multiple circadian-regulated elements contribute to cycling *period* gene expression in *Drosophila*. Embo J *16*, 5006-5018.
Tanoue, S., Krishnan, P., Krishnan, B., Dryer, S. E., and Hardin, P. E. (2004). Circadian clocks in antennal neurons are necessary and sufficient for olfaction rhythms in *Drosophila*. Curr Biol *14*, 638-649.
Thibault, S. T., Singer, M. A., Miyazaki, W. Y., Milash, B., Dompe, N. A., Singh, C. M., Buchholz, R., Demsky, M., Fawcett, R., Francis-Lang, H. L.*, et al.* (2004). A complementary transposon tool kit for *Drosophila melanogaster* using *P* and *piggyBac*. Nat Genet *36*, 283-287.
Tweedie, S., Ashburner, M., Falls, K., Leyland, P., McQuilton, P., Marygold, S., Millburn, G., Osumi-Sutherland, D., Schroeder, A., Seal, R., and Zhang, H. (2009). FlyBase: enhancing *Drosophila* Gene Ontology annotations. Nucleic Acids Res *37*, D555-559.
Veleri, S., Brandes, C., Helfrich-Forster, C., Hall, J. C., and Stanewsky, R. (2003). A self-sustaining, light-entrainable circadian oscillator in the *Drosophila* brain. Curr Biol *13*, 1758-1767.
Yoshii, T., Heshiki, Y., Ibuki-Ishibashi, T., Matsumoto, A., Tanimura, T., and Tomioka, K. (2005). Temperature cycles drive *Drosophila* circadian oscillation in constant light that otherwise induces behavioural arrhythmicity. Eur J Neurosci *22*, 1176-1184.
Zelhof, A. C., Hardy, R. W., Becker, A., and Zuker, C. S. (2006). Transforming the architecture of compound eyes. Nature *443*, 696-699.

7.3 Mechanical stimulation of ch organs synchronizes fly's locomotor activity

Recent findings suggest that chordotonal organs are required for the temperature-dependent entrainment of circadian clocks (Sehadova et al., 2009). Insects use ch organs to convert sound and other mechanical stimuli into action potentials that then are propagated to the central nervous system (Eberl, 1999; Albert et al., 2007). As ch organs are *mechanosensory* organs, I wondered whether the *mechanical* stimulation of ch organs alone could be sufficient for circadian clock entrainment. Specifically, I asked if a vibratory stimulus that was designed to excite ch organs could act as Zeitgeber and therefore entrain the circadian clock. In collaboration with Dr Jörg T. Albert (Ear Institute, University College London, UK), we set-up a mechanical stimulation apparatus which allowed us to measure the circadian patterns of locomotor activity of flies subjected to 12:12 hr "vibration:silence" (VS) cycles (see M&M for more details). Briefly, flies were subjected for 12 hours to a continuous 2-component stimulus of 200 Hz and 40 Hz vibrations followed by 12 hours of "silence" (i.e. background noise with an intensity of the order of a ten-thousandth lower compared to the stimulus applied). The two frequency have been chosen in order to stimulate both the Johnston's Organ (200Hz) and the other, non-hearing, ch organs in the fly's body (40Hz).

Flies were first entrained to 12:12 hr LD cycles and then transferred to DD and the VS was applied "in phase" with the previous LD ("vibration" corresponding to the previous day and "silence" corresponding to the previous night). After 5 days, the VS regime was delayed by 6 hours compared to the previous one and kept like that for 7 days. Next, another 6 hour VS shift (delay) was applied, so that the VS stimulation resulted in opposite phase compared to the initial LD

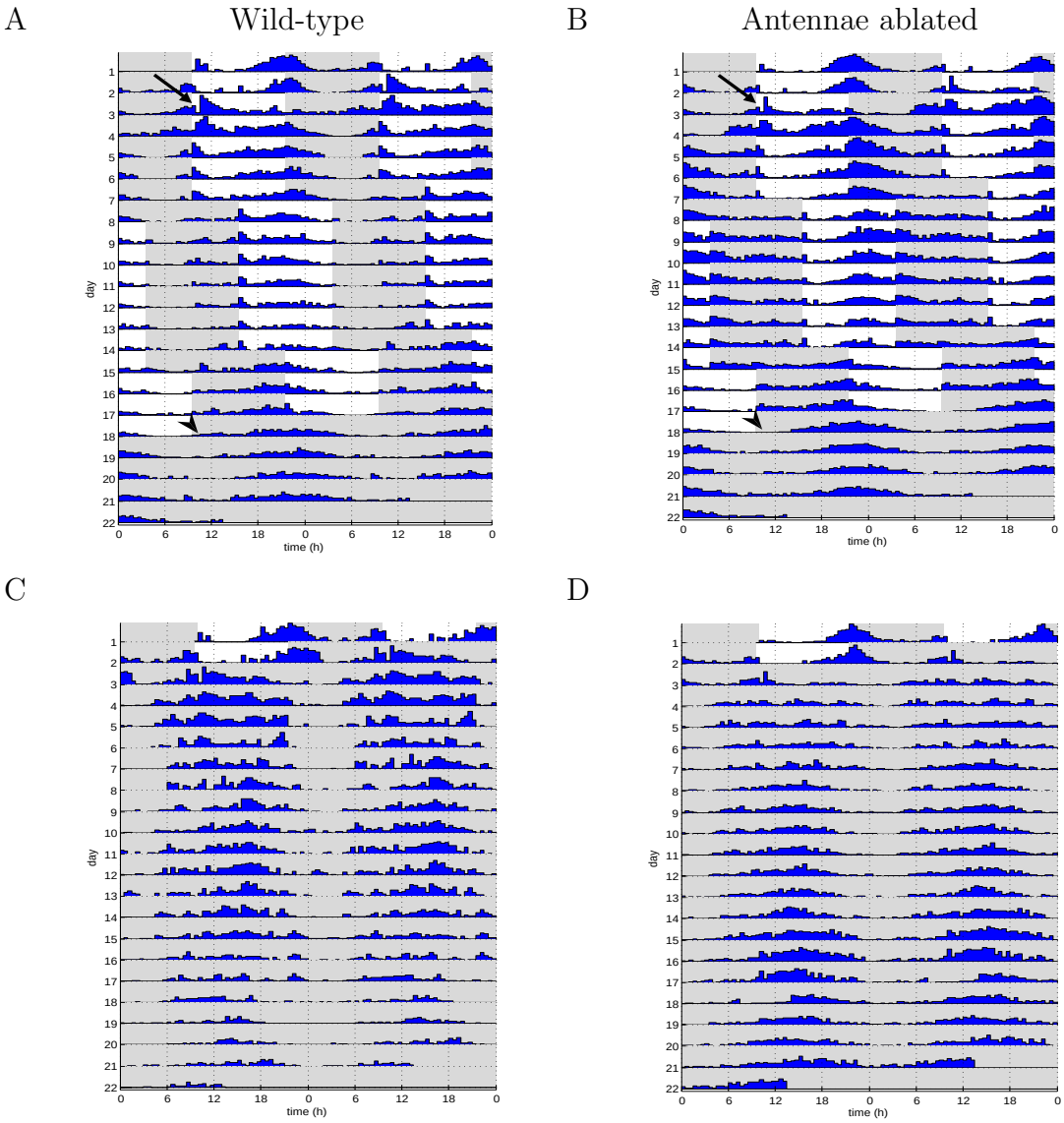

FIGURE 7.1: Average locomotor activity of wild-type and antennae-ablated flies (subjected to VS cycles) and controls (not subjected to VS cycles). A, B) Wt (n=15) and flies with bilateral ablation of all antennal segments (n=16) were first entrained in LD cycles (2 days). Then, flies were transferred to constant darkness and 12:12 hr "vibration-silence" (VS) cycles were applied in phase with the previous LD (arrows). After 5 days, the VS cycles were shifted of 6 hr (delayed) and kept for 7 days. Next, a subsequent 6-hr delayed shift was applied so to have the VS cycles in opposite phase compared to the initial LD regime. After that, flies were release in constant condition (arrow heads) and the phase was calculated (see Figure 7.5). C, D) Wt (n=6) and flies with bilateral ablation of the three antenna segments (n=14) were entrained to LD cycles and then released in DD served as controls. Free-running period are given in Table 7.1. White and grey shades represent "vibration" and "silence", respectively (or light and dark, for the first 2 days).

	Subjected to VS				Not subjected to VS			
	n	Rhythmic	τ	RS	n	Rhythmic	τ	RS
Wild-type	28	96.4%	24.1 ±0.1	2.89 ±0.19	21	100%	23.9 ±0.1	5.78 ±0.38
Ant ablated	26	96.2%	24.1 ±0.1	3.58 ±0.22	24	100%	24.0 ±0.1	4.92 ±0.49

TABLE 7.1: Free-running period of wild-type and antennae ablated flies subjected to vibration-silence (VS) stimulation and control (not subjected to VS). Period (τ) and rhythmicity statistic (RS) are calculated only for rhythmic flies. Total number of flies tested is indicated (n).

entrainment (Figure 7.1A, B). In parallel, flies entrained to the same initial LD cycles and then released to DD conditions without any vibration stimulus were used as controls (Figure 7.1C,D).

Analysis of average actograms and daily activity revealed that wild-type Canton S flies subjected to the VS stimulation exhibit different rest-activity patterns compared to free-running controls (Figure 7.2A–D). They display a sharp increase of locomotor activity after the transition from "silence" to "vibration", plus a major peak of activity during the vibration phase. The main peak of activity of flies subjected to the mechanical vibration occurs at the end of the vibration in the first VS cycles, then moves to the mid of the vibration part during the second VS cycles and after the second shift, it arises soon before the transition from "silence" to "vibration" (Figure 7.2B–D). The increase of activity occurring after vibration-on is reminiscent of the startle response induced by light and temperature. Wild-type flies not subjected to the VS cycles free-run with a period of 24 hours (Figure 7.1 and Table 7.1) and the phase of the main peak of activity follows the previous LD entrainment (Figure 7.2E–H). The differences on the activity phase and pattern induced by the exposure to the mechanical stimulation is conspicuous, and it does not seem to be a reaction (masking) response to the vibration stimulus (see below).

The fly's hearing organ is located in the second antennal segment (Caldwell and Eberl, 2002). It is composed of an array of specialized scolopidial cells, named

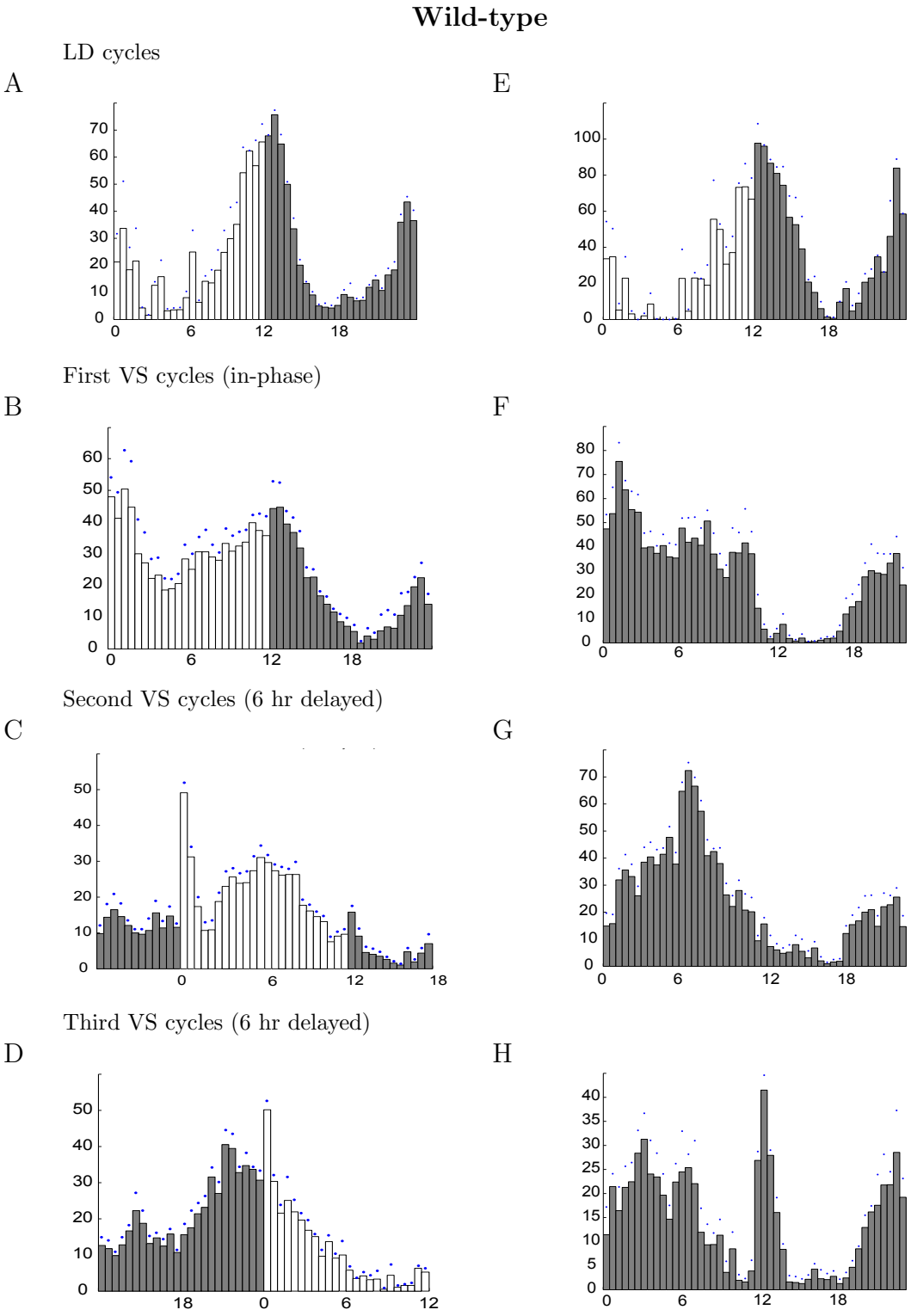

FIGURE 7.2: Daily average activity of wild-type flies subjected to 12:12 hr VS cycles and control. See Figure 7.3 legend for details.

Antennae ablated

LD cycles

A

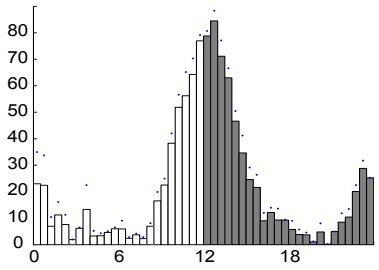

E

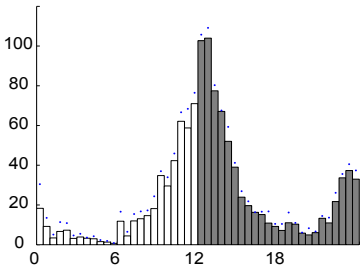

First VS cycles (in-phase)

B

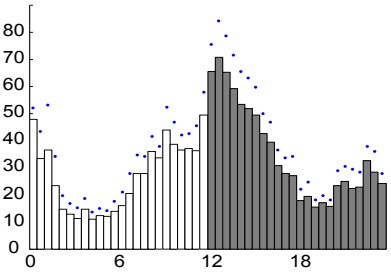

F

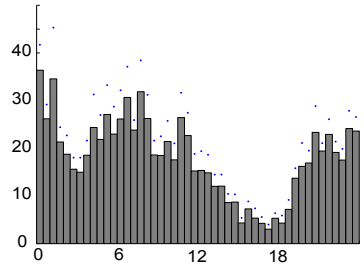

Second VS cycles (6 hr delayed)

C

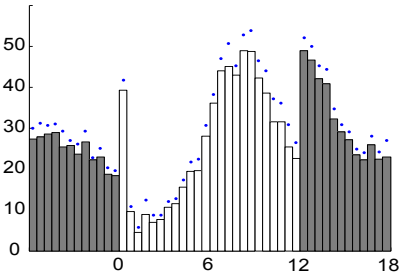

G

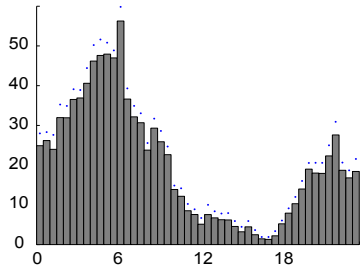

Third VS cycles (6 hr delayed)

D

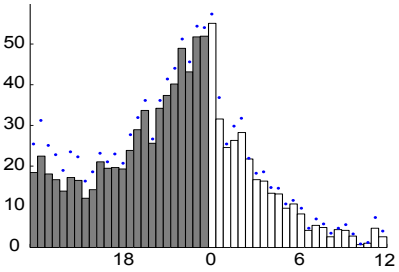

H

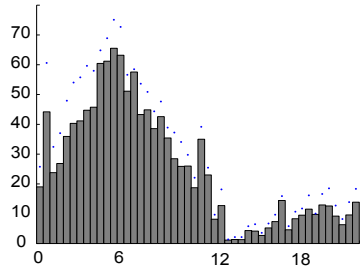

Johnston's organ (JO). Beside the auditory JO, the fly possesses a series of further ch organs which are mainly located in the animals' legs and thought to serve proprioceptive or vibratory functions. In order to assess the role of the fly's antennal ch organ for the observed behavioural changes, we removed the flies' antennae prior to subjecting them to the VS regime. As shown in Figure 7.3A–D, the pattern of activity of antennae-ablated flies is comparable to that of wt flies subjected to the same VS condition (Figure 7.2A–D). In contrast, the activity of antennae-ablated flies not subjected to VS is comparable to that of wild-type (with antennae) not subjected to VS (Figures 7.2E–H and 7.3E–H, respectively). This suggests that the pattern of locomotor activity during VS conditions is not mediated by JO only, and therefore it is not perceived by the flies as an acoustic signal only.

However, we observed two characteristics of the behaviour of antennae ablated flies. The increase of activity just after "vibration-on" is reduced compared to wild-type flies, suggesting that this "response" is mediated by the fly's ear (JO) rather than by the non-antennal ch organs. Secondly, antennae ablated flies are more active during the "silence" phase compared to wild-type flies. This phenomenon is more evident after the VS shift (Figure 7.3C,D). To support this observation, we quantified the relative activity of flies during the "silence" phase of flies subjected to the VS conditions, compared to the control flies kept in DD (free-running conditions). As shown in Figure 7.4, 65% of the total activity of antennae ablated

FIGURE 7.3 *(preceding page)*: Daily average activity of wt (Figure 7.2) and antennae-ablated flies (this Figure) subjected to 12:12 hr VS cycles. A, E) Flies were first entrained to 12:12 hr LD and then (B, F) subjected for 5 days to 12:12 hr "vibration-silence" cycles which were in phase with the previous LD cycles ("vibration" corresponding the previous day and "silence" corresponding to the previous night). C, G) The VS regime was 6 hr shifted (delayed) and kept for 7 days. D, H) An additional 6 hr delayed shift of VS regime was applied, resulting in an opposite phase compared to the initial LD cycles. White and grey bars represent activity during the "vibration" and "silence" phase, respectively. Number of individual tested is same as in Figure 7.1.

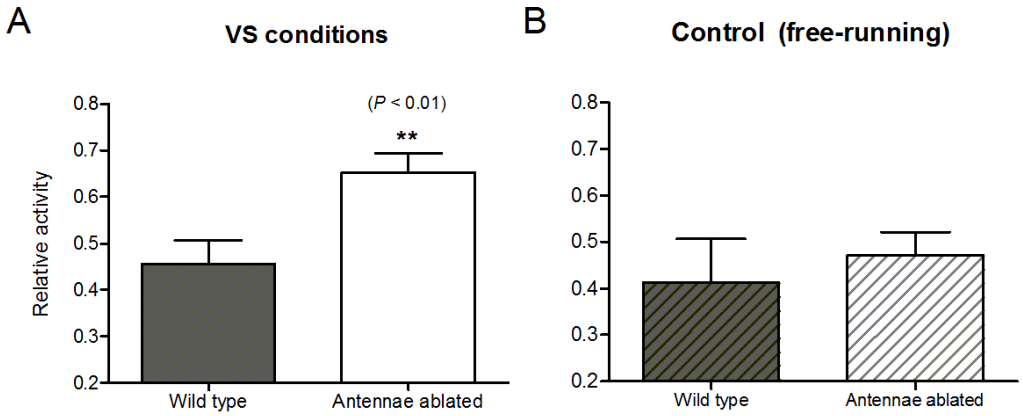

FIGURE 7.4: Relative locomotor activity of wild-type and antennae ablated flies during VS and free-running conditions. A) The plots represent activity during "silence" phase relative to the total activity after the second VS shift only. Ablated antennae flies are significant more active during the "quiet" phase compared to wild-type flies ($F_{(1,5)}$=45.4, $P<$ 0.01, Two-way Anova). B) Relative activity during the corresponding "silence" phase of free-running control flies. No difference between wild-type and antennae ablated flies was observed. Graphs generated by 6 (A) and 2 (B) independent experiments. Error bars indicate SEM.

flies occurs during the "silence" phase, compared to the 45% of wild-type flies with antennae, in a reproducible way between independent experiments ($F_{(1,5)}$=45.4, $P < 0.01$, Two-way Anova). Free-running control flies do not show differences of relative activity in the corresponding part of the day, indicating that the shift of activity is not caused by the ablation of antennae *per se*, but that the effect induced by the lack of antennae depends on the vibration stimulation. The reason for this intriguing phenomenon is still unclear.

To investigate whether the locomotor activity pattern was synchronized to the VS stimulus or the vibration was only masking the locomotor activity inducing a passive response, we analysed the phase of free-running activity after releasing the flies to constant conditions, compared to the phase of flies which have not been exposed to the mechanical stimulation. From the actograms depicted in Figure

7.1 it is already clear that there is a difference in phase between flies exposed to VS (upper part) and controls (lower plots). Nevertheless, we estimated the free-running phase of individual flies and determined the mean phase and intensity in order to quantify the visual impression of the actograms. The circular phase analysis (see Levine et al., 2002a,c and M&M for details) is depicted in Figure 7.5. Every dot in the plot represents the mean free-running peak phase time of single flies plotted in a circular graph with the mean phase of the group depicted by a vector starting from the center and pointing towards the time (expressed in Circadian Time, CT0 = vibration-on, CT12 = vibration-off, or equivalent time for the control). The phase of wild-type and antennae ablated flies (blue stars) is 2.0 and 1.4 hours, respectively. The phase difference compared to the respective controls, which have not been subjected to the vibration (red circle), is 9.8 and 8.5 hours, respectively (Figure 7.5). The mean phase difference between flies subjected to VS and control is strongly significant (M = 100 means $p < 0.001$). Interestingly, the dispersion of phase values (given by the strength of the vector in Figure 7.5) tends to be higher (and the vector smaller) for flies subjected to VS (blue asterisks) compared to control (red circles), both for wt and antennae ablated flies.

Therefore, the VS conditions change both the locomotor activity patters during the stimulation, and during the subsequent free-run. Taken together, these findings indicate that flies can be entrained by the "vibration-silence" cycles and they do not exhibit a passive (masking) response only. The ablation of the antennae does not prevent the flies from synchronizing to the VS stimulation, and thus the antennae are not necessary for this behaviour, as they are not required for the fly to entrain to TC. However, flies lacking antennae exhibit a different behaviour, and the difference can be measured and quantified. The vibration stimulus is per-

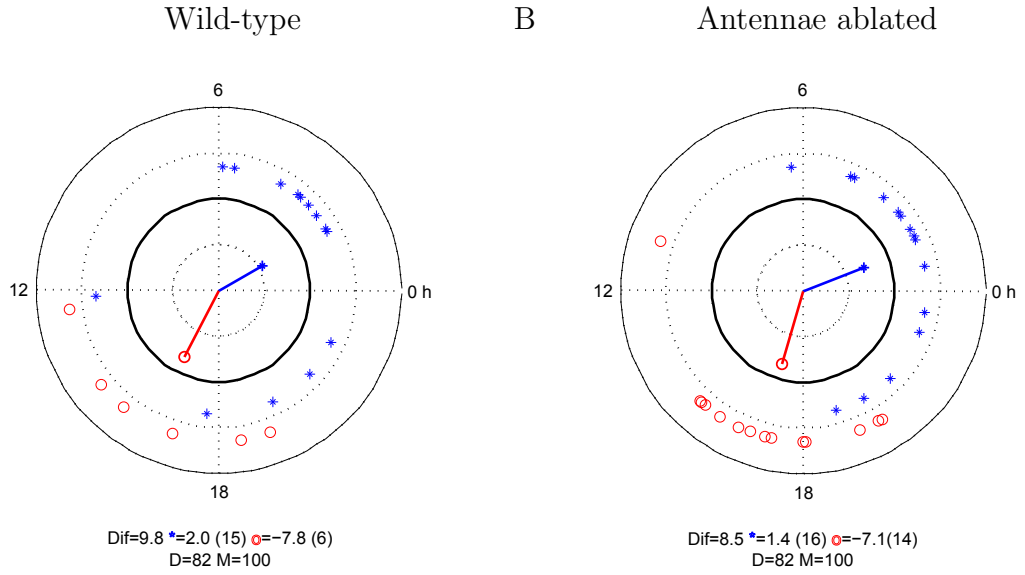

FIGURE 7.5: Circular phase analysis of activity peaks during free-run after VS regime of wt and antennae ablated flies compared to control. The plots represent the mean peak phase time values over the DD days of each individual flies after VS treatment (blue asterisks) and non-treated controls (red circles). The mean phase is represented as a vector with the mean direction indicating the time and the magnitude of the vector indicating the variability (dispersion) within the group. The internal black circumference represents 100% coherence between individuals of the same group. The closer the vector is to the black line, the more coherent the group is. The phase is calculated from the origin (0 h) and within the range $-12 \leqslant phase \leqslant 12$. The phase difference compared to control is 9.8 hours for wild-type (A) and 8.5 hours for flies with antennae ablated (B). M values $\geqslant 95$ indicate statistical significance of the mean phase difference between the two groups (Rayleigh's test). D values indicate dispersion within the group. In my data, the mean phase is statistically significant ($p < 0.001$), whereas the distribution of phase of the two groups cannot be statistically distinguished ($p > 0.5$). Number of individual is given in brackets, next to the phase values of each group.

ceived by the fly's mechanosensory organs, most likely of both type I and type II (i.e. external sensory plus chordotonal organs and multidendritic neurons, respectively, see Introduction). The fly's system is partially redundant, and this explain why removal of antennae does not abolish the response to the vibration stimulus. Therefore, antennae are not necessary for this behaviour, but they contribute to it.

Vibratory stimulus are perceived by fly's mechanosensory organs and predom-

inantly by ch organs. My preliminary work of entrainment of the circadian clock by mechanical stimulation gives additional support to the idea of ch organs being required for the entrainment of the clock. In this respect, we could speculate a model were temperature is perceived by ch organs in a similar way than ch organs perceive vibration. The mechanism underlying this process is still unknown and awaits an explanation.

However, much is still to be done. Analysis of clock mutants and ch organ mutants will reveal if there is a link between the circadian clock and the ch organs which mediate entrainment. Vibration-pulse experiments together with the analysis of locomotor behaviour in different VS regimes ("vibro-period") and application of different stimuli (in terms of frequency, duration and intensity) will provide additional details to the vibration stimulus as novel Zeitgeber.

7.4 Summary

- Isolated *Drosophila* brains are not able to synchronize to TC but need information from the periphery.
- Down-regulation of *nocte* in peripheral sensory (chordotonal) organs mimic the effect of the mutant.
- Mutant for ch organs exhibit defects of temperature entrainment similar to the *nocte* mutants.
- *nocte* is required for signalling the temperature information form the periphery to the brain in order to synchronize the central clock.
- *nocte* exhibits an "uncoordinated" phenotype when expose to 37°C for 90 min, in a similar way to *spam* mutants.

- A functional clock is not required in ch organs to execute temperature entrainment neither are required the ch organs in the antennae.
- Flies can entrain their behaviour to 12:12 hr vibration-silence (VS) cycles that stimulates mechanosensory organs. VS phase the locomotor activity during the stimulation and the subsequent free-running activity.
- The ablation of the antennae does not prevent the flies from synchronizing to the VS regime, suggesting that antennae are not required for entrainment.

Chapter 8

Discussion

8.1 The power of genetic screens: Isolation of novel components for the entrainment of the circadian clock

To address the question of how the circadian clock of *Drosophila melanogaster* can be synchronized to TC, we proceeded by searching for novel components which affect the ability of the fly to entrain. In this work, we made use of several different and complementary approaches all aimed on the isolation of new mutants and genes.

The first approach we used to isolate novel genetic variants was an EMS chemical mutagenesis. EMS mutagenesis reveals itself as an extremely powerful tool of investigation in *Drosophila*. Most of the components of the circadian clock in *Drosophila* have been isolated with EMS variants. In the 1970s the isolation of the *period* mutants by Konopka and Benzer (1971) opened the door to the genetic dissection of complex behaviours, such as those controlled by the circadian clock.

Only two decades after, the EMS-mutagenesis approach gave further important contributions. In 1998 four more components of the circadian clock were isolated: *doubletime* (Kloss et al., 1998; Price et al., 1998), *Clock* (Allada et al., 1998; Bae et al., 1998), *cycle* (Rutila et al., 1998) and *cryptochrome* (Stanewsky et al., 1998) all from EMS mutagenesis screens. The following year, *vrille* was discovered as component required for circadian rhythmicity (Blau and Young, 1999). More recently, the "temperature mutant" *nocte* has been isolated by our group in an EMS screen (Glaser and Stanewsky, 2005), indicating that the temperature entrainment pathway can also be genetically dissected.

My work follows the previous investigations of EMS-induced variants which affect circadian rhythmicity. In this work we screened 1637 chemical-induced mutant lines and the screen has been successful with the isolation of 3 novel variants which show defects in the synchronization of the circadian clock to temperature cycles (Section 3). The 3 mutants were named *2T-30*, *2T-38* and *2P-42*. They all map to chromosome *2* and have been isolated in a bioluminescence assay monitoring real-time expression of *period-luciferase* in isolated legs in a temperature entrainment regime. The two mutants *2T-30* and *2T-38* were isolated from a batch of lines originated in a single EMS treatment, which led the possibility that the two variants affected the same gene and they were potential clones. Complementation tests revealed that the two mutants complement each other (Figure 3.10), excluding the possibility that they map to the same gene.

EMS mutagenesis is unpredictable: it introduces random mutations, it is unbiased and can lead to unexpected results. The extensive use of random mutagenesis screens in the laboratories is supported by power of the fly genetics. The combination of a well-designed experimental read-out, and the feasibility of genetic manipulation, makes *Drosophila* a perfect tool for screening of variants showing

a desired phenotype among a population of random chemical-induced mutants. The downside of the approach is that you need to map the mutation by meiotic recombination, a process which is usually very complex and time consuming (as in my case).

To get around this problem, a complementary approach used a library of RNAi lines targeting specific genes. In *Drosophila* two main libraries are available to the public domain and they cover over 90% of the predicted protein-coding genes (http://www.shigen.nig.ac.jp/fly/nigfly and Dietzl et al., 2007). In this work, we performed two RNAi screens, one targeting 148 randomly-chosen RNAi lines, provided by François Rouyer (and originating from the NIG-FLY Stock Centre, Japan) and a second targeting specifically TRP channels encoding genes (RNAi lines provided by the Vienna Drosophila RNAi Center, VDRC). From the former, we isolated one line which showed impaired synchronization of *per-luc* expression in isolated legs, both during LD cycles and TC conditions. The RNAi line targets the forkhead transcription factor *fd3F*, whose function is still unknown. The latter, TRP-RNAi candidate approach screen, did not give any positive results (see below).

In the post-genomic era, more and more studies make use of RNAi libraries as efficient tools to silence gene expression where mutant alleles are not available (recently reviewed by Boutros and Ahringer, 2008 and Belles, 2010). The RNA interference combined with the UAS-GAL4 system (Brand and Perrimon, 1993) adds the possibility to silence target genes in specific tissues or specific developmental stages, by the use of appropriate *promoter-gal4* driver lines. This allows performing knock-down studies of genes, where mutants might otherwise be lethal, by restricting the effect to specific tissues or cells. There are also some disadvantages of the RNAi technique. The phenotype associated with a certain RNAi line

can be related to positional insertion of the RNAi construct itself. Also, RNAi is often inefficient, resulting in knock-down rather than loss-of-function of the targeted genes, often preventing the desired phenotype from arising. The UAS/GAL4 system can give a false negative result in situation where the expression pattern of the targeted gene is not known. Those last two disadvantages, could be the reasons why we did not obtain any phenotype from the *trp*-targeting RNAi screen approach.

As a complementary approach, we also analysed 12 mutant lines affecting 7 — out of the 13 — *trp* genes. Four mutants (affecting three genes), exhibited defects of entrainment of the circadian clock specifically to temperature cycles. Mutants of the *pyrexia*, *trpA1* and *trpM* genes fail to synchronize locomotor activity to TC, but they are normal under LD conditions. Although the respective RNAi lines did not produce a similar phenotype, the analysis of mutants supported our hypothesis that TRP channels may be involved in the temperature entrainment of the circadian clock.

Therefore, a non complete silencing of TRP channel encoding genes could have been the reason for the absence of phenotypes. Many TRP channels are formed by different subunits and some form heteromultimeric complexes, as reported by the Montell group for TRP and TRPL (Xu et al., 1997). If the double-stranded RNA targets only one subunit, this still might allow the non-silenced subunits to form a functional channel. The efficiency of the interference mechanism can be enhanced by overexpression of components of the RNAi machinery, specifically *Dicer2* (Dietzl et al., 2007). The efficiency increase is particularly evident for the RNAi lines generated by the VDRC compared to the ones from the NIG-FLY Stock Center (this work and François Rouyer, personal communication). In this work, we did not make use of additional *Dicer* to trigger the interference, mainly because of

the difficulty in generating flies carrying simultaneously *UAS-Dicer*, *tim-gal4* and *per-luc*, together with the RNAi construct. The presence of overexpressed DICER is also associated with an increase of false positive results due to off-target effects (Dietzl et al., 2007). When DICER is overexpressed, the process that produce small RNAs from double-stranded RNAs (dsRNAs) is enhanced and it raises the probability of mismatches and gaps in pairing of the small RNA to the targeted genes (Dietzl et al., 2007).

Another reason for the lack of *trp*-RNAi effect could be related to the specific driver line. We restricted our analysis on clock cells-driven RNAi, using a *tim-gal4* driver to knock-down TRP channels. This was based on our initial hypothesis that cells required for temperature entrainment of the circadian clock must indeed possess a clock. Our recent findings (Sehadova et al., 2009) suggest that this is not necessarily the case, and structures required for the temperature entrainment of the clock, namely the chordotonal organs, may not possess a clock. Therefore, the absence of the phenotype arising from *tim-gal4*-driven RNAi can be a results *in se*: this may speak towards the hypothesis that TRP channels are not required in clock cells, but their putative function as thermoreceptors, or at least as components required in the temperature entrainment pathway, is not executed in clock-possessing cells, as suggested by the temperature entrainment defects of "true" TRP channel mutants.

This work shows that genetic screens are a powerful and effective way to investigate and dissect complex biological processes, such as the entrainment of the circadian clock. EMS chemical-mutagenesis continues to be a good resource for the isolation of novel variants, even considering the drawback of the complicated and time consuming mapping process. The specific candidate approach can combine the huge availability of RNAi lines and genetic aberrations (mutants, *P*-element

insertions, deficiencies, etc.) also providing a complementary tool for the isolation of novel components required for specific mechanism.

8.2 *per-luc* expression in novel mutants reveals differences between light and temperature entrainment

The three EMS mutant lines exhibit a drastic reduction of *per-luc* expression in isolated legs, in term of overall expression levels and cycling amplitude specifically during TC conditions, while they exhibit normal *per-luc* expression in LD cycles (Figure 3.3 and 3.6). *per-luc* expression in the whole adult fly during TC entrainment is compromised too (Figure 3.4): *2T-30* and *2T-38* exhibit non-cycling *per* expression, indicating either malfunction at the central pacemaker resulting in complete arrhythmic *per* expression at the whole fly level, or dyssynchrony among central and peripheral clocks, generating an overall flat *per* expression due to different oscillating phases. Adult *per-luc* expression in the line *2P-42* is rhythmic and exhibits an opposite phase compared to controls, both in LL (Figure 3.4) and in DD and TC (Figure 3.8). This can be explained in two ways. *(a)* The mutation alters the endogenous phase of *per* expression and makes it cycling in opposite phase or *(b)* the bioluminescence expression is not circadianly regulated but instead it exhibits a mere reaction to temperature increase and decrease. Given that *per-luc* expression in DD and TC in isolated legs is normal, this suggests that peripheral oscillators are entrained to temperature (at least in DD) and that the overall *per* expression is out of phase between central and peripheral oscillators. Interestingly, a similar phenomenon occurs in $nocte^{1}$ and $norpA^{P41}$ temperature

entrainment mutant flies (Gentile C., Simoni A. and Stanewsky R., in preparation) in which *per-luc* expression entrain to TC in isolated legs but not in the whole fly. From my data it emerges also that a *trp* mutant exhibits the same phenotype: *per-luc* expression in *tim-gal4* driven *trpM*-RNAi is rhythmic in isolated legs, but aperiodic in the adult fly (Figure 5.8) during LL and TC. A similar phenomenon is observed in $trpA1^{ins}$ XLG-*luc* flies: *per-luc* expression in TC in isolated legs is only reduced in terms of amplitude, whereas in the whole fly it is barely cycling (Figure 5.9).

At the moment we still do not have an explanation for this intriguing phenomenon, but it appears a common feature of different mutants affecting the entrainment of *period* expression to temperature cycles. This may reflect a clear difference between the light versus the temperature entrainment pathway. The light entrainment signal acts directly on the central pacemaker, through the light-dependent action of CRY in the clock neurons (Stanewsky et al., 1998; Emery et al., 1998, 2000). As recently reported by our group (Sehadova et al., 2009), it emerges that peripheral structures are instead required to entrain the fly to TC and that the temperature signal is transmitted from the periphery to the brain. The ability of some mutant tissues (legs), to entrain, while the whole mutant fly cannot, may indicate a "hierarchy of entrainment", in which the mutant disrupts part of the pathway required for the entrainment of the whole organisms, while specific isolated components can still be synchronized to temperature.

Interestingly, we observed that *per-luc* expression of *trpM* mutants is not affected in LL and TC, while *tim-gal4*-driven RNAi down-regulation of *trpM* abolishes rhythmic *per-luc* expression in the adult fly (but not in isolated legs, Figure 5.9 and 5.8). This seems to suggest that the RNAi induces a stronger phenotype than the mutant, which is generated by a *P*-element inserted to the coding region

of the gene. However, at the behavioural level, the situation is opposite: *trpM*-RNAi does not induce any effect while the *P*-element does. Recently, TRPM has been indicated as required for the intake of Mg^{2+} from the hemolymph to the Malpighian tubules (Hofmann et al., 2010). In this work, the authors generated two mutant alleles of the *trpM* gene, named $trpm^1$ and $trpm^2$. $trpm^1$ was generated by imprecise excision of the *P*-element *P[EY01618]* that removed three exons (C9–C11). $trpm^2$ was generated by insertion of the w^+ gene in place of the exons C2–C4 by ends-out homologous recombination (Hofmann et al., 2010). Both the alleles generated are pupal lethal (Hofmann et al., 2010). This strongly suggests that the mutant we used in our study (the *P*-element inserted in the 3' splice site of exon C11) is a hypomorphic allele and therefore may explain why the mutant line does not induce mutant phenotype in certain assays (bioluminescence) whereas it does in others (behaviour).

As mentioned in Chapter 3.2, for unknown reasons, the BG-*luc* control did not display consistent rhythmicity between experiments. The 3 mutants have been originated from EMS-fed BG-*luc* flies, therefore they should share the same genetic background. However, as depicted in the crossing scheme in Figure 3.2, the lines we assayed (F_3 generation) have been genetically rearranged (via recombination) on chromosome *1* and *3* with the balancer line $y\ w; \frac{Bl}{CyO}; \frac{+}{+}$ (or $y\ w; \frac{+}{+}; \frac{H}{TM3}$, in case of potential EMS-induced mutants on chromosome *3*). Therefore, although the mutant lines have been originated from BG-*luc*, they do not share the same genetic background (independently of the additional EMS-induced mutations). Although this does not explain why BG-*luc* flies did not exhibit consistent rhythmicity, it may explain why the majority of EMS-fed lines — all minus the 3 isolated as mutants — showed clear rhythmicity and could therefore be used as internal controls for the screen (see for instance line *2X-8* in Table 3.2).

8.3 Behaviour analysis of the novel temperature mutants

8.3.1 Locomotor behaviour in LL and TC

Behavioural analysis of the seven novel mutants shows interesting differences between the lines. Initially, locomotor behaviour has been analysed for the ability to re-entrain to LL and TC after a 12 hour shift compared to the previous LD entrainment (except for *tim-gal*-driven *fd3F*-RNAi, see below). Wild-type control flies resynchronize their rest-activity pattern to LL and TC after 2 transient days (Figure 3.11). The mutants exhibit an abnormal behaviour pattern during LL and TC. They show a drastic increase of activity (unlike Canton S) immediately after temperature goes up (*2T-30*, *2T-38*, *2P-42*, $trpA1^{ins}$) or temperature goes down (*trpM* and *pyx*) and the peak of activity that usually anticipate the transition from warm to cold, is absent (*2T-30* and $trpA1^{ins}$) or only barely visible (*2T-38*, *2P-42*, *pyx* and *trpM*). The activity pattern during LD conditions is normal except for the 3 EMS mutants and *trpM*, which are lacking the morning peak that normally anticipates the transition from dark to light. This could be related to the genetic background, at least for the EMS mutants, since BG-*luc* flies also lack the anticipatory activity before the light goes on, see Figure 5A in Glaser and Stanewsky (2005).

These data show that the isolated mutants exhibit clear defects in adjusting their locomotor behaviour during LL and temperature cycles.

8.3.2 Temperature entrainment differences between LL and DD

The analysis of novel mutants involved in temperature entrainment had initially been performed in constant light and temperature cycles. The reasons why constant light was chosen versus constant darkness were based on the work from Tomioka et al. (1998) and Yoshii et al. (2002), in which they showed that temperature cycles are a stronger Zeitgeber in LL compared to DD, in terms of the ability to entrain either wild-type flies to different thermoperiods, or to synchronize long and short *period* variants to TC. A possible explanation could be the residual (dominant) effect of the previous LD entrainment during DD and TC. Temperature, being a weaker Zeitgeber than light (Pittendrigh et al., 1958; Wheeler et al., 1993), may not be strong enough to conflict the free-running rhythm set by the light-dark cycle.

However, the use of constant light (rather than DD) during temperature entrainment prevents the possibility of monitoring free-running rhythms after releasing the flies to constant conditions (in DD and constant temperature). In order to determine proper entrainment (i.e. the peak of activity aligned with that observed during entrainment) and to investigate any direct effects of light itself on the ability to synchronize to TC, we also compared to the locomotor activity of the novel "temperature mutants" in DD and 12:12 hr 25:16°C TC conditions.

Wild-type locomotor activity in DD and TC exhibits a similar pattern compared to the one in constant light, exhibiting a single unimodal peak of activity (versus the bimodal pattern of activity in LD). However, the phase of activity is advanced, and flies are mainly active at the beginning of the warm day (displaying the main activity peak at ZT3.8, Table 3.3). Previous work studying temperature entrainment in DD has shown that the activity pattern is bimodal, and the main

peak of activity occurs at the end of the warm phase (Tomioka et al., 1998; Yoshii et al., 2002; Busza et al., 2007). These results were based on experiments performed in 30:25℃ and 29:20℃ temperature cycles, respectively, and the different temperature intervals may explain the different patterns of activity in DD. A recent work from Yoshii et al. (2009a) using conditions comparable to mine (26:16℃) also showed a single peak of activity during the first half of the thermophase. In addition, different constant temperatures affect the shape of free-running activity (Majercak et al., 1999), and a higher temperature (29℃) induces the activity to persist with a bimodal pattern for several days in DD, whereas cold temperature (18℃) induce an unimodal pattern of free-run activity. This may be the case also when high-interval (29:20℃ or 30:25℃) temperature cycles are applied, explaining the unimodal activity of my observation at the "low" temperature interval of 25:16℃.

In many cases, it was difficult to judge whether the locomotor activity during DD and TC was entrained, or if the flies were only reacting to the temperature changes, given that the main activity peak partially overlaps with the startle response induced by the increase of temperature. In these situations we need to consider both the activity during the transient days (if present) and the free-running activity once the flies have been released to constant conditions. Considering these difficulties, a picture emerges in which some mutants are able to entrain to DD and 25:16℃ TC (*2T-38*, *2P-42*, *trpM*, pyx^{2} and pyx^{3}, Figure 3.15 and 5.4) in term of *(a)* exhibiting clear transients until resynchronization from LD to TC conditions (comparable to controls) and *(b)* synchronized free-running activity in constant conditions, following the previous TC. Other lines (*2T-30* and $TrpA1^{ins}$) exhibit a mutant phenotype: no transient days but a burst of activity in response to the temperature increase at the first day of TC, and free-running activity is not

synchronized to the previous TC regime (Figure 3.15 and 5.4).

8.3.3 Entrainment to different temperature intervals

The temperature intervals chosen for this study were based on an agreement between several research groups collaborating in an European Integrated Project focused on the entrainment of the *Drosophila* circadian clock (EUCLOCK). The 25:16℃ temperature cycles correspond to average recordings taken in natural conditions at the end of September to the beginning of October (to which correspond 12:12 hr LD cycles), in northern Italy (Yoshii et al., 2009a).

Our idea was to reveal whether entrainment of the mutants at some specific temperature ranges could give us hint about the function of the genes affected in our novel mutants, thus we investigated locomotor activity of flies exposed to different temperature intervals of 29:25℃, 25:20℃ and 20:16℃.

The fly's behaviour adapts to the seasonal variations of photoperiod and temperature, concentrating the activity to the milder part of the day in short and cold days (spring and fall) and shifting the activity towards dawn and dusk in long and warm summer days, perhaps to avoid dessication (Majercak et al., 1999; Collins et al., 2004; Stoleru et al., 2007). We observed this phenomenon after monitoring locomotor activity of wild-type flies in different temperature intervals. Interestingly, the effect of temperature is again more pronounced in LL than in DD (Figures 5.2 and 5.6, respectively), presumably for the reasons described above of "better entrainment" in LL versus DD (Tomioka et al., 1998; Yoshii et al., 2002; Glaser and Stanewsky, 2007). The effect of the seasonal adaptation of the behaviour to different temperature intervals is less pronounced in all novel mutants compared to wild-type flies both in LL and in DD (Figures 3.13, 5.2 and 5.6).

Analysis of behaviour at different temperature intervals showed that some mu-

tant lines can synchronize their locomotor activity in certain ranges, but not in others. Interestingly, line *2P-42* and *2T-38*, for instance, entrain to 25:20℃ and 20:16℃, but not in the 25:16℃ regime. This indicates that the mutant lines, surprisingly, fail to synchronize to larger temperature intervals (25:16℃), while they do at small intervals (25:20℃), suggesting some kind of "entrainment repression" induced by certain temperature ranges. This is also suggested by results obtained with the *trp* mutants (summarized in Table 5.2). *pyx* and *trpM* mutants fail to synchronize their locomotor activity to 20:16℃ TC but they entrain to 25:20℃ and 29:25℃ TC, suggesting indeed that the cold temperature range somehow "represses" entrainment in these TRP channel mutants, whereas the high temperature interval effects more the EMS mutants. $TrpA1^{ins}$ exhibit the the most severe defects in temperature entrainment compared to the other mutant lines we assayed. Locomotor activity in DD and different temperature intervals confirms the idea that some genes are important for certain temperature ranges (29:25℃), whereas other genes are important in different intervals (e.g. *trpM* and *pyx* mutants in 20:16℃), although the effect in DD is less pronounced than in LL. This is even more surprising given that *pyx* and *trpA1* have been isolated as mutants failing to avoid a warm noxious stimulus (Lee et al., 2005; Rosenzweig et al., 2005). This suggests that thermal preference and temperature entrainment, although they may be mediated by the same players — TRP channels — indeed involve different mechanisms (see below). The existence of several thermal TRP channels might be explained by the requirement of the same thermal sensor to play different roles at opposite sides of temperature spectrum. For instance, PYX and TRPA1 may be required either to respond to a warm noxious stimulus (above 40℃) and also to respond to cold TC (below 20℃) in terms of circadian entrainment. This idea is supported by experiments conducted in larvae by the Montell

group, where they propose that TRPA1, in addition to act as thermosensor for noxious temperature, could also function indirectly for temperature sensation in the comfortable range (Kwon et al., 2008).

Although it seems that TRP channels are involved in the entrainment of the clock to temperature cycles, it is still unknown how the temperature stimulus is processed in a circadian manner. The temperature stimulus as a noxious response is mediated in a very small time-scale, in the order of seconds, or milliseconds. This makes sense in the way that the fly must respond immediately to the stimulus to avoid life threatening situations. For a stimulus to be circadianly significant must act in the order of hours and must sense not an absolute temperature value but temperature oscillations (independently of the absolute values). The circadian clock is much less sensitive to temperature than to light, perhaps because it must resist dramatic short-term perturbations of temperature, due to irregular environmental conditions, as proposed by Currie et al. (2009).

In this context, TRP channels mediate entrainment not directly responding to temperature, but rather function through second messenger pathway, or signal amplification mechanism, maybe mediated by a tonic stimulus response of the channels, rather than phasic (transient) stimulus. Recently, it has been shown that TRPA1 controls thermotaxis behaviour acting downstream of a PLC-dependent signalling cascade (Kwon et al., 2008), similar to the PLC-coupled pathway resulting in TRP and TRPL opening in the visual system (Niemeyer et al., 1996). It is already known that PLC is also involved in temperature entrainment (Glaser and Stanewsky, 2005; Sehadova et al., 2009), although its role in the process is still unclear. It is possible that *norpA* mediates a signal cascade associated with TRP channel opening in the temperature entrainment pathway. However, this also implies that the receptor is still elusive. If we compare to the visual transduction

cascade, the "opsin" awaits to be found.

Further studies, and a deeper investigation of the available mutants — also combining TRP mutants with *norpA*, for instance — will help to better understand the role of these proteins in the temperature entrainment of the clock. At the moment of writing, a member of our group is proceeding on mapping the mutations and the isolation of the genes affected by the EMS mutants will hopefully clarify some aspect of the entrainment mechanism. The attempt to map the *2T-30* mutant by meiotic recombination suggests that the mutation lays on the left arm of chromosome *2*.

Also, more analysis in different light and temperature conditions, monitoring the fly's activity in different temperature intervals, are needed. In particular, analyses of the free-running phase of activity after TC at different intervals, in order to discriminate proper synchronization from temperature-driven effect, are necessary. My preliminary work in this direction, discussed in this thesis, shows the benefits of the approach to dissect in more detail the ability of specific mutants to synchronize the locomotor activity in different conditions. It will also be extremely important to monitor real-time *per-luc* expression (or clock protein accumulation and expression) during, and after, temperature entrainment at different intervals, to correlate — and complement — my behavioural results.

8.3.4 2T-30 is a locomotor output mutant

Analysis of free-running locomotor behaviour of the isolated mutants revealed that *2T-30* flies are largely arrhythmic in constant conditions (Table 3.4). To address whether the mutants affect the central clock mechanism, we investigated the eclosion rhythm. Cultures of *2T-30* exhibit a strong rhythm with a period of 23.8 hours when they are released to DD after LD entrainment (Figure 3.19), indi-

cating that the central pacemaker is not compromised. Given that the rhythmic locomotor behaviour is strongly jeopardized, this suggests that the *2T-30* mutant affects a gene related to the locomotor output, in addition to the temperature input pathway.

8.4 Regulation of the eclosion circadian clock

8.4.1 Adult "temperature mutants" do not affect eclosion

In the present thesis we have investigated whether the novel temperature mutants we isolated, in addition to the 2 known temperature mutants, $nocte^{1}$ and $norpA^{P41}$, compromise the ability of the circadian clock to synchronize their eclosion activity to temperature cycles, as much as they do for the adult locomotor activity.

The timing of adult emergence is controlled by the circadian clock and can be synchronized by temperature cycles (Zimmerman et al., 1968; Newby and Jackson, 1993). Wild-type cultures raised in LD, resynchronize the eclosion activity to LL and TC after 2 transient days. The eclosion window, or gate, after they establish a stable phase, occurs at the end of the cold phase, just before the transition to warm (Figure 6.1).

The phase of eclosion rhythm during TC occurs few hours earlier than during LD cycles, in which flies eclose in a broad peak mainly during the first half of the light phase (Qiu and Hardin, 1996). This correlates well with *per-luc* recordings and PER accumulation in LL and TC conditions (Section 3.2 and 4.3), in which we showed that during TC, *per* expression and PER accumulation is 2–3 hours advanced compared to LD conditions. The advance eclosion activity in TC, compared to LD, fits well also with an earlier phase of locomotor activity in TC compared to LD.

We observed also a second peak of eclosion occurring immediately after the temperature rise, likely induced by the steep increase of temperature, promoting the flies developmentally mature enough that missed the eclosion gate, to hatch (also shown by Newby and Jackson, 1993). During LD conditions, the light-on to light-off transition is the moment in which the clock measures the developmental state in order to trigger the eclosion in the next available eclosion gate (Qiu and Hardin, 1996). It is not known at which point during the day this state is determined during temperature entrainment.

The ability to re-entrain to a 6hr temperature shift (Figure 6.2) confirms that TC are indeed a strong Zeitgeber perceived by the clock. However, there is a clear difference between light-dark entrainment and temperature entrainment. The eclosion profile of per^{01} cultures suggests that temperature *per se* induces a clock-independent eclosion event occurring after change of conditions. During temperature cycles, per^{01} cultures exhibit a 12-hr eclosion rhythm, and flies emerge after any temperature transitions, suggesting clock-independent temperature-driven eclosion events (Figure 6.2 and 6.3). During LD conditions, per^{01} eclosion is arrhythmic and the flies emerge throughout the light and dark phase (Konopka and Benzer, 1971; Qiu and Hardin, 1996). Unlike for the locomotor behaviour of per^{01} mutant flies, which shows masking effects, the eclosion rhythm cannot be completely light-driven (Qiu and Hardin, 1996), but it can exhibit a light-induced (light-on) response if a light pulse is applied only after the normal gate is opened (McNabb and Truman, 2008). The ability of temperature changes to drive the eclosion in per^{01} flies, suggests that the second eclosion peak occurring after temperature step-up, in wild-type cultures, is temperature driven (masking), and not clock-controlled.

In the current study we analysed the eclosion activity of seven novel (*2T-30*,

2T-38, *2P-42*, pyx^2, pyx^3, *trpM* and *fd3F*) and 2 already described ($nocte^1$ and $norpA^{P41}$) "temperature mutants" in LL and TC conditions. To our surprise, all the cultures analysed exhibit a normal eclosion activity in TC conditions, synchronizing the emergence to TC after 2 transient days, in a way comparable to wild-type cultures. The only exception is *fd3F*, which exhibits an altered phase of the eclosion rhythm, and will be therefore discussed separately (see below). To our knowledge, this is the first time that adult "temperature mutants" have been assayed in eclosion. My data suggest that the genes which affect temperature entrainment in the adult do not play the same function in the synchronization of the eclosion-regulating clock to TC.

8.4.2 Role of the DN_2 neurons in the regulation of eclosion

The neuronal architecture which eventually triggers the eclosion event in a circadian manner is not fully understood. Even less clear are the differences between light-dark and temperature entrainment. However, recent work from Picot et al. (2009) shed some light on the role of the DN_2 neurons in the larval brain in temperature entrainment. The authors propose that the light-blind CRY-negative DN_2s (Klarsfeld et al., 2004) are necessary (and sufficient) to entrain the larval brain to TC. In LD, the PDF-positive LNs synchronize PER oscillations both through the presence of CRY and through the visual system and they synchronize PER expression in the DN_2s via the neuropeptide PDF. During TC, the DN_2s are directly entrained by temperature and they synchronize the LNs through a PDF-independent pathway. Previous studies in LD have shown that PER cycles in the DN_2s with an opposite phase compared to all other groups of larval neurons (Kaneko et al., 1997; Klarsfeld et al., 2004) and that forced expression of CRY can reverse their internal phase (Klarsfeld et al., 2004), in a PDF-independent manner

(Picot et al., 2009).

My data showed that temperature entrainment applied during development can modulate both the free-running eclosion period and phase. A single light-dark cycle applied as early as at the first larval stage can phase the circadian clock and drive a rhythmic locomotor behaviour (Sehgal et al., 1992; Kaneko et al., 2000; Malpel et al., 2004). Larval-only TC entrainment generates an adult locomotor activity which is in opposite phase compared to larval-only LD entrainment (Picot et al., 2009). My data complement these studies, showing that eclosion activity also exhibits an opposite phase after larval-only TC entrainment (Figure 6.6) compared to LD entrainment. Although the LNs and the prothoracic gland (PG) are required to generate eclosion rhythms (Kaneko et al., 1997; Blanchardon et al., 2001; Myers et al., 2003), my data showed that PDF is not required to generate rhythmic eclosion events both after LD or TC entrainment. We therefore propose that temperature entrainment is mediated by the DN_2s — in agreement with Picot et al.'s results (2009) — and that it is PDF independent. Previous studies have shown that the removal of the larval visual system can change the phase of adult locomotor activity (Malpel et al., 2004). The authors speculated that the DN_2s are responsible to drive the opposite phase of adult activity, given their opposite phase of PER cycling. My results strongly support this idea, suggesting that temperature entrainment could supplement the lack of the information through the visual system and phase the clock to gate a rhythmic eclosion. However, in this respect it is not clear how the DN_2s can be synchronized. Mealey-Ferrara et al. (2003) proposed the existence of 3 pathways for the entrainment of the eclosion circadian clock. The 1st pathway involves the larval visual system (opsin- and *norpA*-mediated); the 2nd requires CRY as photoreceptor and a 3rd, mysterious pathway, suggested by the light-entrainability of the eclosion clock in mutants

lacking the first 2 pathways (Mealey-Ferrara et al., 2003). This mysterious 3rd pathway could mediate the entrainment of the eclosion through the DN_2s, in a situation when the light-pathway is not effective, such as in TC entrainment, consistent with my results.

Very interestingly, we observed that the free-running eclosion period of wild-type cultures entrained in LL and TC is 21 hours (Figure 6.4, 6.7 and 6.9). This is the case for temperature entrainment restricted to both larval-only and pupal-only stages, as well as for TC applied during all developmental time. Based on the hypothesis that during temperature entrainment the DN_2s are the neuron that set phase and period of eclosion, we propose that the free-running period of the DN_2s is shorter than 24 hours. This is strongly supported by the same short eclosion period exhibited by Pdf^{01} mutants and from observation in adult flies: Pdf^{01} mutants are mainly arrhythmic in DD, but the remaining rhythmic flies exhibit a short, 21-hour periodicity (Renn et al., 1999).

The phase of PER oscillations in the adult DN_2s is the same in all clock neurons during LD conditions (Kaneko et al., 1997; Blanchardon et al., 2001). Thus, the adult DN_2s — which derive from the larval DN_2s — change their internal phase of PER cycling during metamorphosis (Kaneko et al., 1997). This is likely due to the synchronization with the LN_vs, which are the only group of neurons which express PER throughout the metamorphosis (Kaneko et al., 1997; Helfrich-Förster et al., 2007) and are also responsible for the developmental time-memory (Kaneko et al., 2000).

In the future, a more detailed analysis of the developmental time at which temperature entrainment can elicit a short free-running period of eclosion is needed. Also, analysis of eclosion period and phase of culture which overexpress CRY in specific groups of larval clock neurons will be performed, together with the modu-

lation of the internal speed of the clock in specific cells, in order to address which are the component that drive the short free-running period.

8.4.3 *fd3F* alters the phase of eclosion

Among the seven novel "temperature mutants" isolated in this work, one exhibited an eclosion phenotype in LL and temperature entrainment. We showed that *tim-gal4*-driven down-regulation of the transcription factor FD3F resulted in an abnormal phase of eclosion activity: flies emerged preferentially during the warm phase and without any defined peak (Figure 4.6). The pattern of emergence is unequivocally different from any other cultures we assayed, including the clock mutant per^{01} (Figure 6.2). The rhythmic free-running eclosion activity excludes the involvement of *fd3F* in the central clock mechanism, but rather suggests a role in the regulation of eclosion gating.

Further investigations are necessary to clarify the effective role of the FD3F transcription factor in this context. Many indications suggests that forkhead transcription factors are expressed during development (see Section 4.5). Lethality in different developmental stages of the *fd3F*-RNAi driven by *tim-gal4*, *repo-gal4* and *nocte-gal4* suggests that FD3F is indeed required development of the fly. The spatial and temporal expression profile of *fd3F* will help to understand which roles it plays. Published data and this work suggest a direct involvement for FD3F in the chordotonal organs (Lee and Frasch, 2004 and below). So far there are no known connections between the chordotonal organs and the regulation of eclosion. Our data showed that ch organs are required for the adult fly to entrain to temperature (see Sehadova et al., 2009 and below) and *fd3F* could be one component that mediates the process.

8.5 Chordotonal organs and temperature entrainment

Accumulating evidence indicates the involvement of chordotonal (ch) organs in the synchronization of the circadian clock of *Drosophila* to temperature cycles. The gene *nocte* plays a crucial role in the temperature entrainment. EMS-induced *nocte*^{1} mutant flies fail to synchronize *per-luc* expression and locomotor activity specifically to temperature cycles as they behave normally in LD conditions (Glaser and Stanewsky, 2005, 2007; Sehadova et al., 2009). Down-regulation of *nocte* with the *F-gal4* driver reproduces the phenotype of the mutant. *F-gal4* (originated by fusion of the *nanchung* promoter to *gal4* sequences) was previously reported to be expressed specifically in ch organs (Kim et al., 2003) but its expression was found also in some external sensory organs and few neurons in the brain (Sehadova et al., 2009). Analysis of ch organs mutants, such as *tilB*, *smetana* and *eyes shut*, confirmed the role of ch organs in temperature entrainment (Sehadova et al., 2009). My work contributed to these findings including new and unpublished data, which support the idea that ch organs are required for temperature entrainment.

The transcription factor FD3F seems to be expressed exclusively in ch organs, at least in the embryo (Lee and Frasch, 2004). We do not have any data concerning the spatial expression profile in the adult. However, *F-gal4*-driven down-regulation of *fd3F* disrupts temperature synchronization of locomotor activity (Figure 4.4) in a similar way as *nocte*-RNAi. This clearly indicates a role for *fd3F* in the adult ch organs too.

Rouyer et al. (1997) described that the *circadian regulated gene 1* (*crg-1*) is rhythmically expressed in phase with the *per* gene and expressed in the same pat-

tern in fly heads. Recently, it turned out that *crg-1* is a chimeric gene, originated by a duplication event that occurred only in *Drosophila melanogaster* (and not in evolutionary related species) which led to the fusion of the 5'-region of *fd3F* and the 3'-UTR region of *Toulsed-like kinase* (*Tlk*) (Hogan and Bettencourt, 2009 and Figure 4.10). Although the *crg-1* cDNA has been detected by PCR (Hogan and Bettencourt, 2009), CRG-1 protein has never been detected (F. Rouyer, personal communication).

It is possible that the circadian regulation of *crg-1* has been gained after the duplication event, occurred probably less than 2.3 mya (Hogan and Bettencourt, 2009). However, it is also possible that the *fd3F* gene is circadianly regulated too, because the regulation region is shared between the two genes. The *fd3F*-RNAi construct does not target *crg-1*, suggesting that the phenotypes we observed in temperature entrainment are specific to FD3F and not to CRG-1. Given the transcription factor nature of the gene, it is very tempting to look for the possible circadian regulation of FD3F itself, and for possible regulation of clock genes, such as *period* and *timeless* by *fd3F*. Although the presence of a functional clock in chordotonal organ neurons (as defined by *F-gal4*) is not required for temperature entrainment (Sehadova et al., 2009), this does not exclude the possibility that *fd3F* is circadianly regulated. In fact, the assumption of ch organs non-clock requirement for temperature entrainment is based on experiments in which the clock was stopped with the *F-gal4* driver, which is expressed in the ch organs neurons (Kim et al., 2003; Sehadova et al., 2009). Neuronal-specific (*elav-gal4*-driven) knock-out of *fd3F* does not give any effects in temperature entrainment (Figure 4.4), suggesting that FD3F could play a role in non-neuronal cells in the chordotonal organs. This is also indicated by pupal lethality induced by *repo-gal4* and *nocte-gal4*, but not by *elav-gal4* driven *fd3F* knock down. *nocte* expression

in the scolopidium is broader than *F-gal4* (Sehadova et al., 2009) although at the moment it is not clear exactly in which additional cells *nocte* is expressed. This could suggest a role for FD3F in glia cells. PER is expressed in glia cells (Zerr et al., 1990; Ewer et al., 1992; Kaneko and Hall, 2000) and analysis of per^{+}/per^{01} mosaics showed that rhythmic behaviour can be observed when PER expression is restricted to glia cells (Ewer et al., 1992). Moreover, a role for the glia cells in circadian rhythms has been proposed (Suh and Jackson, 2007). The glia cells surrounding the ch neurons might be a good location for the presence of a peripheral clock, where FD3F could play its role as a transcription factor. Alternatively, the *F-gal4* is perhaps a "stronger" driver than *elav-gal4*, explaining the non-effect induced with *elav-gal4*. More works need to be done to identify which structures require FD3F and at what level the transcription factor executes its role. *per*, *tim* and *nocte* will be tested as possible targets and, in parallel, *fd3F* expression will be tested in clock and *nocte* mutants.

The structure of the chordotonal organs is determined by the expression of many different genes and proteins which allow the organ to develop and execute the many functions played in *Drosophila*. The implications of ch organs go beyond that of stretch receptor function. In the limb joints ch organs contribute to nociception, whereas the biggest ch organ located in the antennae (named Johnston's organ, JO) mediates hearing (reviewed by Kernan, 2007) and geotaxis (Sun et al., 2009). Several TRP channels belonging to the 3 superfamilies are expressed in ch organs, implicated in transducing touch, sounds and mechanical pain: *nompC* (TRPN), *nanchung*, *incative* (TRPV), and *painless* (TRPA). It has recently been shown that *pyrexia* (TRPA) is involved in regulation of negative geotaxis mediated by the JO and that it is expressed in the cap (or attachment) cells which connect the scolopidium to the cuticle (Sun et al., 2009). *pyx* mutants do not affect

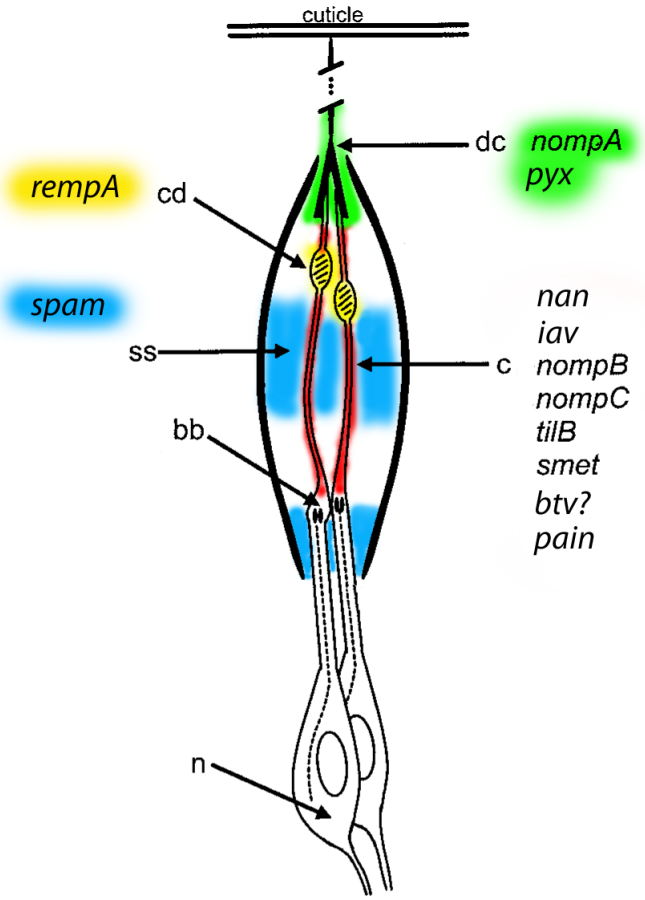

FIGURE 8.1: Drawing of the elements of a scolopidium and the putative location of the genes expressed. Two neurons (n) are present which culminate in a basal body (bb). From the bb, the axoneme of the long cilium (c, red) is assembled, including the ciliary dilation (cd, yellow). The dendritic cap (dc, green) connects the scolopale to the cuticle. The location of the genes expressed in the scolopidium is indicated with colours. *Spam/eye shut* is expressed in the scolopale space (ss, blue) and in the basal region surrounding the basal body. *nompA* is expressed in the dendritic cap and *pyx* in the dendritic cells that surround it (green). Many genes are expressed in the ch neurons and in the cilium, including *nompB*, *nompC*, *smetana* (*smet*) and the TRP channels *nan*, *pain* and *iav*. *Beethoven* (*btv*) is also probably expressed in the cilium. Modified from Caldwell and Eberl (2002).

hearing (Sun et al., 2009), whereas it mediates warm avoidance (Lee et al., 2005) and temperature entrainment (this work). The fly's antennae are also required for thermotaxis behaviour, but this function is executed by the third antennal segment (Sayeed and Benzer, 1996) whereas the JO is located in the second segment. The fly antennae seem not to be required for synchronizing the circadian clock to TC, since its physical removal does not prevent the fly to entrain to temperature cycles (Glaser and Stanewsky, 2005; Sehadova et al., 2009). However, the expression of TRP channels in the ch organs which have been implicated in temperature entrainment is unlikely to be a coincidence. Interestingly, as shown in the Figure 8.1, PYX expression is detected in the proximity of the dendritic cap (the apical part of the scolopale), which is the structure that manifests a morphological defect in *nocte* mutants (Sehadova et al., 2009). Moreover, PYX is not expressed in the chordotonal neurons, in contrast with the other ch TRP channels (Sun et al., 2009), suggesting again that the non-neuronal cells of the ch organs may indeed play a role in the temperature entrainment process. Although *nocte* probably plays its role in the ch organ neurons — based on the observation that *F-gal4* driven *nocte* knock down induces the phenotype —, it may also effect the development of non-neuronal structures, which surround the ch neuron.

We also identify TRPA1 as component required for temperature entrainment. Both PYX and TRPA1 are required for thermotaxis and warm-avoidance (Lee et al., 2005; Rosenzweig et al., 2005, 2008; Hamada et al., 2008). Interestingly, cool and warm avoidance are distinct mechanisms, and involve different TRP channels: cold avoidance is mediated by TRP and TRPL, and warm avoidance by TRPA1, PYX and PAIN, indicating that *Drosophila* use different TRPs to respond to different discrete ranges of temperature (Rosenzweig et al., 2008). However, in contrast to PYX and TRPA1, PAIN is not required for thermotaxis (Rosenzweig

et al., 2008) nor temperature entrainment (this work). *atonal* (*ato*) is a proneural gene required for the specific formation of the ch organs (Jarman et al., 1995). *ato* mutants lack all larval and adult ch organs (Jarman et al., 1995) but exhibit normal thermotaxis behaviour (Rosenzweig et al., 2005). Given that *TrpA1* is not expressed in ch organs (Rosenzweig et al., 2005) this suggest that ch organs are not required for thermotaxis.

Taken together, these data suggest that *(a)* thermotaxis, temperature avoidance and ch organs-mediated temperature entrainment are distinct mechanisms, *(b)* some TRP channels might have different functions mediating some of these mechanisms, but not others, and *(c) Drosophila* use thermosensory reception structures and overlapping players to execute different and distinct sets of behavioural responses.

Each scolopidium in the ch organs contains an internal liquid-filled capsule-like structure called scolopale (see Introduction and Figure 8.1). The EYESHUT (SPAM) protein is located at the border between the ch neurons and the scolopale (Figure 8.1). Interestingly, *eys* mutants exhibit a massive deformation of the scolopale due to loss of water by evaporation in flies that are exposed to high temperature (37°C) for one hour (Cook et al., 2008). This results in an "uncoordination" phenotype, which prevents the flies for walking properly, and eventually they fall over (Cook et al., 2008). Increasing the environmental humidity, avoiding the water to escape the scolopale, can rescue this phenotype. The same "uncoordination" phenotype was observed for *nocte* (Sehadova et al., 2009) and the *2T-30* mutants (Figure 3.20). Since all the three mutants also exhibit similar defects in entraining their locomotor activity to temperature cycles, this suggests they fulfil related functions in maintaining ch organ activity.

Finally, based on the observation that ch organs seem required to mediate temperature entrainment, we tried to synchronize fly locomotor behaviour by direct stimulation of the ch organs with a mechanical stimulus. Our preliminary data showed that cycles between 12 hr of "vibration" stimulus (2-component of frequencies of 40 and 200 Hz) and 12 hr of "silence" (in constant darkness), can synchronize the locomotor behaviour (Figure 7.1, 7.2 and 7.3). Phase analysis of free-running activity after vibration entrainment showed that physical removal of the antennae does not prevent the clock to synchronize to the stimulus. This correlates with previous observations of non-requirement of the antennae for temperature entrainment of the clock (see above), and suggests that the stimulus applied is perceived by the the fly ch organs as a whole and not exclusively as an acoustic response (mediated by the antennae only).

Analysis of clock and temperature mutants combined with molecular studies of clock genes are needed to confirm that the circadian clock is indeed synchronized by the mechanical stimulation. However, these preliminary data strongly suggest the role played by the ch organs in mediating the temperature entrainment of the circadian clock of *D. melanogaster* and provide a new fascinating tool for studying the temperature entrainment pathways.

Chapter 9

Conclusions

In this thesis I showed that genetic screens are still a powerful approach to isolate new components involved in complex mechanisms, such as the temperature entrainment of the circadian clock. By a forward genetic approach I isolated three novel EMS variants that have impaired synchronization of *per-luc* expression and locomotor activity to temperature cycles. In a screen of RNAi lines I identified one forkhead domain transcription factor (*fd3F*) that, when down-regulated, reduces the expression level and cycling amplitude of *per-luc* in isolated legs both during LD and TC conditions. *tim-gal4*-driven knock-down of *fd3F* alters the phase of eclosion and induce lethality in early adults. In a candidate approach screen of mutant lines for *trp* channels encoding genes I identified three TRP channels that are required for entrainment of the circadian clock in LL and TC. Mutants for *pyrexia*, *trpM* and *trpA1* affect entrainment of locomotor activity to temperature cycles and analysis of behaviour at different temperature intervals suggested that *pyx* and *trpM* are required for synchronization to cool temperatures, whereas *TrpA1* is required in any temperature intervals we applied.

With this work I provided additional evidence that temperature entrainment

in *Drosophila* is mediated by the periphery, which autonomously receives temperature signal from the environment and transmit it to the central clock in the brain. In particular, in support of our recent publication (Sehadova et al., 2009), my data indicate that chordotonal organs mediate circadian temperature entrainment. *nocte* expression in the ch neurons and specific ch organ genes are required for temperature entrainment (Sehadova et al., 2009). *fd3F* is also expressed in ch organs (Lee and Frasch, 2004) and I showed that ch neuron down-regulation of *fd3F* affects entrainment of locomotor activity to temperature. In addition, PYX channels is also expressed in ch organs and the *2T-30* mutant exhibits an "uncoordination" behaviour if exposed to high environmental temperature stress probably due to structural defects of ch organs, in a similar way to *nocte* and *spam* (Sehadova et al., 2009). Mechanical stimulation of mechanosensory organs using a vibratory stimulus can entrain fly's locomotor activity, in a similar was as temperature does, providing additional evidence of the importance of ch organs in the temperature entrainment pathway.

Finally, I showed that temperature entrainment of the clock that controls eclosion timing requires different components and structures compared to the adult clock. In this Thesis I showed that temperature entrainment applied during development induce short, 21 hour, free-running eclosion rhythms, which are *Pdf*-independent. In addition, larval-only temperature entrainment reverses the phase of eclosion compared to larval-only LD entrainment. We proposed that the DN_2 group of clock neurons determine the phase of eclosion during temperature entrainment conditions and have an endogenous short free-running period, which is manifested after temperature entrainment conditions.

Appendix A

RNAi lines

List of the 148 RNAi lines generated by the National Institute of Genetics Fly Stock Center (Japan) screened for defects of synchronization of XLG-*luc* to temperature cycles in LL. The lines have been crossed to $\frac{y\ w}{y\ w}$; $\frac{tim-gal4:27}{CyO}$; $\frac{XLG-luc:1-1}{TM3}$. All the lines listed below have been assayed in our bioluminescence assay in constant light and 12:12 hr 25:16℃ temperature cycles.

List of RNAi lines screened							
1401R-1	3412R-1	5087R-2	7288R-2	9144R-2	10952R-2	12345R-1	14884R-3
1401R-2	3412R-3	5279R-2	7399R-1	9497R-2	11324R-2	12345R-4	15010R-2
1441R-2	4005R-1	5279R-3	7399R-3	9645R-1	11324R-3	12359R-4	15093R-2
1441R-3	4005R-2	5610R-1	7425R-2	9645R-3	11734R-1	12359R-2	15093R-3
1512R-3	4006R-1	5610R-2	7555R-3	9649R-3	11734R-3	12632R-1	15150R-4
1692R-1	4006R-3	5671R-2	7555R-1	9668R-1	11796R-1	12632R-2	15437R-1
1692R-2	4200R-2	5709R-3	7656R-2	9952R-2	11823R-1	12752R-2	15437R-2
1877R-1	4200R-3	6190R-3	7656R-1	10198R-3	11823R-4	12752R-3	16720R-1
2096R-3	4244R-1	6211R-1	8147R-1	10523R-1	11861R-2	13109R-1	16720R-3
2275R-1	4244R-2	6211R-3	8184R-1	10523R-2	11891R-1	13109R-3	16740R-4
2525R-1	4574R-2	6382R-1	8206R-1	10539R-3	11891R-2	13343R-3	17386R-1
2525R-3	4574R-3	6382R-2	8206R-3	10553R-1	11987R-3	13343R-4	30085R-1
3016R-1	4899R-1	6759R-1	8290R-2	10553R-2	11988R-3	13758R-3	30085R-2
3131R-2	4919R-1	6759R-3	8346R-3	10693R-1	12030R-3	14228R-1	31160R-1
3131R-3	4919R-2	6772R-2	8725R-3	10888R-2	12082R-1	14228R-2	31160R-3
3200R-2	4943R-1	6798R-3	8881R-3	10888R-1	12082R-2	14619R-1	
3200R-3	4943R-2	6896R-1	8881R-4	10948R-1	12189R-3	14619R-3	
3249R-2	5076R-1	6896R-2	9086R-3	10948R-3	12189R-1	14751R-1	
3249R-3	5076R-2	7288R-1	9144R-1	10952R-1	12227R-2	14884R-1	

TABLE A.1: List of RNAi lines from National Institute of Genetics Fly stock center (Japan) screened for abnormalities in entrainment to temperature cycles when driven by *tim-gal4*. Every line is labelled according the "CG annotation symbol" of the gene (from Flybase) followed by insertion number (R). A total of 148 lines, covering 96 specific genes have been screened (for most of them 2 independent insertion lines were available).

Appendix B

DEG/ENaC Channels

List of RNAi targeting *degenerin/epithelial sodium channels* (DEG/ENaC) genes which have been tested for defect on synchronization of the circadian clock to temperature cycles. The RNAi lines were provided by the Vienna Drosophila RNAi Centre (Vienna) and have been crossed to $\frac{y\ w}{y\ w}$; $\frac{tim-gal4:27}{CyO}$; $\frac{XLG-luc:1-1}{TM3}$. All the lines listed below have been assayed in our bioluminescence assay in constant light and 12:12 hr 25:16℃ temperature cycles. All of them showed normal phenotype, in term of entraining *per-luc* expression to temperature cycles.

Line name	Gene	Gene name
CG1058-T1 CG1058-T2	Rpk	ripped pocket
CG8178-T1 CG8178-T2	Ppk4 (NacH)	Nach
CG11209-T1 CG11209-T2	Ppk6	pickpocket 6
CG9499-T2	Ppk7	pickpocket7
CG14398-T4	Ppk13	pickpocket13
CG9501-T1 CG9501-T2	Ppk14	pickpocket14
CG34059	Ppk16	pickpocket16
CG18287	Ppk19	pickpocket19
CG7577-T1	Ppk20	pickpocket20
CG12048-T1 CG12048-T2	Ppk21	pickpocket21
CG8527-T1 CG8527-T2	Ppk23	pickpocket23
CG15249-T1	Ppk25	pickpocket25
CG4805-T1	Ppk28	pickpocket28
CG32679-T1	CG32679	
CG8546-T3	CG8546	
CG8546-T4	CG8546	

TABLE B.1: List of RNAi targeting DEG/ENaC channel genes which were tested for defects on temperature entrainment of the circadian clock. The "line name" refers to the Flybase annotation symbol followed by insertion number (according to the VDRC).

Bibliography

Adams, D. (2002). *The Hitchhiker's Guide to the Galaxy*. Picador.

Albert, J. T., Nadrowski, B., and Gopfert, M. C. (2007). Drosophila mechanotransduction–linking proteins and functions. *Fly (Austin)*, 1:238–241.

Allada, R., White, N. E., So, W. V., Hall, J. C., and Rosbash, M. (1998). A mutant Drosophila homolog of mammalian Clock disrupts circadian rhythms and transcription of period and timeless. *Cell*, 93:791–804.

Bae, K., Lee, C., Sidote, D., Chuang, K. Y., and Edery, I. (1998). Circadian regulation of a Drosophila homolog of the mammalian Clock gene: PER and TIM function as positive regulators. *Mol. Cell. Biol.*, 18:6142–6151.

Belles, X. (2010). Beyond Drosophila: RNAi in vivo and functional genomics in insects. *Annu. Rev. Entomol.*, 55:111–128.

Blanchardon, E., Grima, B., Klarsfeld, A., Chelot, E., Hardin, P. E., Preat, T., and Rouyer, F. (2001). Defining the role of Drosophila lateral neurons in the control of circadian rhythms in motor activity and eclosion by targeted genetic ablation and PERIOD protein overexpression. *Eur. J. Neurosci.*, 13:871–888.

Blau, J. and Young, M. W. (1999). Cycling vrille expression is required for a functional Drosophila clock. *Cell*, 99:661–671.

Bloomquist, B. T., Shortridge, R. D., Schneuwly, S., Perdew, M., Montell, C., Steller, H., Rubin, G., and Pak, W. L. (1988). Isolation of a putative phospholipase C gene of Drosophila, norpA, and its role in phototransduction. *Cell*, 54:723–733.

Boothroyd, C. E., Wijnen, H., Naef, F., Saez, L., and Young, M. W. (2007). Integration of light and temperature in the regulation of circadian gene expression in Drosophila. *PLoS Genet.*, 3:e54.

Boutros, M. and Ahringer, J. (2008). The art and design of genetic screens: RNA interference. *Nat. Rev. Genet.*, 9:554–566.

Bozek, K., Relogio, A., Kielbasa, S. M., Heine, M., Dame, C., Kramer, A., and Herzel, H. (2009). Regulation of clock-controlled genes in mammals. *PLoS ONE*, 4:e4882.

Brand, A. H. and Perrimon, N. (1993). Targeted gene expression as a means of altering cell fates and generating dominant phenotypes. *Development*, 118:401–415.

Brandes, C., Plautz, J. D., Stanewsky, R., Jamison, C. F., Straume, M., Wood, K. V., Kay, S. A., and Hall, J. C. (1996). Novel features of drosophila period Transcription revealed by real-time luciferase reporting. *Neuron*, 16:687–692.

Brown, S. A., Zumbrunn, G., Fleury-Olela, F., Preitner, N., and Schibler, U. (2002). Rhythms of mammalian body temperature can sustain peripheral circadian clocks. *Curr. Biol.*, 12:1574–1583.

Busza, A., Emery-Le, M., Rosbash, M., and Emery, P. (2004). Roles of the two Drosophila CRYPTOCHROME structural domains in circadian photoreception. *Science*, 304:1503–1506.

Busza, A., Murad, A., and Emery, P. (2007). Interactions between circadian neurons control temperature synchronization of Drosophila behavior. *J. Neurosci.*, 27:10722–10733.

Caldwell, J. C. and Eberl, D. F. (2002). Towards a molecular understanding of Drosophila hearing. *J. Neurobiol.*, 53:172–189.

Ceriani, M. F., Darlington, T. K., Staknis, D., Mas, P., Petti, A. A., Weitz, C. J., and Kay, S. A. (1999). Light-dependent sequestration of TIMELESS by CRYPTOCHROME. *Science*, 285:553–556.

Chatterjee, A., Tanoue, S., Houl, J. H., and Hardin, P. E. (2010). Regulation of gustatory physiology and appetitive behavior by the Drosophila circadian clock. *Curr. Biol.*, 20:300–309.

Clapham, D. E. (2003). TRP channels as cellular sensors. *Nature*, 426:517–524.

Clark, K. L., Halay, E. D., Lai, E., and Burley, S. K. (1993). Co-crystal structure of the HNF-3/fork head DNA-recognition motif resembles histone H5. *Nature*, 364:412–420.

Collins, B. and Blau, J. (2007). Even a stopped clock tells the right time twice a day: circadian timekeeping in Drosophila. *Pflugers Arch.*, 454:857–867.

Collins, B. H., Rosato, E., and Kyriacou, C. P. (2004). Seasonal behavior in Drosophila melanogaster requires the photoreceptors, the circadian clock, and phospholipase C. *Proc. Natl. Acad. Sci. U.S.A.*, 101:1945–1950.

Cook, B., Hardy, R. W., McConnaughey, W. B., and Zuker, C. S. (2008). Preserving cell shape under environmental stress. *Nature*, 452:361–364.

Currie, J., Goda, T., and Wijnen, H. (2009). Selective entrainment of the Drosophila circadian clock to daily gradients in environmental temperature. *BMC Biol.*, 7:49.

Cyran, S. A., Buchsbaum, A. M., Reddy, K. L., Lin, M. C., Glossop, N. R., Hardin, P. E., Young, M. W., Storti, R. V., and Blau, J. (2003). vrille, Pdp1, and dClock form a second feedback loop in the Drosophila circadian clock. *Cell*, 112:329–341.

Damann, N., Voets, T., and Nilius, B. (2008). TRPs in our senses. *Curr. Biol.*, 18:R880–889.

Dietzl, G., Chen, D., Schnorrer, F., Su, K. C., Barinova, Y., Fellner, M., Gasser, B., Kinsey, K., Oppel, S., Scheiblauer, S., Couto, A., Marra, V., Keleman, K., and Dickson, B. J. (2007). A genome-wide transgenic RNAi library for conditional gene inactivation in Drosophila. *Nature*, 448:151–156.

Dolezelova, E., Dolezel, D., and Hall, J. C. (2007). Rhythm defects caused by newly engineered null mutations in Drosophila's cryptochrome gene. *Genetics*, 177:329–345.

Dubruille, R. and Emery, P. (2008). A plastic clock: how circadian rhythms respond to environmental cues in Drosophila. *Mol. Neurobiol.*, 38:129–145.

Dunlap, J. C. (1999). Molecular bases for circadian clocks. *Cell*, 96:271–290.

Dunlap, J. C., Loros, J. J., and DeCoursey, P. J. (2004). *Chronobiology: Biological Timekeeping*. Sinauer Associates, Inc. Publisher.

Eberl, D. F. (1999). Feeling the vibes: chordotonal mechanisms in insect hearing. *Curr. Opin. Neurobiol.*, 9:389–393.

Eberl, D. F. and Boekhoff-Falk, G. (2007). Development of Johnston's organ in Drosophila. *Int. J. Dev. Biol.*, 51:679–687.

Edery, I., Zwiebel, L. J., Dembinska, M. E., and Rosbash, M. (1994). Temporal phosphorylation of the Drosophila period protein. *Proc. Natl. Acad. Sci. U.S.A.*, 91:2260–2264.

Emery, P., So, W. V., Kaneko, M., Hall, J. C., and Rosbash, M. (1998). CRY, a Drosophila clock and light-regulated cryptochrome, is a major contributor to circadian rhythm resetting and photosensitivity. *Cell*, 95:669–679.

Emery, P., Stanewsky, R., Helfrich-Förster, C., Emery-Le, M., Hall, J. C., and Rosbash, M. (2000). Drosophila CRY is a deep brain circadian photoreceptor. *Neuron*, 26:493–504.

Ewer, J., Frisch, B., Hamblen-Coyle, M. J., Rosbash, M., and Hall, J. C. (1992). Expression of the period clock gene within different cell types in the brain of Drosophila adults and mosaic analysis of these cells' influence on circadian behavioral rhythms. *J. Neurosci.*, 12:3321–3349.

Fang, Y., Sathyanarayanan, S., and Sehgal, A. (2007). Post-translational regulation of the Drosophila circadian clock requires protein phosphatase 1 (PP1). *Genes Dev.*, 21:1506–1518.

Field, L. H. and Matheson, T. (1998). Chordotonal organs in insects. *Adv. Insect Physiol.*, 27:1–230.

Frisch, B., Hardin, P. E., Hamblen-Coyle, M. J., Rosbash, M., and Hall, J. C. (1994). A promoterless period gene mediates behavioral rhythmicity and cyclical per expression in a restricted subset of the Drosophila nervous system. *Neuron*, 12:555–570.

Gao, Z., Joseph, E., Ruden, D. M., and Lu, X. (2004). Drosophila Pkd2 is haploid-insufficient for mediating optimal smooth muscle contractility. *J. Biol. Chem.*, 279:14225–14231.

Gao, Z., Ruden, D. M., and Lu, X. (2003). PKD2 cation channel is required for directional sperm movement and male fertility. *Curr. Biol.*, 13:2175–2178.

Glaser, F. T. (2006). *Temperatursynchronisation der circadianen Uhr von Drosophila melanogaster: Eine genetische und molekulare Untersuchung beteiligter Mechanismen und Rezeptoren.* PhD thesis, Universität Regensburg.

Glaser, F. T. and Stanewsky, R. (2005). Temperature synchronization of the Drosophila circadian clock. *Curr. Biol.*, 15:1352–1363.

Glaser, F. T. and Stanewsky, R. (2007). Synchronization of the Drosophila circadian clock by temperature cycles. *Cold Spring Harb. Symp. Quant. Biol.*, 72:233–242.

Gong, Z., Son, W., Chung, Y. D., Kim, J., Shin, D. W., McClung, C. A., Lee, Y., Lee, H. W., Chang, D. J., Kaang, B. K., Cho, H., Oh, U., Hirsh, J., Kernan, M. J., and Kim, C. (2004). Two interdependent TRPV channel subunits, inactive and Nanchung, mediate hearing in Drosophila. *J. Neurosci.*, 24:9059–9066.

Grima, B., Chelot, E., Xia, R., and Rouyer, F. (2004). Morning and evening peaks of activity rely on different clock neurons of the Drosophila brain. *Nature*, 431:869–873.

Halberg, F., Cornelissen, G., Katinas, G., Syutkina, E. V., Sothern, R. B., Zaslavskaya, R., Halberg, F., Watanabe, Y., Schwartzkopff, O., Otsuka, K., Tarquini, R., Frederico, P., and Siggelova, J. (2003). Transdisciplinary unifying implications of circadian findings in the 1950s. *J Circadian Rhythms*, 1:2.

Hall, J. C. (2005). Systems approaches to biological rhythms in Drosophila. *Meth. Enzymol.*, 393:61–185.

Hamada, F. N., Rosenzweig, M., Kang, K., Pulver, S. R., Ghezzi, A., Jegla, T. J., and Garrity, P. A. (2008). An internal thermal sensor controlling temperature preference in Drosophila. *Nature*, 454:217–220.

Hardie, R. C. (2007). TRP channels and lipids: from Drosophila to mammalian physiology. *J. Physiol. (Lond.)*, 578:9–24.

Hase, M., Yagi, Y., Taru, H., Tomita, S., Sumioka, A., Hori, K., Miyamoto, K., Sasamura, T., Nakamura, M., Matsuno, K., and Suzuki, T. (2002). Expression and characterization of the Drosophila X11-like/Mint protein during neural development. *J. Neurochem.*, 81:1223–1232.

Helfrich-Förster, C. (2002). The circadian system of Drosophila melanogaster and its light input pathways. *Zoology (Jena)*, 105:297–312.

Helfrich-Förster, C. (2005). Neurobiology of the fruit fly's circadian clock. *Genes Brain Behav.*, 4:65–76.

Helfrich-Förster, C., Shafer, O. T., Wulbeck, C., Grieshaber, E., Rieger, D., and Taghert, P. (2007). Development and morphology of the clock-gene-expressing lateral neurons of Drosophila melanogaster. *J. Comp. Neurol.*, 500:47–70.

Helfrich-Förster, C., Winter, C., Hofbauer, A., Hall, J. C., and Stanewsky, R. (2001). The circadian clock of fruit flies is blind after elimination of all known photoreceptors. *Neuron*, 30:249–261.

Hermjakob, H., Montecchi-Palazzi, L., Lewington, C., Mudali, S., Kerrien, S., Orchard, S., Vingron, M., Roechert, B., Roepstorff, P., Valencia, A., Margalit,

H., Armstrong, J., Bairoch, A., Cesareni, G., Sherman, D., and Apweiler, R. (2004). IntAct: an open source molecular interaction database. *Nucleic Acids Res.*, 32:D452–455.

Hofmann, T., Chubanov, V., Chen, X., Dietz, A. S., Gudermann, T., and Montell, C. (2010). Drosophila TRPM channel is essential for the control of extracellular magnesium levels. *PLoS ONE*, 5:e10519.

Hogan, C. C. and Bettencourt, B. R. (2009). Duplicate gene evolution toward multiple fates at the Drosophila melanogaster HIP/HIP-Replacement locus. *J. Mol. Evol.*, 68:337–350.

Jarman, A. P., Sun, Y., Jan, L. Y., and Jan, Y. N. (1995). Role of the proneural gene, atonal, in formation of Drosophila chordotonal organs and photoreceptors. *Development*, 121:2019–2030.

Johard, H. A., Yoishii, T., Dircksen, H., Cusumano, P., Rouyer, F., Helfrich-Förster, C., and Nassel, D. R. (2009). Peptidergic clock neurons in Drosophila: ion transport peptide and short neuropeptide F in subsets of dorsal and ventral lateral neurons. *J. Comp. Neurol.*, 516:59–73.

Kadener, S., Stoleru, D., McDonald, M., Nawathean, P., and Rosbash, M. (2007). Clockwork Orange is a transcriptional repressor and a new Drosophila circadian pacemaker component. *Genes Dev.*, 21:1675–1686.

Kamikouchi, A., Inagaki, H. K., Effertz, T., Hendrich, O., Fiala, A., Gopfert, M. C., and Ito, K. (2009). The neural basis of Drosophila gravity-sensing and hearing. *Nature*, 458:165–171.

Kaneko, M. and Hall, J. C. (2000). Neuroanatomy of cells expressing clock genes in Drosophila: transgenic manipulation of the period and timeless genes to mark

the perikarya of circadian pacemaker neurons and their projections. *J. Comp. Neurol.*, 422:66–94.

Kaneko, M., Hamblen, M. J., and Hall, J. C. (2000). Involvement of the period gene in developmental time-memory: effect of the perShort mutation on phase shifts induced by light pulses delivered to Drosophila larvae. *J. Biol. Rhythms*, 15:13–30.

Kaneko, M., Helfrich-Förster, C., and Hall, J. C. (1997). Spatial and temporal expression of the period and timeless genes in the developing nervous system of Drosophila: newly identified pacemaker candidates and novel features of clock gene product cycling. *J. Neurosci.*, 17:6745–6760.

Kang, K., Pulver, S. R., Panzano, V. C., Chang, E. C., Griffith, L. C., Theobald, D. L., and Garrity, P. A. (2010). Analysis of Drosophila TRPA1 reveals an ancient origin for human chemical nociception. *Nature*, 464:597–600.

Katz, B. and Minke, B. (2009). Drosophila photoreceptors and signaling mechanisms. *Front Cell Neurosci*, 3:2.

Kaufmann, E. and Knochel, W. (1996). Five years on the wings of fork head. *Mech. Dev.*, 57:3–20.

Kaushik, R., Nawathean, P., Busza, A., Murad, A., Emery, P., and Rosbash, M. (2007). PER-TIM interactions with the photoreceptor cryptochrome mediate circadian temperature responses in Drosophila. *PLoS Biol.*, 5:e146.

Kernan, M. J. (2007). Mechanotransduction and auditory transduction in Drosophila. *Pflugers Arch.*, 454:703–720.

Kim, E. Y. and Edery, I. (2006). Balance between DBT/CKIepsilon kinase and protein phosphatase activities regulate phosphorylation and stability of Drosophila CLOCK protein. *Proc. Natl. Acad. Sci. U.S.A.*, 103:6178–6183.

Kim, J., Chung, Y. D., Park, D. Y., Choi, S., Shin, D. W., Soh, H., Lee, H. W., Son, W., Yim, J., Park, C. S., Kernan, M. J., and Kim, C. (2003). A TRPV family ion channel required for hearing in Drosophila. *Nature*, 424:81–84.

Klarsfeld, A., Malpel, S., Michard-Vanhee, C., Picot, M., Chelot, E., and Rouyer, F. (2004). Novel features of cryptochrome-mediated photoreception in the brain circadian clock of Drosophila. *J. Neurosci.*, 24:1468–1477.

Kloss, B., Price, J. L., Saez, L., Blau, J., Rothenfluh, A., Wesley, C. S., and Young, M. W. (1998). The Drosophila clock gene double-time encodes a protein closely related to human casein kinase Iepsilon. *Cell*, 94:97–107.

Ko, H. W., Jiang, J., and Edery, I. (2002). Role for Slimb in the degradation of Drosophila Period protein phosphorylated by Doubletime. *Nature*, 420:673–678.

Koh, K., Zheng, X., and Sehgal, A. (2006). JETLAG resets the Drosophila circadian clock by promoting light-induced degradation of TIMELESS. *Science*, 312:1809–1812.

Konopka, R. J. and Benzer, S. (1971). Clock mutants of Drosophila melanogaster. *Proc. Natl. Acad. Sci. U.S.A.*, 68:2112–2116.

Konopka, R. J., Pittendrigh, C., and Orr, D. (1989). Reciprocal behaviour associated with altered homeostasis and photosensitivity of Drosophila clock mutants. *J. Neurogenet.*, 6:1–10.

Kraft, R. and Harteneck, C. (2005). The mammalian melastatin-related transient receptor potential cation channels: an overview. *Pflugers Arch.*, 451:204–211.

Kwon, Y., Shim, H. S., Wang, X., and Montell, C. (2008). Control of thermotactic behavior via coupling of a TRP channel to a phospholipase C signaling cascade. *Nat. Neurosci.*, 11:871–873.

Kyriacou, C. P. and Rosato, E. (2000). Squaring up the E-box. *J. Biol. Rhythms*, 15:483–490.

Lahiri, K., Vallone, D., Gondi, S. B., Santoriello, C., Dickmeis, T., and Foulkes, N. S. (2005). Temperature regulates transcription in the zebrafish circadian clock. *PLoS Biol.*, 3:e351.

Lai, E., Clark, K. L., Burley, S. K., and Darnell, J. E. (1993). Hepatocyte nuclear factor 3/fork head or "winged helix" proteins: a family of transcription factors of diverse biologic function. *Proc. Natl. Acad. Sci. U.S.A.*, 90:10421–10423.

Landskron, J., Chen, K. F., Wolf, E., and Stanewsky, R. (2009). A role for the PERIOD:PERIOD homodimer in the Drosophila circadian clock. *PLoS Biol.*, 7:e3.

Lee, C., Bae, K., and Edery, I. (1999). PER and TIM inhibit the DNA binding activity of a Drosophila CLOCK-CYC/dBMAL1 heterodimer without disrupting formation of the heterodimer: a basis for circadian transcription. *Mol. Cell. Biol.*, 19:5316–5325.

Lee, H. H. and Frasch, M. (2004). Survey of forkhead domain encoding genes in the Drosophila genome: Classification and embryonic expression patterns. *Dev. Dyn.*, 229:357–366.

Lee, J. E. and Edery, I. (2008). Circadian regulation in the ability of Drosophila to combat pathogenic infections. *Curr. Biol.*, 18:195–199.

Lee, Y., Lee, Y., Lee, J., Bang, S., Hyun, S., Kang, J., Hong, S. T., Bae, E., Kaang, B. K., and Kim, J. (2005). Pyrexia is a new thermal transient receptor potential channel endowing tolerance to high temperatures in Drosophila melanogaster. *Nat. Genet.*, 37:305–310.

Levine, J. D., Funes, P., Dowse, H. B., and Hall, J. C. (2002a). Advanced analysis of a cryptochrome mutation's effects on the robustness and phase of molecular cycles in isolated peripheral tissues of Drosophila. *BMC Neurosci*, 3:5.

Levine, J. D., Funes, P., Dowse, H. B., and Hall, J. C. (2002b). Resetting the circadian clock by social experience in Drosophila melanogaster. *Science*, 298:2010–2012.

Levine, J. D., Funes, P., Dowse, H. B., and Hall, J. C. (2002c). Signal analysis of behavioral and molecular cycles. *BMC Neurosci*, 3:1.

Lim, C., Chung, B. Y., Pitman, J. L., McGill, J. J., Pradhan, S., Lee, J., Keegan, K. P., Choe, J., and Allada, R. (2007). Clockwork orange encodes a transcriptional repressor important for circadian-clock amplitude in Drosophila. *Curr. Biol.*, 17:1082–1089.

Lindsley, D. L. and Zimm, G. G. (1992). *The genome of Drosophila melanogaster*. Acadmic Press.

Liu, L., Li, Y., Wang, R., Yin, C., Dong, Q., Hing, H., Kim, C., and Welsh, M. J. (2007). Drosophila hygrosensation requires the TRP channels water witch and nanchung. *Nature*, 450:294–298.

Liu, Y., Merrow, M., Loros, J. J., and Dunlap, J. C. (1998). How temperature changes reset a circadian oscillator. *Science*, 281:825–829.

Luo, L., Liao, Y. J., Jan, L. Y., and Jan, Y. N. (1994). Distinct morphogenetic functions of similar small GTPases: Drosophila Drac1 is involved in axonal outgrowth and myoblast fusion. *Genes Dev.*, 8:1787–1802.

Lyons, L. C. and Roman, G. (2009). Circadian modulation of short-term memory in Drosophila. *Learn. Mem.*, 16:19–27.

Majercak, J., Chen, W. F., and Edery, I. (2004). Splicing of the period gene 3'-terminal intron is regulated by light, circadian clock factors, and phospholipase C. *Mol. Cell. Biol.*, 24:3359–3372.

Majercak, J., Sidote, D., Hardin, P. E., and Edery, I. (1999). How a circadian clock adapts to seasonal decreases in temperature and day length. *Neuron*, 24:219–230.

Malpel, S., Klarsfeld, A., and Rouyer, F. (2002). Larval optic nerve and adult extra-retinal photoreceptors sequentially associate with clock neurons during Drosophila brain development. *Development*, 129:1443–1453.

Malpel, S., Klarsfeld, A., and Rouyer, F. (2004). Circadian synchronization and rhythmicity in larval photoperception-defective mutants of Drosophila. *J. Biol. Rhythms*, 19:10–21.

Martinek, S., Inonog, S., Manoukian, A. S., and Young, M. W. (2001). A role for the segment polarity gene shaggy/GSK-3 in the Drosophila circadian clock. *Cell*, 105:769–779.

McNabb, S. L. and Truman, J. W. (2008). Light and peptidergic eclosion hormone neurons stimulate a rapid eclosion response that masks circadian emergence in Drosophila. *J. Exp. Biol.*, 211:2263–2274.

McNeil, G. P., Zhang, X., Genova, G., and Jackson, F. R. (1998). A molecular rhythm mediating circadian clock output in Drosophila. *Neuron*, 20:297–303.

Mealey-Ferrara, M. L., Montalvo, A. G., and Hall, J. C. (2003). Effects of combining a cryptochrome mutation with other visual-system variants on entrainment of locomotor and adult-emergence rhythms in Drosophila. *J. Neurogenet.*, 17:171–221.

Meissner, R. A., Kilman, V. L., Lin, J. M., and Allada, R. (2008). TIMELESS is an important mediator of CK2 effects on circadian clock function in vivo. *J. Neurosci.*, 28:9732–9740.

Minke, B. and Parnas, M. (2006). Insights on TRP channels from in vivo studies in Drosophila. *Annu. Rev. Physiol.*, 68:649–684.

Miyasako, Y., Umezaki, Y., and Tomioka, K. (2007). Separate sets of cerebral clock neurons are responsible for light and temperature entrainment of Drosophila circadian locomotor rhythms. *J. Biol. Rhythms*, 22:115–126.

Montell, C. (2005). Drosophila TRP channels. *Pflugers Arch.*, 451:19–28.

Montell, C. and Caterina, M. J. (2007). Thermoregulation: channels that are cool to the core. *Curr. Biol.*, 17:R885–887.

Myers, E. M., Yu, J., and Sehgal, A. (2003). Circadian control of eclosion: interaction between a central and peripheral clock in Drosophila melanogaster. *Curr. Biol.*, 13:526–533.

Nässel, D. R. (2000). Functional roles of neuropeptides in the insect central nervous system. *Naturwissenschaften*, 87:439–449.

Newby, L. M. and Jackson, F. R. (1993). A new biological rhythm mutant of Drosophila melanogaster that identifies a gene with an essential embryonic function. *Genetics*, 135:1077–1090.

Niemeyer, B. A., Suzuki, E., Scott, K., Jalink, K., and Zuker, C. S. (1996). The Drosophila light-activated conductance is composed of the two channels TRP and TRPL. *Cell*, 85:651–659.

Oishi, K., Miyazaki, K., Kadota, K., Kikuno, R., Nagase, T., Atsumi, G., Ohkura, N., Azama, T., Mesaki, M., Yukimasa, S., Kobayashi, H., Iitaka, C., Umehara, T., Horikoshi, M., Kudo, T., Shimizu, Y., Yano, M., Monden, M., Machida, K., Matsuda, J., Horie, S., Todo, T., and Ishida, N. (2003). Genome-wide expression analysis of mouse liver reveals CLOCK-regulated circadian output genes. *J. Biol. Chem.*, 278:41519–41527.

O'Tousa, J. E., Baehr, W., Martin, R. L., Hirsh, J., Pak, W. L., and Applebury, M. L. (1985). The Drosophila ninaE gene encodes an opsin. *Cell*, 40:839–850.

Park, J. H., Helfrich-Förster, C., Lee, G., Liu, L., Rosbash, M., and Hall, J. C. (2000). Differential regulation of circadian pacemaker output by separate clock genes in Drosophila. *Proc. Natl. Acad. Sci. U.S.A.*, 97:3608–3613.

Pearn, M. T., Randall, L. L., Shortridge, R. D., Burg, M. G., and Pak, W. L. (1996). Molecular, biochemical, and electrophysiological characterization of Drosophila norpA mutants. *J. Biol. Chem.*, 271:4937–4945.

Peschel, N., Chen, K. F., Szabo, G., and Stanewsky, R. (2009). Light-dependent interactions between the Drosophila circadian clock factors cryptochrome, jetlag, and timeless. *Curr. Biol.*, 19:241–247.

Peschel, N., Veleri, S., and Stanewsky, R. (2006). Veela defines a molecular link between Cryptochrome and Timeless in the light-input pathway to Drosophila's circadian clock. *Proc. Natl. Acad. Sci. U.S.A.*, 103:17313–17318.

Picot, M., Klarsfeld, A., Chelot, E., Malpel, S., and Rouyer, F. (2009). A role for blind DN2 clock neurons in temperature entrainment of the Drosophila larval brain. *J. Neurosci.*, 29:8312–8320.

Pittendrigh, C., Bruce, V., and Kaus, P. (1958). ON THE SIGNIFICANCE OF TRANSIENTS IN DAILY RHYTHMS. *Proc. Natl. Acad. Sci. U.S.A.*, 44:965–973.

Pittendrigh, C. S. (1954). ON TEMPERATURE INDEPENDENCE IN THE CLOCK SYSTEM CONTROLLING EMERGENCE TIME IN DROSOPHILA. *Proc. Natl. Acad. Sci. U.S.A.*, 40:1018–1029.

Pittendrigh, C. S. and Daan, S. (1976). A functional analysis of circadian pacemakers in nocturnal rodents: V. Pacemaker structure: A clock for all seasons. *J. Comp. Physiol.*, 106:333–355.

Plautz, J. D., Straume, M., Stanewsky, R., Jamison, C. F., Brandes, C., Dowse, H. B., Hall, J. C., and Kay, S. A. (1997). Quantitative analysis of Drosophila period gene transcription in living animals. *J. Biol. Rhythms*, 12:204–217.

Price, J. L., Blau, J., Rothenfluh, A., Abodeely, M., Kloss, B., and Young, M. W. (1998). double-time is a novel Drosophila clock gene that regulates PERIOD protein accumulation. *Cell*, 94:83–95.

Qiu, J. and Hardin, P. E. (1996). Developmental state and the circadian clock interact to influence the timing of eclosion in Drosophila melanogaster. *J. Biol. Rhythms*, 11:75–86.

Refinetti, R. (2010). Entrainment of circadian rhythm by ambient temperature cycles in mice. *J. Biol. Rhythms*, 25:247–256.

Renn, S. C., Park, J. H., Rosbash, M., Hall, J. C., and Taghert, P. H. (1999). A pdf neuropeptide gene mutation and ablation of PDF neurons each cause severe abnormalities of behavioral circadian rhythms in Drosophila. *Cell*, 99:791–802.

Rensing, L. and Ruoff, P. (2002). Temperature effect on entrainment, phase shifting, and amplitude of circadian clocks and its molecular bases. *Chronobiol. Int.*, 19:807–864.

Richier, B., Michard-Vanhee, C., Lamouroux, A., Papin, C., and Rouyer, F. (2008). The clockwork orange Drosophila protein functions as both an activator and a repressor of clock gene expression. *J. Biol. Rhythms*, 23:103–116.

Rieger, D., Shafer, O. T., Tomioka, K., and Helfrich-Förster, C. (2006). Functional analysis of circadian pacemaker neurons in Drosophila melanogaster. *J. Neurosci.*, 26:2531–2543.

Roberts, D. (1998). *Drosophila, a practical approach*. Oxford University Press, second edition edition.

Rosato, E., Codd, V., Mazzotta, G., Piccin, A., Zordan, M., Costa, R., and Kyriacou, C. P. (2001). Light-dependent interaction between Drosophila CRY and the clock protein PER mediated by the carboxy terminus of CRY. *Curr. Biol.*, 11:909–917.

Rosenzweig, M., Brennan, K. M., Tayler, T. D., Phelps, P. O., Patapoutian, A., and Garrity, P. A. (2005). The Drosophila ortholog of vertebrate TRPA1 regulates thermotaxis. *Genes Dev.*, 19:419–424.

Rosenzweig, M., Kang, K., and Garrity, P. A. (2008). Distinct TRP channels are required for warm and cool avoidance in Drosophila melanogaster. *Proc. Natl. Acad. Sci. U.S.A.*, 105:14668–14673.

Rouyer, F., Rachidi, M., Pikielny, C., and Rosbash, M. (1997). A new gene encoding a putative transcription factor regulated by the Drosophila circadian clock. *EMBO J.*, 16:3944–3954.

Rutila, J. E., Suri, V., Le, M., So, W. V., Rosbash, M., and Hall, J. C. (1998). CYCLE is a second bHLH-PAS clock protein essential for circadian rhythmicity and transcription of Drosophila period and timeless. *Cell*, 93:805–814.

S. Hari Dass, T. M. and Sharma, V. K. (2008). Egg-laying rhythm in Drosophila melanogaster. *J. Genet.*, 87:495–504.

Saez, L. and Young, M. W. (1996). Regulation of nuclear entry of the Drosophila clock proteins period and timeless. *Neuron*, 17:911–920.

Sakai, T. and Ishida, N. (2001). Circadian rhythms of female mating activity governed by clock genes in Drosophila. *Proc. Natl. Acad. Sci. U.S.A.*, 98:9221–9225.

Sathyanarayanan, S., Zheng, X., Xiao, R., and Sehgal, A. (2004). Posttranslational regulation of Drosophila PERIOD protein by protein phosphatase 2A. *Cell*, 116:603–615.

Sawyer, L. A., Hennessy, J. M., Peixoto, A. A., Rosato, E., Parkinson, H., Costa, R., and Kyriacou, C. P. (1997). Natural variation in a Drosophila clock gene and temperature compensation. *Science*, 278:2117–2120.

Sayeed, O. and Benzer, S. (1996). Behavioral genetics of thermosensation and hygrosensation in Drosophila. *Proc. Natl. Acad. Sci. U.S.A.*, 93:6079–6084.

Schroeder, A. J., Genova, G. K., Roberts, M. A., Kleyner, Y., Suh, J., and Jackson, F. R. (2003). Cell-specific expression of the lark RNA-binding protein in Drosophila results in morphological and circadian behavioral phenotypes. *J. Neurogenet.*, 17:139–169.

Sehadova, H., Glaser, F. T., Gentile, C., Simoni, A., Giesecke, A., Albert, J. T., and Stanewsky, R. (2009). Temperature entrainment of Drosophila's circadian clock involves the gene nocte and signaling from peripheral sensory tissues to the brain. *Neuron*, 64:251–266.

Sehgal, A., Price, J., and Young, M. W. (1992). Ontogeny of a biological clock in Drosophila melanogaster. *Proc. Natl. Acad. Sci. U.S.A.*, 89:1423–1427.

Sehgal, A., Price, J. L., Man, B., and Young, M. W. (1994). Loss of circadian behavioral rhythms and per RNA oscillations in the Drosophila mutant timeless. *Science*, 263:1603–1606.

Sepp, K. J., Schulte, J., and Auld, V. J. (2001). Peripheral glia direct axon guidance across the CNS/PNS transition zone. *Dev. Biol.*, 238:47–63.

Shafer, O. T., Helfrich-Förster, C., Renn, S. C., and Taghert, P. H. (2006). Reevaluation of Drosophila melanogaster's neuronal circadian pacemakers reveals new neuronal classes. *J. Comp. Neurol.*, 498:180–193.

Shafer, O. T., Rosbash, M., and Truman, J. W. (2002). Sequential nuclear accumulation of the clock proteins period and timeless in the pacemaker neurons of Drosophila melanogaster. *J. Neurosci.*, 22:5946–5954.

Shaw, P. J., Cirelli, C., Greenspan, R. J., and Tononi, G. (2000). Correlates of sleep and waking in Drosophila melanogaster. *Science*, 287:1834–1837.

Sidote, D., Majercak, J., Parikh, V., and Edery, I. (1998). Differential effects of light and heat on the Drosophila circadian clock proteins PER and TIM. *Mol. Cell. Biol.*, 18:2004–2013.

Siegmund, T. and Korge, G. (2001). Innervation of the ring gland of Drosophila melanogaster. *J. Comp. Neurol.*, 431:481–491.

Skopik, S. D. and Pittendrigh, C. S. (1967). Circadian systems, II. The oscillation in the individual Drosophila pupa; its independence of developmental stage. *Proc. Natl. Acad. Sci. U.S.A.*, 58:1862–1869.

Stanewsky, R. (2003). Genetic analysis of the circadian system in Drosophila melanogaster and mammals. *J. Neurobiol.*, 54:111–147.

Stanewsky, R., Frisch, B., Brandes, C., Hamblen-Coyle, M. J., Rosbash, M., and Hall, J. C. (1997a). Temporal and spatial expression patterns of transgenes containing increasing amounts of the Drosophila clock gene period and a lacZ reporter: mapping elements of the PER protein involved in circadian cycling. *J. Neurosci.*, 17:676–696.

Stanewsky, R., Jamison, C. F., Plautz, J. D., Kay, S. A., and Hall, J. C. (1997b). Multiple circadian-regulated elements contribute to cycling period gene expression in Drosophila. *EMBO J.*, 16:5006–5018.

Stanewsky, R., Kaneko, M., Emery, P., Beretta, B., Wager-Smith, K., Kay, S. A., Rosbash, M., and Hall, J. C. (1998). The cryb mutation identifies cryptochrome as a circadian photoreceptor in Drosophila. *Cell*, 95:681–692.

Stark, C., Breitkreutz, B. J., Reguly, T., Boucher, L., Breitkreutz, A., and Tyers, M. (2006). BioGRID: a general repository for interaction datasets. *Nucleic Acids Res.*, 34:D535–539.

Stoleru, D., Nawathean, P., Fernandez, M. P., Menet, J. S., Ceriani, M. F., and Rosbash, M. (2007). The Drosophila circadian network is a seasonal timer. *Cell*, 129:207–219.

Stoleru, D., Peng, Y., Nawathean, P., and Rosbash, M. (2005). A resetting signal between Drosophila pacemakers synchronizes morning and evening activity. *Nature*, 438:238–242.

Suh, J. and Jackson, F. R. (2007). Drosophila ebony activity is required in glia for the circadian regulation of locomotor activity. *Neuron*, 55:435–447.

Sun, Y., Liu, L., Ben-Shahar, Y., Jacobs, J. S., Eberl, D. F., and Welsh, M. J. (2009). TRPA channels distinguish gravity sensing from hearing in Johnston's organ. *Proc. Natl. Acad. Sci. U.S.A.*, 106:13606–13611.

Tanoue, S., Krishnan, P., Krishnan, B., Dryer, S. E., and Hardin, P. E. (2004). Circadian clocks in antennal neurons are necessary and sufficient for olfaction rhythms in Drosophila. *Curr. Biol.*, 14:638–649.

Tomioka, K., Sakamoto, M., Harui, Y., Matsumoto, N., and Matsumoto, A. (1998). Light and temperature cooperate to regulate the circadian locomotor rhythm of wild type and period mutants of Drosophila melanogaster. *J. Insect Physiol.*, 44:587–596.

Tracey, W. D., Wilson, R. I., Laurent, G., and Benzer, S. (2003). painless, a Drosophila gene essential for nociception. *Cell*, 113:261–273.

Veleri, S., Brandes, C., Helfrich-Förster, C., Hall, J. C., and Stanewsky, R. (2003). A self-sustaining, light-entrainable circadian oscillator in the Drosophila brain. *Curr. Biol.*, 13:1758–1767.

Veleri, S., Rieger, D., Helfrich-Förster, C., and Stanewsky, R. (2007). Hofbauer-Buchner eyelet affects circadian photosensitivity and coordinates TIM and PER expression in Drosophila clock neurons. *J. Biol. Rhythms*, 22:29–42.

Venkatachalam, K., Long, A. A., Elsaesser, R., Nikolaeva, D., Broadie, K., and Montell, C. (2008). Motor deficit in a Drosophila model of mucolipidosis type IV due to defective clearance of apoptotic cells. *Cell*, 135:838–851.

Venkatachalam, K. and Montell, C. (2007). TRP channels. *Annu. Rev. Biochem.*, 76:387–417.

Vishnu, S., Hertenstein, A., Betschinger, J., Knoblich, J. A., Gert de Couet, H., and Fischbach, K. F. (2006). The adaptor protein X11Lalpha/Dmint1 interacts with the PDZ-binding domain of the cell recognition protein Rst in Drosophila. *Dev. Biol.*, 289:296–307.

Voets, T. and Nilius, B. (2003). TRPs make sense. *J. Membr. Biol.*, 192:1–8.

Walker, R. G., Willingham, A. T., and Zuker, C. S. (2000). A Drosophila mechanosensory transduction channel. *Science*, 287:2229–2234.

Weigel, D., Jurgens, G., Kuttner, F., Seifert, E., and Jackle, H. (1989). The homeotic gene fork head encodes a nuclear protein and is expressed in the terminal regions of the Drosophila embryo. *Cell*, 57:645–658.

Wheeler, D. A., Hamblen-Coyle, M. J., Dushay, M. S., and Hall, J. C. (1993). Behavior in light-dark cycles of Drosophila mutants that are arrhythmic, blind, or both. *J. Biol. Rhythms*, 8:67–94.

Wiener, J. (1999). *Time, Love, Memory: A Great Biologist and His Quest for the Origins of Behavior*. Knopf.

Xu, K., Zheng, X., and Sehgal, A. (2008). Regulation of feeding and metabolism by neuronal and peripheral clocks in Drosophila. *Cell Metab.*, 8:289–300.

Xu, X. Z., Chien, F., Butler, A., Salkoff, L., and Montell, C. (2000). TRPgamma, a drosophila TRP-related subunit, forms a regulated cation channel with TRPL. *Neuron*, 26:647–657.

Xu, X. Z., Li, H. S., Guggino, W. B., and Montell, C. (1997). Coassembly of TRP and TRPL produces a distinct store-operated conductance. *Cell*, 89:1155–1164.

Yang, Z., Emerson, M., Su, H. S., and Sehgal, A. (1998). Response of the timeless protein to light correlates with behavioral entrainment and suggests a nonvisual pathway for circadian photoreception. *Neuron*, 21:215–223.

Yoshii, T., Fujii, K., and Tomioka, K. (2007). Induction of Drosophila behavioral and molecular circadian rhythms by temperature steps in constant light. *J. Biol. Rhythms*, 22:103–114.

Yoshii, T., Heshiki, Y., Ibuki-Ishibashi, T., Matsumoto, A., Tanimura, T., and Tomioka, K. (2005). Temperature cycles drive Drosophila circadian oscillation in constant light that otherwise induces behavioural arrhythmicity. *Eur. J. Neurosci.*, 22:1176–1184.

Yoshii, T., Sakamoto, M., and Tomioka, K. (2002). A temperature-dependent timing mechanism is involved in the circadian system that drives locomotor rhythms in the fruit fly Drosophila melanogaster. *Zool. Sci.*, 19:841–850.

Yoshii, T., Vanin, S., Costa, R., and Helfrich-Förster, C. (2009a). Synergic entrainment of Drosophila's circadian clock by light and temperature. *J. Biol. Rhythms*, 24:452–464.

Yoshii, T., Wülbeck, C., Sehadova, H., Veleri, S., Bichler, D., Stanewsky, R., and Helfrich-Förster, C. (2009b). The neuropeptide pigment-dispersing factor adjusts period and phase of Drosophila's clock. *J. Neurosci.*, 29:2597–2610.

Zanzoni, A., Montecchi-Palazzi, L., Quondam, M., Ausiello, G., Helmer-Citterich, M., and Cesareni, G. (2002). MINT: a Molecular INTeraction database. *FEBS Lett.*, 513:135–140.

Zerr, D. M., Hall, J. C., Rosbash, M., and Siwicki, K. K. (1990). Circadian fluctuations of period protein immunoreactivity in the CNS and the visual system of Drosophila. *J. Neurosci.*, 10:2749–2762.

Zhang, Y., Liu, Y., Bilodeau-Wentworth, D., Hardin, P. E., and Emery, P. (2010). Light and temperature control the contribution of specific DN1 neurons to Drosophila circadian behavior. *Curr. Biol.*, 20:600–605.

Zimmerman, W. F., Pittendrigh, C. S., and Pavlidis, T. (1968). Temperature compensation of the circadian oscillation in drosophila pseudoobscura and its entrainment by temperature cycles. *J. Insect Physiol.*, 14:669–684.